



UNIVERSIDADE TÉCNICA DE LISBOA
INSTITUTO SUPERIOR TÉCNICO



*Periodic and Non-linear Estimators
with Applications to the Navigation of Ocean Vehicles*

Paulo Jorge Coelho Ramalho Oliveira
(Mestre)

Dissertação para a obtenção do Grau de Doutor em
Engenharia Electrotécnica e de Computadores

Orientador: António Manuel dos Santos Pascoal

Presidente: Reitor da Universidade Técnica de Lisboa

Vogais: Doutor José Manuel Nunes Leitão

Doutor Carlos Alberto Varelas da Rocha

Doutor João Manuel Lage de Miranda Lemos

Doutor Isaac Kaminer

Doutor Fernando Manuel Ferreira Lobo Pereira

Doutor Maria Isabel Lobato de Faria Ribeiro

Doutor António Manuel dos Santos Pascoal

Julho de 2002



UNIVERSIDADE TÉCNICA DE LISBOA
INSTITUTO SUPERIOR TÉCNICO



*Periodic and Non-linear Estimators
with Applications to the Navigation of Ocean Vehicles*

Paulo Jorge Coelho Ramalho Oliveira
(Mestre)

Dissertação para a obtenção do Grau de Doutor em
Engenharia Electrotécnica e de Computadores

Orientador: António Manuel dos Santos Pascoal

Presidente: Reitor da Universidade Técnica de Lisboa

Vogais: Doutor José Manuel Nunes Leitão

Doutor Carlos Alberto Varelas da Rocha

Doutor João Manuel Lage de Miranda Lemos

Doutor Isaac Kaminer

Doutor Fernando Manuel Ferreira Lobo Pereira

Doutor Maria Isabel Lobato de Faria Ribeiro

Doutor António Manuel dos Santos Pascoal

Julho de 2002

Acknowledgments

I would like to thank a number of colleagues, friends, and institutions for the support they provided me during the work culminating in this thesis. Foremost among these is my thesis supervisor, Professor António Pascoal, whose patience and insight were invaluable in guiding me down the demanding but rewarding path of research.

Secondly, I must acknowledge the Institute for Systems and Robotics and, in particular, Professor João Sentieiro for providing me with ideal conditions for carrying out the research and development work I set out to do.

Among my colleagues and friends, I particularly wish to thank Carlos Silvestre for his friendship and unflagging support. He was always available to discuss research problems and his interest and feedback helped me to refine solutions. I would also like to thank all my colleagues at the Dynamical Systems and Ocean Robotics Laboratory with whom I had interesting and stimulating discussions, particularly Pedro Aguiar, Pedro Encarnação, Daniel Frixell, and Victor Silva. Very special thanks go to Luis Sebastião, who not only participated in enriching discussions but also helped in preparing some of the figures depicted in this thesis.

The Portuguese Foundation for Science and Technology and the European Community provided financial support in the framework of projects in which I have participated during this period. Their support gave me the opportunity to attend conferences and to work in cooperation with IFREMER at Toulon, France, and with the US Naval Postgraduate School (NPS) in Monterey, CA. I would also like to thank Dr. Vincent Rigaud and Dr. Jan Opderbecke at IFREMER-Toulon for their kind reception and for the interesting challenges they posed in the navigation and positioning of manned and unmanned underwater vehicles. At the NPS I would like to thank Professor Anthony Healey, who received me at the Center for Autonomous Underwater Vehicle Research, for the interesting collaborative work we did during my stay there.

Special thanks must also go to Professor Isaac Kaminer, also from the NPS, for his suggestions and the enlightening discussions we had, as will be apparent throughout this thesis.

Very special thanks go to my wife Maria Margarida and to my parents, Maria Margarida and José Francisco. Without their support and encouragement this long and difficult work would not have been possible. Finally, I would like to dedicate this thesis to my daughter, Ana Margarida, who has recently made me aware of new meanings in life.

Resumo

Esta tese aborda o problema de projecto de estimadores a serem utilizados como sistemas de navegação e de seguimento de alvos para veículos autónomos. A síntese e a análise são suportadas numa metodologia capaz de descrever problemas de optimização convexa - as *Desigualdades Matriciais Lineares* (DMLs). As soluções são obtidas recorrendo a ferramentas de optimização existentes comercialmente, baseadas em métodos eficientes de ponto interior.

Para formalizar e resolver todos os problemas abordados ao longo deste trabalho recorreu-se aos filtros complementares devido às suas propriedades, nomeadamente no que diz respeito à interpretação no domínio da frequência, a qual é de grande valor durante o projecto dos filtros.

São apresentados novos resultados para o cálculo da norma \mathcal{H}_2 de sistemas discretos com dinâmica periódica, baseados num conjunto de LMIs, bem como uma nova metodologia de projecto de estimadores que estende as propriedades dos filtros complementares a esta classe de sistemas. O mesmo exercício é efectuado para sistemas variantes no tempo descritos através de inclusões diferenciais lineares. A estabilidade e o desempenho dos sistemas de navegação obtidos em ambos os casos considerados são estudados. Introduce-se ainda uma nova metodologia de análise, baseada em técnicas de optimização convexa, que possibilita uma interpretação semelhante à análise em frequência clássica.

Finalmente, projectam-se dois seguidores de alvos não lineares que fornecem estimativas da posição e velocidade de um Veículo Submarino Autónomo (VSA) em relação a uma Embarcação Autónoma de Superfície (EAS), baseado em dois conjuntos de sensores alternativos a instalar a bordo. Para esse fim, dois estimadores não lineares são propostos e estudados em detalhe, recorrendo a sistemas lineares com variações temporais paramétricas (LPVs). Garante-se ainda a estabilidade e o desempenho numa região apropriada para os seguidores de alvos resultantes e verificam-se as propriedades habituais dos filtros complementares.

Palavras Chave: Sistemas de Navegação, Seguidores de Alvos Não Lineares, Filtros Complementares, Sistemas Periódicos, Veículos Autónomos, LMIs.

Abstract

This thesis addresses the problem of estimator design to be used as navigation and target tracker systems in autonomous vehicles. Both synthesis and analysis steps are supported by Linear Matrix Inequalities (LMIs), a framework able of describing convex optimization problems. Solutions are found resorting to efficient commercially available interior-point optimization tools.

Complementary filters were chosen as the structure to formulate all problems addressed and solved along this work due to their key properties. Namely, the frequency domain interpretation provides valuable insight into the filtering design process.

New results on the \mathcal{H}_2 norm computation of discrete-time periodic time-varying systems are deduced, based on a set of LMIs written along the systems period and a new methodology for estimator design is introduced, which extends the complementary filters properties to this class of systems. Complementary filter properties are also extended to the time-varying setting by resorting to the theory of linear differential inclusions. The stability and performance properties of the navigation systems obtained are studied in both cases. A new methodology for system analysis using efficient numerical analysis tools that borrow from convex optimization techniques is introduced, allowing for assessment of the "frequency-like" performance of the filters obtained.

Finally, to provide estimates on the position and velocity of an Autonomous Underwater Vehicle (AUV) relative to an Autonomous Surface Craft (ASC), two non-linear target trackers are designed, based on two alternative sensor suites. To that purpose, two non-linear estimators are proposed and studied in detail, resorting to linear parametrically time-varying (LPV) systems. Stability and regional performance of the resulting target trackers are guaranteed and the complementary filters properties are verified.

Keywords: Navigation Systems, Non-linear Target Trackers, Complementary Filters, Periodic Systems, Autonomous Vehicles, LMIs.

Contents

Acknowledgments	i
Resumo	iii
Abstract	v
1 Introduction	1
1.1 Main contributions	3
2 Linear Matrix Inequalities	7
2.1 Introduction	7
2.2 Dissipative systems	8
2.3 Lyapunov stability	11
2.4 Linear matrix inequalities	14
2.5 Norms of systems and linear matrix inequalities	17
2.5.1 \mathcal{H}_∞ norm	17
2.5.2 \mathcal{H}_2 norm	19
2.5.3 Generalized \mathcal{H}_2 norm	21
2.6 Stability regions	22
2.7 Estimator synthesis	24
2.8 Discrete-time systems	32
2.8.1 Norms of discrete-time systems	34
2.8.2 Estimator synthesis for discrete-time systems	37
2.9 Conclusions	40

3	Complementary Filters	41
3.1	Introduction	41
3.2	Linear Estimation	42
3.3	Motivation for the use of complementary filters	48
3.3.1	Complementary filters: basic concepts and definitions	48
4	Synthesis of Periodic Estimators	57
4.1	Introduction	57
4.2	Periodic systems representation	58
4.3	Operator representation of linear systems	60
4.4	<i>Lifting</i> technique	65
4.5	Periodic Riccati based estimators	69
4.5.1	Periodic estimators	69
4.5.2	Existence of a solution for the periodic system	70
4.6	Periodic and invariant estimators equivalence	72
4.7	Norms of periodic systems	74
4.7.1	\mathcal{H}_∞ norm	75
4.7.2	\mathcal{H}_2 norm	77
4.8	Estimator synthesis for periodic systems	80
4.9	Navigation System of DELFIM	83
4.10	Conclusions	94
5	Analysis of Periodic Estimators	99
5.1	Introduction	99
5.2	Digital rate conversion	101
5.2.1	Sampling rate reduction - decimation by an integer factor M	101
5.2.2	Sampling rate increase - interpolation by an integer factor L	102
5.3	Switch Decomposition Method	103
5.3.1	SDM Example of a Quasi Invariant System	108
5.4	Frequency analysis	110
5.4.1	Low and high-pass filters.	111
5.5	Navigation system for the Delfim catamaran	113

5.6	Conclusions and future work	114
6	Time-Varying Estimators	115
6.1	Introduction	115
6.2	Mathematical background	116
6.2.1	Computation of induced operator norms. Polytopic systems.	118
6.2.2	Low and high-pass time-varying filters.	119
6.3	Navigation system design: problem formulation	120
6.3.1	Notation. Vehicle kinematics: a summary.	120
6.3.2	Time-varying complementary filters. Navigation problem formulation. . .	121
6.4	Complementary filter design. Main results.	123
6.4.1	Candidate complementary filter structure.	123
6.4.2	The candidate complementary filter: sufficient conditions for stability and guaranteed break frequency.	126
6.5	Filter Design: a practical algorithm. Simulation results.	132
6.6	Extension to Accelerometers	136
6.7	Conclusions and future work	140
7	Tracker for Joint ASC/AUV Missions	143
7.1	Introduction	143
7.2	Mathematical background	146
7.3	Tracker design: problem formulation	148
7.3.1	Notation	148
7.3.2	Vehicles kinematics and the sensor suite measurements	149
7.3.3	Design Model	152
7.4	Tracker design and analysis	153
7.4.1	Proposed solution	155
7.5	Experimental results	162
7.6	Non-linear tracker revisited	167
7.7	Conclusions	175
8	Conclusion	177

List of Figures

2.7.1 General setup for filtering synthesis.	24
3.3.1 Process model \mathcal{M}	49
3.3.2 Complementary filter.	50
3.3.3 Complementary filter with bias estimation.	52
4.2.1 Multi-rate system with generic sample periods for the inputs and outputs.	58
4.4.1 The operator P associated with the system \mathcal{P} and the <i>lifted</i> operator \bar{P}	66
4.8.1 General setup for periodic filtering synthesis.	80
4.9.1 Location of D. João de Castro bank (on the left). Hydrothermal activity.	84
4.9.2 DELFIM in operation at the D. João de Castro bank.	85
4.9.3 Position estimation: filter design model.	87
4.9.4 $\ T_{x_m \rightarrow e}\ _2$ for a range of q_b and q_x values.	89
4.9.5 $\ T_{u_m \rightarrow \hat{x}}\ _2$ for a range of q_b and q_x values.	90
4.9.6 $\ T_{x_m \rightarrow \hat{x}}\ _\infty$ for a range of q_b and q_x values.	91
4.9.7 Estimator design structure for system (4.9.2).	92
4.9.8 Position x (dashed line) and position estimate \hat{x} , on the top; Velocity u (dashed line) and velocity estimate, in the middle and bias b_x (dashed line) and bias estimate, on the bottom.	93
4.9.9 Trajectory of the Delfim catamaran during a bathymetric survey at sea, in the Setubal canyon.	94
4.9.10 Detail of the trajectory of the Delfim catamaran.	95
4.9.11 $\ T_{x_m \rightarrow e}^*\ _2$ for a series of period values M	95
4.9.12 $\ T_{x_m \rightarrow e}^*\ _2$ for a series of period values M and h	96

4.9.1	Block diagram to estimate ${}^I\hat{\mathbf{v}}_S$, ${}^I\hat{\mathbf{p}}_S$, and ${}^I\hat{\mathbf{v}}_W$	96
4.9.1	Position x (dashed line) and position estimate \hat{x} , on the top; Velocity u (dashed line) and velocity estimate, in the middle and bias b_x (dashed line) and current estimate ${}^I\hat{u}_w$, on the bottom.	97
5.2.1	Sampling rate conversion by a factor L/M , using an interpolator ($\uparrow L$) and a decimator ($\downarrow M$).	103
5.3.1	Multi-rate feedback analysis proposed by Kranc ($\delta = e^{sh/M}$).	104
5.3.2	Digital Decomposition Method.	104
5.3.3	Digital Decomposition Method of Lifted Systems.	107
5.4.1	General setup for frequency analysis.	111
5.5.1	Analysis of the high-pass operator $T_{x_m \rightarrow e}$. Generalized Bode plot.	113
5.5.2	Analysis of the low-pass operator $T_{x_m \rightarrow \hat{x}}$. Generalized Bode plot.	114
6.3.1	Process model.	122
6.4.1	Non-linear time-varying complementary filter.	124
6.5.1	Filter gain K_1 versus iteration number.	135
6.5.2	Generalized bode plots - low-pass property	136
6.5.3	Generalized bode plots - high-pass property	137
6.5.4	Actual and estimated vehicle trajectory.	138
6.5.5	Doppler bias estimate.	139
6.6.1	Process model \mathcal{M}_{pa}	140
6.6.2	Complementary filter \mathcal{E}_{ta}	141
7.1.1	Joint mission of the Delfim ASC and the Infante AUV.	144
7.3.1	Mission coordinate frames and notation.	148
7.3.2	Estimator model.	152
7.4.1	Non-linear tracker structure.	155
7.5.1	ASC and AUV inertial coordinates on the horizontal plane.	163
7.5.2	Relative position coordinates \mathbf{p} (dashed) and estimates $\hat{\mathbf{p}} = [\hat{x} \ \hat{y} \ \hat{z}]^T$	164
7.5.3	AUV velocity in the inertial frame $\{I\}$ ${}^I\mathbf{v}_U = [{}^I\dot{x}_u \ {}^I\dot{y}_u \ {}^I\dot{z}_u]^T$ (dashed) and respective estimates ${}^I\hat{x}_u$, ${}^I\hat{y}_u$ and ${}^I\hat{z}_u$	165

7.5.4 Camera plane coordinates after compensation for the simulated camera parameters. Exact knowledge of the camera position and orientation in the first experiment (continuous line) and misplaced and misdirected (dashed line).	165
7.5.5 Relative position coordinates \mathbf{p} (dashed) and estimates \hat{x} , \hat{y} and \hat{z}	166
7.5.6 AUV velocity in the inertial frame $\{I\}^T \mathbf{v}_U = [{}^I \dot{x}_u \ {}^I \dot{y}_u \ {}^I \dot{z}_u]^T$ (dashed) and respective estimates ${}^I \hat{x}_u$, ${}^I \hat{y}_u$ and ${}^I \hat{z}_u$	166
7.6.1 Relative position coordinates \mathbf{p} (dashed) and estimates \hat{x} , \hat{y} and \hat{z}	172
7.6.2 AUV velocity in the inertial frame $\{I\}^T \mathbf{v}_U = [{}^I \dot{x}_u \ {}^I \dot{y}_u \ {}^I \dot{z}_u]^T$ (dashed) and respective estimates ${}^I \hat{x}_u$, ${}^I \hat{y}_u$ and ${}^I \hat{z}_u$	173
7.6.3 Camera plane coordinates after compensation for the simulated camera parameters.	173
7.6.4 Distance measured d (dashed) and estimated between both vehicles.	174

List of Tables

2.6.1 Generalized stability regions as LMIs.	23
3.3.1 First order complementary filters.	54
7.5.1 Non-linear tracker design parameters.	164
7.6.1 Non-linear tracker design parameters for the new sensor suite.	172

Chapter 1

Introduction

There has been considerable interest recently in the development of navigation systems to provide robotic vehicles with the capability to perform complex missions in an autonomous mode. See [7, 15, 41, 44, 50, 72] and the references therein for in-depth presentations of navigation systems for aircraft and [27, 38, 75, 80] for an overview of similar systems and related research issues in the ocean robotics area.

Central to the development of advanced navigation systems is the availability of powerful theoretical tools for system analysis and synthesis. Among these, Linear Matrix Inequalities (LMIs) [14, 48, 68] - have become the tool *par excellence* to deal with seemingly unwieldy design problems. Interestingly, a series of classic systems and control problems as well as new and more complex problems can be formulated and solved using this framework. Moreover, the recent development of efficient interior-point methods [54] has endowed the scientific community with tools capable of solving multi-criteria convex optimization problems. These interesting features support the choice of LMIs as the synthesis and analysis tool for addressing the problems presented in this work and motivate its introduction in the next chapter. Classic structures for estimator design will also be introduced using LMIs, both in the continuous and in the discrete-time settings, and the solutions obtained will be discussed in detail.

Traditionally, navigation system design is done in a stochastic setting using Kalman-Bucy filtering theory [17]. In the case of non-linear systems, design solutions are usually sought by resorting to Extended Kalman filtering techniques [17]. The stochastic setting requires a complete characterization of process and observation noises, a task that may be difficult, costly,

or not suited to the problem at hand. This issue is argued at length in [18], where the author points out that in a great number of practical applications the filter design process is entirely dominated by constraints that are naturally imposed by the sensor bandwidths. In this case, a design method that explicitly addresses the problem of merging information provided by a given sensor suite over distinct, yet complementary frequency regions is warranted. Complementary filters have been developed to address this issue explicitly and will be presented in chapter 3, supported by both Wiener filtering theory and motivating examples.

In the case where the sensors required in the design of a navigation system are all installed on board and can be sampled at the same period, as in the case of attitude estimation, the corresponding filter operators are linear and time-invariant. This leads to a fruitful interpretation of the filters in the frequency domain. In the case of linear position and velocity estimation, however, the characteristics of the sound channel imply that the position measurements (obtained, for instance, from a Long BaseLine system) are available at a rate that is lower than that of the remaining sensors. To deal with this problem, this thesis proposes a new approach to navigation system design that relies on multi-rate complementary Kalman filtering theory. Design methodologies for such types of multi-rate systems are discussed in chapter 4, and the properties normally associated with single rate complementary filters are shown to be preserved. In chapter 5 some analysis tools are introduced and it is shown that multi-rate filters can be viewed as input-output operators exhibiting “frequency-like” properties that are the natural generalization of those obtained for the single rate case. Performance of the resulting navigation system is assessed from the results obtained with an autonomous catamaran during sea trials.

Chapter 6 further extends complementary filter design and analysis techniques to a time-varying setting, and offers a solution to the problem of estimating the linear position and velocity of a vehicle using time-varying complementary filters. Time-dependence is imposed by the fact that some of the sensors provide measurements in inertial coordinates, while other measurements are naturally expressed in body axis. To merge the information from both types of sensors - while compensating for sensor biases - requires that the rotation matrix from inertial to body axis be explicitly included in the navigation filters. The resulting filters are bilinear and time-varying, but the time-dependence is well structured. By exploiting this structure, the problem of filter design and analysis can be converted into that of determining the feasibility of a set of Linear Matrix Inequalities (LMIs) [14, 68] supported by the theory of linear differential inclusions [8, 14].

As a consequence, the stability of the resulting filters as well as their frequency-like performance can be assessed using efficient numerical analysis tools that borrow from convex optimization techniques [14, 48]. The performance of the resulting navigation system is assessed in simulation.

In recent years there has also been an increasing interest in the use of a fleet of autonomous vehicles to perform complex missions. Military [70] and civil [4] applications are becoming more complex and demanding in terms of joint (*formation*) performance. Air, land, and sea examples of such cooperative missions can be found in [70] and in the references therein. As an example in oceanography, the main thrust of the ASIMOV project [3] is the development and integration of advanced technological systems to achieve coordinated operation of an Autonomous Surface Craft (ASC) and an Autonomous Underwater Vehicle (AUV) while ensuring a fast communication link between the two vehicles. The ASC / AUV ensemble is being used to study the extent of shallow water hydro-thermalism and to determine patterns of community diversity at vents in the D. João de Castro bank in the Azores. To that purpose, on-board sensors such as a video camera and a sonar are envisioned to be carried by the AUV Infante to collect scientific data in a pre-specified survey area.

In order to have access to higher bandwidth acoustic communications, the vertical channel must be used [3]. This constraint motivates the design of joint cooperative missions where the ASC Delfim will be positioned in a vicinity of the vertical position of the AUV Infante with minimal or no exchange of navigation data between the two platforms. These requirements lead naturally to the need for a target tracker on-board the ASC to provide access to estimates on the relative position and velocity of both platforms. The sensor suite to be installed on board will be discussed and alternatives, such as the AUV depth or the distance between the two vehicles that can be provided by a depth cell or by an acoustic ranging sensor, respectively, will be discussed in detail in chapter 7. Stability and performance of the proposed structure will be studied and the resulting architecture will be assessed with realistic simulations.

1.1 Main contributions

The main purpose of this work is to address estimation problems using new and powerful synthesis and analysis tools. It is relevant to outline the following contributions present in this thesis:

- In chapter 4 new results on the \mathcal{H}_2 norm computation of discrete-time, linear, periodic time-varying systems using LMIs are introduced. The resulting LMIs are a natural extension of the classic discrete-time invariant setup and pave the way for common design methodologies for the synthesis and analysis of these two classes of systems. The results obtained are also promising as a design framework for periodic feedback control, periodic output feedback, and periodic filter synthesis.

The synthesis of (periodic) estimators is extended to the class of periodic time-varying systems, resorting to a set of LMIs describing the constraints along the system period, and the properties of the resulting solution are established. The methodology proposed, resorting to convex optimization procedures, is based on the minimization of the \mathcal{H}_2 or \mathcal{H}_∞ norms from auxiliary inputs to auxiliary outputs, constrained by the norms of other input/output signals in a generalized plant.

- A new methodology for the analysis of periodic systems is introduced in chapter 5 where it is shown that the multi-rate complementary filters can be viewed as input-output operators exhibiting frequency-like properties that are the natural generalization of those obtained for the single rate case. The main advantages of the proposed method is its close relation to classical frequency-response analysis (the Bode plot) and the broad class of systems that can be analyzed using the proposed methodology.
- The design of navigation systems for autonomous vehicles using simple time-varying kinematic relationships is addressed in chapter 6. The problem is solved by resorting to special bilinear time-varying filters that are the natural generalization of linear time-invariant complementary filters. Sufficient conditions for stability and guaranteed break frequency are introduced.

The analysis tool introduced for discrete-time, periodic systems is further extended to time-varying systems resorting to differential inclusions (polytopic systems). A design example, incorporating directly constraints described by the aforementioned analysis tool, is discussed in detail. The extension to other structures of the results obtained is also taken into consideration.

- In chapter 7 two non-linear target trackers are proposed to provide estimates of the position

and velocity of an Autonomous Underwater Vehicle (AUV) relative to an Autonomous Surface Craft (ASC), based on two alternative sensor suites. To that purpose, two non-linear estimators are designed and studied resorting to linear parametrically time-varying (LPV) systems. Stability and regional performance of the resulting target trackers are guaranteed and the complementary filters properties are verified.

Chapter 2

Linear Matrix Inequalities

2.1 Introduction

In systems and control theory there are many problems that can be written using Linear Matrix Inequalities (LMIs). In preparation for the applications that will be presented in the course of this thesis some classical problems in systems theory will be revisited and written in this framework. Some supporting tools that help manipulate LMIs will also be presented with an emphasis on the convex characteristics of the resulting constraints. Convex optimization problems can be formulated using LMIs, and numerical solutions can be found by resorting to recently developed efficient interior-point methods [54]. For the sake of completeness, the book [14] must be mentioned, as it provides a fruitful description of many interesting problems where the constraints are set as LMIs and methodologies to find the numerical solutions are summarized.

The structure of this chapter is as follows: section 2.2 introduces the concept of dissipativity for non-linear and linear continuous-time driven systems, and section 2.3 describes the concept of stability as introduced by Aleksandr Lyapunov more than one century ago. In both cases the emphasis is on the description of the concepts under study resorting to the use of LMIs. Section 2.4 describes in detail the structure and properties of linear matrix inequalities. The \mathcal{H}_∞ , \mathcal{H}_2 , and the generalized \mathcal{H}_2 norms for continuous-time driven, finite-dimensional, linear, time-invariant systems are presented in section 2.5. Section 2.6 describes how constraints on the eigenvalues of linear systems can be formulated as LMIs. That task builds on the definition

of convex constraints for the minimization problems at hand. Section 2.7 presents two general setups for estimator synthesis. Moreover, the computation of the norms introduced previously are presented for the structures under study. Section 2.8 revisits the subjects described for continuous-time systems in the framework of discrete-time systems. Finally, section 2.9 presents some conclusions.

2.2 Dissipative systems

The notion of dissipativity is of utmost importance in systems theory, both from a theoretical point of view and as a practical concept. A dissipative system can not supply as much energy to the environment as it receives, due to the fact that part of it is absorbed and transformed into heat, entropy increase or other *energy losses*. In the following it will be shown that linear matrix inequalities (LMIs) occur in the study of dissipative systems. The solutions of these LMIs can be interpreted as *storage functions* playing a key role in understanding stability, robustness, and other system design requirements.

The pioneering work of Aleksandr Lyapunov near the end of the XIX century [47], where he studied the stability of autonomous differential equations of the form

$$\dot{\mathbf{x}}(t) = a(\mathbf{x}(t)), \quad (2.2.1)$$

where $a : \mathbb{R}^n \rightarrow \mathbb{R}^n$ is some analytic function and $\mathbf{x}(t)$ is a vector of position and velocities in \mathbb{R}^n along the time $t \in \mathbb{R}$, has been an inspiring guideline ever since.

Consider a finite-dimensional, time-invariant dynamical system \mathcal{S} described by

$$\begin{aligned} 0 &= f(\dot{\mathbf{x}}(t), \mathbf{x}(t), \mathbf{u}(t)), \\ \mathbf{y}(t) &= g(\mathbf{x}(t), \mathbf{u}(t)), \end{aligned} \quad (2.2.2)$$

where $\mathbf{x}(t) \in \mathbb{R}^n$ is the state vector, $\mathbf{u}(t) \in \mathbb{R}^m$ is the input vector, and $\mathbf{y}(t)$ is the output vector which assumes its values in \mathbb{R}^p , with the initial state $\mathbf{x}(t_0) = x_0$. This system generates outputs \mathbf{y} , according to the inputs \mathbf{u} , given the initial conditions considered. Let $s : [\mathbf{u}^T \mathbf{y}^T]^T \rightarrow \mathbb{R}$ be a mapping, referred to as *supply rate function* or *supply function*, and assume for all instants $t \in \mathbb{R}$ and for all input-output pairs satisfying (2.2.2) the composite function $s(t) := s(\mathbf{u}(t), \mathbf{y}(t))$ is locally absolutely integrable, i.e.,

$$\int_{t_0}^{t_1} |s(t)| dt < \infty.$$

Definition 2.2.1 Dissipativity [77] *The system $\mathcal{S} : \mathbf{u} \rightarrow \mathbf{y}$ with supply rate $s(t)$ is said to be strictly dissipative if there exists a non-negative function $V : \mathbf{x} \rightarrow \mathbb{R}$ such that*

$$V(\mathbf{x}(t_0)) + \int_{t_0}^{t_1} s(\mathbf{u}(t), \mathbf{y}(t)) dt > V(\mathbf{x}(t_1)), \quad (2.2.3)$$

for all $t_0 < t_1$ and for all trajectories $(\mathbf{u}(t), \mathbf{x}(t), \mathbf{y}(t))$ of the system \mathcal{S} .

Note that in the instants where the supply function is positive, work is supplied to the system and in the opposite case, work is being done by the system. $V(\mathbf{x})$, with $\mathbf{x} : \mathbb{R} \rightarrow \mathbb{R}^n$, is called a storage function and generalizes the notion of an energy function for a dissipative system. Moreover, if the function $V(t)$, with $t \in \mathbb{R}$, is differentiable as a function of time the relation $\dot{V}(t) < s(t)$ holds.

The classical motivation for the storage function comes from circuit theory, where the product of tensions and currents at a given point of a circuit reveals that a subsystem is instantaneously receiving or providing energy. In mechanical systems and in thermodynamics, similar notions of storage functions have been in use for long time.

Consider now the dissipativity definition of linear, time-invariant systems $\mathcal{F} : \mathbf{u} \rightarrow \mathbf{y}$, described as a finite-dimensional operator with state-space realization

$$\Sigma_{\mathcal{F}} := \begin{cases} \dot{\mathbf{x}}(t) &= A\mathbf{x}(t) + B\mathbf{u}(t) \\ \mathbf{y}(t) &= C\mathbf{x}(t) + D\mathbf{u}(t) \end{cases} \quad (2.2.4)$$

with the quadratic supply function

$$s(\mathbf{u}(t), \mathbf{y}(t)) = \begin{bmatrix} \mathbf{y}(t) \\ \mathbf{u}(t) \end{bmatrix}^T \begin{bmatrix} Q_{yy} & Q_{yu} \\ Q_{uy} & Q_{uu} \end{bmatrix} \begin{bmatrix} \mathbf{y}(t) \\ \mathbf{u}(t) \end{bmatrix}, \quad (2.2.5)$$

where no assumptions are made on the matrix $Q \in \mathbb{R}^{(p+m) \times (p+m)}$

$$Q = \begin{bmatrix} Q_{yy} & Q_{yu} \\ Q_{uy} & Q_{uu} \end{bmatrix}.$$

Using the equation for the output \mathbf{y} in (2.2.4), the supply function can be expressed in terms of $\mathbf{u}(t)$ and $\mathbf{x}(t)$ as

$$s(\mathbf{u}(t), \mathbf{x}(t)) = \begin{bmatrix} \mathbf{x}(t) \\ \mathbf{u}(t) \end{bmatrix}^T \begin{bmatrix} C & D \\ 0 & I_m \end{bmatrix}^T \begin{bmatrix} Q_{yy} & Q_{yu} \\ Q_{uy} & Q_{uu} \end{bmatrix} \begin{bmatrix} C & D \\ 0 & I_m \end{bmatrix} \begin{bmatrix} \mathbf{x}(t) \\ \mathbf{u}(t) \end{bmatrix}, \quad (2.2.6)$$

where I_m is the identity matrix of dimensions $m \times m$. Along this thesis we will use the same symbol \mathcal{F} to denote both a system and its particular realization $\Sigma_{\mathcal{F}}$, as the meaning will become clear from the context.

In what follows, the definition of positive definite matrices will be required.

Definition 2.2.2 *A matrix $P \in \mathbb{R}^{n \times n}$ is positive definite, denoted in compact form as $P > 0$ if and only if $\mathbf{x}^T P \mathbf{x} > 0$, for any non-null column vector $\mathbf{x} \in \mathbb{R}^n$.*

This definition will be revisited later in section 2.4. In a similar way, a semi-definite positive matrix, denoted $P \geq 0$ verifies $\mathbf{x}^T P \mathbf{x} \geq 0$ for all non-null \mathbf{x} . For a negative definite matrix, denoted $P < 0$, the expression $\mathbf{x}^T P \mathbf{x} < 0$, for all non-null inputs is verified. The next theorem provides necessary and sufficient conditions for the system \mathcal{F} , with the supply function $s(\mathbf{u}(t), \mathbf{y}(t))$ to be dissipative, see [68]. Moreover, it is the first example of a systems's property described as LMIs.

Theorem 2.2.3 *Suppose the system $\mathcal{F} : \mathbf{u} \rightarrow \mathbf{y}$ with realization $\Sigma_{\mathcal{F}}$ is controllable and let the supply function $s(\mathbf{u}(t), \mathbf{x}(t))$ be defined by (2.2.5). The following statements are equivalent:*

1. *The system is strictly dissipative;*
2. *The system admits a quadratic storage function $V(\mathbf{x}(t)) = \mathbf{x}^T(t) P \mathbf{x}(t)$, where $P \in \mathbb{R}^{n \times n}$ is a positive definite symmetric matrix;*
3. *There exists a positive definite, symmetric matrix $P \in \mathbb{R}^{n \times n}$ such that*

$$F(P) := - \begin{bmatrix} A^T P + P A & P B \\ B^T P & 0 \end{bmatrix} + \begin{bmatrix} C & D \\ 0 & I_m \end{bmatrix}^T \begin{bmatrix} Q_{yy} & Q_{yu} \\ Q_{uy} & Q_{uu} \end{bmatrix} \begin{bmatrix} C & D \\ 0 & I_m \end{bmatrix} > 0; \quad (2.2.7)$$

4. *The transfer function $F : \mathbb{C} \rightarrow \mathbb{C}^{p \times m}$ of the system with realization $\Sigma_{\mathcal{F}}$ can be written in compact form as $F(\mathbf{s}) = C(\mathbf{s}I_n - A)^{-1}B + D$, where \mathbf{s} is the Laplace transform indeterminate. When evaluated along $\mathbf{s} = j\omega$, for all $\omega \in \mathbb{R}$ and with $\det(j\omega I_n - A) \neq 0$, it satisfies¹*

$$\begin{bmatrix} F(j\omega) \\ I_m \end{bmatrix}^* \begin{bmatrix} Q_{yy} & Q_{yu} \\ Q_{uy} & Q_{uu} \end{bmatrix} \begin{bmatrix} F(j\omega) \\ I_m \end{bmatrix} > 0. \quad (2.2.8)$$

¹The operator $[\]^*$ stands for the transpose conjugate of a vector or matrix.

Moreover, if one of the above statements holds, then $V(\mathbf{x}(t)) = \mathbf{x}^T(t)P\mathbf{x}(t)$ is a quadratic storage function if and only if $P > 0$ and $F(P) > 0$.

Proof: The complete proof can be found in [68]. However, it is interesting to show how the LMI in (2.2.7) appears. Given the analytic storage function $V(\mathbf{x}(t)) = \mathbf{x}^T(t)P\mathbf{x}(t)$, with $P \geq 0$, the dissipativity relation (2.2.3) can be written as

$$\int_{t_0}^{t_1} -\frac{d}{dt} (\mathbf{x}^T(t)P\mathbf{x}(t)) + s(\mathbf{u}(t), \mathbf{y}(t)) dt > 0,$$

with $t_1 > t_0$. Using (2.2.4) and (2.2.6) this relation results in

$$\int_{t_0}^{t_1} \begin{bmatrix} \mathbf{x}(t) \\ \mathbf{u}(t) \end{bmatrix}^T F(P) \begin{bmatrix} \mathbf{x}(t) \\ \mathbf{u}(t) \end{bmatrix} dt > 0. \quad (2.2.9)$$

Since this relation holds for all inputs \mathbf{u} and for all instants $t_1 > t_0$, the dissipativity property implies the LMI (2.2.7). The reverse is obvious, i.e., if the LMI (2.2.7) holds, the system \mathcal{F} satisfies (2.2.9) and, therefore, assuming a quadratic storage function, the strictly dissipative property is verified. ■

The matrix $F(P)$ is usually called the *dissipation matrix*. The characterization of dissipative systems is a key result in systems theory and the frequency characterization counterpart in (2.2.8) is often referred to as the *Kalman-Yakubovich Lemma* [40, 79].

2.3 Lyapunov stability

As mentioned earlier Aleksandr Lyapunov studied the stability of mechanical systems about equilibrium points. A major contribution has been the evidence that stability can be discussed based on the existence of functions called *Lyapunov functions*. For general non-linear systems, there are no systematic procedures to find such functions. However, for linear systems the problem of finding a quadratic Lyapunov function leads to a feasibility test for the unknowns in a linear matrix inequality. This fact will be stressed next in the definition of Lyapunov functions and in a proposition summarizing the stability properties for linear and non-linear systems [47]. For real valued signals $\mathbf{x}(t) : \mathbb{R}^+ \rightarrow \mathbb{R}^n$,

$$\|x\|_2^2 = \int_0^\infty \mathbf{x}^T(\tau)\mathbf{x}(\tau)d\tau$$

is the classical Euclidean norm.

Definition 2.3.1 A function $V : \mathbf{x} \rightarrow \mathbb{R}$ is a Lyapunov function in a neighborhood $\mathcal{N}(\mathbf{x}_{eq}) \in \mathbb{R}^n$ of an equilibrium point \mathbf{x}_{eq} if

1. V is continuous at \mathbf{x}_{eq} ;
2. V has a strong local minimum at \mathbf{x}_{eq} , i.e., there exists a continuous function $\alpha : \mathbb{R}^+ \rightarrow \mathbb{R}^+$, strictly increasing with $\alpha(0) = 0$, such that

$$V(\mathbf{x}) - V(\mathbf{x}_{eq}) \geq \alpha(\|\mathbf{x} - \mathbf{x}_{eq}\|_2)$$

for all $\mathbf{x} \in \mathcal{N}(\mathbf{x}_{eq})$;

3. V is monotone non-increasing along all solutions of (2.2.1), with initial conditions $\mathbf{x}_0 \in \mathcal{N}(\mathbf{x}_{eq})$, i.e., $V(\mathbf{x}(t))$ is monotone non-increasing as a function of t for all $\mathbf{x}_0 \in \mathcal{N}(\mathbf{x}_{eq})$.

An intuitive way of interpreting Lyapunov functions is in terms of storage functions, as introduced above. In fact, energy decreases along the trajectories of a dissipative system. Next, some properties of equilibria points will be described.

Definition 2.3.2 Consider the differential equation $\dot{\mathbf{x}}(t) = f(\mathbf{x})$.

1. An equilibrium point $\mathbf{x}_{eq} \in \mathbb{R}^n$ is called stable in the Lyapunov sense if given $\epsilon > 0$, there exists $\delta_\epsilon > 0$ such that if $\|\mathbf{x}_{eq} - \mathbf{x}_0\| \leq \delta_\epsilon$ then $\|\mathbf{x}(t) - \mathbf{x}_{eq}\| \leq \epsilon$ for all $t \geq 0$.
2. The equilibrium point \mathbf{x}_{eq} is an attractor if there exists $\epsilon > 0$ such that if $\|\mathbf{x}_{eq} - \mathbf{x}_0\| \leq \epsilon$ then $\lim_{t \rightarrow \infty} \mathbf{x}(t) = \mathbf{x}_{eq}$.
3. The equilibrium point is called asymptotically stable, in the sense of Lyapunov if \mathbf{x}_{eq} is stable and an attractor.

Proposition 2.3.3 Lyapunov Theorem: Consider the non-linear system described by (2.2.1) with the equilibrium point $\mathbf{x}_{eq} \in \mathbb{R}^n$.

1. The equilibrium point is stable if there exists a Lyapunov function V in a neighborhood $\mathcal{N}(\mathbf{x}_{eq})$ of \mathbf{x}_{eq} ;

2. \mathbf{x}_{eq} is an asymptotic stable equilibrium if there exists a Lyapunov function V in a neighborhood $\mathcal{N}(\mathbf{x}_{eq})$ of \mathbf{x}_{eq} such that the only solution of (2.2.1) in $\mathcal{N}(\mathbf{x}_{eq})$ for which $\dot{V}(\mathbf{x}(t)) = 0$ is $\mathbf{x}(t) = \mathbf{x}_{eq}$.

Consider the non-linear autonomous system (2.2.1) expressed explicitly in terms of its components as

$$\dot{\mathbf{x}}(t) = \begin{bmatrix} a_1(\mathbf{x}(t)) \\ \vdots \\ a_n(\mathbf{x}(t)) \end{bmatrix},$$

where $\mathbf{x}(t) = \begin{bmatrix} x_1(t) & \cdots & x_n(t) \end{bmatrix}^T$. The equilibrium point \mathbf{x}_{eq} is such that $a(\mathbf{x}_{eq}) = 0$. Introducing the perturbation variable $\delta\mathbf{x}(t) = \mathbf{x}(t) - \mathbf{x}_{eq}$, this non-linear relation admits the first order Taylor expansion in the neighborhood of the equilibrium

$$\dot{\delta\mathbf{x}}(t) = A\delta\mathbf{x}(t), \quad (2.3.1)$$

where $A : \mathbb{R}^n \rightarrow \mathbb{R}^n$ is a linear map described by an $n \times n$ matrix, defined as

$$A := \left[\begin{array}{ccc} \frac{\partial}{\partial x_1} a_1(\mathbf{x}) & \cdots & \frac{\partial}{\partial x_n} a_1(\mathbf{x}) \\ \vdots & \ddots & \vdots \\ \frac{\partial}{\partial x_1} a_n(\mathbf{x}) & \cdots & \frac{\partial}{\partial x_n} a_n(\mathbf{x}) \end{array} \right]_{\mathbf{x}=\mathbf{x}_{eq}}.$$

The next result characterizes the only equilibrium point candidate - the origin of the resulting linear map - when A is invertible, in terms of asymptotic stability.

Proposition 2.3.4 *Let the linear system in (2.3.1) be the linearization of the non-linear autonomous system (2.2.1) at the equilibrium \mathbf{x}_{eq} . The following statements are equivalent:*

1. *The origin is an asymptotically stable equilibrium point for the linear system under study;*
2. *The origin is a global asymptotically stable equilibrium point for the linear system considered;*
3. *All eigenvalues $\lambda(A)$ of A have strictly negative real part;*
4. *The linear matrix inequalities on the symmetric matrix $P \in \mathbb{R}^{n \times n}$*

$$A^T P + P A < 0 \quad \text{and} \quad P > 0$$

are feasible.

Moreover, if these statements hold, the equilibrium point of the non-linear differential equation under study is asymptotically stable.

The stability of the non-linear system near the equilibrium point \mathbf{x}_{eq} , can be discussed based on the eigenvalues of the linearization matrix A . This fact reduces the complexity of the problem at hand and provides an insight to the behaviour of very general non-linear systems. In the same way, the existence of a quadratic Lyapunov function $V(\mathbf{x}(t)) = \mathbf{x}^T(t)P\mathbf{x}(t)$ for the linear system, with negative time derivative along the trajectories expressed as

$$\dot{V}(\mathbf{x}(t)) = \mathbf{x}^T(t)(A^T P + PA)\mathbf{x}(t) < 0,$$

allows one to conclude on the stability of the corresponding non-linear system. Once again the feasibility study of linear matrix inequalities reveals intrinsic properties on systems' theory.

2.4 Linear matrix inequalities

In the previous sections some classical problems in systems theory were revisited. Solutions were deduced in the form of matrix inequalities, linear in some unknown parameters (which can be also matrices). This was the motivation for the study of this type of relations -*linear matrix inequalities* (LMI) expressed in the form (see [14] for details)

$$F(\mathbf{x}) := F_0 + x_1 F_1 + \cdots + x_k F_k = F_0 + \sum_{i=1}^k x_i F_i > 0,$$

where the vector $\mathbf{x} = [x_1 \cdots x_k]^T$ is the vector of k real numbers (also called free decision variables) and F_0, \dots, F_k are symmetric matrices $F_i = F_i^T \in \mathbb{R}^{n \times n}$ known *a priori*. The inequality in the equation above should be read as *positive definite*, i.e., for all non-null \mathbf{u} of proper dimensions $\mathbf{u}^T F(\mathbf{x}) \mathbf{u} > 0$ and all eigenvalues of $F(\mathbf{x})$ are positive. This type of relation can also be denominated as the function F being affine in the unknowns.

An important fact is that the set $\mathcal{S} := \{\mathbf{x} : F(\mathbf{x}) > 0\}$ related with the linear matrix inequality $F(\mathbf{x}) > 0$ defines a convex constraint on \mathbf{x} . To prove this fact, note that if x_1 and $x_2 \in \mathcal{S}$ and $\alpha \in [0, 1]$, then

$$\begin{aligned} F(\alpha x_1 + (1 - \alpha)x_2) &= F_0 + \sum_{i=1}^k (\alpha x_{1i} + (1 - \alpha)x_{2i}) F_i \\ &= F_0 + \alpha \sum_{i=1}^k x_{1i} F_i + (1 - \alpha) \sum_{i=1}^k x_{2i} F_i = \alpha F(x_1) + (1 - \alpha) F(x_2), \end{aligned}$$

which allows one to conclude that $F(\alpha x_1 + (1-\alpha)x_2) > 0$ and, therefore, that $\alpha x_1 + (1-\alpha)x_2 \in \mathcal{S}$ also.

In the case where a system of LMIs $F_1(\mathbf{x}) > 0, \dots, F_m(\mathbf{x}) > 0$ in the same unknowns is considered, an important fact is that they can be written in a block diagonal LMI of the form

$$F(\mathbf{x}) := \begin{bmatrix} F_1(\mathbf{x}) & 0 & \cdots & 0 \\ 0 & F_2(\mathbf{x}) & \cdots & 0 \\ \vdots & \vdots & \ddots & \vdots \\ 0 & 0 & \cdots & F_m(\mathbf{x}) \end{bmatrix} > 0, \quad (2.4.1)$$

due to the fact that each LMI is symmetric. Moreover, as the eigenvalues of $F(\mathbf{x})$ are the union of the eigenvalues of all $F_i(\mathbf{x}), i = 1, \dots, m$, any \mathbf{x} that satisfies (2.4.1) also satisfies the system of LMIs.

Another important property of LMIs that allows some non-linear relations to be converted into linear inequalities are the so-called Schur complements, as presented in the following proposition.

Proposition 2.4.1 *Consider a symmetric matrix $M \in \mathbb{R}^{n \times n}$ affine in \mathbf{x} , with a partition*

$$M(\mathbf{x}) = \begin{bmatrix} Q(\mathbf{x}) & S(\mathbf{x}) \\ S^T(\mathbf{x}) & R(\mathbf{x}) \end{bmatrix},$$

where $Q(\mathbf{x}) = Q^T(\mathbf{x})$ and $R(\mathbf{x}) = R^T(\mathbf{x})$. The matrix $M(\mathbf{x}) > 0$ if and only if $R(\mathbf{x}) > 0$ and

$$Q(\mathbf{x}) - S(\mathbf{x})R^{-1}(\mathbf{x})S^T(\mathbf{x}) > 0. \quad (2.4.2)$$

Proof: This equivalence can be obtained by introducing two auxiliary matrices

$$U(\mathbf{x}) := \begin{bmatrix} I & S(\mathbf{x})R^{-1}(\mathbf{x}) \\ 0 & I \end{bmatrix} > 0, \quad V(\mathbf{x}) := \begin{bmatrix} I & -S(\mathbf{x})R^{-1}(\mathbf{x}) \\ 0 & I \end{bmatrix} > 0 \quad (2.4.3)$$

that verify $U(\mathbf{x})V(\mathbf{x}) = I$.

From the algebraic identity $M(\mathbf{x}) = U(\mathbf{x})V(\mathbf{x})M(\mathbf{x})V^T(\mathbf{x})U^T(\mathbf{x})$ it follows that

$$M(\mathbf{x}) = U(\mathbf{x}) \begin{bmatrix} Q(\mathbf{x}) - S(\mathbf{x})R^{-1}(\mathbf{x})S^T(\mathbf{x}) & 0 \\ 0 & R(\mathbf{x}) \end{bmatrix} U^T(\mathbf{x}) > 0. \quad (2.4.4)$$

With the argument that all matrices must be positive definite in the previous expression, the equivalence follows from the elements in the diagonal of the matrix detailed in (2.4.4). \blacksquare

In the following, a result used to eliminate variables and to simplify LMIs will be presented.

Lemma 2.4.2 [68] *Let A and B be arbitrary matrices and P be a symmetric matrix of proper dimensions. The LMI*

$$A^T X B + B^T X A + P < 0$$

in the unstructured variable X has a solution if and only if

$$(Ax = 0 \vee Bx = 0) \Rightarrow (x^T P x < 0 \vee x = 0).$$

where \vee stands for the logical disjunction. Moreover, let A_\perp and B_\perp denote the generic matrices whose columns form bases for the null spaces of A and B , respectively. The previous implication can therefore be written as

$$\begin{cases} A_\perp^T P A_\perp < 0 \\ B_\perp^T P B_\perp < 0 \end{cases}$$

The reasons for the recent surge of interest in LMIs are twofold: there are a plethora of problems in systems and control theory that can be cast in a general structure of this kind and convex optimization problems using convex constraints on \mathbf{x} in the form of $F(\mathbf{x}) > 0$ can be solved by resorting to computational methods. Moreover, efficient interior-point algorithms for convex optimization have been developed recently [54] and commercially available optimization packages [48] provide easy tools for setting up and solving the aforementioned problems.

The history on LMIs is not recent. It goes back to the contributions of Lyapunov near the end of the XIX century. During the 1940s, Lure, Postnikov, and others in the Soviet Union applied Lyapunov's methods to engineering problems [46]. The next breakthrough took place in the 1960s when Yakubovich, Popov, Kalman, and others introduced what we now call the positive-real lemma. Some LMIs were then solved using graphical methods. In the late 1960s, the relations of LMIs with passivity, with the small gain theorem (introduced by Zames and Sandberg), and with quadratic optimal control were evident. By 1971, the positive-real lemma could not only be solved graphically but also by solving a certain algebraic Riccati equation [77]. It was only in the 1980s that it was stated that many LMIs could be solved by computer via convex optimization methods [62]. The final step occurred in the late 1980s when interior-point algorithms were developed [54], allowing the solution of LMIs to be found using efficient computational methods. In [14] and in the references therein, a more in-depth history of LMIs can be found.

2.5 Norms of systems and linear matrix inequalities

This section addresses the computation of induced operator norms for finite-dimensional, continuous-time driven, linear, time-invariant systems \mathcal{F} described by a set of first order differential equations with realization

$$\Sigma_{\mathcal{F}} := \begin{cases} \dot{\mathbf{x}}(t) &= A\mathbf{x}(t) + B\mathbf{w}(t) \\ \mathbf{z}(t) &= C\mathbf{x}(t) + D\mathbf{w}(t) \end{cases} \quad (2.5.1)$$

where $\mathbf{x}(t) \in \mathbb{R}^n$ is the state vector, $\mathbf{w}(t) \in \mathbb{R}^m$ is the vector of inputs and disturbances and $\mathbf{z}(t) \in \mathbb{R}^p$ is the output vector. Norm computations will be done in terms of LMIs for stable systems, that is, for the case when

$$\operatorname{Re}(\lambda_i(A)) < 0, \quad i = 1, \dots, n.$$

The transfer function for this system can be written using the Laplace transform as

$$F(\mathbf{s}) = C(\mathbf{s}I - A)^{-1}B + D. \quad (2.5.2)$$

2.5.1 \mathcal{H}_∞ norm

Suppose that the input \mathbf{w} to system (2.5.1) is taken from the set \mathcal{L}_2 of Lebesgue measurable, real valued, square integrable functions of time with finite Euclidean norm

$$\|\mathbf{w}\|_2 = \left(\int_0^{+\infty} \mathbf{w}^T(t)\mathbf{w}(t)dt \right)^{1/2} < +\infty.$$

Due to the linearity and asymptotic stability of the system the output \mathbf{z} is also a signal from the set \mathcal{L}_2 . One of the classical performance criteria for system (2.5.1) is its maximum gain amplification

$$\sup_{\mathbf{w} \in \mathcal{L}_2} \frac{\|\mathbf{z}\|_2}{\|\mathbf{w}\|_2},$$

also denoted as the \mathcal{L}_2 induced norm of $\Sigma_{\mathcal{F}}$.

The *Hardy space* \mathcal{H}_∞ consists of all complex valued functions $F : \mathbb{C}^+ \rightarrow \mathbb{C}^{p \times m}$ which are analytic, with \mathcal{H}_∞ norm defined as

$$\|F\|_\infty := \sup_{\mathbf{s} \in \mathbb{C}^+} \sigma_{\max}(F(\mathbf{s})) < \infty,$$

where \mathbb{C}^+ is the open right half complex plane, $\sigma(F(\mathbf{s})) = \lambda(F^*(\mathbf{s})F(\mathbf{s}))$ is the spectrum of $F(\mathbf{s})$, i.e., the set of all singular values, and $\sigma_{max}(F(\mathbf{s}))$ denotes the largest one. It can be shown that there exists an extension for each of these functions to the imaginary axis with the \mathcal{H}_∞ norm given by

$$\|F\|_\infty := \sup_{\omega \in \mathbb{R}} \sigma_{max}(F(j\omega)).$$

The proposition below plays a key role in the development that follows.

Proposition 2.5.1 [68] *Let the system $\mathcal{F} : \mathbf{w} \rightarrow \mathbf{z}$ described by (2.5.1) be asymptotically stable and let $\gamma > 0$ be a real number. The following statements are equivalent:*

1. $\|F\|_\infty < \gamma$;

2. *The gain of the system verifies*

$$\sup_{\mathbf{w} \in \mathcal{L}_2} \frac{\|\mathbf{z}\|_2}{\|\mathbf{w}\|_2} < \gamma,$$

with null initial conditions, $\mathbf{x}(t_0) = \mathbf{x}_0 = 0$;

3. *The system is strictly dissipative with respect to the supply function*

$$s(\mathbf{w}, \mathbf{z}) = \gamma^2 \|\mathbf{w}\|_2^2 - \|\mathbf{z}\|_2^2;$$

4. *There exists a symmetric matrix $P = P^T \in \mathbb{R}^{n \times n}$ that enables the LMI*

$$\begin{bmatrix} A^T P + P A + C^T C & P B + C^T D \\ B^T P + D^T C & D^T D - \gamma^2 I_m \end{bmatrix} < 0. \quad (2.5.3)$$

The equivalence of the two first items comes from the well known fact that for a stable system the \mathcal{H}_∞ and the induced \mathcal{L}_2 norm are equal (see e.g. [68] for a detailed explanation).

The third item can be obtained using theorem 2.2.3 with

$$Q = \begin{bmatrix} -I_p & 0 \\ 0 & \gamma^2 I_m \end{bmatrix}.$$

Using Schur complements, the LMI (2.5.3) can be presented in an alternative form as

$$\begin{bmatrix} A^T P + P A & P B \\ B^T P & -\gamma^2 I_m \end{bmatrix} + \begin{bmatrix} C^T \\ D^T \end{bmatrix} \begin{bmatrix} C & D \end{bmatrix} = \begin{bmatrix} A^T P + P A & P B & C^T \\ B^T P & -\gamma^2 I_m & D^T \\ C & D & -I_p \end{bmatrix} < 0.$$

Once again the feasibility of an LMI can provide numerical solutions for the computation of a commonly used performance index in system theory.

2.5.2 \mathcal{H}_2 norm

The \mathcal{H}_2 norm of a system $\Sigma_{\mathcal{F}}$, denoted $\|F\|_2$ is relevant in a stochastic setting. For the linear, time-invariant system described by (2.5.1), consider the input \mathbf{w} as white-noise with zero mean $E[\mathbf{w}] = 0$ and unitary variance $E[\mathbf{w}\mathbf{w}^T] = I$. Define the covariance of the state as

$$W(t) = E[\mathbf{x}(t)\mathbf{x}^T(t)] = \int_{-\infty}^t e^{A\tau} B B^T e^{A^T \tau} d\tau. \quad (2.5.4)$$

Using the Leibnitz's rule it can be easily shown that the time derivative of the covariance verifies the matrix differential equation

$$\dot{W}(t) = AW(t) + W(t)A^T + BB^T.$$

Assuming that the system is asymptotically stable and controllable, in steady state this equation becomes the algebraic relation $AW + WA^T + BB^T = 0$, where $W = \lim_{t \rightarrow +\infty} W(t)$. The solution can be written as

$$W_{ctr} = \int_0^{+\infty} e^{At} B B^T e^{A^T t} dt,$$

and is denominated as the *controllability Grammian*. The output variance is equal to the square of $\|F\|_2$ and can be written, assuming $D = 0$, as

$$\|F\|_2^2 = E[\mathbf{z}\mathbf{z}^T] = E[C\mathbf{x}\mathbf{x}^T C^T] = \mathbf{tr}(C W_{ctr} C^T). \quad (2.5.5)$$

Notice that if the matrix D is non-zero, then the \mathcal{H}_2 norm is infinite.

A similar result can be obtained considering the *observability Grammian*

$$W_{obs} = \int_0^{+\infty} e^{A^T t} C^T C e^{At} dt,$$

which is the solution to the algebraic matrix equation $A^T V + V A + C^T C = 0$. As the trace of the product of matrices is commutative, the output variance can also be computed as

$$\|F\|_2^2 = \mathbf{tr}(B^T W_{obs} B).$$

The duality of these two alternative results has been known long ago in systems theory.

Another possible way of interpreting the \mathcal{H}_2 norm of a system is by viewing it as a member of the Hardy space \mathcal{H}_2 . This space consists of all complex valued functions which are analytic in \mathbb{C}^+ , with an extension to the imaginary axis, with finite norm computed as

$$\|F\|_2^2 = \frac{1}{2\pi} \mathbf{tr} \int_{-\infty}^{+\infty} F(j\omega) F^*(j\omega) d\omega < \infty,$$

where $\omega \in \mathbb{R}$. Injecting as inputs the Dirac functions $\mathbf{w}_i(t) = \delta(t), i = 1, \dots, m$, in the causal system (2.5.1) with null initial state $\mathbf{x}(0) = 0$, the output is $\mathbf{z}(t) = Ce^{At}B\mathbf{w}(t), t > 0$. Using Parseval's theorem, the \mathcal{H}_2 norm of the aforementioned system can also be written as

$$\|F\|_2^2 = \mathbf{tr} \int_0^{+\infty} Ce^{At}BB^T e^{A^T t}C^T dt = \mathbf{tr}(CW_{ctr}C^T),$$

where the controllability Grammian definition was used. Note that the same relation as stated in (2.5.5) was recovered.

The next proposition characterizes the \mathcal{H}_2 norm in terms of LMIs, as well as the relations between these two possible interpretations for the norm.

Proposition 2.5.2 [68] *Let the system $\mathcal{F} : \mathbf{w} \rightarrow \mathbf{z}$ described by (2.5.1) be asymptotically stable with the transfer function (2.5.2). Then $\|F\|_2 < +\infty$ if and only if $D = 0$. Furthermore, the following statements are equivalent:*

1. $\|F\|_2 < \gamma$, for $\gamma > 0$;
2. There exists a positive definite, symmetric matrix $P \in \mathbb{R}^{n \times n}$ and an auxiliary variable $X \in \mathbb{R}^{p \times p}$ such that

$$\begin{bmatrix} A^T P + PA & PB \\ B^T P & -I_m \end{bmatrix} < 0, \quad \begin{bmatrix} X & C \\ C^T & P \end{bmatrix} > 0, \quad \mathbf{tr}(X) < \gamma^2; \quad (2.5.6)$$

3. There exists a positive definite, symmetric matrix $P \in \mathbb{R}^{n \times n}$ and an auxiliary variable $X \in \mathbb{R}^{m \times m}$ such that

$$\begin{bmatrix} AP + PA^T & PC^T \\ CP & -I_p \end{bmatrix} < 0, \quad \begin{bmatrix} X & B^T \\ B & P \end{bmatrix} > 0, \quad \mathbf{tr}(X) < \gamma^2. \quad (2.5.7)$$

In light of the above, the controllability Grammian is the unique positive definite solution of the Lyapunov equation $AW + WA^T + BB^T = 0$, which is equivalent to saying that there exists a symmetric matrix $Z > 0$ such that

$$AZ + ZA^T + BB^T < 0.$$

Introducing the variable $P = Z^{-1}$ and pre and post-multiplying this relation by P results in

$$PA + A^T P + PBB^T P < 0.$$

Using Schur complements the first LMI in (2.5.6) is obtained. Note that the \mathcal{H}_2 norm is obtained according to the relation (2.5.5). Using the auxiliary or *slack* variable $X > 0$, this relation can be expressed alternatively as $X > CP^{-1}C^T$ and $\mathbf{tr}(X) < \gamma^2$, which are the remaining LMIs in (2.5.6). By using the observability Grammian definition a similar circle of ideas leads to the set of LMIs in (2.5.7).

In both cases, the minimization of $\mathbf{tr}(X)$ can be viewed as the minimization of the norm of the corresponding system \mathcal{F} and will be used in the synthesis of estimators and trackers throughout this thesis.

2.5.3 Generalized \mathcal{H}_2 norm

Often, it is of interest to find out how an input signal of bounded energy to the stable system (2.5.1) impact on the peak of the corresponding signal at the output. To this effect, define \mathcal{L}_∞ as the space of Lebesgue measurable real valued functions of time, endowed with the norm

$$\|F\|_{2,\infty} = \sup_{\mathbf{w} \in \mathcal{L}_2} \frac{\|\mathbf{z}\|_\infty}{\|\mathbf{w}\|_2} \quad (2.5.8)$$

and satisfies

$$\|F\|_{2,\infty} = \frac{1}{2\pi} \lambda_{\max} \left(\int_{-\infty}^{+\infty} F(j\omega)F^*(j\omega)d\omega \right) < \infty,$$

where $\lambda_{\max}(\cdot)$ denotes the maximum eigenvalue of a matrix. When $\mathbf{z}(t)$ is a scalar quantity, this relation degenerates into the previously introduced \mathcal{H}_2 norm, which is the reason why the definition now introduced is usually called the generalized \mathcal{H}_2 norm. The proposition that follows characterizes the computation of the aforementioned norm in terms of LMIs.

Proposition 2.5.3 [68] *Let the system $\mathcal{F} : \mathbf{w} \rightarrow \mathbf{z}$ described by (2.5.1) be asymptotically stable with the transfer function (2.5.2). Assuming $D = 0$, $\|F\|_{2,\infty} < \gamma$, for $\gamma > 0$, if and only if there exists a symmetric positive definite matrix $P \in \mathbb{R}^{n \times n}$ for the LMIs*

$$\begin{bmatrix} A^T P + PA & PB \\ B^T P & -I_m \end{bmatrix} < 0, \quad \begin{bmatrix} P & C^T \\ C & \gamma^2 I_p \end{bmatrix} > 0. \quad (2.5.9)$$

The first LMI in (2.5.9) can be inferred from the application of the dissipativity theorem (2.2.3) relative to the supply function $s(\mathbf{x}, \mathbf{w}) = \mathbf{w}^T \mathbf{w}$. Therefore,

$$V(\mathbf{x}(t)) = \mathbf{x}^T(t)P\mathbf{x}(t) \leq \int_0^t \mathbf{w}^T(\tau)\mathbf{w}(\tau)d\tau. \quad (2.5.10)$$

Given $\epsilon > 0$ such that $C^T C < (\gamma^2 - \epsilon^2)P$, using Schur complements, the the second LMI in (2.5.9) is obtained. This expression allows one to write

$$\langle \mathbf{z}(t), \mathbf{z}(t) \rangle = \mathbf{x}^T(t) C^T C \mathbf{x}(t) \leq (\gamma^2 - \epsilon^2) \mathbf{x}^T(t) P \mathbf{x}(t)$$

where $\langle \cdot, \cdot \rangle$ represents the internal product between signals. Using these relations, it results that

$$\langle \mathbf{z}(t), \mathbf{z}(t) \rangle \leq (\gamma^2 - \epsilon^2) \|\mathbf{w}\|_2^2.$$

Dividing this later expression by $\|\mathbf{w}\|_2^2$ and taking the supremum over all $\mathbf{w} \in \mathcal{L}_2$, the relation (2.5.8) is recovered.

2.6 Stability regions

Frequency domain analysis for finite-dimensional, linear, time-invariant systems provides insight into systems characteristics such as stability, norm interpretation, and spectral factorization, to name but a few. In the case of estimator synthesis using LMIs, the specification of constraints for regional placement of the closed loop eigenvalues of the resulting systems may be required to avoid solutions with dynamics that are too fast, with poorly damped modes, or with high frequency gain.

Let \mathbf{s} be the complex valued indeterminate in the Laplace transforms of the systems under study. In this case the corresponding characteristic equations are polynomials in \mathbf{s} , with real coefficients. Let $\lambda_i, i = 1, \dots, n$ be the roots of such equations verifying $\lambda_i \in \mathbb{C}_{st} \Rightarrow \bar{\lambda}_i \in \mathbb{C}_{st}$, where \mathbb{C}_{st} is the stability region to be specified and the over-line stands for the complex conjugate operation. Assume the required stability region is a convex region of \mathbb{C} .

Some typical regions and the corresponding LMIs are summarized in table (2.6.1). In [21] it was proven that the standard Lyapunov stability can be generalized to the case of LMI regions of stability \mathbb{C}_{st} using a technique summarized in the next theorem.

Theorem 2.6.1 [21] *The closed loop dynamics matrix A has all its eigenvalues in the generalized LMI region*

$$\mathbb{C}_{st} = \{s \in \mathbb{C} : p_{ij} + q_{ij}s + q_{ji}\bar{s} < 0, i, j = 1 \dots n\} \quad (2.6.1)$$

if and only if a symmetric, positive definite matrix X exists such that

$$P + QAX + Q^T A^T X < 0,$$

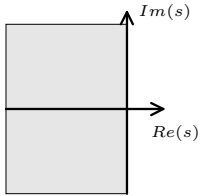
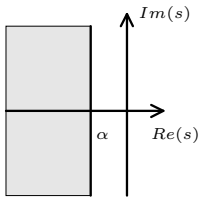
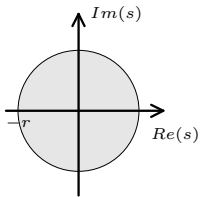
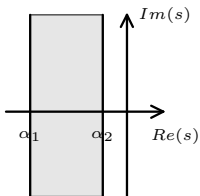
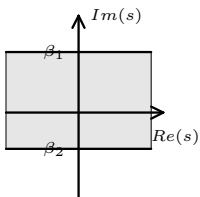
Description	Math relation	C_{st}	Inequality (< 0)
Open left half complex plane	$Re(s) < 0$		$s + \bar{s}$
Guaranteed damping	$Re(s) < \alpha$		$s + \bar{s} - 2\alpha$
Maximal damping	$ s < r$		$\begin{bmatrix} -r & s \\ \bar{s} & -r \end{bmatrix}$
Vertical strip	$\alpha_1 < Re(s) < \alpha_2$		$\begin{bmatrix} s + \bar{s} - 2\alpha_2 & 0 \\ 0 & -s - \bar{s} + 2\alpha_1 \end{bmatrix}$
Horizontal strip	$\beta_1 < Im(s) < \beta_2$		$\begin{bmatrix} s - \bar{s} - 2\beta_1 & 0 \\ 0 & -s + \bar{s} + 2\beta_2 \end{bmatrix}$

Table 2.6.1: Generalized stability regions as LMIs.

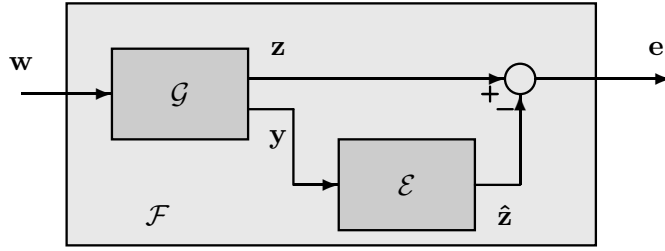


Figure 2.7.1: General setup for filtering synthesis.

where p_{ij} and q_{ij} are the entries of line i and column j in the P and Q matrices, respectively. Moreover, the characteristic equation of the closed loop system is given by $P + Qs + Q^T\bar{s}$.

Circular sectors, ellipses, and conic sectors, as well as the regions presented in the previous table, can all be written as in (2.6.1). The required stability region can be obtained from the intersection of a set of convex regions, resulting in a convex region.

2.7 Estimator synthesis

In the course of this thesis some estimation problems will be formulated. The corresponding analysis and synthesis methodologies will be presented, along with some relevant properties for the proposed structures. Performance, stability, and robustness requirements will be described in terms of constraints on norms to be minimized, by resorting to auxiliary inputs and outputs to be defined. The problem of estimator design based on LMIs is therefore of utmost importance in the present thesis.

The general setup for estimation design is presented in figure 2.7.1, where the nominal system \mathcal{G} is a linear, time-invariant system described by the realization

$$\Sigma_{\mathcal{G}} = \begin{cases} \dot{\mathbf{x}}(t) = A \mathbf{x}(t) + B_w \mathbf{w}(t) \\ \mathbf{z}(t) = C_z \mathbf{x}(t) + D_{zw} \mathbf{w}(t) \\ \mathbf{y}(t) = C_y \mathbf{x}(t) + D_{yw} \mathbf{w}(t), \end{cases} \quad (2.7.1)$$

where $\mathbf{x}(t) \in \mathbb{R}^n$ is the state vector, $\mathbf{w}(t) \in \mathbb{R}^m$ is the vector of external inputs, $\mathbf{z}(t) \in \mathbb{R}^p$ is the vector of outputs from the system, $\mathbf{y}(t) \in \mathbb{R}^q$ represents the measurement vector, and the

matrices used have the compatible dimensions. Assuming stationary conditions, the estimator under design \mathcal{E} is also a linear, time-invariant dynamical system [2] with realization

$$\Sigma_{\mathcal{E}} = \begin{cases} \dot{\hat{\mathbf{x}}}(t) &= A_f \hat{\mathbf{x}}(t) + B_f \mathbf{y}(t) \\ \hat{\mathbf{z}}(t) &= C_f \hat{\mathbf{x}}(t) + D_f \mathbf{y}(t), \end{cases} \quad (2.7.2)$$

where $\hat{\mathbf{x}}(t) \in \mathbb{R}^{n_f}$ is the estimated state vector and $\hat{\mathbf{z}}(t) \in \mathbb{R}^p$ are the output estimates. Note that no constraints on the dimension of the estimator state-space $\hat{\mathbf{x}}$ are imposed.

Interconnecting these two dynamical systems, as depicted in figure 2.7.1, yields a system \mathcal{F} with input \mathbf{w} and with the estimation error $\mathbf{e} = \mathbf{z} - \hat{\mathbf{z}}$ as output, described by

$$\Sigma_{\mathcal{F}} = \begin{cases} \begin{bmatrix} \dot{\hat{\mathbf{x}}}(t) \\ \dot{\hat{\mathbf{x}}}(t) \end{bmatrix} &= \begin{bmatrix} A & 0 \\ B_f C_y & A_f \end{bmatrix} \begin{bmatrix} \mathbf{x}(t) \\ \hat{\mathbf{x}}(t) \end{bmatrix} + \begin{bmatrix} B_w \\ B_f D_{yw} \end{bmatrix} \mathbf{w}(t) \\ \mathbf{e}(t) &= \begin{bmatrix} C_z - D_f C_y & -C_f \end{bmatrix} \begin{bmatrix} \mathbf{x}(t) \\ \hat{\mathbf{x}}(t) \end{bmatrix} + [D_{zw} - D_f D_{yw}] \mathbf{w}(t), \end{cases} \quad (2.7.3)$$

or, in compact form,

$$\Sigma_{\mathcal{F}} = \begin{cases} \dot{\tilde{\mathbf{x}}}(t) &= \tilde{A} \tilde{\mathbf{x}}(t) + \tilde{B} \mathbf{w}(t) \\ \mathbf{e}(t) &= \tilde{C} \tilde{\mathbf{x}}(t) + \tilde{D} \mathbf{w}(t). \end{cases}$$

The design of observers, where the variable to be estimated is the state variable $\mathbf{x}(t)$, goes back to the work of Luenberger [45]. The optimal estimator with minimum output error variance was first derived by Kalman in the late 1950s, by resorting to the solution of a Riccati equation. This work motivated what is now considered the modern theory of estimation and control. See [74] for details, where a selection of the original papers on the subject are available on this subject.

As convincingly argued in [2], for nominal systems that are linear, the optimum estimator, in the sense of providing the state estimate with minimum variance, is a finite-dimensional, linear, time-invariant, dynamical system with the particular structure given by

$$\Sigma_{\mathcal{E}_k} = \begin{cases} \dot{\hat{\mathbf{x}}}(t) &= A \hat{\mathbf{x}}(t) + K(\mathbf{y}(t) - C_y \hat{\mathbf{x}}(t)) \\ \hat{\mathbf{z}}(t) &= C_z \hat{\mathbf{x}}(t), \end{cases} \quad (2.7.4)$$

where $K \in R^{n \times q}$ is a constant observer gain to be determined and $\hat{\mathbf{x}}(t)$ and $\hat{\mathbf{z}}(t)$ have the same dimensions of $\mathbf{x}(t)$ and $\mathbf{z}(t)$, respectively. Moreover, note that the proposed structure is a particular case of the general setup described by the realization in (2.7.2). The solution for

this simpler, however, generic case will be presented next and will clarify the general solution presented later in this section.

Let the state estimation error be defined as $\tilde{\mathbf{x}} = \mathbf{x} - \hat{\mathbf{x}}$. Using the relations in (2.7.1) and (2.7.4) yields a system \mathcal{F}_k with dynamics

$$\Sigma_{\mathcal{F}_k} = \begin{cases} \dot{\tilde{\mathbf{x}}}(t) &= (A - KC_y) \tilde{\mathbf{x}}(t) + (B_w - KD_{yw}) \mathbf{w}(t) \\ \mathbf{e}(t) &= C_z \tilde{\mathbf{x}}(t) + D_{zw} \mathbf{w}(t). \end{cases} \quad (2.7.5)$$

Applying to this system the results introduced in section 2.5, the norms computation can be performed through the use of matrix inequalities. However, it can be easily foreseen that the matrix inequalities are not linear in the unknown parameters, which precludes the use of convex optimization tools to solve the problem at hand. The next two propositions present the solutions for the \mathcal{H}_2 and \mathcal{H}_∞ norms, respectively, after introducing a non-linear transformation in the unknowns.

Proposition 2.7.1 *Consider a system $\mathcal{F}_k : \mathbf{w} \rightarrow \mathbf{z}$, composed of a nominal system $\mathcal{G} : \mathbf{w} \rightarrow [\mathbf{z}^T \mathbf{y}^T]^T$ and an estimator $\mathcal{E}_k : \mathbf{y} \rightarrow \hat{\mathbf{z}}$ interconnected as described in figure 2.7.1, with realization (2.7.5). Suppose $D_{zw} = 0$ and that $\Sigma_{\mathcal{F}_k}$ is asymptotically stable. The \mathcal{H}_2 norm of the system obtained, from the input \mathbf{w} to the output estimation error \mathbf{e} is such that, for $\gamma > 0$, the following statements are equivalent:*

1. $\|F_k\|_2 < \gamma$;
2. *There exists a symmetric, positive definite matrix $P \in \mathbb{R}^{n \times n}$, an auxiliary variable $X \in \mathbb{R}^{p \times p}$, and an auxiliary variable $Y \in \mathbb{R}^{n \times q}$ verifying $Y = PK$, such that*

$$\begin{aligned} & \begin{bmatrix} A^T P + PA - C_y^T Y^T - Y C_y & PB_w - Y D_{yw} \\ B_w^T P - D_{yw}^T Y^T & -I_m \end{bmatrix} < 0, \\ & \begin{bmatrix} X & C_z \\ C_z^T & P \end{bmatrix} > 0, \\ & \text{tr}(X) < \gamma^2; \end{aligned} \quad (2.7.6)$$

3. *There exists a symmetric, positive definite matrix $P \in \mathbb{R}^{n \times n}$, an auxiliary variable $X \in \mathbb{R}^{m \times m}$, and an auxiliary variable $Y \in \mathbb{R}^{n \times q}$ verifying $Y = PK$, such that*

$$\begin{bmatrix} PA + A^T P - Y C_y - C_y^T Y^T & C_z^T \\ C_z & -I_p \end{bmatrix} < 0,$$

$$\begin{bmatrix} X & B_w^T P - D_{yw} Y^T \\ P B_w - Y D_{yw} & P \end{bmatrix} > 0, \quad \text{tr}(X) < \gamma^2. \quad (2.7.7)$$

Proof: Applying the definition of the \mathcal{H}_2 norm presented in proposition 2.5.2 to the system described by (2.7.5), the first LMI from the set (2.5.6) results in the matrix inequality

$$\begin{bmatrix} A^T P + P A - C_y^T K^T P - P K C_y & P B_w - P K D_{yw} \\ B_w^T P - D_{yw}^T K^T P & -I_m \end{bmatrix} < 0,$$

which is not an LMI, as there are products of unknowns, namely P and K . Introducing the auxiliary variable $Y = PK$ results in the first LMI of (2.7.6). This can be understood as the use of a non-linear transformation that allows the bilinear matrix inequality to become an LMI. The remaining LMIs in (2.7.6) are those introduced in proposition 2.5.6, so the need for them is obvious. The sufficient condition for this case closely follows the sufficiency proof on proposition 2.5.2.

The same circle of ideas can be used to derive the corresponding LMIs in (2.7.7), after pre and post-multiplying the first two LMIs in (2.5.7) by

$$\begin{bmatrix} P^{-1} & 0 \\ 0 & I_p \end{bmatrix} \quad \text{and} \quad \begin{bmatrix} I_m & 0 \\ 0 & P^{-1} \end{bmatrix},$$

respectively. ■

Proposition 2.7.2 *Consider a system $\mathcal{F}_k : \mathbf{w} \rightarrow \mathbf{z}$, composed of a nominal system $\mathcal{G} : \mathbf{w} \rightarrow [\mathbf{z}^T \mathbf{y}^T]^T$ and an estimator $\mathcal{E}_k : \mathbf{y} \rightarrow \hat{\mathbf{z}}$ interconnected as described in figure 2.7.1, with realization (2.7.5). Suppose that $\Sigma_{\mathcal{F}_k}$ is asymptotically stable and assume that there exists $\gamma > 0$. The \mathcal{H}_∞ norm from the input \mathbf{w} to the output estimation error \mathbf{e} verifies $\|\mathcal{F}_k\|_\infty < \gamma$ if and only if there exists a symmetric, positive definite matrix $P \in \mathbb{R}^{n \times n}$ and an auxiliary variable $Y \in \mathbb{R}^{n \times q}$ verifying $Y = PK$, such that*

$$\begin{bmatrix} A^T P + P A - C_y^T Y^T - Y C_y & P B_w - Y D_{yw} & C_z^T \\ B_w^T P - D_{yw}^T Y^T & -\gamma^2 I_m & D_{zw}^T \\ C_z & D_{zw} & -I_p \end{bmatrix} < 0. \quad (2.7.8)$$

The proof of this proposition is omitted as it follows the application of the same non-linear transformation to the results presented in proposition 2.5.1, for the system described by (2.7.5).

In estimation and control theory the problems of designing stable estimators with the structure described in (2.7.4) and constant feedback stabilizable controllers for linear systems, or $\mathbf{u}(t) = L\mathbf{x}(t)$ in (2.2.4), are dual. The parametrization of all stabilizable controllers as a convex optimization problem is known for more than a decade [9]. However, the solution for the set of all stabilizable estimators as a convex optimization problem has only recently been brought to light [28]. The procedure to solve this problem for the \mathcal{H}_2 norm computation will be presented next following the steps outlined in [56].

Consider the matrix \tilde{K}_f that results from packing the unknown parameters in the generic realization of the system (2.7.2), that is,

$$\tilde{K}_f = \begin{bmatrix} A_f & B_f \\ C_f & D_f \end{bmatrix},$$

and define the auxiliary matrices

$$\tilde{X} = \begin{bmatrix} Z^{-T} & U^T \\ U & \hat{X} \end{bmatrix}, \quad \tilde{X}^{-1} = \begin{bmatrix} Y^T & V^T \\ V^T & \hat{Y}^T \end{bmatrix} \quad \text{and} \quad \tilde{T} = \begin{bmatrix} Z^T & Y^T \\ 0 & V^T \end{bmatrix}, \quad (2.7.9)$$

such that the product

$$\tilde{X}\tilde{T} = \begin{bmatrix} I & I \\ UZ^T & 0 \end{bmatrix}.$$

The next lemma presents some algebraic results that will be required later on.

Lemma 2.7.3 *Consider the auxiliary matrices introduced in (2.7.9). The variable transformations*

$$\begin{bmatrix} Q & F \\ L & R \end{bmatrix} = \begin{bmatrix} V & 0 \\ 0 & I \end{bmatrix} \tilde{K}_f \begin{bmatrix} UZ^T & 0 \\ 0 & I \end{bmatrix} \quad \text{and} \quad S = VUZ^T \quad (2.7.10)$$

linearize the matrices

$$\begin{aligned} \tilde{T}^T \tilde{A} \tilde{X} \tilde{T} &= \begin{bmatrix} ZA & ZA \\ YA + FC_y + Q & YA + FC_y \end{bmatrix}, & \tilde{T}^T \tilde{B} &= \begin{bmatrix} ZB_w \\ YB_w + FD_{yw} \end{bmatrix}, \\ \tilde{C} \tilde{X} \tilde{T} &= \begin{bmatrix} C_z - RC_y - L & C_z - RC_y \end{bmatrix} \quad \text{and}, & \tilde{T}^T \tilde{X} \tilde{T} &= \begin{bmatrix} Z & Z \\ Y + S & Y \end{bmatrix} \end{aligned}$$

in the unknown variables $Q \in \mathbb{R}^{n \times n}$, $F \in \mathbb{R}^{n \times q}$, $L \in \mathbb{R}^{p \times n}$, $R \in \mathbb{R}^{p \times q}$, $U = U^T \in \mathbb{R}^{n \times n}$, $V = V^T \in \mathbb{R}^{n \times n}$, $Z = Z^T \in \mathbb{R}^{n \times n}$, $Y = Y^T \in \mathbb{R}^{n \times n}$, and $S = S^T \in \mathbb{R}^{n \times n}$.

We are now in position to present the result on the \mathcal{H}_2 norm minimization based on LMIs for an estimator with general structure.

Theorem 2.7.4 *Consider an asymptotically stable system $\mathcal{F} : \mathbf{w} \rightarrow \mathbf{z}$, composed of a nominal system $\mathcal{G} : \mathbf{w} \rightarrow [\mathbf{z}^T \mathbf{y}^T]^T$ and an estimator $\mathcal{E} : \mathbf{y} \rightarrow \hat{\mathbf{z}}$ interconnected as described in figure 2.7.1, with realization (2.7.3). The \mathcal{H}_2 norm of the resulting system, from the input \mathbf{w} to the output estimation error \mathbf{e} , is such that, for $\gamma > 0$, the following statements are equivalent:*

1. $\|F\|_2 < \gamma$;
2. *There exist matrices $Z = Z^T \in \mathbb{R}^{n \times n}$, $Y = Y^T \in \mathbb{R}^{n \times n}$, $Q \in \mathbb{R}^{n \times n}$, $F \in \mathbb{R}^{n \times q}$, $L \in \mathbb{R}^{p \times n}$, and $R \in \mathbb{R}^{p \times q}$ such that*

$$\begin{bmatrix} A^T Z + Z A & Z A + A^T Y + C_y^T F^T + Q^T & Z B_w \\ A^T Z + Y A + F C_y + Q & A^T Y + C_y^T F^T + Y A + F C_y & Y B_w + F D_{yw} \\ B_w^T Z & B_w^T Y + D_{yw}^T F^T & -I_m \end{bmatrix} < 0, \quad (2.7.11)$$

and there exists a symmetric matrix $W \in \mathbb{R}^{p \times p}$ that verifies

$$\begin{bmatrix} W & C_z - R C_y - L & C_z - R C_y \\ C_z^T - C_y^T R^T - L^T & Z & Z \\ C_z^T - C_y^T R^T & Z & Y \end{bmatrix} > 0, \quad (2.7.12)$$

$$D_{zw} - R D_{yw} = 0 \quad (2.7.13)$$

$$\mathbf{tr}(W) < \gamma^2; \quad (2.7.14)$$

3. *There exist matrices $Z = Z^T \in \mathbb{R}^{n \times n}$, $Y = Y^T \in \mathbb{R}^{n \times n}$, $Q \in \mathbb{R}^{n \times n}$, $F \in \mathbb{R}^{n \times q}$, $L \in \mathbb{R}^{p \times n}$, and $R \in \mathbb{R}^{p \times q}$ such that*

$$\begin{bmatrix} A^T Z + Z A & Z A + A^T Y + C_y^T F^T + Q^T & C_z^T - C_y^T R^T - L^T \\ A^T Z + Y A + F C_y + Q & A^T Y + C_y^T F^T + Y A + F C_y & C_z^T - C_y^T R^T \\ C_z - R C_y - L & C_z - R C_y & -I_p \end{bmatrix} < 0, \quad (2.7.15)$$

and there exists a symmetric matrix $W \in \mathbb{R}^{m \times m}$ such that

$$\begin{bmatrix} W & B_w^T Z & B_w^T Y + D_{yw}^T F^T \\ Z B_w & Z & Z \\ Y B_w + F D_{yw} & Z & Y \end{bmatrix} > 0, \quad (2.7.16)$$

$$D_{zw} - R D_{yw} = 0 \quad (2.7.17)$$

$$\mathbf{tr}(W) < \gamma^2. \quad (2.7.18)$$

Proof: The definition of \mathcal{H}_2 norm, presented in proposition 2.5.2, will be used to compute the norm of the system that results from the interconnection of the estimator and the nominal system, described in compact form by (2.7.3). To prove the necessity of item *ii*), the matrix inequality resulting from the first LMI in the set (2.5.6) is pre and post-multiplied by adequate matrices to obtain

$$\begin{bmatrix} \tilde{T}^T \tilde{P}^{-1} & 0 \\ 0 & I_m \end{bmatrix} \begin{bmatrix} \tilde{A}^T \tilde{P} + \tilde{P} \tilde{A} & \tilde{P} \tilde{B} \\ \tilde{B}^T \tilde{P} & -I_m \end{bmatrix} \begin{bmatrix} \tilde{P}^{-1} \tilde{T} & 0 \\ 0 & I_m \end{bmatrix} < 0$$

and thus

$$\begin{bmatrix} \tilde{T}^T \tilde{P}^{-1} \tilde{A}^T \tilde{T} + \tilde{T}^T \tilde{A} \tilde{P}^{-1} \tilde{T} & \tilde{T}^T \tilde{B} \\ \tilde{B}^T \tilde{T} & -I_m \end{bmatrix} < 0.$$

Using the results presented in lemma 2.7.3 and considering $X = \tilde{P}^{-1}$, the LMI in (2.7.11) is obtained. The relation (2.7.12) can be obtained from the second LMI in the set (2.5.6), using lemma 2.7.3 and the auxiliary relation $Y + S = Z$,

$$\begin{bmatrix} I_p & 0 \\ 0 & \tilde{T}^T \tilde{P}^{-1} \end{bmatrix} \begin{bmatrix} W & \tilde{C} \\ \tilde{C}^T & \tilde{P} \end{bmatrix} \begin{bmatrix} I_p & 0 \\ 0 & \tilde{P}^{-1} \tilde{T} \end{bmatrix} = \begin{bmatrix} W & \tilde{C} \tilde{P}^{-1} \tilde{T} \\ \tilde{T}^T \tilde{P} \tilde{C}^T & \tilde{T}^T \tilde{P}^{-1} \tilde{T} \end{bmatrix} > 0.$$

The constraint (2.7.13) is necessary for the existence of the \mathcal{H}_2 norm. Finally, the relation (2.7.14) is the third LMI in the set (2.5.6).

To prove sufficiency, the construction of an estimator with the required \mathcal{H}_2 norm from feasible variables that constitute the solution to the LMIs (2.7.11), (2.7.12), and (2.7.14) (with the constraint (2.7.13)) is required. In this case the realization matrices for the estimator can be obtained from the relation (2.7.10) as

$$\tilde{K}_f = \begin{bmatrix} V^{-1} & 0 \\ 0 & I \end{bmatrix} \begin{bmatrix} Q & F \\ L & R \end{bmatrix} \begin{bmatrix} Z^{-T} U^{-1} & 0 \\ 0 & I \end{bmatrix}, \quad (2.7.19)$$

where the non-singularity of U and V are required.

The Schur complement of LMI (2.7.12) implies $Y > 0$ and $Z(Y - Z) > 0$. Rewriting the auxiliary relation $Y + S = Y + VUZ^T = Z$ as

$$VU = (Y - Z)Z^{-T},$$

the right side of the relation is positive definite and, therefore, non-singularity of U and V are guaranteed. Moreover, the non-singularity of the transformation \tilde{T} is also guaranteed. Since the equivalence between the first and third items follows exactly the same line of arguments as the proof just outlined, it will be omitted here. ■

The following corollary to this result can be useful in interpreting the results obtained.

Corollary 2.7.5 *The full rank estimator obtained by minimizing the \mathcal{H}_2 norm as presented in theorem 2.7.4 is the optimal linear estimator from the class of all linear estimators.*

This corollary paves the way for a broader view of the result obtained. For nominal linear systems, the generic estimator given by (2.7.2) has the optimal structure among all causal estimators, including the class of non-linear filters [2]. An interesting consequence of this fact is that the optimum estimator under stationary conditions can be obtained from the solution of an algebraic Riccati equation, and it is on the boundary of the convex space of solutions given by theorem 2.7.4 (see [56] for details).

A result for the \mathcal{H}_∞ norm minimization, based on the non-linear transformation presented in lemma 2.7.3 for a general linear estimator is presented next.

Theorem 2.7.6 *Consider an asymptotically stable system $\mathcal{F} : \mathbf{w} \rightarrow \mathbf{z}$, composed of a nominal system $\mathcal{G} : \mathbf{w} \rightarrow [\mathbf{z}^T \mathbf{y}^T]^T$ and an estimator $\mathcal{E} : \mathbf{y} \rightarrow \hat{\mathbf{z}}$ interconnected as described in figure 2.7.1, with realization (2.7.3). The \mathcal{H}_∞ norm of such system, from the input \mathbf{w} to the output estimation error \mathbf{e} , verifies $\|F\|_\infty < \gamma$, for $\gamma > 0$ if and only if there exist matrices $Z = Z^T \in \mathbb{R}^{n \times n}$, $Y = Y^T \in \mathbb{R}^{n \times n}$, $Q \in \mathbb{R}^{n \times n}$, $F \in \mathbb{R}^{n \times q}$, $L \in \mathbb{R}^{p \times n}$, $R \in \mathbb{R}^{p \times q}$, and $W \in \mathbb{R}^{m \times m}$ such that*

$$\begin{bmatrix} A^T Z + ZA & ZA + A^T Y + C_y^T F^T + Q^T & ZB_w & C_z^T - C_y^T R^T - L^T \\ A^T Z + YA + FC_y + Q & A^T Y + C_y^T F^T + YA + FC_y & YB_w + FD_{yw} & C_z^T - C_y^T R^T \\ B_w^T Z & B_w^T Y + D_{yw}^T F^T & -\gamma^2 I_m & D_{zw}^T - D_{yw}^T R^T \\ C_z - RC_y - L & C_z - RC_y & D_{zw} - RD_{yw} & -I_p \end{bmatrix} \quad (2.7.20)$$

is negative definite and

$$Y > Z > 0. \quad (2.7.21)$$

Since the proof of this theorem follows the same steps as that of the \mathcal{H}_2 norm, it will be omitted here. As in the previous theorem, a corollary similar to 2.7.5 is immediate. Following the same arguments, the \mathcal{H}_∞ central estimator can be obtained on the boundary of the linear inequalities under consideration.

2.8 Discrete-time systems

Some of the concepts presented in the previous sections will be revisited next and written in a discrete-time setup. The term discrete-time expresses the fact that the signals and systems only change in an infinite countable set of instants equally spaced in time. It is therefore possible to index the elements of this set using an isomorphism to \mathbb{Z}^+ . A signal can be represented as a column vector with the discrete-time components stacked as in

$$\mathbf{u} = \begin{bmatrix} u(0) \\ u(1) \\ \vdots \\ u(k) \\ \vdots \end{bmatrix} \quad k \in \mathbb{Z}^+,$$

where $u(k) \in \mathbb{R}^n$ and the Euclidean norm can be computed according to

$$\|\mathbf{u}\|_2 = \left(\sum_{k=0}^{\infty} u^T(k)u(k) \right)^{\frac{1}{2}} < +\infty.$$

The space of such signals with finite Euclidean norm is denoted as $l_2(\mathbb{Z}^+, \mathbb{R}^n)$, or as $l_2(\mathbb{Z}^+)$ if the vector dimension is not relevant, or simply l_2 when the instant index domain is obvious.

A discrete-time, finite-dimensional, linear, time-invariant system \mathcal{F} can be described by a set of difference equations with state-space realization

$$\Sigma_{\mathcal{F}} := \begin{cases} \mathbf{x}(k+1) &= A\mathbf{x}(k) + B\mathbf{w}(k) \\ \mathbf{y}(k) &= C\mathbf{x}(k) + D\mathbf{w}(k) \end{cases} \quad (2.8.1)$$

where $\mathbf{x}(k) \in \mathbb{R}^n$ is the state vector, $\mathbf{w}(k) \in \mathbb{R}^m$ is the input vector, and $\mathbf{y}(k) \in \mathbb{R}^p$ is the output vector which assumes its values in \mathbf{y} , with the initial state $\mathbf{x}(k_0) = x_0$. This type of systems can

be regarded as a linear transformation from the spaces $l_2(\mathbb{Z}^+, \mathbb{R}^m) \rightarrow l_2(\mathbb{Z}^+, \mathbb{R}^p)$. In this case the set of positive integers of the time index can be interpreted as if the signals were undefined for all negative time-instants.

This isomorphism can be also used in sampled-data systems where the outputs of a continuous-time system, such as the one in (2.2.4), are sampled and the outputs from the controller/estimator are applied to the system input at the time instants $t_k = kh, k \in \mathbb{Z}^+$, where $h > 0$ is the sampling period. Moreover, by discretizing the plant and introducing fictitious sample and hold blocks at the output and at the input, respectively, an interpretation for the resulting system in the discrete-time setup is possible (see [19] for an interesting overview on sampled-data systems).

The concept of dissipativity can be introduced with an obvious adaptation to this setup, as stated in the following definition.

Definition 2.8.1 Dissipativity *The system $\mathcal{F} : \mathbf{w} \rightarrow \mathbf{y}$ with the quadratic supply rate function $s : [\mathbf{w}^T \mathbf{y}^T]^T \rightarrow \mathbb{R}$,*

$$s(\mathbf{w}(k), \mathbf{y}(k)) = \begin{bmatrix} \mathbf{y}(k) \\ \mathbf{w}(k) \end{bmatrix}^T \begin{bmatrix} Q_{yy} & Q_{yw} \\ Q_{wy} & Q_{ww} \end{bmatrix} \begin{bmatrix} \mathbf{y}(k) \\ \mathbf{w}(k) \end{bmatrix}, \quad (2.8.2)$$

is said to be strictly dissipative if there exists a non-negative function $V : X \rightarrow \mathbb{R}$ such that

$$V(\mathbf{x}(k_0)) + \sum_{k=k_0}^{k_1} s(\mathbf{w}(k), \mathbf{y}(k)) > V(\mathbf{x}(k_1 + 1)), \quad (2.8.3)$$

for all $k_0 < k_1$ and for all trajectories $(\mathbf{w}(k), \mathbf{x}(k), \mathbf{y}(k))$ of the system \mathcal{F} .

Note once again that no assumptions were made on the matrix $Q \in \mathbb{R}^{(p+m) \times (p+m)}$. Using the telescopic property the previous relation can be written as

$$\sum_{k=k_0}^{k_1} (s(\mathbf{w}(k), \mathbf{y}(k)) - V(\mathbf{x}(k+1)) + V(\mathbf{x}(k))) > 0,$$

which must be valid for all time-instants $k_1 > k_0$. The next theorem provides necessary and sufficient conditions for the system \mathcal{F} with the supply function $s(\mathbf{w}(k), \mathbf{y}(k))$ to be dissipative. Moreover, it will constitute the bridge between the class of dissipative discrete-time systems and their characterization in terms of LMIs.

Theorem 2.8.2 *Suppose the system \mathcal{F} with realization $\Sigma_{\mathcal{F}}$ is controllable, and let the supply function $s(\mathbf{w}(k), \mathbf{y}(k))$ be defined as in 2.8.2. The following statements are equivalent:*

1. The system is strictly dissipative;
2. The system admits a quadratic storage function $V(\mathbf{x}(k)) = \mathbf{x}^T(k)P\mathbf{x}(k)$, where $P \in \mathbb{R}^{n \times n}$ is a positive definite, symmetric matrix and $P = P^T > 0$;
3. There exists a positive definite matrix $P = P^T \in \mathbb{R}^{n \times n}$ such that

$$F(P) := - \begin{bmatrix} A^T P A - P & A^T P B \\ B^T P A & B^T P B \end{bmatrix} + \begin{bmatrix} C & D \\ 0 & I_m \end{bmatrix}^T \begin{bmatrix} Q_{yy} & Q_{yw} \\ Q_{wy} & Q_{ww} \end{bmatrix} \begin{bmatrix} C & D \\ 0 & I_m \end{bmatrix} > 0. \quad (2.8.4)$$

4. The transfer function of the system with realization $\Sigma_{\mathcal{F}}$, obtained with the z -transform, written as

$$F(\mathbf{z}) = C(\mathbf{z}I_n - A)^{-1}B + D, \quad (2.8.5)$$

where \mathbf{z} is the time-shift operator, evaluated along $\mathbf{z} = e^{j\omega}$ for all $\omega \in [0, 2\pi[$, and with $\det(j\omega I_n - A) \neq 0$ satisfies

$$\begin{bmatrix} F(e^{j\omega}) \\ I_m \end{bmatrix}^* \begin{bmatrix} Q_{yy} & Q_{yw} \\ Q_{wy} & Q_{ww} \end{bmatrix} \begin{bmatrix} F(e^{j\omega}) \\ I_m \end{bmatrix} > 0; \quad (2.8.6)$$

Moreover, if one of the above statements holds, then $V(\mathbf{x}(k)) = \mathbf{x}^T(k)P\mathbf{x}(k)$ is a quadratic storage function if and only if $P > 0$ and $F(P) > 0$.

The proof follows the same circle of ideas as in the continuous-time version. In the deduction of (2.8.4) the dissipativity of the system under consideration implies that the relation (2.8.3) is verified for all time-instants.

2.8.1 Norms of discrete-time systems

The computation of the \mathcal{H}_∞ norm of system $\Sigma_{\mathcal{F}}$ with realization (2.8.1), from the input \mathbf{w} to the output \mathbf{y} , both considered to be signals in the set $l_2(\mathbb{Z}^+)$, can be performed based on the system dissipativity property as stated by the next proposition.

Proposition 2.8.3 *Let the system $\mathcal{F} : \mathbf{w} \rightarrow \mathbf{y}$ in (2.8.1) be asymptotically stable, with all roots inside the unit circle and let $\gamma > 0$ be a real number. The following statements are equivalent:*

1. $\|F\|_\infty < \gamma$;

2. The gain of the system verifies

$$\sup_{\mathbf{w} \in l_2} \frac{\|\mathbf{y}\|_2}{\|\mathbf{w}\|_2} < \gamma,$$

with null initial conditions, $\mathbf{x}(0) = 0$;

3. The system is strictly dissipative, with respect to the supply function

$$s(\mathbf{w}, \mathbf{y}) = \gamma^2 \|\mathbf{w}\|_2^2 - \|\mathbf{y}\|_2^2;$$

4. There exists a symmetric matrix $P = P^T \in \mathbb{R}^{n \times n}$, that enables the LMI

$$\begin{bmatrix} -P & 0 & A^T P & C^T \\ 0 & -\gamma^2 I_m & B^T P & D^T \\ PA & PB & -P & 0 \\ C & D & 0 & -I_p \end{bmatrix} < 0. \quad (2.8.7)$$

Note that the third item can be obtained using theorem 2.8.2 with

$$Q = \begin{bmatrix} -I_p & 0 \\ 0 & \gamma^2 I_m \end{bmatrix},$$

after organizing the terms in the resulting LMI. Note also that for linear and stable systems the \mathcal{H}_∞ norm and the induced $l_2(\mathbb{Z}^+)$ norm are equal.

The \mathcal{H}_2 norm of discrete-time systems can also be interpreted in a stochastic setup in a similar way as described in section 2.5, however, a deterministic interpretation will be presented in the Hardy space \mathcal{H}_2 . This space corresponds to the class of complex valued functions which are analytic in \mathbb{C}^+ . They do have an extension to the unitary circle and the norm of these systems can be computed as

$$\|F\|_2^2 = \frac{1}{2\pi} \mathbf{tr} \int_0^{2\pi} F(j\omega) F^*(j\omega) d\omega < \infty,$$

where $\omega \in [0, 2\pi[$, due to the properties of the discrete-time Fourier transform. Injecting as inputs the discrete-time Dirac functions $\mathbf{w}_i(k) = \delta(k)$, $i = 1, \dots, m$, in the causal system with

realization (2.8.1), and $y(0) = 0$ the resulting output is

$$\mathbf{y} = \begin{bmatrix} D \\ CB \\ \vdots \\ CA^{k-1}B \\ \vdots \end{bmatrix} \quad k \in \mathbb{Z}^+.$$

Using Parseval's theorem, the \mathcal{H}_2 norm of the aforementioned system can also be written as

$$\|F\|_2^2 = \mathbf{tr}(D^T D) + \mathbf{tr} \sum_{k=0}^{+\infty} CA^k BB^T A^{T^k} C^T = \mathbf{tr}(D^T D) + \mathbf{tr}(CW_{ctr}C^T),$$

where the discrete-time controllability Grammian $W_{ctr} = \sum_{k=0}^{+\infty} A^k BB^T A^{T^k}$ was introduced.

Interestingly enough, the controllability Grammian verifies the Lyapunov equation

$$W(k+1) = AW(k)A^T + BB^T.$$

Assuming that the system is asymptotically stable and controllable, this equation becomes the algebraic relation $W = AWA^T + BB^T$, where $W = \lim_{k \rightarrow +\infty} W(k)$. In light of the above, the next proposition summarizes the \mathcal{H}_2 norm computation as relations involving linear matrix inequalities.

Proposition 2.8.4 *Let the system $\mathcal{F} : \mathbf{w} \rightarrow \mathbf{y}$ in (2.8.1) be asymptotically stable with the transfer function described by (2.8.5) and let $\gamma > 0$ be a real number. The following statements are equivalent:*

1. $\|F\|_2 < \gamma$;
2. There exists a positive definite, symmetric matrix $P \in \mathbb{R}^{n \times n}$ and an auxiliary variable $X \in \mathbb{R}^{p \times p}$ such that

$$\begin{bmatrix} P & AP & B \\ PA^T & P & 0 \\ B^T & 0 & I_m \end{bmatrix} > 0, \quad \begin{bmatrix} X & C \\ C^T & P \end{bmatrix} > 0, \quad \mathbf{tr}(X) + \mathbf{tr}(D^T D) < \gamma^2; \quad (2.8.8)$$

3. There exists a positive definite, symmetric matrix $P \in \mathbb{R}^{n \times n}$ and an auxiliary variable $X \in \mathbb{R}^{m \times m}$ such that

$$\begin{bmatrix} P & A^T P & C^T \\ PA & P & 0 \\ C & 0 & I_p \end{bmatrix} > 0, \quad \begin{bmatrix} X & B^T \\ B & P \end{bmatrix} > 0, \quad \text{tr}(X) + \text{tr}(D^T D) < \gamma^2. \quad (2.8.9)$$

The proof, based on the Grammians previously introduced, follows the same steps as for continuous-time systems and thus will be omitted here. In both cases, minimization of $\text{tr}(X)$ can be viewed as the minimization of the norm of the corresponding system \mathcal{F} and will be used in the synthesis of estimators in the next subsection.

2.8.2 Estimator synthesis for discrete-time systems

The general setup for estimator design in the discrete-time is also based on the structure presented in figure 2.7.1, where the nominal system \mathcal{G} is a linear time-invariant system with realization

$$\Sigma_{\mathcal{G}} = \begin{cases} \mathbf{x}(k+1) &= A \mathbf{x}(k) + B_w \mathbf{w}(k) \\ \mathbf{z}(k) &= C_z \mathbf{x}(k) + D_{zw} \mathbf{w}(k) \\ \mathbf{y}(k) &= C_y \mathbf{x}(k) + D_{yw} \mathbf{w}(k), \end{cases} \quad (2.8.10)$$

$\mathbf{x}(k) \in \mathbb{R}^n$ is the state vector, $\mathbf{w}(k) \in \mathbb{R}^m$ is the vector of external inputs, $\mathbf{z}(k) \in \mathbb{R}^p$ is the vector of outputs from the system, $\mathbf{y}(k) \in \mathbb{R}^q$ represents the measurement vector, and the remaining matrices have the required dimensions. As stated for continuous-time systems, under stationary conditions the estimator \mathcal{E} is also a discrete-time, linear, time-invariant dynamical system [2], described by

$$\Sigma_{\mathcal{E}} = \begin{cases} \hat{\mathbf{x}}(k+1) &= A_f \hat{\mathbf{x}}(k) + B_f \mathbf{y}(k) \\ \hat{\mathbf{z}}(k) &= C_f \hat{\mathbf{x}}(k) + D_f \mathbf{y}(k), \end{cases} \quad (2.8.11)$$

where $\hat{\mathbf{x}}(k) \in \mathbb{R}^{n_f}$ is the estimated state vector and $\hat{\mathbf{z}}(k) \in \mathbb{R}^p$ are the output estimates. Note that no constraints on the dimension of the state estimator $\hat{\mathbf{x}}$ are imposed. The study of such an estimator with a generic structure could be exploited in the same way as presented earlier for the continuous-time systems. However, as convincingly argued in [2], for linear nominal systems described by a set of difference equations, the optimum estimator, in the sense of providing

the state estimate with minimum variance consists of a finite-dimensional linear time-invariant estimator with realization

$$\Sigma_{\mathcal{E}_k} = \begin{cases} \hat{\mathbf{x}}(k+1) &= A \hat{\mathbf{x}}(k) + K(\mathbf{y}(k) - C_y \hat{\mathbf{x}}(k)) \\ \hat{\mathbf{z}}(k) &= C_z \hat{\mathbf{x}}(k) \end{cases} \quad (2.8.12)$$

where $K \in \mathbb{R}^{n \times q}$ is a constant observer gain to be determined and $\hat{\mathbf{x}}(k)$ and $\hat{\mathbf{z}}(k)$ have the same dimensions of $\mathbf{x}(k)$ and $\mathbf{z}(k)$, respectively.

Let the state estimation error be defined as $\tilde{\mathbf{x}} = \mathbf{x} - \hat{\mathbf{x}}$ and the estimation error as $\mathbf{e} = \mathbf{z} - \hat{\mathbf{z}}$. Using the relations in (2.8.10) and (2.8.12) the dynamics is

$$\Sigma_{\mathcal{F}_k} = \begin{cases} \tilde{\mathbf{x}}(k+1) &= (A - KC_y) \tilde{\mathbf{x}}(k) + (B_w - KD_{yw}) \mathbf{w}(k) \\ \mathbf{e}(k) &= C_z \tilde{\mathbf{x}}(k) + D_{zw} \mathbf{w}(k). \end{cases} \quad (2.8.13)$$

Applying the results introduced earlier in this section to this system, the \mathcal{H}_2 and \mathcal{H}_∞ norms can be computed using the same non-linear transformation on the unknown variables as for the continuous-time version.

Proposition 2.8.5 *Consider the discrete-time asymptotically stable system $\mathcal{F}_k : \mathbf{w} \rightarrow \mathbf{z}$ composed of a nominal system $\mathcal{G} : \mathbf{w} \rightarrow [\mathbf{z}^T \mathbf{y}^T]^T$ and an estimator $\mathcal{E}_k : \mathbf{y} \rightarrow \hat{\mathbf{z}}$ interconnected as described in figure 2.7.1, with realization (2.8.13). The \mathcal{H}_2 norm of this system, from the input \mathbf{w} to the output estimation error \mathbf{e} , is such that, given $\gamma > 0$, the following statements are equivalent:*

1. $\|F_k\|_2 < \gamma$;
2. There exists a symmetric, positive definite matrix $P \in \mathbb{R}^{n \times n}$, an auxiliary variable $X \in \mathbb{R}^{p \times p}$, and an auxiliary variable $Y \in \mathbb{R}^{n \times q}$ verifying $Y = PK$ such that

$$\begin{aligned} & \begin{bmatrix} P & PA - YC_y & PB_w - YD_{yw} \\ A^T P - C_y^T Y^T & P & 0 \\ B_w^T W - D_{yw}^T Y^T & 0 & I_m \end{bmatrix} > 0, \\ & \begin{bmatrix} X & C_z P \\ PC_z^T & P \end{bmatrix} > 0, \\ & \mathbf{tr}(X) + \mathbf{tr}(D_{zw}^T D_{zw}) < \gamma^2; \end{aligned} \quad (2.8.14)$$

3. There exists a symmetric, positive definite matrix $P \in \mathbb{R}^{n \times n}$, an auxiliary variable $X \in \mathbb{R}^{m \times m}$, and an auxiliary variable $Y \in \mathbb{R}^{n \times q}$ verifying $Y = PK$ such that

$$\begin{aligned} & \begin{bmatrix} P & A^T P - C_y^T Y^T & C_z^T \\ PA - Y C_y & P & 0 \\ C_z & 0 & I_p \end{bmatrix} > 0, \\ & \begin{bmatrix} X & B_w^T P - D_{yw}^T Y^T \\ PB_w - Y D_{yw} & P \end{bmatrix} > 0, \\ & \text{tr}(X) + \text{tr}(D_{zw}^T D_{zw}) < \gamma^2. \end{aligned} \quad (2.8.15)$$

Proof: Applying the definition of the \mathcal{H}_2 norm presented in proposition 2.8.4 to the system described by (2.8.13), the first LMI from the set (2.8.8) in the variable $W = P^{-1}$, after pre and post-multiplying by

$$\begin{bmatrix} P & 0 & 0 \\ 0 & P & 0 \\ 0 & 0 & I_m \end{bmatrix}$$

results in the matrix inequality

$$\begin{bmatrix} P & PA - PKC_y & PB_w - PKD_{yw} \\ A^T P - C_y^T K^T P & P & 0 \\ B_w^T P - D_{yw}^T K^T P & 0 & I_m \end{bmatrix} > 0,$$

which is not an LMI, as there are products of unknowns, namely P and K . Introducing the auxiliary variable $Y = PK$ results in the first LMI of (2.8.14). This can be understood as the use of a non-linear transformation that allows the bilinear matrix inequality to become an LMI. The second LMI in (2.8.14) is obtained from the second LMI in the set (2.8.8) written in the variable $W = P^{-1}$ after pre and post-multiplying by

$$\begin{bmatrix} I_p & 0 \\ 0 & P \end{bmatrix}.$$

The sufficiency of the result follows the sufficiency proof of proposition 2.8.4. Moreover, the same set of arguments could be used to derive the corresponding LMIs in (2.5.7). ■

Proposition 2.8.6 *Consider the discrete-time asymptotically stable system $\mathcal{F}_k : \mathbf{w} \rightarrow \mathbf{z}$ composed of a nominal system $\mathcal{G} : \mathbf{w} \rightarrow \mathbf{z} \times \mathbf{y}$ and an estimator $\mathcal{E}_k : \mathbf{y} \rightarrow \hat{\mathbf{z}}$ interconnected as described in figure 2.7.1, with realization (2.8.13). The \mathcal{H}_∞ norm from the input \mathbf{w} to the output estimation error \mathbf{e} verifies $\|F_k\|_\infty < \gamma$, for $\gamma > 0$, if and only if there exists a symmetric, positive definite matrix $P \in \mathbb{R}^{n \times n}$ and an auxiliary variable $Y \in \mathbb{R}^{n \times q}$ verifying $Y = PK$ such that*

$$\begin{bmatrix} -P & 0 & A^T P - C_y^T Y^T & C_z^T \\ 0 & -\gamma^2 I_m & B_w^T P - D_{yw}^T Y^T & D_{zw}^T \\ PA - Y C_y & PB_w - Y D_{yw} & -P & 0 \\ C_z & D_{zw} & 0 & -I_p \end{bmatrix} < 0. \quad (2.8.16)$$

The proof of this proposition is omitted as it follows exactly the same steps as those outlined in the proof of the previous proposition.

The procedures to synthesize discrete-time estimators with generic structure that are the counterpart of $\Sigma_{\mathcal{E}}$ in (2.7.2) are omitted. See [56] for a complete exposition of this material, as well as for the non-linear transformation required to convert the constraints into LMIs. The proofs that the estimators derived are the \mathcal{H}_2 and the central \mathcal{H}_∞ estimators, respectively, are also available in [56]. Moreover, in the same way as in the continuous-time versions, they can be found on the boundaries of the convex spaces associated with the generic cases.

2.9 Conclusions

This chapter introduced an LMI characterization of closed loop estimators, in the continuous and discrete-time settings. An LMI approach to \mathcal{H}_∞ and \mathcal{H}_2 design was performed and convex constraints on the regional placement of the eigenvalues in terms of LMIs were presented.

The results obtained are easily implementable using commercially available packages such as the MATLAB LMI Optimization Toolbox and play a key role in the design of estimators with multiple constraints. Some application examples will be found along this thesis.

Chapter 3

Complementary Filters

3.1 Introduction

Classically, the design of controllers, filters, and estimators was supported in the theoretical results introduced by Wiener during the 1940s (see [39] and the references therein for an overview of the work). The framework proposed, based on a stationary stochastic characterization of the signals used and on linear time-invariant systems, leads to a linear time-invariant solution resorting to spectral factorization techniques.

In the case of a general stochastic setting, the design of feedback systems and in particular the design of estimators (the main focus of this thesis) is done using Kalman-Bucy filtering theory [17]. In the case of non-linear systems, design solutions are usually sought by resorting to Extended Kalman filtering techniques [17]. The stochastic setting requires a complete characterization of process and observation noises, a task that may be difficult, costly, or not suited to the problem at hand. This issue is argued at length in [18], where the author points out that in a great number of practical applications the filter design process is entirely dominated by constraints that are naturally imposed by the sensor bandwidths. In this case, a design method that explicitly addresses the problem of merging information provided by a given sensor suite over distinct, yet complementary frequency regions is warranted.

Complementary filters have been developed to address this issue explicitly. See for example [18, 50] for a concise introduction to complementary filters and their applications. In the linear time-invariant setting, filter design is ultimately reduced to the problem of decomposing an

identity operator into stable low and high-pass transfer functions that operate on complementary sensor information. The bandwidth of the low-pass transfer function becomes a tuning parameter aimed at matching the physical characteristics of the “low frequency” sensor. Therefore, the emphasis is shifted from a stochastic to a deterministic framework, where the main objective is to shape the filter closed-transfer functions. Interestingly this is the structure that results from using the classical approach introduced by Wiener.

This chapter is organized as follows: section 3.2 introduces linear estimation techniques, namely the Wiener filtering technique and section 3.3 sets the motivation for the sections that follow with simple filtering problems. Complementary filters are characterized in terms of an algebraic relation involving the transfer functions from the sensors inputs to the estimated outputs. Moreover, the relations of complementary filters with the Wiener and Kalman filters will be discussed.

3.2 Linear Estimation

In this section the work of Norbert Wiener, developed in the early 1940s at the MIT Radiation Laboratory, will be briefly presented. Some definitions on stochastic processes and on linear estimation optimization will also be introduced.

In preparation to what follows lets start by introducing some properties for scalar stochastic processes, i.e., a non-countable infinite collection of random variables, over the time domain $t \in \mathbb{R}$. The random variable obtained from a stochastic process $\mathbf{x}(t)$, when a particular instant t considered, has the distribution

$$F(\mathbf{x}, t) = P\{\mathbf{x}(t) < x\},$$

and its first-order function $f(\mathbf{x}, t)$ is defined as

$$f(\mathbf{x}, t) = \frac{dF(\mathbf{x}, t)}{dt}.$$

The n^{th} -order distribution of $\mathbf{x}(t)$ has a joint distribution $F(\mathbf{x}_1, \dots, \mathbf{x}_n; t_1, \dots, t_n)$ of the random variables $\mathbf{x}(t_1), \dots, \mathbf{x}(t_n)$, and it is a generalization of the distribution introduced above. The statistic properties of a stochastic process are mainly determined in terms of this function. In some special cases, only the expected values of $\mathbf{x}(t)$ and $\mathbf{x}^2(t)$ are important (see [60] and the

references therein for a detailed discussion on stochastic processes and random variables). Note that a n -dimensional stochastic process $\mathbf{x} : \mathbb{R} \rightarrow \mathbb{R}^n$ can be represented as a stacked column vector of stochastic processes as introduced above. The second order statistics for a stochastic process are introduced next.

Definition 3.2.1 *The mean $\eta_x(t)$ of the random variable $\mathbf{x}(t)$ is its expected value*

$$\eta_x(t) = E[\mathbf{x}(t)] = \int_{-\infty}^{+\infty} \mathbf{x} f(\mathbf{x}, t) d\mathbf{x}.$$

Definition 3.2.2 *The auto-correlation $R_{xx}(t_1, t_2)$ of the stochastic process $\mathbf{x}(t)$, at the time-instants t_1 and t_2 , is the expected value of the product $\mathbf{x}(t_1)\mathbf{x}^T(t_2)$*

$$R_{xx}(t_1, t_2) = E[\mathbf{x}(t_1)\mathbf{x}^T(t_2)] = \int_{-\infty}^{+\infty} \int_{-\infty}^{+\infty} \mathbf{x}_1 \mathbf{x}_2^T f(\mathbf{x}_1, \mathbf{x}_2; t_1, t_2) d\mathbf{x}_1 d\mathbf{x}_2 = R_{xx}^T(t_2, t_1).$$

Note that the auto-correlation is positive definite due to the identity

$$0 \leq E\left[\left|\sum_i a_i \mathbf{x}(t_i)\right|^2\right] = \sum_{i,j} a_i a_j E[\mathbf{x}(t_i)\mathbf{x}^T(t_j)],$$

and the average power of $\mathbf{x}(t)$ is obtained when the time-instants considered are equal, i.e., $R(t, t) = E[\mathbf{x}^2(t)] \geq 0$.

Definition 3.2.3 *The auto-covariance $C_{xx}(t_1, t_2)$ of the stochastic process $\mathbf{x}(t)$, at the time-instants t_1 and t_2 , is the covariance of the random variables $\mathbf{x}(t_1)$ and $\mathbf{x}(t_2)$*

$$C_{xx}(t_1, t_2) = R_{xx}(t_1, t_2) - \eta_x(t_1)\eta_x^T(t_2).$$

In the case where the same time-instants are considered $C_{xx}(t, t)$ equals the variance of the random variable $\mathbf{x}(t)$. Moreover, for null-mean random variables the auto-covariance and the auto-correlation are equal.

Definition 3.2.4 *The cross-correlation of two processes $\mathbf{x}(t)$ and $\mathbf{y}(t)$ is the function $R_{xy}(t_1, t_2) = E[\mathbf{x}(t_1)\mathbf{y}^T(t_2)] = R_{yx}^T(t_2, t_1)$. Similarly, the cross-covariance of these two processes is*

$$C_{xy}(t_1, t_2) = R_{xy}(t_1, t_2) - \eta_x(t_1)\eta_y^T(t_2).$$

Two stochastic processes with null cross-correlation $R_{xy}(t_1, t_2) = 0$, for all $t_1, t_2 \in \mathbb{R}$ are called orthogonal. If $C_{xy}(t_1, t_2) = 0$ independently of the time-instants considered, the processes $\mathbf{x}(t)$ and $\mathbf{y}(t)$ are uncorrelated.

The definition of stationarity is central to the discussion that will be presented along this work. A stochastic process $\mathbf{x}(t)$ is stationary in strict-sense if its statistical properties are invariant to a shift in the time variable, i.e., the processes $\mathbf{x}(t)$ and $\mathbf{x}(t + c)$ have the same statistics for any $c \in \mathbb{R}$. Moreover, two processes are jointly stationary if the joint statistics of $\mathbf{x}(t)$ and $\mathbf{y}(t)$ are the same as the statistics of $\mathbf{x}(t + c)$ and $\mathbf{y}(t + c)$, respectively, for any c . A stochastic process is called wide-sense stationary if its mean is constant $E[\mathbf{x}(t)] = \eta_x$ and its auto-correlation depends only on the time difference $\tau = t_1 - t_2$,

$$R_{xx}(\tau) = E[\mathbf{x}(t + \tau)\mathbf{x}^T(t)].$$

In particular $R_{xx}(0) = E[|\mathbf{x}^2(t)|]$, therefore the average power of a wide-sense stationary process is constant over time and the auto-covariance depends only on $\tau = t_1 - t_2$ and verify

$$C_{xx}(\tau) = R_{xx}(\tau) - \eta_x \eta_x^T.$$

The estimation problem formulated by Wiener belongs to a broad class of optimization problems that can be described as follows:

Proposition 3.2.5 *Based on measurements of a random variable y with a known joint probability density function $f_{xy}(\mathbf{x}, \mathbf{y})$, how to obtain an estimate $\hat{\mathbf{x}}$ of a non-directly measurable variable $\mathbf{x}(t)$ that minimizes the expected value of a quadratic function on the estimate error $\mathbf{e}(t) = \mathbf{x}(t) - \hat{\mathbf{x}}(t)$.*

Note that in general the estimate $\hat{\mathbf{x}} = h(\mathbf{y})$ can be a linear or non-linear function of the measurable variable \mathbf{y} . The solution of these optimization problems are called mean-square error estimates or least squares estimates, for short. There are multiple reasons to address this type of problems: i) the least squares estimates can be specified as a conditional mean; ii) for gaussian variables they are linear functions of the observations; iii) suboptimal solutions are easy to obtain in general and in the case where the estimates are linear functions of the observations, only knowledge on the first and second order statistics is required; iv) a rich

geometric interpretation for the solution obtained exists. For a survey study on the classic optimization problems briefly described above see [39] and the references therein.

In the case where the estimate $\hat{\mathbf{x}}$ is assumed to be linear on the observations the following theorem provides an enlightening interpretation for the linear least squares estimates, that constitute the solution to the optimization problem at hand.

Theorem 3.2.6 [39] *The error estimate $\mathbf{e} = \mathbf{x} - \hat{\mathbf{x}}$ for the random variable \mathbf{x} , assuming a linear combination of the observations $\hat{\mathbf{x}} = \sum_i a_i x_i$, has a minimum that is orthogonal to all data, i.e., verifies*

$$E[(\mathbf{x} - \sum_i a_i x_i)x_i] = 0, \quad i = 1, \dots, n.$$

Proof: To minimize the function $J = E[(\mathbf{x} - \hat{\mathbf{x}})^2]$ relative to the unknowns a_i can be obtained by differentiation

$$\frac{\partial}{\partial a_i} J = E[2((\mathbf{x} - \sum_i a_i x_i))(-x_i)] = 0, \quad i = 1, \dots, n,$$

which results on the orthogonal condition stated in the theorem. ■

Note that this result paves the way for a rich interpretation on the minimization problem under study.

The general problem addressed by Wiener will be presented next in a stochastic setting, based on the stochastic processes and on the linear estimation optimization problem briefly introduced above.

Given two zero-mean wide sense stationary random processes $\mathbf{x}(t)$ and $\mathbf{y}(t)$, with zero mean $\eta_x = \eta_y = 0$ and known auto-covariances and cross-covariance $R_{xx}(\tau)$, and $R_{yy}(\tau)$, and $R_{xy}(\tau)$, respectively, solve the following problem:

Proposition 3.2.7 (Wiener) *Given the observations $\mathbf{y}(\tau)$, with $-\infty < \tau < t$ find the linear least mean-square error estimate of $\mathbf{x}(t + \lambda)$, for a fixed positive constant λ .*

Considering that a linear dependence on the observations is sought, then the estimate $\hat{\mathbf{x}}(t + \lambda)$ can be written as

$$\hat{\mathbf{x}}(t + \lambda) = \int_{-\infty}^t h(t, \tau) \mathbf{y}(\tau) d\tau,$$

where $h(t, \tau)$ is the impulsive response of a causal linear system whose response at time t , \mathbf{y} is the system input, and $\hat{\mathbf{x}}(t + \lambda)$ is the desired value, which minimizes

$$E[(\mathbf{x}(t + \lambda) - \hat{\mathbf{x}}(t + \lambda))^2].$$

According with the projection theorem presented above,

$$E[(\mathbf{x}(t + \lambda) - \hat{\mathbf{x}}(t + \lambda))\mathbf{y}(\sigma)] = 0, \quad \text{for } -\infty < \sigma < t,$$

which yields

$$E[\mathbf{x}(t + \lambda)\mathbf{y}(\sigma)] = \int_{-\infty}^t h(t, \tau)E[\mathbf{y}(\tau)\mathbf{y}(\sigma)]d\tau,$$

where the linear characteristics of the expected value and the integral were used. From the definitions of auto and cross-correlation introduced above and after the coordinate transformations $\tau' = t - \tau$ and $t - \sigma = t'$ it is straightforward to obtain

$$R_{xy}(t' + \lambda) = \int_0^{\infty} h(t' + \sigma, t' + \sigma - \tau')R_{yy}(t' - \tau')d\tau', \quad \text{for } t > 0.$$

The auto and cross-correlation functions do not depend on σ , therefore $h(t' + \sigma, t' + \sigma - \tau')$ must be a function only of the difference of its arguments. With some abuse of notation the above expression can be rewritten as

$$R_{xy}(t + \lambda) = \int_0^{\infty} h(\tau)R_{yy}(t - \tau)d\tau, \quad \text{for } t > 0, \quad (3.2.1)$$

where $h(t) = 0$, for $t < 0$. The equations of this form are usually called Wiener-Hopf equations. It might appear that the Laplace transform could be used to solve this equation, however the fact that this relation holds only for positive values of t precludes the use of such methodology (see [39] for a detailed discussion of this fact).

A more sophisticated technique, developed by Wiener and Hopf in 1931, must be used to solve the aforementioned type of equations. This technique will be briefly discussed next for stationary processes with rational power spectral density functions. Interestingly, this set corresponds also to the processes obtained when white-noise is used as input for finite-dimensional, linear, continuous time-invariant systems.

Consider the Laplace transform of the transfer function of the single-input, single-output system $H : \mathbf{u} \rightarrow \mathbf{y}$, where $\mathbf{u} \in R$ is a zero-mean and unitary variance white-noise input and $\mathbf{y} \in R$ is the output, when null initial conditions are considered. The bilateral Laplace transform

of the covariance of the output $\mathbf{y}(t)$ verifies $S_{yy}(\mathbf{s}) = H(\mathbf{s})H(-\mathbf{s})$. It is immediate that $S_{yy}(\mathbf{s}) = S_{yy}(-\mathbf{s})$ and that the numerator (zeros) and denominator roots (poles) present the following properties:

- they are symmetric relative to the real axis, as $S_{yy}(\mathbf{s})$, when $\mathbf{s} = j\omega$, is real;
- they are symmetric relative to the imaginary axis, due to the fact that $S_{yy}(\mathbf{s})$ is even;
- there are an even number of zeros on the imaginary axis, as $S_{yy}(\mathbf{s}) \geq 0$
- there are no poles on the imaginary axis, because in that case it could not be a covariance function.

The constraints on $H(\mathbf{s})$ imply that all poles should be on the left-half-plane, i.e., all roots of the denominator have a negative real part. Moreover, a canonical factorization of the form $S_{yy}(\mathbf{s}) = S_{yy}^+(\mathbf{s})S_{yy}^-(\mathbf{s})$ will be possible, where $S_{yy}^+(\mathbf{s})$ is the stable and minimum-phase power spectral density function, composed by the poles and zeros on the left-half-plane.

The solution to the problem at hand can be obtained using the following result:

Proposition 3.2.8 (Wiener)[39] *The Wiener-Hopf equation (3.2.1)*

$$R_{xy}(t + \lambda) = \int_0^\infty h(\tau)R_{yy}(t - \tau)d\tau, \quad \text{for } t > 0,$$

where $h(t) = 0$, for $t < 0$ has the solution ¹

$$H(\mathbf{s}) = \frac{1}{S_{yy}^+(\mathbf{s})} \left\{ \frac{S_{xy}(\mathbf{s})e^{\mathbf{s}\lambda}}{S_{yy}^-(\mathbf{s})} \right\}_+ \quad (3.2.2)$$

Proof: Lets start by introducing the auxiliary function

$$g(t) = R_{xy}(t + \lambda) - \int_0^\infty h(\tau)R_{yy}(t - \tau)d\tau,$$

where $\mathbf{g}(t) = 0$ for $t > 0$ and unknown for the negative values of the time index. The Laplace transform of $\mathbf{g}'(t) = \mathbf{g}(t)u(t)$ is $G(\mathbf{s}) = \mathcal{L}\{\mathbf{g}'(t)\}$, where $\mathbf{u}(t)$ is the Heaviside step function, has no poles on the left-half-plane $\mathbf{s} < 0$. Using this fact to compute the Laplace transform of the previous expression leads to

$$G(\mathbf{s}) = S_{xy}(\mathbf{s})e^{(\mathbf{s})\lambda} - H((\mathbf{s}))S_{yy}(\mathbf{s}).$$

¹The notation $\{\cdot\}_+$ stands to the operation of choosing the poles on the right-half-plane of the function under consideration.

Using the canonical factorization introduced above, this expression can be written as

$$\frac{G(\mathbf{s})}{S_{yy}^-(\mathbf{s})} = \frac{S_{xy}(\mathbf{s})e^{(\mathbf{s})\lambda}}{S_{yy}^-(\mathbf{s})} - H(\mathbf{s})S_{yy}^+(\mathbf{s}).$$

Note that from this expression the equation (3.2.2) results taking into account that poles on the left-half-plane exists only in the terms on the right side of the equation. ■

Extensions to the original Wiener theory have been developed along the last fifty years, namely for non-stationary processes and to non-scalar processes. A special application of Wiener filtering - complementary filters - where the estimate of an unknown variable is sought, based on redundant measures corrupted by noise will be introduced next, through the use of some motivating examples.

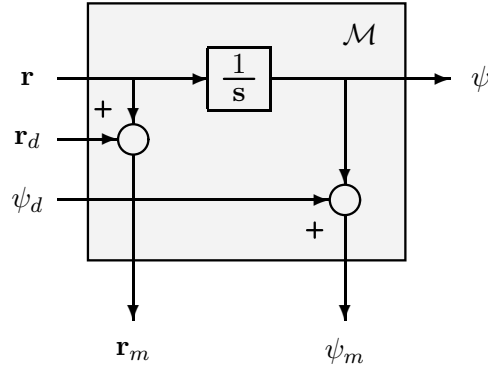
3.3 Motivation for the use of complementary filters

This section reviews the basic structure of complementary filters through a motivation example. To that purpose an attitude navigation system will be formulated and the structure of the solution will be discussed in detail.

3.3.1 Complementary filters: basic concepts and definitions

Complementary filters arise naturally in the context of signal estimation based on measurements provided by sensors over distinct, yet complementary regions of frequency. Brown [18] was the first author to stress the importance of complementary filters in navigation system design. Since then, this subject has been studied in a number of publications that address theoretical as well as practical implementation issues; see for example [7, 44, 50, 53, 72] and the references therein. The key ideas in complementary filtering are very intuitive, and can be simply introduced by referring to the example of the process model \mathcal{M} depicted in figure 3.3.1. The figure captures the practical situation where the heading ψ of a vehicle must be estimated based on measurements \mathbf{r}_m and ψ_m of $\mathbf{r} = \dot{\psi}$ and ψ provided, respectively, obtained using a rate gyro and a flux-gate compass. The measurements are corrupted by disturbances \mathbf{r}_d and ψ_d as depicted in the model \mathcal{M} .

Let $\psi(\mathbf{s})$ and $\mathbf{r}(\mathbf{s})$ denote the Laplace Transforms of ψ and \mathbf{r} , respectively. Then, for every

Figure 3.3.1: Process model \mathcal{M} .

$k > 0$, $\psi(\mathbf{s})$ admits the stable decomposition

$$\begin{aligned}\psi(\mathbf{s}) &= \frac{\mathbf{s} + k}{\mathbf{s} + k} \psi(\mathbf{s}) = \frac{k}{\mathbf{s} + k} \psi(\mathbf{s}) + \frac{\mathbf{s}}{\mathbf{s} + k} \psi(\mathbf{s}) \\ &= T_1(\mathbf{s})\psi(\mathbf{s}) + T_2(\mathbf{s})\psi(\mathbf{s}),\end{aligned}\tag{3.3.1}$$

where $T_1(\mathbf{s}) = k/(\mathbf{s} + k)$ and $T_2(\mathbf{s}) = \mathbf{s}/(\mathbf{s} + k)$ satisfy the equality

$$T_1(\mathbf{s}) + T_2(\mathbf{s}) = I.\tag{3.3.2}$$

Using the relationship $\mathbf{r}(\mathbf{s}) = \mathbf{s}\psi(\mathbf{s})$, it follows from the above equations that

$$\psi(\mathbf{s}) = F_\psi(\mathbf{s})\psi(\mathbf{s}) + F_r(\mathbf{s})\mathbf{r}(\mathbf{s}),$$

where $F_\psi(\mathbf{s}) = T_1(\mathbf{s}) = k/(\mathbf{s} + k)$ and $F_r(\mathbf{s}) = 1/(\mathbf{s} + k)$. This suggests a filter with the structure

$$\hat{\psi} = \mathcal{F}_\psi\psi_m + \mathcal{F}_r\mathbf{r}_m,$$

where \mathcal{F}_ψ and \mathcal{F}_r are linear time-invariant operators with transfer functions $F_\psi(\mathbf{s})$ and $F_r(\mathbf{s})$, respectively. Clearly, the filter admits the state-space realization \mathcal{F}

$$\begin{aligned}\dot{\hat{\psi}} &= -k\hat{\psi} + k\psi_m + \mathbf{r}_m \\ &= \mathbf{r}_m + k(\psi_m - \hat{\psi})\end{aligned}\tag{3.3.3}$$

that is represented in figure 3.3.2.

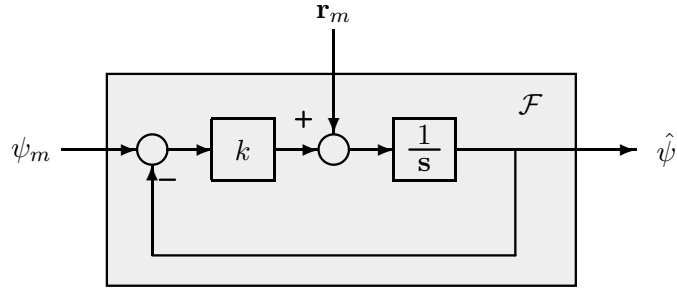


Figure 3.3.2: Complementary filter.

Let \mathcal{T}_1 and \mathcal{T}_2 denote linear time-invariant operators with transfer functions $T_1(\mathbf{s})$ and $T_2(\mathbf{s})$, respectively. Simple computations show that

$$\hat{\psi} = (\mathcal{T}_1 + \mathcal{T}_2)\psi + \mathcal{F}_\psi\psi_d + \mathcal{F}_r\mathbf{r}_d,$$

that is, the estimate $\hat{\psi}$ consists of an undistorted copy $(\mathcal{T}_1 + \mathcal{T}_2)\psi = \psi$ of the original signal ψ , together with corrupting terms that depend on the measurement disturbances ψ_d and \mathbf{r}_d .

Notice the following important properties:

- $T_1(\mathbf{s})$ is low-pass: the filter relies on the information provided by the compass at low frequency only.
- $T_2(\mathbf{s}) = I - T_1(\mathbf{s})$: the filter blends the information provided by the compass in the low frequency region with that available from the rate gyro in the complementary region.
- the break frequency is simply determined by the choice of the parameter k .

The frequency decomposition induced by the complementary filter structure holds the key to its practical success, since it mimics the natural frequency decomposition induced by the physical nature of the sensors themselves: the compass provides reliable information at low frequency only, whereas the rate gyro exhibits bias and drift phenomena in the same frequency region and is therefore useful at higher frequencies.

Complementary filter design is then reduced to computing the gain k so as to meet a target break frequency that is entirely dictated by the physical characteristics of the sensors. From this point of view, the emphasis is shifted from a stochastic framework, which relies heavily on a

correct description of process and measurement noise [18] and the minimization of filter errors, to a deterministic framework that aims at shaping the filter closed-transfer functions.

As convincingly argued in [18], the latter approach is best suited to tackle a large number of practical situations where the characterization of process and measurement disturbances in a stochastic context does not fit the problem at hand, the filter design process being entirely dominated by the constraints imposed by sensor bandwidths. Once this setup is adopted, however, one is free to use any efficient design method, the design parameters being viewed simply as "tuning knobs" to shape the characteristics of the closed loop operators. In this context, filter design can be done using \mathcal{H}_2 or \mathcal{H}_∞ design techniques [17, 30, 31, 34, 53]. Filter analysis is easily carried out in the frequency domain using Bode plots. In the simple case described here, the underlying process model \mathcal{M} can be written relying on the realization

$$\Sigma_{\mathcal{M}} := \begin{cases} \dot{\psi} & = \mathbf{r}_m - \mathbf{r}_d \\ \psi_m & = \psi + \psi_d \end{cases}, \quad (3.3.4)$$

where \mathbf{r}_d and ψ_d play the roles of process and measurement disturbances, respectively. Notice the important fact that ψ_m (the measured value of ψ) is an input to the system. In an \mathcal{H}_2 setting, the objective is to minimize the estimation error $\psi - \hat{\psi}$ for given values of the covariances of ψ_d and \mathbf{r}_d . The optimal solution to this problem has the complementary filter structure described in relation (3.3.3). The covariances of ψ_d and \mathbf{r}_d are simply viewed as design parameters to vary the break frequency.

In practice, the simple complementary structure described above can be modified to meet additional constraints. For example, to achieve steady state rejection of the rate gyro bias, the filter must be augmented with an integrator to obtain the new complementary filter depicted in figure 3.3.3 with the realization

$$\Sigma_{\mathcal{M}} := \begin{cases} \begin{bmatrix} \dot{x}_1 \\ \dot{x}_2 \end{bmatrix} & = \begin{bmatrix} -k_1 & 1 \\ -k_2 & 0 \end{bmatrix} \begin{bmatrix} x_1 \\ x_2 \end{bmatrix} + \begin{bmatrix} k_1 \\ k_2 \end{bmatrix} \psi_m + \begin{bmatrix} 1 \\ 0 \end{bmatrix} \mathbf{r}_m \\ \hat{\psi} & = \begin{bmatrix} 0 & 1 \end{bmatrix} \begin{bmatrix} x_1 \\ x_2 \end{bmatrix} \end{cases}, \quad (3.3.5)$$

where x_1 and x_2 denote the states associated with $\hat{\psi}$ and the bias term, respectively, and k_1 and k_2 are filter gains. To illustrate its relationship with a conventional Kalman filter, the expression

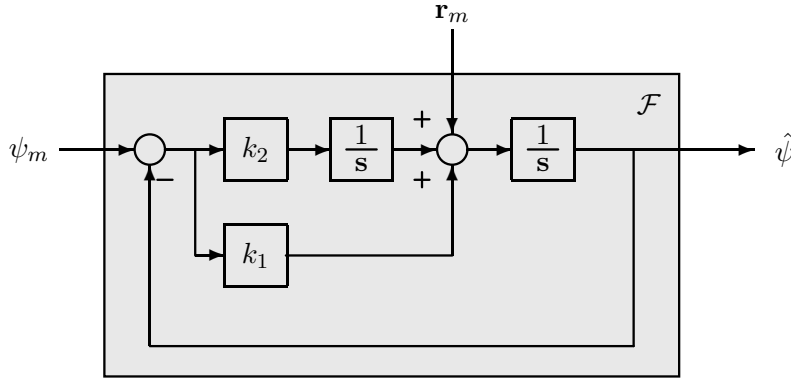


Figure 3.3.3: Complementary filter with bias estimation.

above can be rewritten as

$$\begin{cases} \dot{\mathbf{x}} &= A\mathbf{x} + Bu + K(y - \hat{y}) \\ \hat{y} &= C\mathbf{x} \end{cases} \quad (3.3.6)$$

where $\mathbf{x} = \begin{bmatrix} x_1 \\ x_2 \end{bmatrix}^T$, $\mathbf{u} = \mathbf{r}_m$, $\mathbf{y} = \psi_m$, and

$$A = \begin{bmatrix} 0 & 1 \\ 0 & 0 \end{bmatrix}, B = \begin{bmatrix} 1 \\ 0 \end{bmatrix}, C = \begin{bmatrix} 1 & 0 \end{bmatrix}, \text{ and } K = \begin{bmatrix} k_1 \\ k_2 \end{bmatrix}.$$

Simple computations show that in this case

$$\hat{\psi} = (\mathcal{T}_1 + \mathcal{T}_2)\psi + \eta,$$

where

$$T_1(\mathbf{s}) = \frac{k_1\mathbf{s} + k_2}{\mathbf{s}^2 + k_1\mathbf{s} + k_2}, T_2(\mathbf{s}) = \frac{\mathbf{s}^2}{\mathbf{s}^2 + k_1\mathbf{s} + k_2},$$

and $\eta = \mathcal{F}_\psi\psi_d + \mathcal{F}_r\mathbf{r}_d$ is a noise term, the intensity of which depends on $F_\psi(\mathbf{s}) = T_1(\mathbf{s})$ and

$$F_r(\mathbf{s}) = \frac{\mathbf{s}}{\mathbf{s}^2 + k_1\mathbf{s} + k_2}.$$

Again, notice that $T_1(\mathbf{s}) + T_2(\mathbf{s}) = I$, $T_1(\mathbf{s})$ is low-pass, and $T_2(\mathbf{s})$ is high-pass. The filter blends the information provided by the compass at low frequency with that available from the rate gyro in the complementary frequency range, leaving the original signal ψ undistorted. Furthermore,

any constant terms in \mathbf{r}_d (rate gyro bias) will be naturally rejected at the output since $F_r(0) = 0$. Notice also that the filter rejects high frequency noise present in the flux-gate measurements.

In view of the discussion above, we henceforth adopt a deterministic framework for complementary filter design and analysis where the objective is to shape the filter transfer functions to obtain desired bandwidths. Furthermore, in preparation for the work that follow, it is convenient to formally introduce the definition of a complementary filter for the underlying process model (3.3.4) (with $\mathbf{r}_d = \psi_d = 0$) in a state-space framework (see figure 3.3.1).

Definition. (r, ψ) Complementary Filter. Consider the process model

$$\mathcal{M}_{\psi r} := \begin{cases} \dot{\psi} & = \mathbf{r} \\ \psi_m & = \psi \\ \mathbf{r}_m & = \mathbf{r} \end{cases} \quad (3.3.7)$$

and a filter \mathcal{F} with realization

$$\begin{aligned} \dot{\mathbf{x}} &= A\mathbf{x} + B_r\mathbf{r}_m + B_\psi\psi_m \\ \hat{\psi} &= C\mathbf{x}. \end{aligned}$$

Then, \mathcal{F} is said to be a complementary filter for $\mathcal{M}_{\psi r}$ if

- \mathcal{F} is internally stable.
- For any initial conditions $\psi(0)$ and $\mathbf{x}(0)$ $\lim_{t \rightarrow \infty} \{\psi(t) - \hat{\psi}(t)\} = 0$.
- \mathcal{F} satisfies a bias rejection property, that is, $\lim_{t \rightarrow \infty} \hat{\psi} = 0$ when $\psi_m = 0$ and \mathbf{r}_m is an arbitrary constant.
- The operator $\mathcal{F}_\psi : \psi_m \rightarrow \hat{\psi}$ is a finite bandwidth low-pass filter.

Clearly, for every $k_1, k_2 > 0$ the filter with realization (3.3.5) is a complementary filter for the process $\mathcal{M}_{\psi r}$ in (3.3.7).

It is important to point out that, according to the definition above, filter (3.3.5) is but one representative of a large class of complementary filters for $\mathcal{M}_{\psi r}$. See table (3.3.1), where two separate intervals of frequency are considered: a low band frequency ranging from zero to a pre-specified finite value and a high band frequency that can be considered to end at

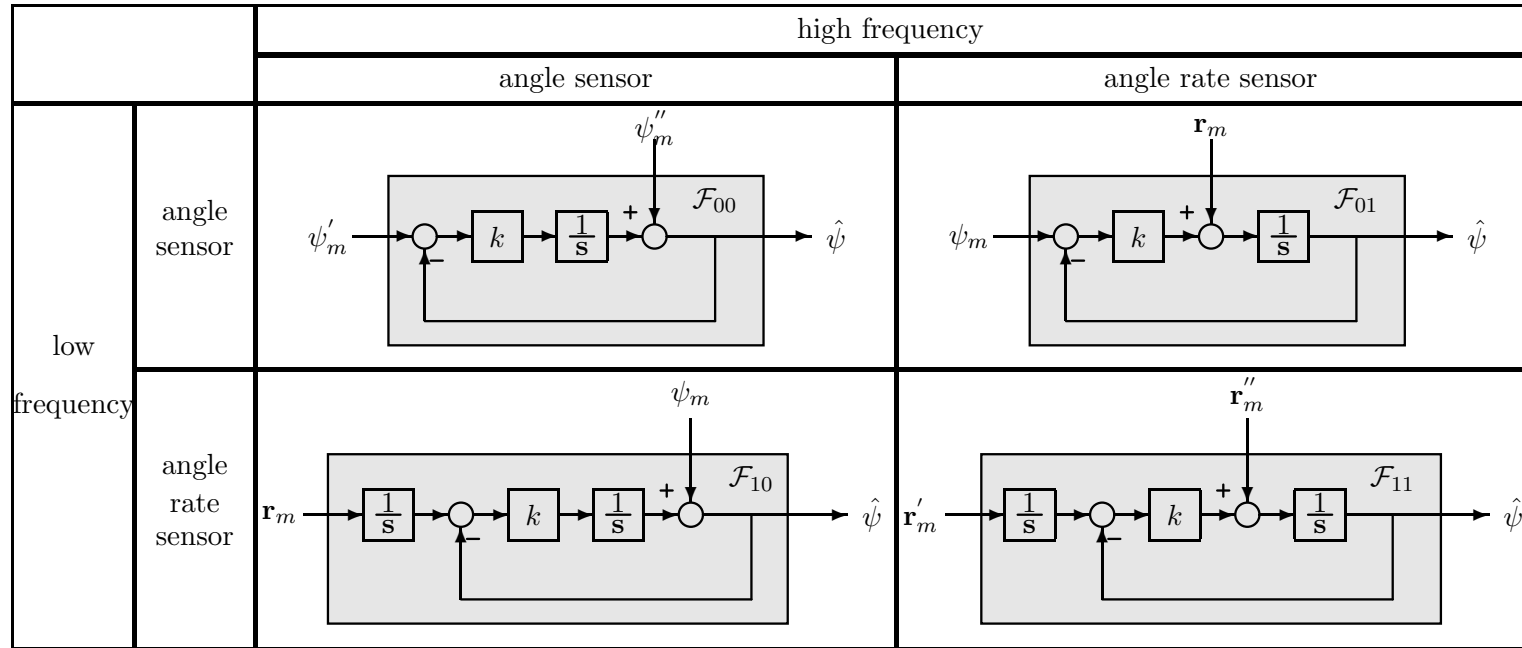


Table 3.3.1: First order complementary filters.

infinite frequency. Consider that there are sensors available providing measurements on the angle variable and on the rate of variation of that variable. Moreover, assume that it is possible to have these sensors providing reliable measurements on each of the frequency regions defined above, based on different physical principles.

The upper right position of table (3.3.1) corresponds to the first order complementary filter introduced above. The remaining complementary filters on the table correspond to alternative structures that can be used to solve the estimation problem at hand in cases where the available sensors are not the ones considered in the aforementioned filter problem. The process of deducing the structures presented in this table is similar to the one used above and expressed in relation (3.3.1). Moreover, all structures obey to the fundamental relation expressed by relation (3.3.2).

Chapter 4

Synthesis of Periodic Estimators

4.1 Introduction

The study of dynamic systems where more than one sampling rate is used has received special attention in recent decades, due to the theoretical results that have become available for this particular class of time-varying systems [20]:

- In complex systems, where several variables must be sampled, it is difficult to sample all variables at the same rate. Some of the variables may need long processing intervals (e.g., chemical based samplers); or delays in the propagation of physical phenomena of interest restrict the sampling rate (e.g., acoustic based sensors).
- Performance, in general, is improved with faster sampling strategies but the computational burden also increases. For loops with higher bandwidths, better trade-offs are obtained with faster sampling rates and performance can be increased using multi-rate systems.
- The superiority of periodic linear time-varying discrete-time controllers was shown in [42]. The stabilization of any linear time-invariant plant with improvements on the gain and phase margins, and the stabilization of any finite collection of discrete time-invariant plants resorting to stable periodic time-varying controllers are examples of such situations.

In this chapter the synthesis of periodic estimators for periodic and multi-rate systems will be described in detail. To that purpose, the definition of multi-rate systems as periodic systems will be presented in section 4.2. A description of linear systems as operators will be introduced

in section 4.3, with an emphasis on the properties of linear, periodically time-varying systems. A technique that establishes the equivalence of linear, periodic systems with a sub class of linear time-invariant systems will be presented in section 4.4 along with a relation on the properties of both classes of systems. The Kalman filter for the periodic systems at hand will be briefly introduced in section 4.5. Recent work on the existence and uniqueness of solutions of the Lyapunov and Kalman periodic equations [10, 73] associated with the discrete-time estimators will also be presented in this section. An invariant version for the off-line Kalman filter design will be introduced in section 4.6.

New theoretical results on the \mathcal{H}_2 and \mathcal{H}_∞ norms of periodic systems will be presented in section 4.7. A synthesis solution to the estimators with the structure proposed in chapter 2 will be presented in section 4.8. The methodology proposed, resorting to convex optimization procedures, is based on the minimization of the \mathcal{H}_2 or \mathcal{H}_∞ norms from auxiliary inputs to auxiliary outputs, constrained by the norms of other input/output signals of a generalized system. This powerful methodology paves the way for the use of such framework in periodic control, in multi-rate filter design, etc. Finally, these new synthesis methodologies will be applied to a classic example in section 4.9 and some conclusions will be presented in section 4.10.

4.2 Periodic systems representation

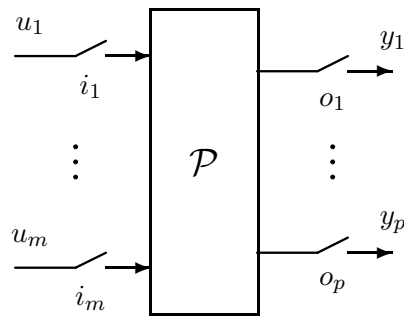


Figure 4.2.1: Multi-rate system with generic sample periods for the inputs and outputs.

Let \mathcal{P} be a multi-rate discrete-time system with m inputs and p outputs, as depicted in figure 4.2.1. This system can result from the use of a linear time-invariant, finite-dimensional,

continuous-time system where appropriate sample and hold devices are used in the inputs and outputs, respectively. However, in this thesis the discrete-time periodic systems under study do not have to be the result of the discretization of continuous-time systems. The approach presented next follows the same circle of ideas as in [63] and constitutes a generalization of the $(P-M)$ -shift-invariant operator introduced in [51].

Consider the system \mathcal{P} with the inputs and outputs sampled at positive time intervals (in appropriate units) denoted i_j , $j = 1, \dots, m$ and o_j , $j = 1, \dots, p$, respectively. Let h be the *base time period* $h = \text{lcd}\{\{i_j, j = 1, \dots, m\}, \{o_j, j = 1, \dots, p\}\}$ and let $Mh = \text{lcm}\{\{i_j, j = 1, \dots, m\}, \{o_j, j = 1, \dots, p\}\}$ be the *system time period*. Let $I_j = \frac{Mh}{i_j}$, $j = 1, \dots, m$ and $O_j = \frac{Mh}{o_j}$, $j = 1, \dots, p$ be the sampling schedule for the inputs and for the outputs, respectively. Throughout this thesis M will denote the system period.

Using the isomorphism previously introduced relating the base sampling time-instants $t_k = hk$, $k = 0, \dots, \infty$ and the set of integer numbers \mathbb{Z}^+ , and assuming \mathcal{P} as a linear, finite dimension system, its dynamics can be represented by a set of difference equations with realization

$$\Sigma_{\mathcal{P}} := \begin{cases} \mathbf{x}(k+1) &= A(k)\mathbf{x}(k) + B(k)\mathbf{u}(k) \\ \mathbf{y}(k) &= C(k)\mathbf{x}(k) + D(k)\mathbf{u}(k), \end{cases} \quad (4.2.1)$$

where the p outputs $\mathbf{y} \in \mathbb{R}^p$ can be expressed as a linear dependence on the state $\mathbf{x} \in \mathbb{R}^n$ and on the m inputs $\mathbf{u} \in \mathbb{R}^m$. Note that this realization is not unique because there is freedom in assigning the time-instant $k = 0$ for the beginning of the period.

In order to express the aforementioned relations, the system matrices must satisfy other constraints, namely ¹:

- $B_{ij}(k) = 0$ if $k \text{ MOD } i_j \neq 0$, i.e., the j^{th} input only influences the system each I_j sample;
- $C_{ij}(k) = 0$ if $k \text{ MOD } o_i \neq 0$, i.e., the i^{th} output is updated only at each O_i sample;
- $D_{ij}(k) \neq 0$ if $k \text{ MOD } i_j = 0$, and $k \text{ MOD } o_i = 0$.

The use of the function MOD in the system matrix indexes together with the definition of M makes it clear that the multi-rate system \mathcal{P} just defined is a periodic system.

¹The subscripts in the system matrices stand for the i^{th} line and j^{th} column. $(.)\text{MOD}(\cdot)$ stands to represent the integer division of the first argument by the second argument.

4.3 Operator representation of linear systems

A number of concepts in mathematics and in feedback systems theory can be described using operator theory [65]. Causality, time-invariance, periodicity, and stability are some of the concepts, to name a few, that can be described using this framework for linear time-invariant systems and that can be naturally extended to the class of periodic time-varying systems.

Consider a discrete-time, finite-dimensional, linear, time-invariant system \mathcal{F} described by a set of difference equations with state-space realization

$$\Sigma_{\mathcal{F}} := \begin{cases} \mathbf{x}(k+1) &= A\mathbf{x}(k) + B\mathbf{u}(k) \\ \mathbf{y}(k) &= C\mathbf{x}(k) + D\mathbf{u}(k), \end{cases} \quad (4.3.1)$$

where $\mathbf{x}(k) \in \mathbb{R}^n$ is the state vector, $\mathbf{u}(k) \in \mathbb{R}^m$ is the input vector, and $\mathbf{y}(k) \in \mathbb{R}^p$ is the output vector, with null initial state $\mathbf{x}(0) = 0$. This system can also be regarded as a linear operator from the spaces $F : \mathbb{R}^m \rightarrow \mathbb{R}^p$. The set of all bounded linear operators will be denoted as $\mathcal{L}(\mathbb{R}^m, \mathbb{R}^p)$ and constitutes the focus of the results presented below. In the case where the domain and the range spaces are the same, this set will be denoted as $\mathcal{L}(\mathbb{R}^m)$. To correctly interpret these statements the following basic definitions for linear spaces are required. Consider \mathcal{U} as a linear space over the field $F = \mathbb{R}$.

Definition 4.3.1 A norm is a function $\|\cdot\| : \mathcal{U} \rightarrow \mathbb{R}_0^+$ which satisfies for every $x, y \in \mathcal{U}$ and for every $\alpha \in F$:

1. $\|\alpha x\| = |\alpha| \|x\|$;
2. $\|x\| = 0$ if and if x is the null vector;
3. $\|x + y\| \leq \|x\| + \|y\|$;

Definition 4.3.2 Let \mathcal{U} and \mathcal{Y} be normed linear spaces. The operator $\mathcal{M} : \mathcal{U} \rightarrow \mathcal{Y}$ is:

Linear if given $\alpha, \beta \in F$ and any $x, y \in \mathcal{U}$,

$$\mathcal{M}(\alpha x + \beta y) = \alpha \mathcal{M}(x) + \beta \mathcal{M}(y);$$

Bounded if the norm of \mathcal{M} $\|\mathcal{M}\|$ is finite, i.e.,

$$\|\mathcal{M}\| = \sup_{x \in \mathcal{U}} \frac{\|\mathcal{M}x\|}{\|x\|} < \infty;$$

Normed if there exists a functional $\langle \cdot, \cdot \rangle: \mathcal{U} \times \mathcal{U} \rightarrow \mathbb{R}$ satisfying for any $x, y, z \in \mathcal{U}$, and $\alpha, \beta \in F$:

1. $\langle \alpha x + \beta y, z \rangle = \alpha \langle x, z \rangle + \beta \langle y, z \rangle$;
2. $\langle x, y \rangle = \overline{\langle y, x \rangle}$;
3. $\langle x, x \rangle \geq 0$, $\langle x, x \rangle = 0$ if and only if x is the null vector.

A normed space is said to be *complete* if any Cauchy sequence $u(k) : k = 1, \dots, \infty$ converges, or more precisely if it satisfies

$$\lim_{n \rightarrow \infty, m \rightarrow \infty} \|\mathbf{u}(n) - \mathbf{u}(m)\| = 0.$$

A complete inner product space is called a Hilbert space and a complete normed space is called a Banach space.

The matrix operator associated with the system with realization described in (4.3.1) can be obtained stacking the inputs and outputs as vectors as presented in the following relation:

$$\begin{bmatrix} \mathbf{y}(0) \\ \mathbf{y}(1) \\ \mathbf{y}(2) \\ \vdots \\ \mathbf{y}(k) \\ \vdots \end{bmatrix} = \begin{bmatrix} D & 0 & 0 & \cdots & 0 & \cdots \\ CB & D & 0 & \cdots & 0 & \cdots \\ CAB & CB & D & \cdots & 0 & \cdots \\ \vdots & \vdots & \vdots & \ddots & \vdots & \vdots \\ CA^{k-1}B & CA^{k-2}B & CA^{k-3}B & \cdots & D & \cdots \\ \vdots & \vdots & \vdots & \vdots & \vdots & \ddots \end{bmatrix} \begin{bmatrix} \mathbf{u}(0) \\ \mathbf{u}(1) \\ \mathbf{u}(2) \\ \vdots \\ \mathbf{u}(k) \\ \vdots \end{bmatrix} \quad (4.3.2)$$

or in compact form as $\mathbf{y} = F\mathbf{u}$. This infinite-dimensional matrix is also known as the impulse response matrix due to the fact that column k is the output to an impulse applied to the system at the time-instant k . The Toeplitz structure of the matrix is evident and causality is closely related to the low-triangular structure of matrix D as will be seen later in this section.

Consider now some auxiliary bounded and linear operators. The forward shift operator $\Lambda : l_2(\mathbb{Z}^+, \mathbb{R}^m) \rightarrow l_2(\mathbb{Z}^+, \mathbb{R}^p)$ can be defined as

$$\Lambda(k) = \begin{cases} \mathbf{u}(k-1) & k > 1 \\ 0 & k \leq 1, \end{cases}$$

where $\mathbf{u}(k)$ is the input signal and the associated matrix operator is given by

$$\Lambda = \begin{bmatrix} 0 & 0 & 0 & \cdots \\ I_{p \times m} & 0 & 0 & \cdots \\ 0 & I_{p \times m} & 0 & \cdots \\ \vdots & \vdots & \vdots & \ddots \end{bmatrix}.$$

The backward shift operator $\Lambda^* : l_2(\mathbb{Z}^+, \mathbb{R}^p) \rightarrow l_2(\mathbb{Z}^+, \mathbb{R}^m)$ defined as $\Lambda^*(k) = \mathbf{u}(k+1)$ can be associated with the matrix operator

$$\Lambda^* = \begin{bmatrix} 0 & I_{m \times p} & 0 & \cdots \\ 0 & 0 & I_{m \times p} & \cdots \\ 0 & 0 & 0 & \cdots \\ \vdots & \vdots & \vdots & \ddots \end{bmatrix},$$

where the non-causal nature of this system is evident. Moreover, it can be easily proven that the \mathcal{H}_∞ and \mathcal{H}_2 norms of Λ are unitary and that the composition of Λ^* with Λ is the identity operator, $\Lambda^* \Lambda = I$. The composition of such operators is therefore an isometry.

Another interesting operator, crucial in the definition of causality, is the truncation operator $\Pi_K : l_2(\mathbb{Z}^+, \mathbb{R}^m) \rightarrow l_2(\mathbb{Z}^+, \mathbb{R}^p)$, defined as

$$\Pi_K(k) = \begin{cases} u(k) & k \leq K \\ 0 & k > K, \end{cases}$$

which corresponds to the matrix operator

$$\Pi_K = \left. \begin{bmatrix} I_{p \times m} & 0 & \cdots & 0 & 0 & \cdots \\ 0 & I_{p \times m} & \cdots & 0 & 0 & \cdots \\ \vdots & \vdots & \ddots & \vdots & \vdots & \vdots \\ 0 & 0 & \cdots & I_{p \times m} & 0 & \cdots \\ 0 & 0 & \cdots & 0 & 0 & \cdots \\ \vdots & \vdots & \vdots & \vdots & \vdots & \ddots \end{bmatrix} \right\} K \text{ blocks of size } p \times m.$$

These functions allow elegant definitions of some key concepts on systems theory presented in the next propositions.

Proposition 4.3.3 *A discrete-time system is time-invariant if its corresponding matrix operator F commutes with the shift operator or, stated mathematically, if it verifies*

$$F\Lambda = \Lambda F.$$

This proposition can be interpreted as time-invariance leads to the same output signals: when the shift operator is applied to the output of the operator F , and when the operator F is applied to a shifted version of the input signal.

Proposition 4.3.4 *A discrete-time system is causal if its corresponding matrix operator verifies the relation*

$$\Pi_K F \Pi_K = \Pi_K F.$$

Proposition 4.3.5 *A discrete-time system is periodic time-variant with period M if its corresponding matrix operator F commutes with the M^{th} power shift operator, expressed as*

$$F\Lambda^M = \Lambda^M F.$$

Two more operators relating signals expressed at different time scales will be introduced next. Given an n dimensional signal \mathbf{u} , represented as an infinite sequence, the *de-multiplexing* operator $W_M : l_2(\mathbb{Z}^+, \mathbb{R}^n) \rightarrow l_2(\mathbb{Z}^+, \mathbb{R}^{nM})$ can be defined as

$$\mathbf{u} = \begin{bmatrix} \mathbf{u}(0) \\ \mathbf{u}(1) \\ \vdots \\ \mathbf{u}(M-1) \\ \mathbf{u}(M) \\ \mathbf{u}(M+1) \\ \vdots \end{bmatrix} \rightarrow \bar{\mathbf{u}} = W_M \mathbf{u} = \begin{bmatrix} \mathbf{u}(0) & \mathbf{u}(1) & \cdots & \mathbf{u}(M-1) \\ \mathbf{u}(M) & \mathbf{u}(M+1) & \cdots & \mathbf{u}(2M-1) \\ \mathbf{u}(2M) & \mathbf{u}(2M+1) & \cdots & \mathbf{u}(3M-1) \\ \vdots & \vdots & \vdots & \vdots \end{bmatrix}, \quad (4.3.3)$$

resulting in M sub-sequences extracted from the original one. From the definitions of the forward shift operator Λ and the de-multiplexing operator W_M , the relation

$$\Lambda W_M = W_M \Lambda^M \quad (4.3.4)$$

is obvious and can be interpreted as the equivalence between one forward shift in the de-multiplexed signal and M forward shifts in the original signal space.

The inverse of the de-multiplexing operator (4.3.3) is the multiplexing operator defined as $W_M^{-1} : l_2(\mathbb{Z}^+, \mathbb{R}^{nM}) \rightarrow l_2(\mathbb{Z}^+, \mathbb{R}^n)$

$$\bar{\mathbf{u}} = \begin{bmatrix} \mathbf{u}(0) & \mathbf{u}(1) & \cdots & \mathbf{u}(M-1) \\ \mathbf{u}(M) & \mathbf{u}(M+1) & \cdots & \mathbf{u}(2M-1) \\ \mathbf{u}(2M) & \mathbf{u}(2M+1) & \cdots & \mathbf{u}(3M-1) \\ \vdots & \vdots & \vdots & \vdots \end{bmatrix} \rightarrow \mathbf{u} = W_M^{-1} \bar{\mathbf{u}} = \begin{bmatrix} \mathbf{u}(0) \\ \mathbf{u}(1) \\ \vdots \\ \mathbf{u}(M-1) \\ \mathbf{u}(M) \\ \mathbf{u}(M+1) \\ \vdots \end{bmatrix}, \quad (4.3.5)$$

verifying the relation $\Lambda^M W_M^{-1} = W_M^{-1} \Lambda$, which states the same equivalence as expressed by (4.3.4). Moreover, from the definitions of W_M and W_M^{-1} it is immediate that they are isometric as they verify $W_M W_M^{-1} = I = W_M^{-1} W_M$.

The stability of a system is a property of utmost importance. Several classic definitions of stability exist in the systems theory literature. Next, an input/output definition will be presented, based on the ratio of energy in the output of a system \mathcal{G} , given the energy fed into its input.

Definition 4.3.6 *The operator G associated with the linear system $\mathcal{G} : l_2(\mathbb{Z}^+, \mathbb{R}^m) \rightarrow l_2(\mathbb{Z}^+, \mathbb{R}^p)$ is input-output stable if and only if*

$$\|G\| = \sup_{\substack{\mathbf{u} \in l_2 \\ \Pi_K \mathbf{u} \neq 0}} \frac{\|\Pi_K G \mathbf{u}\|_2}{\|\Pi_K \mathbf{u}\|_2} < \infty, \quad \forall K \in \mathbb{Z}.$$

Note that in this definition no constraints on the system time-invariance are imposed, which constitutes an interesting feature to be explored. Moreover, this definition presents the advantage of implying causality for the system under study, as expressed in the next theorem. For periodic time-varying systems the concept of stability will be further worked out using the \mathcal{H}_2 and the \mathcal{H}_∞ induced norms, in section 4.7.

Theorem 4.3.7 *If the operator G associated with the linear system \mathcal{G} as defined in 4.3.6 is stable, then the system under study is causal.*

Proof: Assume that the system is not causal. In this case, there exists an input \mathbf{w} such that

$$\Pi_K G \mathbf{w} \neq \Pi_K G \Pi_K \mathbf{w}.$$

Applying the auxiliary input $\mathbf{u} = \mathbf{w} - \Pi_K \mathbf{w}$ then

$$\Pi_K \mathbf{u} = \Pi_K (\mathbf{w} - \Pi_K \mathbf{w}) = \Pi_K \mathbf{w} - \Pi_K \Pi_K \mathbf{w} = 0.$$

However, if the linear system under study is not causal, then

$$\Pi_K G \mathbf{u} = \Pi_K G (\mathbf{w} - \Pi_K \mathbf{w}) = \Pi_K G \mathbf{w} - \Pi_K G \Pi_K \mathbf{w} \neq 0.$$

Note that the previous two relations were used in the definition of the stability introduced above and in this case (null denominator with non-null numerator) there exists an infinite amplification for this input and therefore the system is not stable, which is a contradiction and concludes the proof of the result at hand. ■

4.4 *Lifting technique*

In this section an equivalence between discrete-time periodic systems and a subset of the linear, time-invariant, discrete-time systems introduced by Friedland [26] will be presented. This technique is commonly denominated as *lifting*. Davis [24] used the same technique for stability analysis of the feedback connection of a linear, time-invariant plant and a periodic memoryless controller. In [42, 63] Khargonekar showed the superiority of linear, periodic time-varying discrete-time controllers, resorting also to this technique. These were some of the steps that paved the way for the use of periodic dynamic systems in filtering, estimation, and control of multi-rate discrete-time systems and in multi-rate sampled-data systems.

Consider the discrete-time linear system \mathcal{P} , with m inputs, p outputs, and period M , expressed as in (4.2.1). This system has a realization, repeated in the following for convenience,

$$\Sigma_{\mathcal{P}} := \begin{cases} \mathbf{x}(k+1) & = A(k)\mathbf{x}(k) + B(k)\mathbf{u}(k) \\ \mathbf{y}(k) & = C(k)\mathbf{x}(k) + D(k)\mathbf{u}(k) \end{cases},$$

where the periodic characteristic of the system implies that the matrices in the state space representation verify $A(k+M) = A(k)$, $B(k+M) = B(k)$, $C(k+M) = C(k)$, and $D(k+M) = D(k)$, independent of the realization used. The state of the system (4.2.1) at instant k can be

evaluated in terms of the initial state $\mathbf{x}(k_0)$ and the input \mathbf{u} , along the interval $j = k_0, \dots, k-1$ according to

$$\mathbf{x}(k) = \Phi_{(k,k_0)}\mathbf{x}(k_0) + \sum_{j=k_0}^{k-1} \Phi_{(k,j+1)}B(j)u(j),$$

where the auxiliary function $\Phi_{(i,j)}$, defined as

$$\Phi_{(i,j)} = \begin{cases} A(i-1)A(i-2)\cdots A(j+1)A(j) & i > j \\ I_{n \times n} & i = j \\ 0 & i < j \end{cases} \quad (4.4.1)$$

was used. Note the similarity between this auxiliary function and the classical transition matrix, for $i \geq j$. Given the evolution of the state of the dynamic system (4.2.1) expressed above, the output signal can be written as

$$\mathbf{y}(k) = C(k)\Phi_{(k,k_0)}\mathbf{x}(k_0) + C(k)\sum_{j=k_0}^{k-1} \Phi_{(k,j+1)}B(j)u(j) + D(k)\mathbf{u}(k).$$

Applying the de-multiplexing operator W_M to the inputs and outputs of system \mathcal{P} described by (4.2.1), a new operator $\bar{P} : l_2(\mathbb{Z}^+, \mathbb{R}^{mM}) \rightarrow l_2(\mathbb{Z}^+, \mathbb{R}^{pM})$ named the *lift* of system \mathcal{P} can be defined. The relations among the signals and operators involved are resumed in the commutative diagram presented in figure 4.4.1. Based on the operators (4.3.3), and (4.3.5), previously intro-

$$\begin{array}{ccc} & \tilde{P} & \\ l_2(\mathbb{Z}^+, \mathbb{R}^{mM}) & \longrightarrow & l_2(\mathbb{Z}^+, \mathbb{R}^{pM}) \\ W_M \uparrow & & \uparrow W_M \\ l_2(\mathbb{Z}^+, \mathbb{R}^m) & \xrightarrow{P} & l_2(\mathbb{Z}^+, \mathbb{R}^p) \end{array}$$

Figure 4.4.1: The operator P associated with the system \mathcal{P} and the *lifted* operator \bar{P} .

duced and taking into account the maps expressed in the above diagram, the lift operator can be written as $\Omega_M : P \rightarrow W_M P W_M^{-1}$, resulting in this case that $\bar{P} = W_M P W_M^{-1}$. Using the definition of time-invariance introduced in proposition 4.3.3, \bar{P} can be proven to be time-invariant. The proof follows along the set of identities

$$\bar{P}\Lambda = W_M P W_M^{-1}\Lambda = W_M P \Lambda^M W_M^{-1} = W_M \Lambda^M P W_M^{-1} = \Lambda \bar{P},$$

where the relations (4.3.4) and (4.3.5) were used.

The inverse lift operator Ω^{-1} can be defined as $\Omega^{-1} : \bar{P} \rightarrow W_M^{-1}\bar{P}W_M$. According to the definition 4.3.5, it can be proven to be M -periodic, i.e.,

$$P\Lambda^M = W_M^{-1}\bar{P}W_M\Lambda^M = W_M^{-1}\bar{P}\Lambda W_M = W_M^{-1}\Lambda\bar{P}W_M = \Lambda^M P.$$

A realization for the lifted version of the periodic system (4.2.1) can be obtained by defining a stacked version for the input and output vectors along the \mathcal{K}^{th} period

$$\mathbf{u}(\mathcal{K}) = \begin{bmatrix} \mathbf{u}(kM) \\ \mathbf{u}(kM+1) \\ \vdots \\ \mathbf{u}(kM+M-1) \end{bmatrix}, \quad \mathbf{y}(\mathcal{K}) = \begin{bmatrix} \mathbf{y}(kM) \\ \mathbf{y}(kM+1) \\ \vdots \\ \mathbf{y}(kM+M-1) \end{bmatrix}, \quad (4.4.2)$$

respectively, where \mathcal{K} ranges from kM to $kM+M-1$. The system state at instant $\mathcal{K}+1 = kM+M$, based on the state at instant \mathcal{K} and on the inputs specified in (4.4.2), has the realization

$$\Sigma_{\bar{P}} := \begin{cases} x(\mathcal{K}+1) &= \bar{A}x(\mathcal{K}) + \bar{B}u(\mathcal{K}) \\ y(\mathcal{K}) &= \bar{C}x(\mathcal{K}) + \bar{D}u(\mathcal{K}). \end{cases} \quad (4.4.3)$$

To obtain the matrices for the realization (4.4.3) the dynamics of the periodic system (4.2.1) must be computed along the M instants of a period and written in matrix form, resulting in

$$\bar{C} = \begin{bmatrix} \bar{A} = \Phi_{(M,0)}, & \bar{B} = [\Phi_{(M,1)}B(0) \quad \cdots \quad \Phi_{(M,M-1)}B(M-2) \quad B(M-1)], \\ C(0) & D(0) & \cdots & 0 & 0 \\ C(1)\Phi_{(1,0)} & C(1)B(0) & \cdots & 0 & 0 \\ \vdots & \vdots & \ddots & \vdots & \vdots \\ C(M-2)\Phi_{(M-2,0)} & C(M-2)\Phi_{(M-2,1)}B(0) & \cdots & D(M-2) & 0 \\ C(M-1)\Phi_{(M-1,0)} & C(M-1)\Phi_{(M-1,1)}B(0) & \cdots & C(M-1)B(M-2) & D(M-1) \end{bmatrix}. \quad (4.4.4)$$

The operator \bar{P} associated with the lifted system \bar{P} , assuming null initial conditions, is given by

$$\bar{P} = \begin{bmatrix} D(0) & \cdots & 0 & \cdots & \cdots \\ \vdots & \ddots & \vdots & \cdots & \cdots \\ C(M-1)\Phi_{(M-1,1)}B(0) & \cdots & D(M-1) & 0 & \cdots \\ C(M)\Phi_{(M,1)}B(0) & \cdots & C(M)B(M-1) & D(M) & \cdots \\ \vdots & \vdots & \vdots & \vdots & \ddots \end{bmatrix},$$

where the upper-left block with dimensions $pM \times mM$ coincides with the \bar{D} matrix. Using the time-invariance nature of this system, the associated system operator can be proven to have the Toeplitz structure

$$\bar{P} = \begin{bmatrix} M_0 & 0 & 0 & \cdots \\ M_1 & M_0 & 0 & \ddots \\ M_2 & M_1 & M_0 & \ddots \\ \vdots & \ddots & \ddots & \ddots \end{bmatrix},$$

where each block M_i has the dimensions $pM \times mM$ and $M_0 = \bar{D}$.

Some properties of the lift operator Ω_M are outlined next. For an in-depth characterization of the lift operator as well as proofs of the statements presented, see [35], and the references therein.

- The operator Ω_M is time-invariant;
- The operators Ω_M and Ω_M^{-1} preserve the matrix representation of the linear system (invariant or time-varying);
- The operators Ω_M and Ω_M^{-1} are isomorphisms, i.e., they are bijective and linear.
- The operators Ω_M and Ω_M^{-1} are isometric, and they preserve the induced norms of the original systems.
- The operators Ω_M and Ω_M^{-1} preserve the input/output stability characteristics of the causal linear periodic systems.
- The operator Ω_M preserves the periodic characteristic of the composition of periodic operators, i.e.,

$$\Omega_M(GoF) = \Omega_M(G)o\Omega_M(F),$$

where o is the composition operator and the operators F and G are of appropriate dimensions. Moreover, it also preserves the linearity, causality, and time-invariance characteristics of the composition operation.

4.5 Periodic Riccati based estimators

In this section recent solutions for minimization of the \mathcal{H}_2 norm of the estimation error for linear discrete-time periodic systems resorting to the solution of Riccati equations using an indirect technique based on the lift operator will be presented. The reasons for presenting these results are twofold: to introduce the technical conditions for the existence and uniqueness of solutions of the periodic estimation problem at hand; and to compare these solutions with a new synthesis methodology of estimators for periodic systems, based on the \mathcal{H}_2 and \mathcal{H}_∞ norms minimization, resorting to convex optimization problems expressed in the form of LMIs. This new methodology will be presented in section 4.8. The technical conditions presented in this section will also play an important role in establishing the feasibility conditions for such new design methods.

4.5.1 Periodic estimators

In control and estimation problems, where actuation variables or sensor measurements are available at different sampling rates, a multi-rate system is naturally obtained as described in section 4.2. The estimators for periodic systems, conducing to periodic Kalman filters, are presented in the following.

Consider a discrete-time, finite-dimensional, linear, periodically time-varying system $\mathcal{P}_s : \mathbf{u} \rightarrow \mathbf{y}$. This system is described by a set of difference equations with state-space realization

$$\Sigma_{\mathcal{P}_s} := \begin{cases} \mathbf{x}(k+1) &= A(k)\mathbf{x}(k) + B(k)\mathbf{u}(k) + G(k)\mathbf{w}(k) \\ z(k) &= C(k)\mathbf{x}(k) + \mathbf{v}(k) \end{cases} \quad (4.5.1)$$

where $\mathbf{x}(k) \in \mathbb{R}^n$ is the state vector, $\mathbf{u}(k) \in \mathbb{R}^m$ is the input vector, and $\mathbf{y}(k) \in \mathbb{R}^p$ is the output vector. Note that the state and the measurements are corrupted by white, gaussian noise, with zero mean and with covariance matrices

$$\begin{aligned} E[w(k)w(j)^T] &= Q(k)\delta(k-j) \\ E[v(k)v(j)^T] &= R(k)\delta(k-j) \end{aligned}$$

where $\delta(k-j)$ is the Kronecker δ and $Q(k) \geq 0$ and $R(k) > 0$. The periodic characteristic of the system implies that the matrices in the state-space representation verify $A(k+M) = A(k)$, $B(k+M) = B(k)$, $C(k+M) = C(k)$, $G(k+M) = G(k)$, $Q(k+M) = Q(k)$ and $R(k+M) = R(k)$.

Under the technical conditions that will be detailed next, the estimator that presents the minimum expected error variance is a periodic Kalman filter, as convincingly argued in [10, 74].

The structure of such filter is given by

$$\hat{\mathbf{x}}(k+1) = A(k)\hat{\mathbf{x}}(k) + B(k)\mathbf{u}(k) + K(k)[\mathbf{z}(k) - C(k)\hat{\mathbf{x}}(k)], \quad (4.5.2)$$

where $\hat{\mathbf{x}}(k) \in \mathcal{X}$ is the state estimate and the Kalman gain $K(k) \in \mathbb{R}^{n \times m}$ is defined as

$$K(k) = P(k)C^T(k) (C(k)P(k)C^T(k) + R(k))^{-1}, \quad (4.5.3)$$

where $P(k) = E[(\hat{\mathbf{x}}(k) - \mathbf{x}(k))(\hat{\mathbf{x}}(k) - \mathbf{x}(k))^T]$ is the covariance of the error which verifies, at each step, the Riccati equation with periodic parameters

$$\begin{aligned} P(k+1) &= A(k)P(k)A^T(k) + G(k)Q(k)G^T(k) \\ &\quad - A(k)P(k)C^T(k) (C(k)P(k)C^T(k) + R(k))^{-1} C(k)P(k)A^T(k). \end{aligned} \quad (4.5.4)$$

The solution of this periodic Riccati equation is in general, not periodic. However, as in the invariant case, the periodic stationary positive semi-definite solution for an infinite prediction interval is sought.

4.5.2 Existence of a solution for the periodic system

The periodic Riccati equation associated with the prediction problem at hand has been presented in [10], for non-reversible and non-stabilizable systems. The existence, uniqueness, and stability properties of Symmetric Periodic Positive Semi-definite (SPPS) solutions for the periodic Riccati equation (4.5.4) have been studied in [73]. The notation $X(\cdot)$ will be used to denote any of the matrices $X(k)$ involved in the periodic description of the system. The following definitions are central to the results that follows:

Definition 4.5.1 $\Phi_k = \Phi(k+M, k)$ is the monodromy of the periodic system (4.5.1), at instant k .

Note that the eigenvalues of Φ_k are independent of k and are named the characteristic multipliers of $A(\cdot)$. In general a periodic system is asymptotically stable if and only if the characteristic multipliers are all inside the unit circle.

Definition 4.5.2 An eigenvalue λ of Φ_k is called $(A(\cdot), B(\cdot))$ reachable at time-instant k if and only if it is a reachable mode of $(\Phi_k, W_{rea}(k+M, k))$, where

$$W_{rea}(k+M, k) = \sum_{i=k}^{k+M-1} \Phi(k+M, i) B(i-1) B^T(i-1) \Phi^T(k+M, i)$$

is the reachability grammian matrix of $(A(\cdot), B(\cdot))$.

Definition 4.5.3 The pair $(A(\cdot), C(\cdot))$ is detectable at time k if and only if the pair $(W_{obs}(k+M, k), \Phi_k)$ is detectable, where

$$W_{obs}(k+M, k) = \sum_{i=k}^{k+M-1} \Phi(i, k)^T C^T(i) C(i) \Phi(i, k)$$

is the observability grammian matrix of $(A(\cdot), C(\cdot))$.

The real symmetric periodic non-negative definite solutions of the periodic Riccati equation that, after computing the Kalman gain, give rise to a system with characteristic multipliers inside, or on, the unit circle, are called strong solutions. Existence, uniqueness, and stability properties of strong solutions are vital for periodic estimator synthesis and are presented next.

Lemma 4.5.4 [73] Let $P(\cdot)$ be a periodic strong solution of the periodic Riccati difference equation (PRDE). Then:

- a) if the eigenvalues of Φ_k on the unit circle are $(A(\cdot), B(\cdot))$ reachable, then $P(\cdot)$ is stabilizing;
- b) if the eigenvalues of $\Phi(k)$ inside, or on, the unit circle are $(A(\cdot), B(\cdot))$ reachable for all k , then $P(\cdot)$ is stabilizing and positive definite for all k .

Lemma 4.5.5 [73] If the eigenvalues of $\Phi(k+M, k)$ outside the unit circle are $(A(\cdot), B(\cdot))$ reachable, then every symmetric periodic non-negative definite solution of the PRDE is a strong solution.

Theorem 4.5.6 [73] The periodic stabilizing solution of the PRDE exists and is unique if and only if $(A(\cdot), C(\cdot))$ is detectable and the eigenvalues of Φ_k on the unit circle are $(A(\cdot), B(\cdot))$ reachable.

Theorem 4.5.7 [73] The periodic stabilizing solution of the PRDE exists and is the only symmetric periodic non-negative definite solution of the PRDE if and only if $(A(\cdot), C(\cdot))$ is detectable and the eigenvalues of Φ_k outside the unit circle are $(A(\cdot), B(\cdot))$ reachable.

Theorem 4.5.8 [73] *The periodic stabilizing solution of the PRDE exists and is positive definite for all k if and only if $(C(\cdot), A(\cdot))$ is detectable and the eigenvalues of Φ_k inside, or on, the unit circle are $(A(\cdot), B(\cdot))$ reachable for all k .*

Stability conditions for periodic systems were set by Bittanti in the *Periodic Lyapunov Lemma* [11] presented next, which is closely linked to the framework that will be introduced later in this chapter.

Lemma 4.5.9 [11] *The periodic system (4.5.1) is stable if and only if for any periodic $C(\cdot)$ such that the pair $(A(\cdot), C(\cdot))$ is detectable, there exists a periodic, positive semi-definite solution $Q(\cdot)$ for the Lyapunov equation*

$$Q(k+1) = A^T(k)Q(k)A(k) + C^T(k)C(k). \quad (4.5.5)$$

Given the existence and uniqueness of solutions and the technical conditions for the stability of the periodic systems at hand, the final question is how to obtain the periodic Kalman gain matrices to use in the filter? Due to the periodic nature of the Riccati equation involved, the stationary solution of the discrete-time algebraic Riccati equation setting $P(k+1) = P(k)$ does not result in the required periodic solution. A solution will be presented next.

4.6 Periodic and invariant estimators equivalence

Based on the lifting technique, the periodic estimator introduced in section 4.5.1 can be synthesized using the equivalent invariant system [22]. The lifted version of the periodic system (4.5.1) has the realization

$$\Sigma_{\bar{p}_s} := \begin{cases} \mathbf{x}(\mathcal{K}+1) &= \bar{A}\mathbf{x}(\mathcal{K}) + \bar{B}\mathbf{u}(\mathcal{K}) + \bar{G}\mathbf{w}(\mathcal{K}) \\ \mathbf{z}(\mathcal{K}) &= \bar{C}\mathbf{x}(\mathcal{K}) + \bar{D}_u\mathbf{u}(\mathcal{K}) + \bar{D}_w\mathbf{w}(\mathcal{K}) + \mathbf{v}(\mathcal{K}), \end{cases}$$

where $\mathbf{w}(\mathcal{K})$ and $\mathbf{v}(\mathcal{K})$ are the stacked versions of state and observation noises. The associated prediction estimator is

$$\hat{\mathbf{x}}(\mathcal{K}+1) = \bar{A}\hat{\mathbf{x}}(\mathcal{K}) + \bar{B}\mathbf{u}(\mathcal{K}) + \bar{K}[\mathbf{z}(\mathcal{K}) - \bar{C}\hat{\mathbf{x}}(\mathcal{K}) - \bar{D}_u\mathbf{u}(\mathcal{K})].$$

The estimation error dynamics $\tilde{\mathbf{x}}(\mathcal{K}) = \hat{\mathbf{x}}(\mathcal{K}) - \mathbf{x}(\mathcal{K})$, using the previous relations, is

$$\tilde{\mathbf{x}}(\mathcal{K} + 1) = (\bar{A} - \bar{K}\bar{C})\tilde{\mathbf{x}}(\mathcal{K}) - \bar{G}\mathbf{w}(\mathcal{K}) + \bar{K}\bar{D}_w\mathbf{w}(\mathcal{K}) + \bar{K}\mathbf{v}(\mathcal{K})$$

and the estimation error covariance $P(\mathcal{K}) = E[\tilde{\mathbf{x}}(\mathcal{K})\tilde{\mathbf{x}}^T(\mathcal{K})]$ verifies the relation

$$\begin{aligned} P(\mathcal{K} + 1) &= \bar{A}P(\mathcal{K})\bar{A}^T + \bar{G}\bar{Q}\bar{G}^T + \bar{K}(\bar{R} + \bar{C}P(\mathcal{K})\bar{C}^T + \bar{D}_w\bar{Q}\bar{D}_w^T)\bar{K}^T \\ &\quad - \bar{K}(\bar{C}P(\mathcal{K})\bar{A}^T + \bar{D}_w\bar{Q}\bar{G}^T) - (\bar{A}P(\mathcal{K})\bar{C}^T + \bar{G}\bar{Q}\bar{D}_w^T)\bar{K}^T, \end{aligned} \quad (4.6.1)$$

where \bar{Q} and \bar{R} are the covariance of the state and observation noises $w(\mathcal{K})$ and $v(\mathcal{K})$, respectively. Only the last three terms have a quadratic matrix polynomial in the unknown \bar{K} . The matrix $(\bar{R} + \bar{C}P(\mathcal{K})\bar{C}^T + \bar{D}_w\bar{Q}\bar{D}_w^T)$ is symmetric and non-negative definite and therefore can be written as the product of SS^T . Using the two relations, the Riccati equation can be written as

$$\begin{aligned} P(\mathcal{K} + 1) &= \bar{A}P(\mathcal{K})\bar{A}^T + \bar{G}\bar{Q}\bar{G}^T \\ &\quad - (\bar{A}P(\mathcal{K})\bar{C}^T + \bar{G}\bar{Q}\bar{D}_w^T)(\bar{R} + \bar{C}P(\mathcal{K})\bar{C}^T + \bar{D}_w\bar{Q}\bar{D}_w^T)^{-1}(\bar{C}P(\mathcal{K})\bar{A}^T + \bar{D}_w\bar{Q}\bar{G}^T) \\ &\quad \{ \bar{K}S - (\bar{A}P(\mathcal{K})\bar{C}^T + \bar{G}\bar{Q}\bar{D}_w^T)S^{-T} \} \{ \bar{K}S - (\bar{A}P(\mathcal{K})\bar{C}^T + \bar{G}\bar{Q}\bar{D}_w^T)S^{-T} \}^T \end{aligned}$$

where only the last term depends on \bar{K} . The minimum covariance is obtained when

$$\bar{K}S = \bar{A}P(\mathcal{K})\bar{C}^T + \bar{G}\bar{Q}\bar{D}_w^T)S^{-T}$$

or using the definition of SS^T

$$\bar{K} = (\bar{A}P(\mathcal{K})\bar{C}^T + \bar{G}\bar{Q}\bar{D}_w^T)(\bar{R} + \bar{C}P(\mathcal{K})\bar{C}^T + \bar{D}_w\bar{Q}\bar{D}_w^T)^{-1}.$$

The resulting Riccati equation is

$$\begin{aligned} P(\mathcal{K} + 1) &= \bar{A}P(\mathcal{K})\bar{A}^T + \bar{G}\bar{Q}\bar{G}^T \\ &\quad - (\bar{A}P(\mathcal{K})\bar{C}^T + \bar{G}\bar{Q}\bar{D}_w^T)(\bar{R} + \bar{C}P(\mathcal{K})\bar{C}^T + \bar{D}_w\bar{Q}\bar{D}_w^T)^{-1}(\bar{C}P(\mathcal{K})\bar{A}^T + \bar{D}_w\bar{Q}\bar{G}^T), \end{aligned} \quad (4.6.2)$$

which is a non-standard Riccati equation. Introducing the new variables

$$\begin{aligned} \tilde{R} &= \bar{R} + \bar{D}_w\bar{Q}\bar{D}_w^T, \\ \tilde{A} &= \bar{A} - \bar{G}\bar{Q}\bar{D}_w^T\tilde{R}^{-1}\bar{C}, \quad \text{and} \\ \tilde{G}\tilde{G}^T &= \bar{G}\bar{Q}\bar{G}^T - \bar{G}\bar{Q}\bar{D}_w^T\tilde{R}^{-1}\bar{D}_w\bar{Q}\bar{G}^T \end{aligned} \quad (4.6.3)$$

the following standard Riccati equation is obtained:

$$P(\mathcal{K} + 1) = \tilde{A}P(\mathcal{K})\tilde{A}^T + \tilde{G}\tilde{G}^T - \tilde{A}P(\mathcal{K})\tilde{C}^T(\tilde{R} + \tilde{C}P(\mathcal{K})\tilde{C}^T)^{-1}\tilde{C}P(\mathcal{K})\tilde{A}^T. \quad (4.6.4)$$

The established equivalence allows the design of the periodic stationary estimator using an off-line procedure, composed of the following steps:

Algorithm 1:

Step 1: Obtain the lifted system

Given the system described by (4.5.1), the system is lifted using the method described by (4.4.4).

Step 2: Estimation error covariance computation

Compute the auxiliary variables \bar{R} , \bar{A} , and $\bar{G}\bar{G}^T$ and solve the Riccati equation (4.6.4).

The stationary estimate error covariance matrix $P(\mathcal{K})$ is equal to that obtained using (4.5.4) at the instant kM . Therefore, that equation can be iterated along the period to obtain P_i and the Kalman gain K_i , using (4.5.4) and (4.5.3), respectively.

Step 3: Initialization

Initialize the filter state $\hat{\mathbf{x}}(0) = \mathbf{x}_0$ and the error covariance estimate $P(0)$.

Step 4: On-line estimator

Iterate the estimator given by (4.5.2), where the subscript k denotes the matrices at instant $(k \text{ MOD } M)$. Set $k = k + 1$ and repeat Step 4.

In this off-line method no system of non-linear equations must be solved. Numerical error propagation is avoided and, with minor computations, well known Riccati equation solvers can be used.

4.7 Norms of periodic systems

This section will introduce two new methodologies to evaluate the \mathcal{H}_∞ and the \mathcal{H}_2 norms of periodic systems using LMIs. The approach used borrows from the results presented in chapter 2

and constitutes theoretical results that can be used in the synthesis of periodic feedback systems in the same manner as described in the aforementioned chapter. In this thesis, as the main focus is on estimation, the periodic estimators with the Luenberger's observer structure that minimize the \mathcal{H}_∞ and the \mathcal{H}_2 norms of an auxiliary signal will be presented.

4.7.1 \mathcal{H}_∞ norm

Consider a discrete-time, finite-dimensional, linear, periodically time-varying system \mathcal{P}_M , with system time period M described by

$$\Sigma_{\mathcal{P}_M} := \begin{cases} \mathbf{x}(k+1) &= A(k)\mathbf{x}(k) + B(k)\mathbf{w}(k) \\ \mathbf{y}(k) &= C(k)\mathbf{x}(k) + D(k)\mathbf{w}(k), \end{cases} \quad (4.7.1)$$

where $\mathbf{x}(k) \in \mathbb{R}^n$ is the state vector, $\mathbf{w}(k) \in \mathbb{R}^m$ is the input vector with m components, and $\mathbf{y}(k) \in \mathbb{R}^p$. Let the initial state $\mathbf{x}(k_0)$ be 0.

The square \mathcal{H}_∞ norm of such systems was presented in [61] as a particular case for general time-varying systems. The approach presented was based on linear matrix inequalities of infinite dimension, which generally precludes the use of commercial software packages available. In the case of periodic systems, finite-dimensional inequalities were recovered. However, the square \mathcal{H}_∞ norm is a different concept from the classical definition which corresponds to the approach presented in chapter 2.

Due to the linearity and causality characteristics of (4.7.1), the definition presented for the \mathcal{H}_∞ norm

$$\|P\|_\infty = \sup_{\mathbf{w} \in l_2} \frac{\|\mathbf{y}\|_2}{\|\mathbf{w}\|_2},$$

is also valid (see [25] for details). The isometric properties of the W_M and W_M^{-1} operators imply that the \mathcal{H}_∞ norms of the original and lifted system $\bar{P}_M = W_M P_M W_M^{-1}$ are the same. Moreover, an immediate consequence of this fact is that the lift operator preserves any induced norm (see [35]).

The \mathcal{H}_∞ norm computation for the system described by (4.7.1), from the input $\mathbf{w}(k)$ to the output $\mathbf{y}(k)$, both considered to be signals in the set $l_2(\mathbb{Z}^+)$, can be performed based on the system dissipativity property as stated in the next theorem.

Theorem 4.7.1² Let the system $\mathcal{P}_M : \mathcal{U} \rightarrow \mathcal{Y}$ in (4.7.1) be $(A(\cdot), C(\cdot))$ detectable with all the eigenvalues of Φ_k on the unit circle being $(A(\cdot), B(\cdot))$ reachable and let $\gamma > 0$ be a real number.

The following statements are equivalent:

1. $\|P_M\|_\infty < \gamma$;

2. The gain of the system verifies

$$\sup_{\mathbf{w} \in \ell_2} \frac{\|\mathbf{y}\|_2}{\|\mathbf{w}\|_2} < \gamma,$$

with null initial conditions, $\mathbf{x}(0) = 0$;

3. The system is strictly dissipative with respect to the supply function

$$s(\mathbf{w}, \mathbf{y}) = \gamma^2 \|\mathbf{w}\|_2^2 - \|\mathbf{y}\|_2^2;$$

4. There exist symmetric matrices $P(i) = P^T(i) \in \mathbb{R}^{n \times n}$, $i = 0, \dots, M-1$, such that the set of LMIs

$$\begin{bmatrix} -P(i) & 0 & A^T(i)P(i+1) & C^T(i) \\ 0 & -\gamma^2 I_m & B^T(i)P(i+1) & D^T(i) \\ P(i+1)A(i) & P(i+1)B(i) & -P(i+1) & 0 \\ C(i) & D(i) & 0 & -I_p \end{bmatrix} < 0 \quad (4.7.2)$$

for $i = 0, \dots, M-1$.

Proof: Under the technical conditions presented, the existence and the uniqueness of a periodic stabilizing solution is guaranteed, see section 4.5.1. In that case, the equivalence among the first three items follows the same lines of argument used for the continuous and the discrete time-invariant cases. The fourth item can be obtained using the dissipativity concept introduced earlier in 2.8.2, with the supply function

$$s(\mathbf{w}, \mathbf{y}) = \gamma^2 \|\mathbf{w}\|_2^2 - \|\mathbf{y}\|_2^2,$$

leading to the set of LMIs for $i = 0, \dots, M-1$

$$\begin{bmatrix} A^T(i)P(i+1)A(i) - P(i) & A^T(i)P(i+1)B(i) \\ B^T(i)P(i+1)A(i) & B^T(i)P(i+1)B(i) \end{bmatrix}$$

²This theorem was derived independently. Later it came to the knowledge of the author that in [12] the same result was presented.

$$+ \begin{bmatrix} C^T(i)C(i) & C^T(i)D(i) \\ D^T(i)C(i) & D^T(i)D(i) - \gamma^2 I_m \end{bmatrix} < 0.$$

The i^{th} LMI in the aforementioned set can be written as

$$\begin{bmatrix} -P(i) & 0 \\ 0 & -\gamma^2 I_m \end{bmatrix} + \begin{bmatrix} A^T(i) \\ B^T(i) \end{bmatrix} P(i+1) [A(i)B(i)] + \begin{bmatrix} C^T(i) \\ D^T(i) \end{bmatrix} [C(i)D(i)] < 0,$$

resulting in

$$\begin{bmatrix} -P(i) & 0 & A^T(i) & C^T(i) \\ 0 & -\gamma^2 I_m & B^T(i) & D^T(i) \\ A(i) & B(i) & -P^{-1}(i+1) & 0 \\ C(i) & D(i) & 0 & -I_p \end{bmatrix} < 0.$$

Pre and post-multiplying each one of these LMIs in $P(i)$, and in $P^{-1}(i+1)$, $i = 0, \dots, M-1$ by

$$\begin{bmatrix} I_n & 0 & 0 & 0 \\ 0 & I_m & 0 & 0 \\ 0 & 0 & P(i+1) & 0 \\ 0 & 0 & 0 & I_p \end{bmatrix},$$

and taking into consideration that the set of matrices $P(i)$ verify $P(i+M) = P(i)$, the set of LMIs (4.7.2) is obtained. ■

4.7.2 \mathcal{H}_2 norm

In the literature of periodic control a solution for the problem of computing the \mathcal{H}_2 norm of a given system appeared in [78]. However, a two step solution is proposed. The first step consists of finding a periodic matrix using the projection result presented in lemma 2.4.2, and a second step is required to subsequently compute a periodic controller. The first set is solved by resorting to a convex minimization. The second step, based on a feasibility problem, does not guarantee optimality of the controller found. Moreover, the methodology proposed cannot be used with other convex constraints on the controller under synthesis, thereby precluding its use in a more generic framework required on a mixed or on a multi-objective optimization problem.

Next, a new method for the \mathcal{H}_2 norm computation of periodic systems will be introduced, based on LMIs. As a motivation to the approach that follows, consider the basic relation with

respect to the \mathcal{H}_2 norm of a periodic system and the lifted system that results from applying the operator Ω_M introduced previously in this chapter.

Lemma 4.7.2 *The \mathcal{H}_2 norms of the periodic system \mathcal{P}_M and the lifted system $\bar{P} = W_M P W_M^{-1}$, obtained using the lift operator Ω_M , are related as*

$$\|\bar{P}_M\|_2^2 = M \|P_M\|_2^2.$$

See [35] for a proof based on the stochastic interpretation of the norm under discussion. In order to preserve the deterministic interpretation presented in chapter 2, a generalization of the \mathcal{H}_2 norm definition should be used (see [78, 5] for similar definitions), considering as input a train of Dirac signals, non-null at the time-instants of the first period, i.e., for $k = 0, \dots, M - 1$. In both cases the computed norm can be interpreted as the average energy on the outputs for the inputs under consideration.

For the periodic system described by (4.7.1), consider the set of inputs $\mathbf{w}_i(k) = \delta(k - i)$, $i = 0, \dots, M - 1$, where $\delta(\cdot)$ is the discrete-time Dirac function. The outputs will be denoted next as \mathbf{y}_i and can be written as

$$\mathbf{y}_i = \begin{bmatrix} D(i) \\ C(i+1)\Phi_{(i+1,i+1)}B(i) \\ C(i+2)\Phi_{(i+2,i+1)}B(i) \\ \vdots \\ C(k)\Phi_{(k,i+1)}B(i) \\ \vdots \end{bmatrix}.$$

In light of the above, the generalized \mathcal{H}_2 norm can be obtained as

$$\|P_M\|_2^2 = \frac{1}{M} \sum_{i=0}^{M-1} \|P_M \mathbf{w}_i\|_2^2 = \frac{1}{M} \sum_{i=0}^{M-1} \|\mathbf{y}_i\|_2^2.$$

The \mathcal{H}_2 norm of each of the signals $\mathbf{y}_i(k)$ can be written using the definition presented in section 2.8 of chapter 2 and the observability Grammian considered in the definition of detectability for periodic systems 4.5.3 as

$$\|\mathbf{y}_i\|_2^2 = \mathbf{tr}(D^T(i)D(i)) + \mathbf{tr}(B^T(i)W_{obs}(\infty, i)B(i)). \quad (4.7.3)$$

Interesting enough, the observability Grammian considered above verifies the periodic Lyapunov equation

$$A^T(i)W_{obs}(\infty, i+1)A(i) + C^T(i)C(i) = W_{obs}(\infty, i),$$

which has the form of the Lyapunov equation (4.5.5) introduced in lemma 4.5.9, running backwards on the time variable.

The \mathcal{H}_2 norm for the system in (4.7.1) from the input \mathbf{w} to the output \mathbf{y} can therefore be computed using these results as stated in the next theorem.

Theorem 4.7.3 *Let the system $\mathcal{P}_M : \mathbf{u} \rightarrow \mathbf{y}$ in (4.7.1) be $(A(\cdot), C(\cdot))$ detectable with all the eigenvalues of Φ_k on the unit circle $(A(\cdot), B(\cdot))$ reachable and let $\gamma > 0$ be a real number. The $\|P_M\|_2 < \gamma$ if and only if there exist positive definite symmetric matrices $P(i) \in \mathbb{R}^{n \times n}$, $i = 0, \dots, M-1$, and auxiliary matrices $X(i) \in \mathbb{R}^{p \times p}$, $i = 0, \dots, M-1$ such that*

$$\begin{aligned} & \begin{bmatrix} P(i) & A(i)P(i+1) & C^T(i) \\ P(i+1)A^T(i) & P(i+1) & 0 \\ C(i) & 0 & I_p \end{bmatrix} > 0, \quad i = 0, \dots, M-1; \\ & \begin{bmatrix} X(i+1) & B^T(i)P(i+1) \\ P(i+1)B(i) & P(i+1) \end{bmatrix} > 0, \quad i = 0, \dots, M-1; \\ & \sum_{i=0}^{M-1} \text{tr}(X(i)) + \text{tr}(D^T(i)D(i)) < M\gamma^2. \end{aligned} \tag{4.7.4}$$

Proof: Based on the technical conditions introduced above, existence and uniqueness of a periodic stabilizing solution, as expressed by theorem 4.5.6, is guaranteed. Applying the definition of the \mathcal{H}_2 norm based on deterministic signals presented above and the relation with the observability Grammian expressed in relation (4.7.3), the solution for the set of Lyapunov equations $A^T(i)W(i+1)A(i) + C^T(i)C(i) - W(i) = 0$, $i = 0, \dots, M-1$ is sought, where the notation was simplified, using the abbreviate notation $W_{obs}(\infty, i) = W(i)$.

Given a set of auxiliary positive definite variables $P(i) \in \mathbb{R}^{n \times n}$, $i = 0, \dots, M-1$, verifying $P(i) > W(i)$, the set of Lyapunov equations verified by the observability grammians used in the norm computation of the outputs \mathbf{y}_i introduced above can be expressed as a set of matrix inequalities

$$A^T(i)P(i+1)A(i) + C^T(i)C(i) - P(i) < 0, \quad i = 0, \dots, M-1.$$

Using Schur complements, the first set of LMIs presented above are obtained. The norm computation can be written using a set of auxiliary variables $X(i) \in \mathbb{R}^{p \times p}$, $i = 0, \dots, M-1$ such

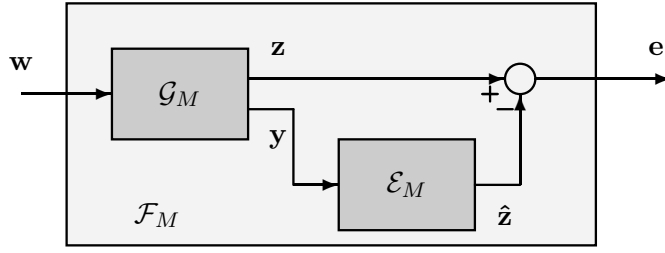


Figure 4.8.1: General setup for periodic filtering synthesis.

that

$$X(i+1) > B^T(i)P(i+1)B(i), \quad i = 0, \dots, M-1,$$

and finally

$$\sum_{i=0}^{M-1} (\text{tr}(D^T(i)D(i)) + \text{tr}(B^T(i)W(i)B(i))) \leq \sum_{i=0}^{M-1} (\text{tr}(D^T(i)D(i)) + \text{tr}X(i)) < M\gamma^2,$$

which can be written as the second set of LMIs introduced above and the relation with γ for a periodic system, respectively. ■

The last two theorems are the key results for the synthesis of estimators that will be presented in the next section. The results obtained, sharing the same structure with the ones obtained for linear, discrete-time, invariant systems, allow for the development of common design methodologies for the synthesis and analysis of these two classes of systems.

The results obtained are also promising as a design framework for periodic feedback control, periodic output feedback, and periodic filter synthesis. They will be the focus of future research.

4.8 Estimator synthesis for periodic systems

The general setup for estimation design for periodically time-varying, discrete-time systems consists of the interconnections presented in figure 4.8.1, which exhibit the same structure as in chapter 2. The nominal system \mathcal{G}_M is a linear, periodically time-varying discrete-time system

with realization

$$\Sigma_{\mathcal{G}_M} = \begin{cases} \mathbf{x}(k+1) &= A(k) \mathbf{x}(k) + B_w(k) \mathbf{w}(k) \\ \mathbf{z}(k) &= C_z(k) \mathbf{x}(k) + D_{zw}(k) \mathbf{w}(k) \\ \mathbf{y}(k) &= C_y(k) \mathbf{x}(k) + D_{yw}(k) \mathbf{w}(k) \end{cases}, \quad (4.8.1)$$

where $\mathbf{x}(k) \in \mathbb{R}^n$ is the state vector, $\mathbf{w}(k) \in \mathbb{R}^m$ is the vector of external inputs, $\mathbf{z}(k) \in \mathbb{R}^p$ is the vector of outputs from the system, $\mathbf{y}(k) \in \mathbb{R}^q$ represents the measurement vector, and the remaining matrices have compatible dimensions. Following the arguments presented for the linear, time-invariant case (based on the arguments of [2]), the optimum estimator in the sense of providing the state estimate with minimum variance for the system (4.8.1) consists of a finite-dimensional linear, periodically time-varying estimator with realization

$$\Sigma_{\mathcal{E}_M} = \begin{cases} \hat{\mathbf{x}}(k+1) &= A(k) \hat{\mathbf{x}}(k) + K(k)(\mathbf{y}(k) - C_y(k)\hat{\mathbf{x}}(k)) \\ \hat{\mathbf{z}}(k) &= C_z(k) \hat{\mathbf{x}}(k) \end{cases}, \quad (4.8.2)$$

where $K \in \mathbb{R}^{n \times q}$ is a periodically varying observer gain to be determined, $\hat{\mathbf{x}}(k)$, and $\hat{\mathbf{z}}(k)$ have the same dimensions of $\mathbf{x}(k)$ and $\mathbf{z}(k)$, respectively.

Let the state estimation error be defined as before $\tilde{\mathbf{x}} = \mathbf{x} - \hat{\mathbf{x}}$ and the estimation error as $\mathbf{e} = \mathbf{z} - \hat{\mathbf{z}}$. The corresponding dynamics using the relations in (4.8.1) and (4.8.2) have the realization

$$\Sigma_{\mathcal{F}_M} = \begin{cases} \tilde{\mathbf{x}}(k+1) &= (A(k) - K(k)C_y(k)) \tilde{\mathbf{x}}(k) + (B_w(k) - K(k)D_{yw}(k)) \mathbf{w}(k) \\ \mathbf{e}(k) &= C_z(k) \tilde{\mathbf{x}}(k) + D_{zw}(k) \mathbf{w}(k). \end{cases} \quad (4.8.3)$$

Applying the results introduced in the previous section to this system, the \mathcal{H}_2 and \mathcal{H}_∞ norms can be computed. Similar non-linear transformations on the unknown variables as those used for the linear, time-invariant, discrete-time versions will also be required.

Theorem 4.8.1 *Consider the periodically time-varying discrete-time system $\mathcal{F}_M : \mathbf{w} \rightarrow \mathbf{z}$ composed of a nominal system $\mathcal{G}_M : \mathbf{w} \rightarrow [\mathbf{z}^T \mathbf{y}^T]^T$ and an estimator $\mathcal{E}_M : \mathbf{y} \rightarrow \hat{\mathbf{z}}$ interconnected as described in figure 4.8.1, with realization (4.8.3). The \mathcal{H}_2 norm of such a system, from the input \mathbf{w} to the output estimation error \mathbf{e} , is such that $\|\mathcal{F}_M\|_2 < \gamma$ if and only if there exists a set of symmetric, positive definite matrices $P(i) \in \mathbb{R}^{n \times n}$, $i = 0, \dots, M-1$, a set of auxiliary variables $X(i) \in \mathbb{R}^{m \times m}$, $i = 0, \dots, M-1$ and a set of auxiliary variables $Y(i) \in \mathbb{R}^{n \times q}$, $i = 0, \dots, M-1$*

verifying $Y(i) = P(i+1)K(i)$, such that

$$\begin{aligned}
 & \begin{bmatrix} P(i) & A(i)P(i+1) - C_y^T(i)Y^T(i) & C_z^T(i) \\ P(i+1)A^T(i) - Y(i)C_y(i) & P(i+1) & 0 \\ C_z(i) & 0 & I_p \end{bmatrix} > 0, \\
 & \qquad \qquad \qquad i = 0, \dots, M-1; \\
 & \begin{bmatrix} X(i+1) & B_w^T(i)P(i+1) - D_{yw}^T(i)Y^T(i) \\ P(i+1)B_w(i) - Y(i)D_{yw}(i) & P(i+1) \end{bmatrix} > 0, \\
 & \qquad \qquad \qquad i = 0, \dots, M-1; \\
 & \sum_{i=0}^{M-1} \text{tr}(X(i)) + \text{tr}(D^T(i)D(i)) < M\gamma^2.
 \end{aligned} \tag{4.8.4}$$

Proof: Applying the definition of the \mathcal{H}_2 norm presented in theorem 4.7.3 to the system described by (4.8.3), the following set of inequalities for $i = 0, \dots, M-1$ is obtained

$$\begin{bmatrix} P(i) & \star & \star \\ P(i+1)A^T(i) - P(i+1)K(i)C_y(i) & P(i+1) & \star \\ C_z(i) & 0 & I_p \end{bmatrix} > 0,$$

which is not an LMI as there are products of unknowns, namely $P(i+1)$ and $K(i)$. The same products were also found in the definition of the \mathcal{H}_2 norm computation based on LMIs in the time-invariant cases. Note that in this case, a periodic set of matrices are sought verifying $P(M+i) = P(i)$. Introducing the set of auxiliary variables $Y(i) = P(i+1)K(i)$, $i = 0, \dots, M-1$ results in the first set of LMIs described above. This can be understood as the use of a periodic non-linear transformation (a Lyapunov transformation) that allows the bilinear matrix inequalities to become LMIs. The second set of LMIs introduced in (4.8.4) is obtained from the second set of LMIs in (4.7.4). The last LMI is obvious.

The sufficiency of the result follows the same lines as sufficiency proof on proposition 2.8.4 and will be omitted here. ■

Theorem 4.8.2 Consider the discrete-time system $\mathcal{F}_M : \mathbf{w} \rightarrow \mathbf{z}$, composed of a nominal system $\mathcal{G}_M : \mathbf{w} \rightarrow [\mathbf{z}^T \mathbf{y}^T]^T$ and an estimator $\mathcal{E}_M : \mathbf{y} \rightarrow \hat{\mathbf{z}}$ interconnected as described in figure 4.8.1, with realization (4.8.3). The \mathcal{H}_∞ norm from the input \mathbf{w} to the output estimation error \mathbf{e} verifies $\|F_k\|_\infty < \gamma$ if and only if there exists a symmetric, positive definite set of matrices $P(i) \in \mathbb{R}^{n \times n}$, $i = 0, \dots, M-1$ and a set of auxiliary variables $Y(i) \in \mathbb{R}^{n \times q}$, $i = 0, \dots, M-1$

verifying $Y(i) = P(i+1)K(i)$, such that

$$\begin{bmatrix} -P(i) & \star & \star & \star \\ 0 & -\gamma^2 I_m & \star & \star \\ P(i+1)A(i) - Y(i)C_y(i) & P(i+1)B_w(i) - Y(i)D_{yw}(i) & -P(i+1) & \star \\ C_z(i) & D_{zw}(i) & 0 & -I_p \end{bmatrix} < 0, \quad i = 0, \dots, M-1. \quad (4.8.5)$$

The proof of this theorem is omitted as it follows exactly the same steps as those outlined in the proof of the previous theorem, in this case based on theorem 4.7.1.

The results obtained for the synthesis of \mathcal{H}_2 and \mathcal{H}_∞ norms allow the design of mixed $\mathcal{H}_2/\mathcal{H}_\infty$ estimators and multi-objective estimators from auxiliary inputs to auxiliary outputs as a generic design framework. In the next section, an example will be presented for a classical complementary filter structure, with both simulation results and results obtained with an autonomous catamaran performing a mission at sea.

4.9 Multi-rate navigation system design for the Delfim catamaran

The design of a multi-rate navigation system for an Autonomous Surface Craft (ASC) will be presented next as an example of application of the new synthesis methodologies introduced in this chapter. Implementing and testing the aforementioned navigation system has been made possible through the EC MAST-III ASIMOV project. Results obtained during sea trials will be presented next, allowing for the assessment of the navigation system performance under realistic work conditions.

The main thrust of the ASIMOV project (see [3] for details) is the development and integration of advanced technological systems to achieve coordinated operation of an Autonomous Surface Craft and an Autonomous Underwater Vehicle (AUV) while ensuring a fast communication link between the two vehicles. The ASC / AUV ensemble is being used to study the extent of shallow water hydrothermalism and to determine patterns of community diversity at the vents in the D. João de Castro bank in the Azores (see figure 4.9.1).

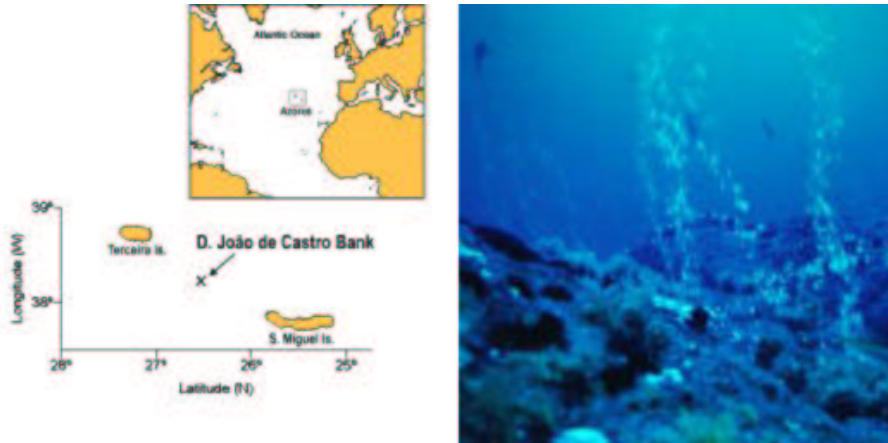


Figure 4.9.1: Location of D. João de Castro bank (on the left). Hydrothermal activity.

By properly maneuvering the ASC to always remain in the vicinity of a vertical line directed along the AUV, a fast communication link can be established to transmit navigational data from the ASC to the AUV, as well as acoustic / vision data from the AUV to the ASC. The ASC can therefore be used as a communications relay to an end-user located on-board a support ship or on-shore. An accurate and reliable navigation system running on-board the ASC, providing estimates of the position and velocity is central for the success of the ASIMOV project.

The DELFIM ASC was designed and built by the Institute for Systems and Robotics of the Instituto Superior Técnico to carry out automatic marine data acquisition and to serve as an acoustic relay between the submerged craft and a support vessel. This will enable the transmission of sonar and video images through a specially developed acoustic communication channel that is optimized to transmit in the vertical. The DELFIM ASC can also be used as a stand-alone unit, capable of maneuvering autonomously and performing precise path following (see [1] for details) while carrying out automatic marine data acquisition (including bathymetric data) and transmitting data to an operating center installed on-board a support vessel or on-shore. This is in line with the current trend to develop systems that will lower the costs and improve the efficiency of operation of oceanographic vessels at sea.

The DELFIM is a small Catamaran 3.5 m long and 2.0 m wide, with a mass of 320 kg, see figure 4.9.2. The propulsion system consists of two propellers driven by electrical motors. The vehicle is equipped with on-board resident systems for navigation, guidance, and control, as well as for mission control. Navigation is done by integrating motion sensor data obtained from an

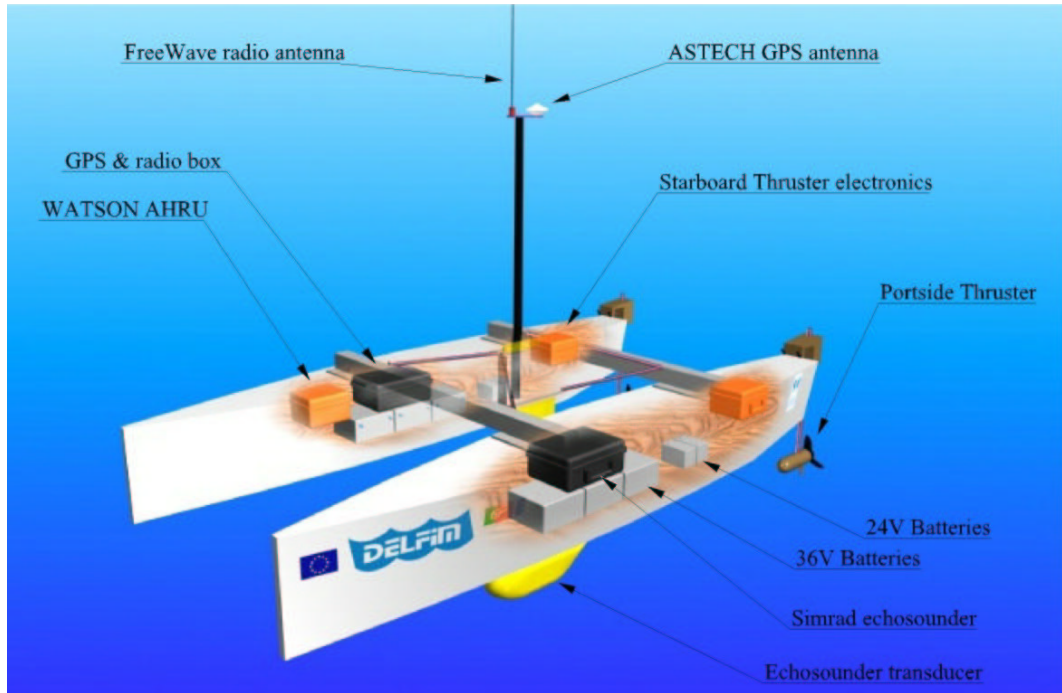


Figure 4.9.2: DELFIM in operation at the D. João de Castro bank.

attitude reference unit, a Doppler log, and a DGPS (Differential Global Positioning System) receiver. The guidance and control systems consist of simplified versions of the $s - y$ controller described in [71].

Transmissions between the vehicle, its support vessel, the fixed GPS station and the on-shore control center installed on-shore are achieved by means of a radio link with a range of 80 km. The vehicle has a wing shaped central structure that is lowered during operations at sea. At the bottom of this structure a hydrodynamically shaped body is installed that carries all acoustic transducers, including those used to communicate with the underwater craft.

In what follows, $\{I\}$ is a fixed reference frame located at the origin of the pre-specified mission area and $\{S\}$ is a body-fixed coordinate that moves with the ASC. The vehicle motion is subject to the influence of a constant unknown current ${}^I\mathbf{v}_w = [{}^Iu_w \ {}^Iv_w \ 0]^T$ expressed in $\{I\}$, which is equivalent to assuming that there is a coordinate frame $\{W\}$ attached hypothetically to a point in the water. The following notation is required:

${}^I\mathbf{p}_S$	$:=$	$\begin{bmatrix} {}^Ix_s & {}^Iy_s & {}^Iz_s \end{bmatrix}^T$	- position of the origin of $\{S\}$ measured in $\{I\}$;
${}^I\mathbf{v}_S$	$:=$	$\begin{bmatrix} {}^Iu_s & {}^Iv_s & {}^Iw_s \end{bmatrix}^T$	- relative velocity of the origin of $\{S\}$ with respect to the fixed frame $\{I\}$;
${}^W\mathbf{v}_S$	$:=$	$\begin{bmatrix} {}^Wu_s & {}^Wv_s & {}^Ww_s \end{bmatrix}^T$	- relative velocity of the origin of $\{S\}$ with respect to the water attached coordinate frame $\{W\}$;
λ	$:=$	$\begin{bmatrix} \phi & \theta & \psi \end{bmatrix}^T$	- vector of roll, pitch, and yaw angles that parametrize locally the orientation of $\{S\}$ relative to $\{I\}$;
I_sR	(λ)		- rotation matrix from $\{S\}$ to $\{I\}$.

With this notation, the relevant kinematics of the ASC can be written in compact form as

$$\frac{d}{dt}{}^I\mathbf{p}_S = {}^I\mathbf{v}_S + \mathbf{b}, \quad (4.9.1)$$

where \mathbf{b} is an installation bias to be estimated.

As briefly mentioned above, the AUV is equipped with the following motion sensors:

1. a *NAVSTAR GPS* (Global Positioning System) receiver that computes the latitude, longitude, and altitude in the WGS-84 datum based on the travel time delays of an electromagnetic pulse from a synchronized constellation of satellites orbiting the earth.
2. a *Doppler log sonar* that provides on-board referenced measurements of the body-fixed velocities ${}^S({}^I\mathbf{v}_S) = {}^S_I R {}^I\mathbf{v}_S$ and ${}^S({}^W\mathbf{v}_S)$ of the vehicle with respect to the sea bottom and to the water, respectively.
3. An attitude reference unit is also available to provide accurate estimates of the vector λ of roll, pitch, and yaw angles.

Based on the coordinates provided by the GPS, after a suitable transformation for the local coordinate frame $\{I\}$, the position of the ASC $({}^I\mathbf{p}_S)_m := \begin{bmatrix} ({}^Ix_s)_m & ({}^Iy_s)_m & ({}^Iz_s)_m \end{bmatrix}^T$ of ${}^I\mathbf{p}_S$ is available. The GPS receiver, running recently developed algorithms for positioning, namely the Real Time Kinematics (RTK), can achieve centimetric accuracy in the fixed version and decimetric accuracy in the float version. The Doppler data are simply converted from the body to the reference coordinate frame using the relation ${}^I\mathbf{v}_S = {}^I_sR(\lambda)({}^S\mathbf{v}_S)$ to obtain measurements $({}^I\mathbf{v}_S)_m = \begin{bmatrix} ({}^Iu_s)_m & ({}^Iv_s)_m & ({}^Iw_s)_m \end{bmatrix}^T$. The interrogation rates for the GPS

and for the Doppler sonar are 2 Hz and 4 Hz , respectively. According to the definitions for the multi-rate systems introduced in the beginning of this chapter, the basic time period is $h = 0.25\text{ s}$ and the period is $M = 2$.

Following an integrated approach in the design of the navigation, guidance, and control systems, presented in detail in [1], the following specifications for the navigation system are the guidelines for the design of a multi-rate complementary filter:

1. Obtain accurate estimates ${}^I\hat{\mathbf{p}}_S = [{}^I\hat{x}_s \quad {}^I\hat{y}_s \quad {}^I\hat{z}_s]^T$ and $\hat{\mathbf{v}}_S = [{}^I\hat{u}_s \quad {}^I\hat{v}_s \quad {}^I\hat{w}_s]^T$ of the vehicle position and velocity, respectively;
2. Achieve a settling time of 240 s on the estimate of the mis-installation bias.
3. Achieve a settling time of 6 s on the position estimate.

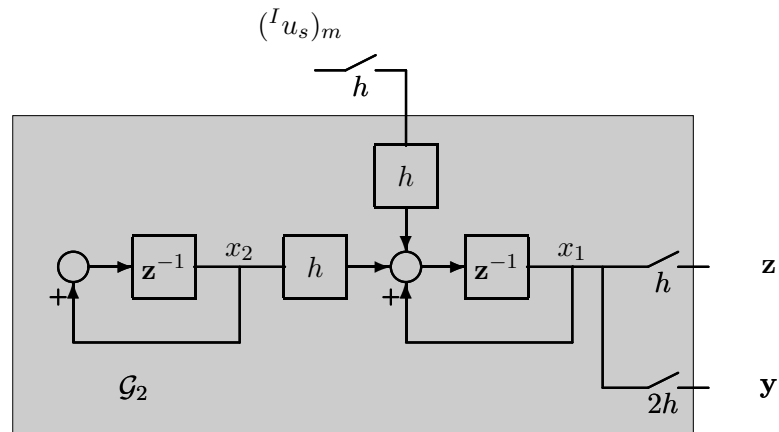


Figure 4.9.3: Position estimation: filter design model.

Following the guidelines introduced in chapter 3, the design model for the complementary navigation filter is easily obtained from the kinematic equations of the AUV, leading to three sets of decoupled equations that correspond to the three linear coordinates x , y , and z . See figure 4.9.3 for the design model that captures the motion of the AUV along the coordinate x . The output integrator captures the relationship ${}^I\dot{x}_s = {}^Iu_s + b_x$ and the input integrator was inserted to estimate the installation bias, assumed constant. Adopting the basic sampling period

$h = 0.25$ s, the design model admits the realization

$$\Sigma_{\mathcal{G}_2} = \begin{cases} \mathbf{x}(k+1) = A(k) \mathbf{x}(k) + B_u(k) \mathbf{u}(k) \\ \mathbf{z}(k) = C_z(k) \mathbf{x}(k) \\ \mathbf{y}(k) = C_y(k) \mathbf{x}(k) \end{cases}, \quad (4.9.2)$$

where $\mathbf{x} = \begin{bmatrix} x_1 & x_2 \end{bmatrix}^T$, $\mathbf{u} = ({}^I u_s)_m$, and $\mathbf{z} = \mathbf{y} = ({}^I x_s)_m$. Furthermore,

$$A(k) = \begin{bmatrix} 1 & h \\ 0 & 1 \end{bmatrix}, \quad B_u(k) = \begin{bmatrix} h \\ 0 \end{bmatrix},$$

$$C_z(k) = \begin{bmatrix} 1 & 0 \end{bmatrix}, \quad \text{and} \quad C_y(k) = \begin{cases} \begin{bmatrix} 1 & 0 \end{bmatrix}^T & \text{if } k \text{ MOD } M = 0 \\ \begin{bmatrix} 0 & 0 \end{bmatrix}^T & \text{if } k \text{ MOD } M = 1 \end{cases},$$

where the periodic nature of the matrix $C_y(k)$ is obvious.

In preparation for the approach that will be introduced later, the project of a linear, time-invariant system where $C_y = C_z = \begin{bmatrix} 1 & 0 \end{bmatrix}^T$ will be presented using classical design tools. To that purpose, the system (4.9.2) will be considered to be driven by null mean, gaussian white-noise $\mathbf{v}(k)$ and the output is assumed to be corrupted by gaussian white-noise, with null mean, i.e. $E[\mathbf{w}(k)] = 0$, leading to the realization $\Sigma_{\mathcal{G}_n}$

$$\Sigma_{\mathcal{G}_n} = \begin{cases} \mathbf{x}(k+1) = A \mathbf{x}(k) + B_u \mathbf{u}(k) + \mathbf{v}(k) \\ \mathbf{y}(k) = C_y \mathbf{x}(k) + \mathbf{w}(k). \end{cases} \quad (4.9.3)$$

The state covariance, considered as a tuning mechanism in the estimator design is

$$Q_v = \begin{bmatrix} q_x & 0 \\ 0 & q_b \end{bmatrix},$$

and an unitary output covariance Q_w was considered, without loss of generality. Moreover, define a set of auxiliary transfer functions that will help introduce the constraints in the design of the estimator at hand, namely

- $T_{x_m \rightarrow e}$ - transfer function from the position measurement $({}^I x_s)_m$ to the estimate error $e = ({}^I x_s)_m - {}^I \hat{x}_s$;
- $T_{u_m \rightarrow \hat{x}}$ - transfer function from the velocity measurement $({}^I u_s)_m$ to the position estimate ${}^I \hat{x}_s$;
- $T_{x_m \rightarrow \hat{x}}$ - transfer function from the position measurement $({}^I x_s)_m$ to the position estimate ${}^I \hat{x}_s$.

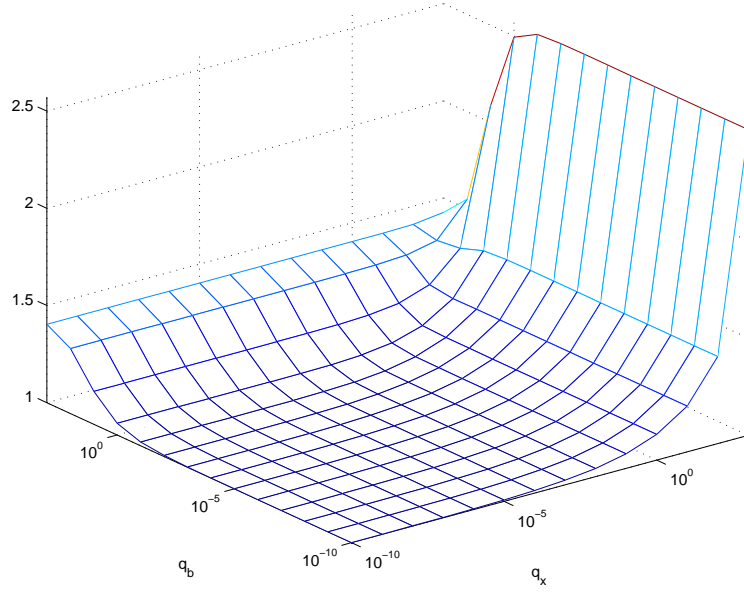


Figure 4.9.4: $\|T_{x_m \rightarrow e}\|_2$ for a range of q_b and q_x values.

Figures 4.9.4, 4.9.5, and 4.9.6 depict the values for the norms obtained for the aforementioned transfer functions when the tuning knobs (q_b and q_x) are used in the specified ranges. Note that the transfer function $T_{x_m \rightarrow e}$, depicted in figure 4.9.4, has a smaller \mathcal{H}_2 norm when the gains are smaller and the bandwidth from the position sensor to the error estimate is smaller. Figure 4.9.5, where the $\|T_{u_m \rightarrow \hat{x}}\|_2$ is depicted for the same range of design parameters, shows opposite behaviour. Note that the overall structure of the system under consideration is a complementary filter. Finally, figure 4.9.6 depicts the $\|T_{x_m \rightarrow \hat{x}}\|_\infty$, where a value over 1 is always obtained.

The approach to the design of the estimator at hand as a convex optimization problem is clearly validated from the results described in the aforementioned figures and can be stated as

$$\begin{aligned}
 & \min \|T_{x_m \rightarrow e}\|_2 \\
 & \text{subject to:} \\
 & \|T_{u_m \rightarrow \hat{x}}\|_2 < \gamma_v \\
 & \|T_{x_m \rightarrow \hat{x}}\|_\infty < \gamma_p
 \end{aligned} \tag{4.9.4}$$

The rationale for this choice is to decrease the dependence on the sensor that will be available at higher sampling periods. However, this minimization will not lead to a degenerated solution as the transfer function $T_{u_m \rightarrow \hat{x}}$ should be chosen in such a way that the influence from the faster sensor on the position estimate is guaranteed, as depicted in figure 4.9.5, and the fundamental

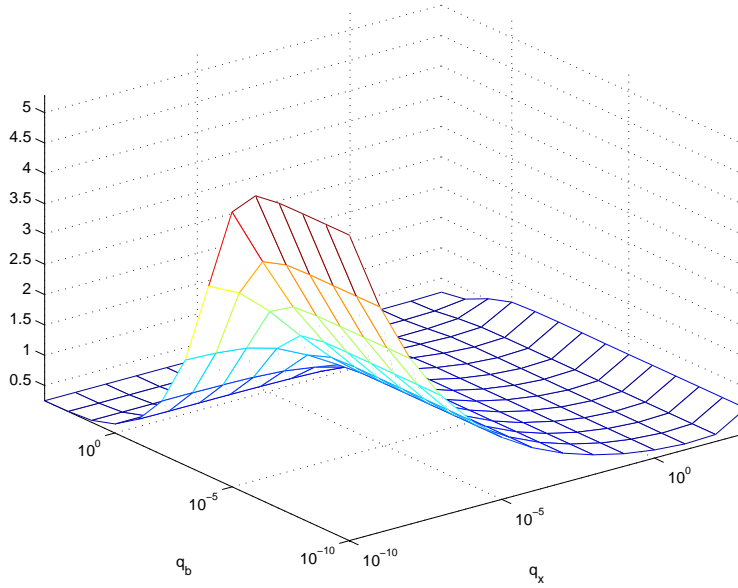


Figure 4.9.5: $\|T_{u_m \rightarrow \hat{x}}\|_2$ for a range of q_b and q_x values.

relation for complementary filters is valid for the proposed structure. Moreover, to aid in the estimator design, a bound on the errors in the position estimate due to possible errors introduced by the position sensor is set through the constraint on the magnitude of the transfer function $T_{x_m \rightarrow \hat{x}}$.

The structure presented in figure 4.8.1 is repeated in the case shown in figure 4.9.7, where the sampling rates associated with the underlying signals were left in to highlight the multi-rate nature of the estimator under design. To achieve the design requirements introduced above, the bounds $\gamma_v = 0.65$ and $\gamma_p = 1.8$ were used leading to the filter gains

$$K(k) = \begin{cases} \begin{bmatrix} 0.1890 & 0.0027 \end{bmatrix}^T & \text{if } k \text{ MOD } M = 0 \\ \begin{bmatrix} 0 & 0 \end{bmatrix}^T & \text{if } k \text{ MOD } M = 1 \end{cases}$$

for a minimum value of $\|T_{x_m \rightarrow e}^*\|_2 = 1.0651$.

The performance of the navigation system was evaluated *in simulation* for an initial 10 m error on the position estimate. The installation bias was setup to 0.1 m/s and the initial estimate was $\hat{b}_x = 0 \text{ m/s}$. The temporal evolution of the estimates is depicted in figure 4.9.8.

As mentioned earlier, this navigation system was tested in the DELFIM catamaran performing a mission at sea. Figure 4.9.9 depicts the trajectory, in local coordinates for latitude

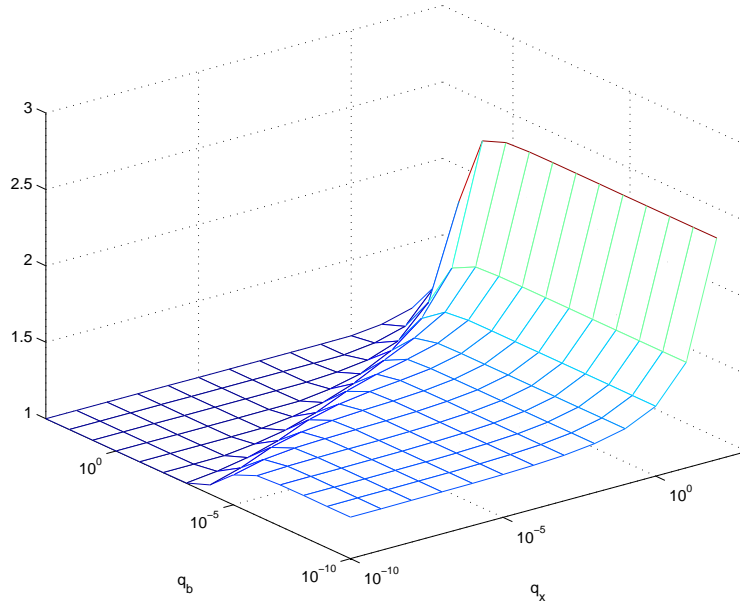


Figure 4.9.6: $\|T_{x_m \rightarrow \hat{x}}\|_\infty$ for a range of q_b and q_x values.

and longitude, during a bathymetric survey performed at sea in October 2000 off the coast of Setubal. The stability and reliability of the filter used show great promise for the use of such simple structures as reliable navigation systems for autonomous vehicles. Figure 4.9.10 presents a zoom over a period of 50 samples (= 12.5 s), to emphasize the multi-rate characteristic of the navigation system as well as the low-pass characteristics from the measured position to the estimated position, as required due to the complementary nature of the filter chosen.

To acquire a better understanding of the multi-rate system used a series of simulation tests were performed. In order to gain some insight into the evolution of the attainable norm for $\|T_{x_m \rightarrow e}^*\|_2$, a set of experiments were performed where the ratio M of the the fastest sampled sensor (velocity sensor) to the slowest one (position sensor) was tested for the range starting at $M = 1$ (the time-invariant case) and finishing at $M = 9$. The auxiliary bounds were set to $\gamma_v = 0.8$ and $\gamma_p = 3$, respectively, leading to the results presented in figure 4.9.11. Interesting to remark, is the graceful degradation experienced by the lower bound on the norm under minimization for this system in the interval under consideration. Moreover, for a period of $M = 9$ and above, the convex optimization problem is infeasible.

The influence of the basic sampling rate for this system was also studied under simulation by performing a series of tests where the same minimization problem was solved using the MATLAB

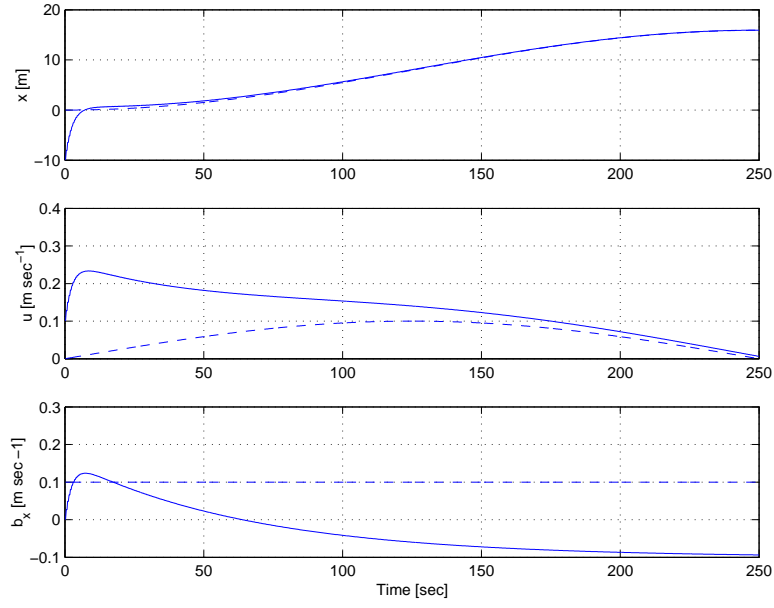


Figure 4.9.8: Position x (dashed line) and position estimate \hat{x} , on the top; Velocity u (dashed line) and velocity estimate, in the middle and bias b_x (dashed line) and bias estimate, on the bottom.

$({}^{\mathcal{W}}\mathbf{v}_S)_m$ were used to estimate the installation bias, the position estimate ${}^{\mathcal{I}}\hat{\mathbf{p}}_S$, and the unknown current ${}^{\mathcal{I}}\hat{\mathbf{v}}_W$. Assuming that the same installation bias \mathbf{b} affects both velocity measurements, the following relations hold:

$$\Sigma_{\mathcal{G}_a} \left\{ \begin{array}{l} \frac{d}{dt} {}^{\mathcal{I}}\mathbf{p}_S = ({}^{\mathcal{I}}\mathbf{v}_S)_m \\ \frac{d}{dt} \mathbf{b} = 0 \\ ({}^{\mathcal{I}}\mathbf{v}_S)_m = {}^{\mathcal{I}}\mathbf{v}_W + {}^{\mathcal{W}}\mathbf{v}_S + \mathbf{b} \\ ({}^{\mathcal{W}}\mathbf{v}_S)_m = {}^{\mathcal{W}}\mathbf{v}_S + \mathbf{b} \end{array} \right. ,$$

and the block diagram of the systems used are represented in figure 4.9.13, where each of the blocks has a structure as defined above.

The performance of the navigation system obtained with these interconnections was evaluated *in simulation* for an initial 10 m error on the position estimate. The installation bias was set to 0.1 m/s, but the initial estimate was $\hat{b}_x = 1.0$ m/s, with a temporal evolution as depicted in figure 4.9.14. Moreover, a constant current along the x direction with a value of 1 m/s was included, with a null initial estimate. The results obtained allow one to draw some conclusions about the promising characteristics of the new methodology proposed and used.

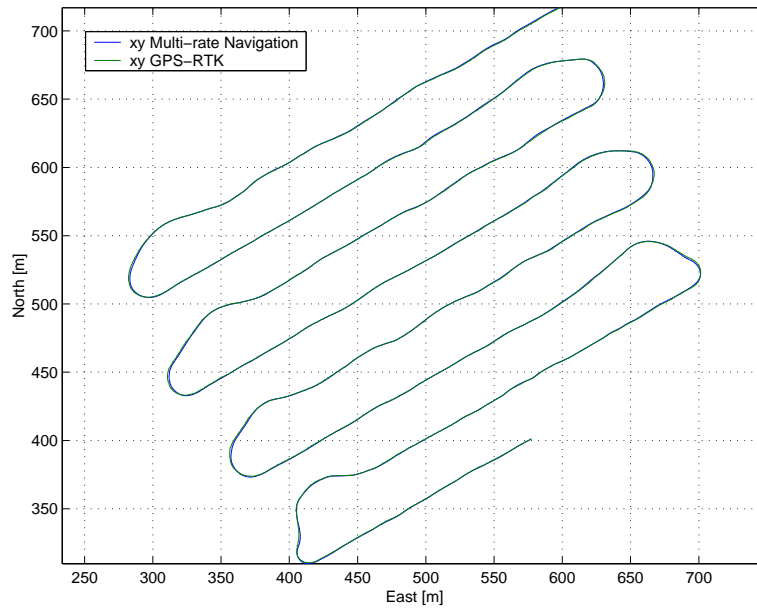


Figure 4.9.9: Trajectory of the Delfim catamaran during a bathymetric survey at sea, in the Setubal canyon.

4.10 Conclusions

This chapter introduced new theoretical results on the \mathcal{H}_2 and \mathcal{H}_∞ norms of periodic systems. For a generic structure of periodic estimators, a synthesis solution was proposed with well established properties. The methodology proposed, resorting to convex optimization procedures, is based on minimization of the \mathcal{H}_2 or \mathcal{H}_∞ norms from auxiliary inputs to auxiliary outputs, constrained by the norms of other input/output signals. This powerful methodology paves the way for the use of such framework in other problems such as periodic feedback control and multi-rate filter design. Finally, this new synthesis methodology has been applied to a classic example leading to promising simulation results. The proposed navigation system was later validated with results obtained during sea trials performed with an autonomous surface craft.

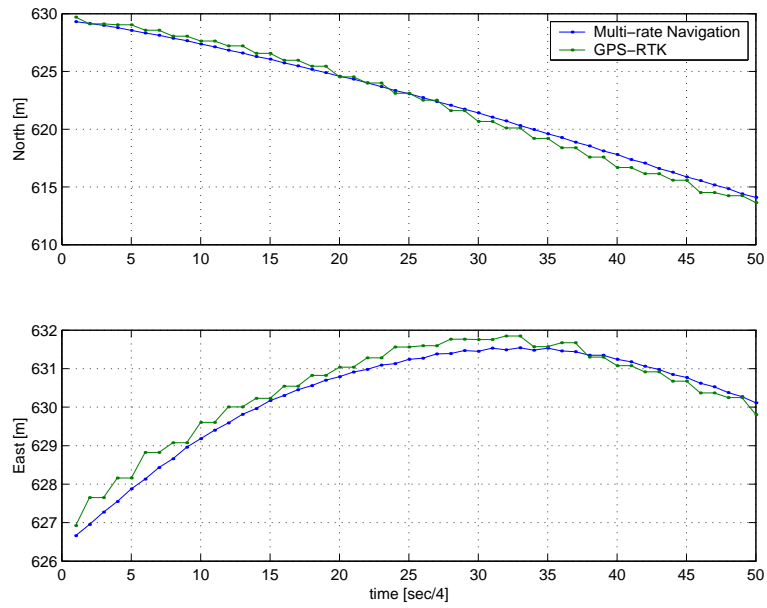


Figure 4.9.10: Detail of the trajectory of the Delfim catamaran.

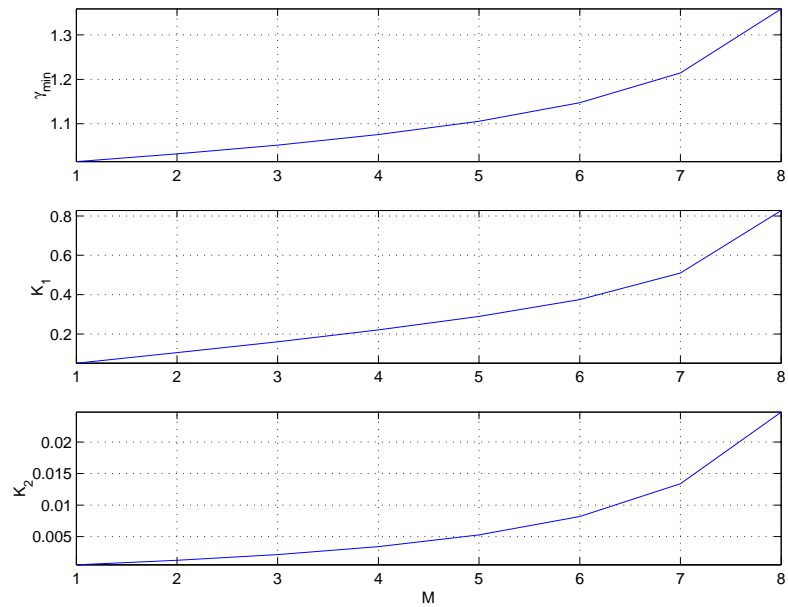


Figure 4.9.11: $\|T_{x_m \rightarrow \epsilon}^*\|_2$ for a series of period values M .

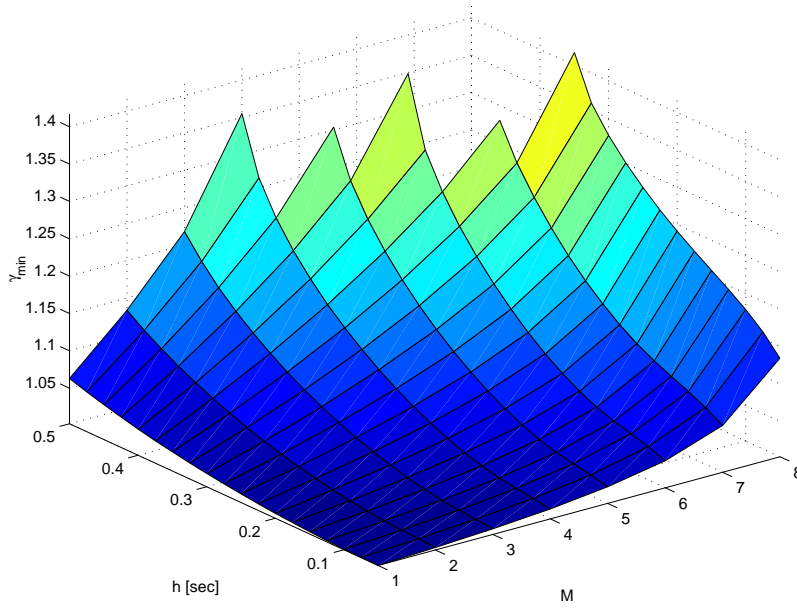


Figure 4.9.12: $\|T_{x_m \rightarrow \epsilon}^*\|_2$ for a series of period values M and h .

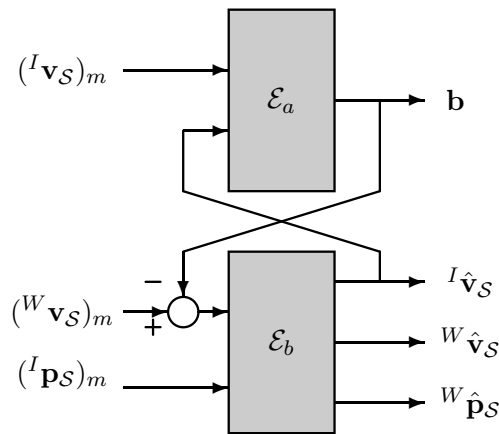


Figure 4.9.13: Block diagram to estimate $I \hat{\mathbf{v}}_S$, $I \hat{\mathbf{p}}_S$, and $I \hat{\mathbf{v}}_w$.

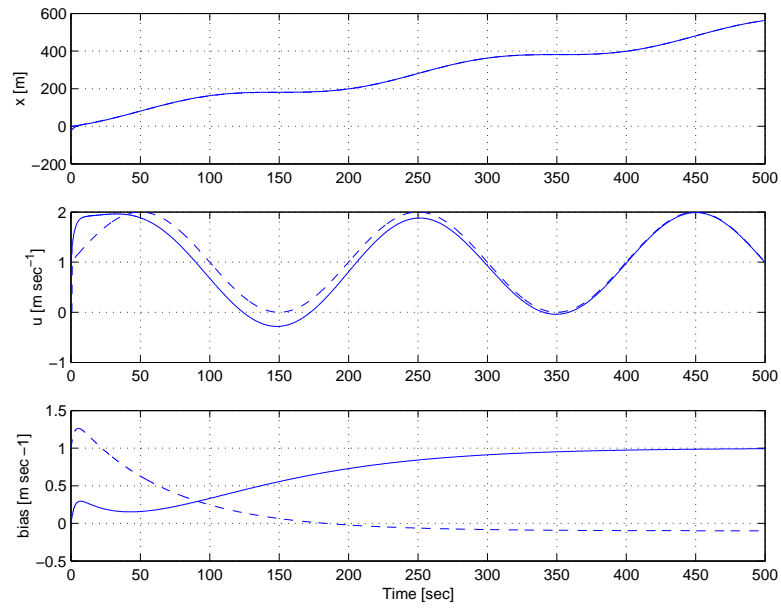


Figure 4.9.14: Position x (dashed line) and position estimate \hat{x} , on the top; Velocity u (dashed line) and velocity estimate, in the middle and bias b_x (dashed line) and current estimate ${}^I\hat{u}_w$, on the bottom.

Chapter 5

Analysis of Periodic Estimators

5.1 Introduction

The synthesis of feedback systems to solve a given estimation problem, resorting to optimization tools, requires that the performance of the final design be evaluated according to a number of relevant features. Time response characteristics of the output signals when pre-specified inputs are fed into the system and analysis of its frequency-response, as criteria to evaluate system performance, have been used for a long time and shown to be of utmost importance.

The requirements for the problem at hand, expressed in the form of technical specifications, should be used in the synthesis methodology leading to an *optimal* solution if possible. In the case that some technical requirements can not be incorporated in the synthesis directly they should be verified a posteriori after a solution is obtained. This can lead to a redesign process conducing to a new solution. However, some reasons can preclude a solution to be obtained:

- Given a set of constraints, some of them contradictory, the resulting optimization problem can be infeasible;
- Qualitative features of the solution may be hard or impossible to be formulated in terms of quantitative characteristics to be used in the synthesis methodology;
- Some of the constraints can be incompatible with the framework used. For instance, in a methodology using LMIs and where the solution is obtained resorting to convex optimization algorithms, constraints on the rank and structure of the solution sought are

non-convex (see [13] for an enlightening characterization of that technical requirements).

Apart from the constraints enumerated above, there are time-response characteristics that can be formulated as convex constraints in the design parameters as presented in section 2.6.1 of chapter 2. Moreover, using the isomorphic properties of the \mathbf{z} transform, some of the frequency-response constraints can also be setup as convex constraints on the location of the eigenvalues of the specified closed loop solution. In the case of linear, time-invariant systems this approach is commonly used. However, in the case of linear, periodically time-varying system the notion of frequency-response is not clear and the system designer is thus left without an important tool to assess system performance. This chapter aims to clarify these issues and to explain how a frequency-like interpretation can be obtained even for a broad class of time-varying systems.

To this purpose, a classical method for representing multi-rate feedback systems by equivalent single rate systems that goes back to the pioneering work of Kranc [43] in the late 1950s - the switch decomposition method - will be summarized later in this chapter. See also [52], where this technique was exploited, leading to the study of linear periodic time-varying systems in the time and frequency domain. The underlying technique, also called polyphase decomposition when applied to the lift system, will be also presented for reference in this chapter. However, as will be clear, the technique does not afford system designers a versatile tool for system analysis in the frequency domain.

To overcome this difficulty a new methodology for system analysis is introduced that builds on work described in previous chapters and allows for an interpretation in the frequency domain.

The organization of this chapter is as follows: The operations associated with digital rate conversion are presented in section 5.2 and the switch decomposition method is reviewed in section 5.3. In section 5.4 a new methodology for the analysis of linear systems is introduced and the resulting properties are discussed. The natural extension to the class of discrete, periodic time-varying systems will be presented with emphasis on the physical meaning of the methodology presented. Interestingly, this method can be applied to a broad class of linear and non-linear systems as will be shown in chapter 6. In order to provide insight into the proposed method, the periodic estimation problem solved in the previous chapter is analyzed, with the results presented in section 5.5. Moreover, based on the new methodology the design of periodic systems incorporating the frequency domain properties directly is proposed. Finally, conclusions

will be drawn and some future work will be outlined in section 5.6.

5.2 Digital rate conversion

The frequency analysis of a multi-rate system implies the conversion of the sampling rates of the discrete signals involved. The signals can be converted using multi-rate signal processing techniques - interpolators and decimators - described in the following [23].

The process of sampling a continuous signal $\mathbf{x}(t)$ using an ideal sample and hold device is assumed to be uniform, occurring h time apart. A sequence $\mathbf{x}(kh)$ results, referred to as $\mathbf{x}(k)$ when only one rate is used. In order to be able to reconstruct the band-limited signal $\mathbf{x}(k)$, the sampling period h should be chosen to satisfy the Nyquist sampling theorem.

The process of digitally converting the sampling rate of a signal from a given rate $F = 1/h$ to $F' = 1/h'$ is called sampling rate conversion and takes the name of interpolation if $F' > F$ and decimation if $F' < F$.

The rate conversion system, given an input signal $\mathbf{x}(k)$, outputs a signal $\mathbf{y}(m)$ with a new sampling rate $F' = 1/h'$. In the following it is assumed that the sampling periods of the input and output signals are related by a rational fraction

$$\frac{h'}{h} = \frac{F}{F'} = \frac{M}{L}.$$

Systems that can perform such rate conversion are linear time-varying discrete systems where the output $\mathbf{y}(m)$ at instant m is the response to an input at the time $(\lfloor \frac{mM}{L} \rfloor - k)$ and can be expressed as

$$\mathbf{y}(m) = \sum_{k=-\infty}^{\infty} \mathbf{g}_m(k) \mathbf{x} \left(\lfloor \frac{mM}{L} \rfloor - k \right),$$

where $\lfloor u \rfloor$ denotes the integer less or equal to u . The system response $\mathbf{g}_m(k)$ is periodic in m with period L , verifying $\mathbf{g}_m(k) = \mathbf{g}_{m+rL}(k)$ with $r = 0, \pm 1, \pm 2, \dots$. In the case where $h = h'$ the above expression degenerates into the classic convolution sum.

5.2.1 Sampling rate reduction - decimation by an integer factor M

The operation of sampling rate reduction by an integer factor M , relating the input and output sampling periods by $h/h' = F/F' = M$, produces a signal with the new sampling rate

$F' = F/M$. This operation is generally called decimation ¹.

Given a full band signal $\mathbf{x}(k)$ with a non-zero spectrum in all frequencies such that $-\frac{F}{2} \leq f \leq \frac{F}{2}$ with $\omega = 2\pi fh$

$$|X(e^{j\omega})| \neq 0, \quad |\omega| = |2\pi fh| \leq \frac{2\pi Fh}{2} = \pi$$

the rate reduction is achieved by generating a sequence $y(m)$ such that each M^{th} input sample is copied to the output resulting a sequence $\mathbf{y}(m) = \mathbf{x}(Mk)$.

To obtain the relationship on the \mathbf{z} transforms of the signals, the definition of an auxiliary signal $\mathbf{x}'(n)$, defined as

$$\mathbf{x}'(k) = \begin{cases} \mathbf{x}(k), & k = 0, \pm M, \pm 2M, \dots \\ 0, & \text{otherwise} \end{cases},$$

verifying that $\mathbf{x}'(k) = \mathbf{x}(k) \left\{ \frac{1}{M} \sum_{l=0}^{M-1} e^{j2\pi lk/M} \right\}$ results that $Y(\mathbf{z})$ can be expressed as

$$Y(\mathbf{z}) = \frac{1}{M} \sum_{l=0}^{M-1} X \left(e^{-j2\pi l/M} \mathbf{z}^{1/M} \right). \quad (5.2.1)$$

Evaluating $Y(\mathbf{z})$ on the unit circle $\mathbf{z} = e^{jw'}$

$$Y(e^{jw'}) = \frac{1}{M} \sum_{l=0}^{M-1} X \left(e^{j(w'-2\pi l)/M} \right)$$

where $w' = 2\pi fh'$, the above equation allows an interpretation of sample rate reduction as the sum of frequency shifted versions of the input signal spectrum. If an anti-aliasing filter with bandwidth π/M is used then

$$Y(e^{jw'}) = \frac{1}{M} X \left(e^{jw'/M} \right), \quad |w'| \leq \pi.$$

5.2.2 Sampling rate increase - interpolation by an integer factor L

The operation of sample rate increase is usually called interpolation. If a signal is interpolated by an integer factor L , the sampling period relation is $h'/h = F/F' = 1/L$ and a signal with a new update rate $F' = LF$ is produced.

¹To be precise, decimation should be the reduction by a factor of 10. However, the scientific community has adopted this term as the generic rate reduction denomination.

Sample rate increase is obtained by interpolating the input signal $\mathbf{x}(k)$ with $L - 1$ null samples, resulting in a signal $y(m)$ that can be described by

$$\mathbf{y}(m) = \begin{cases} \mathbf{x}(\frac{m}{L}), & m = 0, \pm L, \pm 2L, \dots \\ 0, & \text{otherwise} \end{cases},$$

which has a \mathbf{z} transform

$$Y(\mathbf{z}) = \sum_{i=-\infty}^{\infty} \mathbf{x}(i/L)\mathbf{z}^{-i} = X(\mathbf{z}^L). \quad (5.2.2)$$

Evaluating $Y(\mathbf{z})$ on the unit circle $\mathbf{z} = e^{j\omega'}$, $Y(e^{j\omega'}) = X(e^{j\omega'L})$, which corresponds to a frequency expansion.

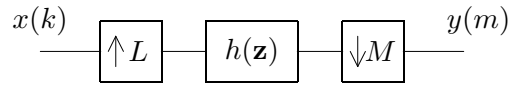


Figure 5.2.1: Sampling rate conversion by a factor L/M , using an interpolator ($\uparrow L$) and a decimator ($\downarrow M$).

In the case where a generic (rational) relation on the sampling rates of the input and output signals is seek, i.e. $F'/F = L/M$, a cascade of interpolators and decimators can be used. See one such example in figure 5.2.1, where one interpolator and one decimator were used, represented with the symbols $\uparrow L$ and $\downarrow M$, respectively. A low-pass filter $h(\mathbf{z})$ can be used to eliminate components in the interpolated signal.

5.3 Switch Decomposition Method

The analysis of discrete or sampled-data systems where different sample intervals are present goes back to the work of George Kranc [43]. The purpose of that work was to study multi-rate feedback systems using the **switch decomposition method**-SDM to change the different sampling periods to a common one (h), with the period of the least common multiple. In figure 5.3.1 a) the structure that implements this equivalence is presented.

A feedback system with different sampling rates, as represented in figure 5.3.1 b), should be reduced to the equivalent single rate and the transfer functions should be evaluated using

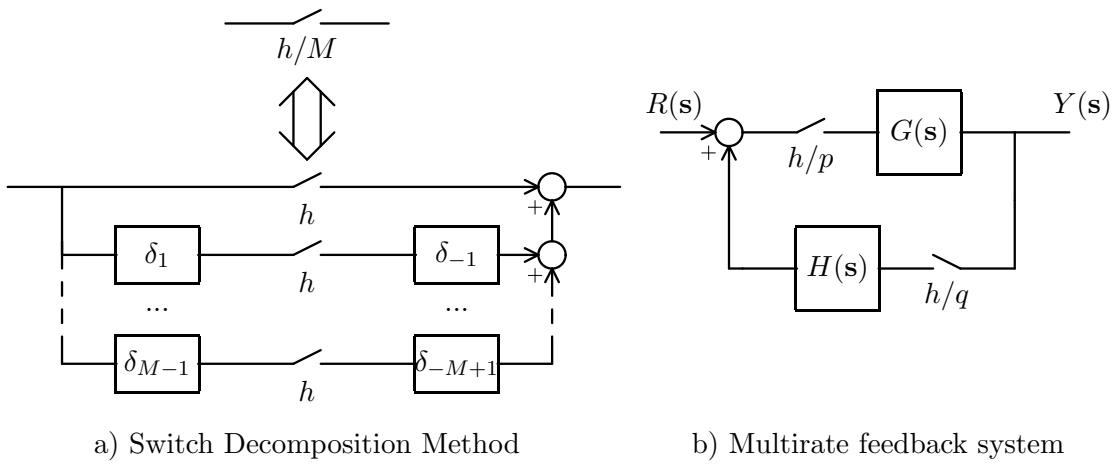


Figure 5.3.1: Multi-rate feedback analysis proposed by Kranc ($\delta = e^{sh/M}$).

superposition. The approach proposed by Kranc did not use zero order hold systems at the sampling mechanism, but a similar approach will be used to study the frequency-response of a system using discrete multi-rate data processing.

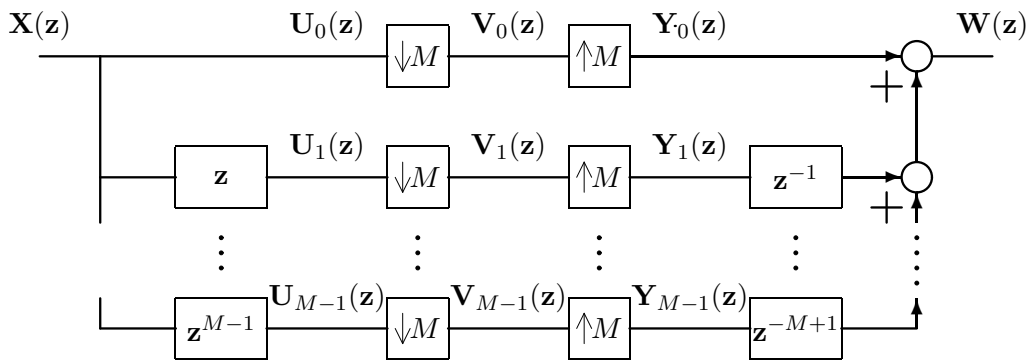


Figure 5.3.2: Digital Decomposition Method.

A decomposition method similar to the one proposed by Kranc is presented in figure 5.3.2. The equivalent system uses a set of advances to generate a set of M replicas of the input signal that are feed to the decimators stage. The low rate outputs of the decimators are connected to

a set of interpolators and their outputs are delayed and summed to obtain the output signal. The following lemma formalizes this structure:

Lemma 5.3.1 *Given the M sub-sequences $\mathbf{x}(pM+k)$ of a signal with \mathbf{z} transform $X(\mathbf{z})$ obtained using a set of tapped advances and M decimators, the relationship among sequences is*

$$X(\mathbf{z}) = X_0(\mathbf{z}^M) + \mathbf{z}^{-1}X_1(\mathbf{z}^M) + \dots + \mathbf{z}^{-(M-1)}X_{M-1}(\mathbf{z}^M).$$

and a set of M interpolators performing a 1 to M rate increase with tapped delays can recover the original signal.

Proof:

Assuming $X(\mathbf{z})$ as the \mathbf{z} transform of the impulse response $h(k)$ and $X_j(\mathbf{z}) = \sum_{i=0}^{\infty} h(Mi + j)\mathbf{z}^{-i}$ the \mathbf{z} transform of the subsequences $h(mM + j)$, the following relation is obvious from the \mathbf{z} transform definition

$$X(\mathbf{z}) = X_0(\mathbf{z}^M) + \mathbf{z}^{-1}X_1(\mathbf{z}^M) + \dots + \mathbf{z}^{-(M-1)}X_{M-1}(\mathbf{z}^M). \quad (5.3.1)$$

Defining the auxiliary signals $U_l(\mathbf{z}) = \mathbf{z}^l X(\mathbf{z})$, and using the frequency relation on a decimator by a factor of M (see relation (5.2.1)), the expression for $V_l(\mathbf{z})$ can be written as

$$V_l(\mathbf{z}) = \frac{1}{M} \sum_{i=0}^{M-1} U_l(e^{-\frac{j2\pi i}{M}} \mathbf{z}^{\frac{1}{M}}) = \frac{1}{M} \sum_{i=0}^{M-1} (e^{-\frac{j2\pi il}{M}} \mathbf{z}^{\frac{l}{M}}) X(e^{-\frac{j2\pi i}{M}} \mathbf{z}^{\frac{1}{M}}).$$

The signals $V_l(m)$, composed by a set of aliased components, have a rate M times lower than the full band original signal $\mathbf{x}(k)$. However, the proposed structure can be used to recover the original signal considering the interpolator and delay structure of the output. Defining $Y_l(\mathbf{z})$ as the \mathbf{z} transform of the interpolator output, according to (5.2.2),

$$Y_l(\mathbf{z}) = V_l(\mathbf{z}^M) = \frac{1}{M} \sum_{i=0}^{M-1} (e^{-\frac{j2\pi il}{M}} (\mathbf{z}^M)^{\frac{l}{M}}) X(e^{-\frac{j2\pi i}{M}} (\mathbf{z}^M)^{\frac{1}{M}}).$$

Simplifying this relation it can be written as

$$Y_l(\mathbf{z}) = \frac{1}{M} \sum_{i=0}^{M-1} (e^{-\frac{j2\pi il}{M}} \mathbf{z}^l) X(e^{-\frac{j2\pi i}{M}} \mathbf{z}), \quad (5.3.2)$$

and finally given that $W(\mathbf{z}) = \sum_{p=0}^{M-1} \mathbf{z}^{-p} Y_p(\mathbf{z})$, or using relation (5.3.2),

$$W(\mathbf{z}) = \sum_{p=0}^{M-1} \mathbf{z}^{-p} \frac{1}{M} \sum_{i=0}^{M-1} (e^{-\frac{j2\pi ip}{M}} \mathbf{z}^p) X(e^{-\frac{j2\pi i}{M}} \mathbf{z});$$

after cancelling the advance and delay factors and using the $X(\mathbf{z})$ definition

$$W(\mathbf{z}) = \frac{1}{M} \sum_{p=0}^{M-1} \sum_{i=0}^{M-1} e^{-\frac{j2\pi ip}{M}} \sum_{q=0}^{\infty} \mathbf{x}(q) (e^{-\frac{j2\pi i}{M}} \mathbf{z})^{-q}.$$

Changing the summations and collecting the terms on $e^{j2\pi i/M}$, the previous expression becomes

$$W(\mathbf{z}) = \frac{1}{M} \sum_{p=0}^{M-1} \sum_{q=0}^{\infty} \mathbf{x}(q) \mathbf{z}^{-q} \sum_{i=0}^{M-1} e^{\frac{j2\pi i(q-p)}{M}}.$$

Note that the last sum is given by

$$\sum_{i=0}^{M-1} e^{\frac{j2\pi i(q-p)}{M}} = \begin{cases} M & q - p = \pm rM \\ 0 & \text{otherwise} \end{cases}.$$

$W(\mathbf{z})$ can be expressed as

$$W(\mathbf{z}) = \sum_{p=0}^{M-1} \sum_{r=0}^{\infty} \mathbf{x}(rM + p) \mathbf{z}^{-(rM+p)},$$

and after a summation change,

$$W(\mathbf{z}) = \sum_{r=0}^{\infty} \sum_{p=0}^{M-1} \mathbf{x}(rM + p) \mathbf{z}^{-(rM+p)} = \sum_{r=0}^{\infty} \mathbf{x}(r) \mathbf{z}^{-r} = X(\mathbf{z})$$

obtaining the identity on the lemma. ■

Attention should be paid to the following points in the interpretation of the previous result:

- The sampling rate in the input signal $X(\mathbf{z})$ and on the output signal $W(\mathbf{z})$ is greater, by a factor of M , than the sampling rates of the signals $V_l(\mathbf{z})$.
- The decimators outputs $V_l(\mathbf{z})$ are closely related to the vector signals in the lifting technique presented in section 4.4. This scheme can be used with a lifted system, as will be seen later.
- To implement the proposed method as a causal system, a delay \mathbf{z}^M in the input signal should be used.

The equivalence described in lemma 5.3.1 can be further exploited in the implementation of lifted systems. In the structure introduced above, note that the signals between the decimator

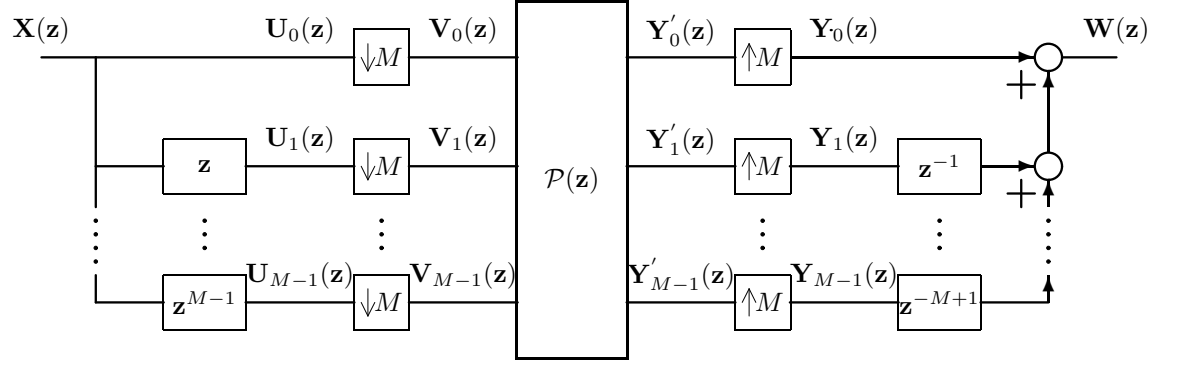


Figure 5.3.3: Digital Decomposition Method of Lifted Systems.

and interpolator stages are the ones stacked in equation (4.4.2) leading to the lifted system described by (4.4.3). The lifted system transfer function 5.3.6 is incorporated (see figure 5.3.3) and the following lemma can be enunciated:

Lemma 5.3.2 *The transfer function $P(\mathbf{z})$ of a time-invariant discrete-time linear system is recovered when the system is considered as M -periodic and is incorporated in the structure presented in lemma 5.3.1.*

Proof:

Introducing the outputs from the lifted system Y'_l ,

$$\begin{cases} Y'_0(\mathbf{z}) &= P_0(\mathbf{z})V_0(\mathbf{z}) + \mathbf{z}^{-1}P_{M-1}(\mathbf{z})V_1(\mathbf{z}) + \dots + \mathbf{z}^{-1}P_1(\mathbf{z})V_{M-1}(\mathbf{z}) \\ Y'_1(\mathbf{z}) &= P_1(\mathbf{z})V_0(\mathbf{z}) + P_0(\mathbf{z})V_1(\mathbf{z}) + \dots + \mathbf{z}^{-1}P_2(\mathbf{z})V_{M-1}(\mathbf{z}) \\ \dots & \dots \\ Y'_{M-1}(\mathbf{z}) &= P_{M-1}(\mathbf{z})V_0(\mathbf{z}) + P_{M-2}(\mathbf{z})V_1(\mathbf{z}) + \dots + P_0(\mathbf{z})V_{M-1}(\mathbf{z}) \end{cases}$$

and using the \mathbf{z} transform of the interpolators (see equation 5.2.2) $Y_l(\mathbf{z}) = Y'(\mathbf{z}^M)$, the set of signals $Y(\mathbf{z})$ can be expressed as

$$\begin{cases} Y_0(\mathbf{z}) &= P_0(\mathbf{z}^M)V_0(\mathbf{z}^M) + \mathbf{z}^{-M}P_{M-1}(\mathbf{z}^M)V_1(\mathbf{z}^M) + \dots + \mathbf{z}^{-M}P_1(\mathbf{z}^M)V_{M-1}(\mathbf{z}^M) \\ Y_1(\mathbf{z}) &= P_1(\mathbf{z}^M)V_0(\mathbf{z}^M) + P_0(\mathbf{z}^M)V_1(\mathbf{z}^M) + \dots + \mathbf{z}^{-M}P_2(\mathbf{z}^M)V_{M-1}(\mathbf{z}^M) \\ \dots & \dots \\ Y_{M-1}(\mathbf{z}) &= P_{M-1}(\mathbf{z}^M)V_0(\mathbf{z}^M) + P_{M-2}(\mathbf{z}^M)V_1(\mathbf{z}^M) + \dots + P_0(\mathbf{z}^M)V_{M-1}(\mathbf{z}^M) \end{cases}$$

The output $W(\mathbf{z})$ can be obtained multiplying each relation by \mathbf{z}^{-l} and summing

$$\begin{aligned} W(\mathbf{z}) &= P(\mathbf{z})V_0(\mathbf{z}^M) + \mathbf{z}^{-1}P(\mathbf{z})V_1(\mathbf{z}^M) + \dots + \mathbf{z}^{-M+1}P(\mathbf{z})V_{M-1}(\mathbf{z}^M) \\ &= P(\mathbf{z}) \sum_{p=0}^{M-1} \mathbf{z}^{-p}V_p(\mathbf{z}^M), \end{aligned}$$

where the relations $W(\mathbf{z}) = \sum_{p=0}^{M-1} \mathbf{z}^{-p}Y_p(\mathbf{z})$ and (5.3.1) were used. Following along the lines of the proof in lemma 5.3.1, the input-output relation is

$$W(\mathbf{z}) = P(\mathbf{z})X(\mathbf{z}).$$

■

This lemma provides a bridge between the lift system technique and the interpretation of the switch decomposition method. The well known fact that the transfer function of a periodic system does not exist, is also clear from figure 5.3.3. In the following, a counter-example, that highlights this fact is presented.

5.3.1 SDM Example of a Quasi Invariant System

Suppose a scalar discrete-time system, with the state $x \in \mathbb{R}$, the input $u \in \mathbb{R}$, the output $y \in \mathbb{R}$, period M , and where only the output equation is periodic. The dynamics of such system can be described by

$$\mathbf{x}(k+1) = a_k\mathbf{x}(k) + b_k\mathbf{u}(k),$$

and the output equation is

$$\mathbf{y}(k) = c_k\mathbf{x}(k) + d_k\mathbf{u}(k)$$

verifying $a_k = a$, $b_k = b$, $d_k = d$ and

$$c_k = \begin{cases} c_0 & \text{if } k \text{ MOD } M = 0 \\ c_{\bar{0}} & \text{if } k \text{ MOD } M \neq 0 \end{cases}.$$

Using the same arguments as in relation (5.3.6) the following relation for the lifted system can be found:

$$\tilde{P}(\mathbf{z}) = \begin{bmatrix} P'_0(\mathbf{z}), & \mathbf{z}^{-1}P'_{M-1}(\mathbf{z}), & \dots & \mathbf{z}^{-1}P'_1(\mathbf{z}) \\ P_1(\mathbf{z}), & P_0(\mathbf{z}), & \dots & \mathbf{z}^{-1}P_2(\mathbf{z}) \\ \vdots & \vdots & \ddots & \vdots \\ P_{M-1}(\mathbf{z}), & P_{M-2}(\mathbf{z}), & \dots & P_0(\mathbf{z}) \end{bmatrix}, \quad (5.3.3)$$

where $P_j(\mathbf{z})$ and $P'_j(\mathbf{z})$ are the \mathbf{z} transform of the sequences obtained from auxiliary invariant systems with $c_k = c_{\bar{0}}$ and $c_k = c_0$, respectively. Note that $P'_j(\mathbf{z}) = c_0/c_{\bar{0}} P_j(\mathbf{z})$.

Following along the proof of lemma 4, the outputs from the lifted system Y'_l are given by

$$\begin{cases} Y'_0(\mathbf{z}) &= P'_0(\mathbf{z})V_0(\mathbf{z}) + \mathbf{z}^{-1}P'_{M-1}(\mathbf{z})V_1(\mathbf{z}) + \dots + \mathbf{z}^{-1}P'_1(\mathbf{z})V_{M-1}(\mathbf{z}) \\ Y'_1(\mathbf{z}) &= P_1(\mathbf{z})V_0(\mathbf{z}) + P_0(\mathbf{z})V_1(\mathbf{z}) + \dots + \mathbf{z}^{-1}P_2(\mathbf{z})V_{M-1}(\mathbf{z}) \\ \dots & \dots \\ Y'_{M-1}(\mathbf{z}) &= P_{M-1}(\mathbf{z})V_0(\mathbf{z}) + P_{M-2}(\mathbf{z})V_1(\mathbf{z}) + \dots + P_0(\mathbf{z})V_{M-1}(\mathbf{z}). \end{cases}$$

The interpolators outputs, according to relation (5.2.2), are given by $Y_l(\mathbf{z}) = Y'(\mathbf{z}^M)$, and the set of signals $Y(\mathbf{z})$ can be expressed as

$$\begin{cases} Y_0(\mathbf{z}) &= P'_0(\mathbf{z}^M)V_0(\mathbf{z}^M) + \mathbf{z}^{-M}P'_{M-1}(\mathbf{z}^M)V_1(\mathbf{z}^M) + \dots + \mathbf{z}^{-M}P'_1(\mathbf{z}^M)V_{M-1}(\mathbf{z}^M) \\ Y_1(\mathbf{z}) &= P_1(\mathbf{z}^M)V_0(\mathbf{z}^M) + P_0(\mathbf{z}^M)V_1(\mathbf{z}^M) + \dots + \mathbf{z}^{-M}P_2(\mathbf{z}^M)V_{M-1}(\mathbf{z}^M) \\ \dots & \dots \\ Y_{M-1}(\mathbf{z}) &= P_{M-1}(\mathbf{z}^M)V_0(\mathbf{z}^M) + P_{M-2}(\mathbf{z}^M)V_1(\mathbf{z}^M) + \dots + P_0(\mathbf{z}^M)V_{M-1}(\mathbf{z}^M). \end{cases}$$

The output $W(\mathbf{z})$ can be obtained multiplying each relation by \mathbf{z}^{-l} and then summing all the terms, resulting

$$\begin{aligned} W(\mathbf{z}) &= P(\mathbf{z}) \sum_{p=0}^{M-1} \mathbf{z}^{-p} V_p(\mathbf{z}^M) \\ &+ \left[(P'_0(\mathbf{z}^M) - P_0(\mathbf{z}^M))V_0(\mathbf{z}^M) + \sum_{p=1}^{M-1} \mathbf{z}^{-M} (P'_p(\mathbf{z}^M) - P_p(\mathbf{z}^M))V_{M-p}(\mathbf{z}^M) \right], \end{aligned}$$

where the relations $W(\mathbf{z}) = \sum_{p=0}^{M-1} \mathbf{z}^{-p} Y_p(\mathbf{z})$ and (5.3.1) were used.

The first term in the previous equation can be simplified and the remaining terms are computed using the expression for $V_l(\mathbf{z})$, as defined in the proof of the lemma 5.3.1, resulting in the relation

$$\begin{aligned} W(\mathbf{z}) &= P(\mathbf{z})X(\mathbf{z}) \\ &+ \left[(P'_0(\mathbf{z}^M) - P_0(\mathbf{z}^M)) \frac{1}{M} \sum_{i=0}^{M-1} X(e^{-\frac{j2\pi i}{M}} \mathbf{z}^{\frac{1}{M}}) \right. \\ &+ \left. \sum_{p=1}^{M-1} \mathbf{z}^{-M} ((P'_p(\mathbf{z}^M) - P_p(\mathbf{z}^M))) \frac{1}{M} \sum_{i=0}^{M-1} (e^{-\frac{j2\pi i(M-p)}{M}} \mathbf{z}^{\frac{(M-p)}{M}}) X(e^{-\frac{j2\pi i}{M}} \mathbf{z}^{\frac{1}{M}}) \right] \end{aligned} \quad (5.3.4)$$

The above expression emphasizes the well known fact that a periodic system presents a transfer function with replicas of the input shifted and scaled in the frequency. The transfer functions, from the mM inputs to the pM outputs associated with the lifted system, can be computed using the general relation

$$\bar{P}(\mathbf{z}) = \bar{C}(\mathbf{z}^M I - \bar{A})^{-1} \bar{B} + \bar{D} = [\bar{P}_{i,j}].$$

An invariant discrete-time system can be taken as M periodic for any $M \geq 1$. In that case the expressions for \bar{A} , \bar{B} , \bar{C} , and \bar{D} are respectively

$$\bar{A} = A^M, \quad \bar{B} = (A^{M-1}B, A^{M-2}B, \dots, AB, B),$$

$$\bar{C} = \begin{bmatrix} C \\ CA \\ \vdots \\ CA^{M-2} \\ CA^{M-1} \end{bmatrix}, \quad \text{and} \quad \bar{D} = \begin{bmatrix} D, & \dots & 0, & 0 \\ CB, & \dots & 0, & 0 \\ \vdots & \ddots & \vdots & \vdots \\ CA^{M-3}B, & \dots & D, & 0 \\ CA^{M-2}B, & \dots & CB, & D \end{bmatrix}. \quad (5.3.5)$$

Given the impulse signal $h(k)$ and denoting as $P_j(\mathbf{z}) = \sum_{i=0}^{\infty} h(Mi + j)\mathbf{z}^{-i}$ the \mathbf{z} transform of the subsequences $h(mM + j)$, given the Markov parameters' matrix for the lifted system, the following relation can be found

$$\bar{P}(\mathbf{z}) = \begin{bmatrix} P_0(\mathbf{z}), & \mathbf{z}^{-1}P_{M-1}(\mathbf{z}), & \dots & \mathbf{z}^{-1}P_1(\mathbf{z}) \\ P_1(\mathbf{z}), & P_0(\mathbf{z}), & \dots & \mathbf{z}^{-1}P_2(\mathbf{z}) \\ \vdots & \vdots & \ddots & \vdots \\ P_{M-1}(\mathbf{z}), & P_{M-2}(\mathbf{z}), & \dots & P_0(\mathbf{z}) \end{bmatrix}. \quad (5.3.6)$$

Moreover, if the poles of the original system are λ_i the poles of the lifted system are λ_i^M . It can hardly be overemphasized the difficulties that the designer encounters in analyzing a system with the tools presented above. To obviate such difficulties a new methodology is proposed.

5.4 Frequency analysis

The rest of the chapter departs considerably from the classical analysis derived above. The key ideas exposed build on the usual concepts of low-pass and high-pass filters that play a key role in assessing the performance of complementary filters and are well understood in the case of

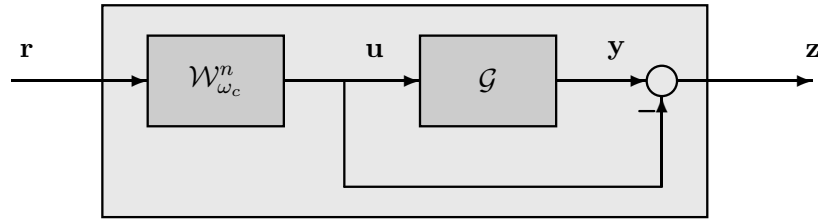


Figure 5.4.1: General setup for frequency analysis.

linear time-invariant systems. We now extend these concepts to the class of linear time-varying systems.

5.4.1 Low and high-pass filters.

Definition. Low-pass property. Let \mathcal{G} be a linear, internally stable time-varying system and let \mathcal{W}_ω^n be a low-pass, linear time-invariant Chebyshev filter of order n and cutoff frequency ω . The system \mathcal{G} is said to satisfy a low-pass property with indices (ϵ, n) over $[0, \omega_c]$ if

$$\|(\mathcal{G} - I)\mathcal{W}_{\omega_c}^n\|_\infty < \epsilon. \quad (5.4.1)$$

Definition. Low-pass filter with bandwidth ω_c . A linear, internally stable time-varying system \mathcal{G} is said to be an (ϵ, n) *low-pass filter* with bandwidth ω_c if

- $\lim_{\omega \rightarrow 0} \|(\mathcal{G} - I)\mathcal{W}_\omega^n\|_\infty$ is well defined and equals 0.
- $\omega_c := \sup\{\omega : \|(\mathcal{G} - I)\mathcal{W}_\omega^n\|_\infty < \epsilon\}$, i.e., \mathcal{G} satisfies a low-pass property with indices (ϵ, n) over $[0, \omega]$ for all $\omega \in [0, \omega_c)$ but fails to satisfy that property whenever $\omega \geq \omega_c$.
- For every $\delta > 0$, there exists $\omega^* = \omega^*(\delta)$ such that $\|\mathcal{G}(I - \mathcal{W}_\omega^n)\|_\infty < \delta$ for $\omega > \omega^*$.

Definition. High-pass Filter with break frequency ω_c . A linear, internally stable time-varying system \mathcal{G} is said to be an (ϵ, n) *high-pass filter* with break frequency ω_c if $(I - \mathcal{G})$ is an (ϵ, n) low-pass filter with bandwidth ω_c .

The conditions in the definition of low-pass filters generalize the following facts that are obvious in the linear time-invariant case:

- the filter must provide a gain equal to one at zero frequency.
- there is a finite band of frequencies over which the system behaviour replicates very closely that of an identity operator.
- the system gain rolls off to zero at high frequency.

Notice the role played by the weighting operator \mathcal{W}_ω^n , which was arbitrarily selected as a Chebyshev filter. In practice, the order of the filter can be made sufficiently large so as to make it effectively select the “low frequency components” of the input signal.

Consider the following conceptual experience that justifies the analysis methodology for periodic systems, taking into consideration figure 5.4.1:

1. Given all non-null signals \mathbf{r} , with finite energy, i.e., $\|\mathbf{r}\|_2 < \infty$, consider the signal $\mathbf{u} = \mathcal{W}_{\omega_c}^n \mathbf{r}$ obtained at the output of a low-pass filter with bandwidth $\omega_c > 0$ arbitrary small. The signal thus obtained has energy in the bandwidth $]0, \omega_c[$.
2. Inject the signal \mathbf{u} in the system under test and in an auxiliary identity operator.
3. Compute the signal $\mathbf{z} = (\mathcal{G} - I)\mathbf{u}$ as the difference from the output of the two signals obtained in the previous step.
4. The maximum energy amplification can be expressed as

$$\sup_{\mathbf{r} \in \mathcal{L}_2} \frac{\|\mathbf{z}\|_2}{\|\mathbf{r}\|_2} = \|(\mathcal{G} - I)\mathcal{W}_\omega^n\|_\infty$$

and provides a measurement on the low-pass characteristics of the system under consideration.

5. Repeat all the previous steps for increasing values of the bandwidth ω_c , plotting the values for the maximum amplification obtained.

This intuitive methodology results in a practical tool to evaluate the low (or high) pass characteristics of the systems under analysis. Its application to the navigation system designed in the previous chapter will be presented next.

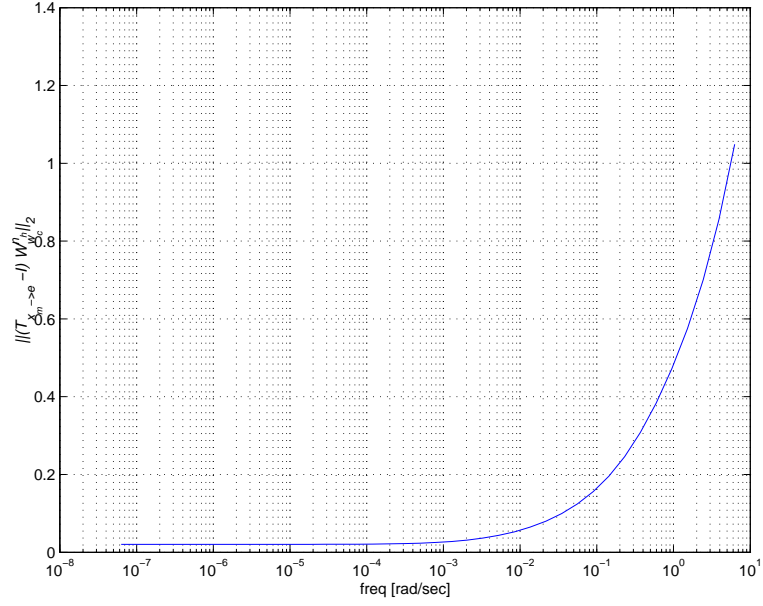


Figure 5.5.1: Analysis of the high-pass operator $T_{x_m \rightarrow e}$. Generalized Bode plot.

5.5 Navigation system for the Delfim catamaran

The analysis of a multi-rate navigation system for an Autonomous Surface Craft (ASC) designed in the previous chapter will be presented next, as an example of application of the new synthesis methodologies proposed in this chapter.

See figures 5.5.1 and 5.5.2, where the operators $T_{x_m \rightarrow e}$ and $T_{x_m \rightarrow \hat{x}}$ introduced previously are analyzed. The analysis procedure outlined above was performed with 4th order low-pass Chebyshev filters.

Frequency constraints can be directly incorporated in the synthesis of the periodic estimator presented in the previous chapter. For that purpose, the theorem 4.7.1 is instrumental to incorporate the expression (5.4.1), introduced above. The optimization problem can then be restated as

$$\begin{aligned}
 & \min \|T_{x_m \rightarrow e}\|_2 \\
 & \text{subject to:} \\
 & \|T_{u_m \rightarrow \hat{x}}\|_2 < \gamma_v \\
 & \|T_{x_m \rightarrow \hat{x}}(I - \mathcal{W}_{\omega}^n)\|_{\infty} < \gamma_p
 \end{aligned} \tag{5.5.1}$$

Note that the resulting program is a non-convex optimization problem, due to the fact that the system under synthesis has a reduced order, when compared with the underlying model

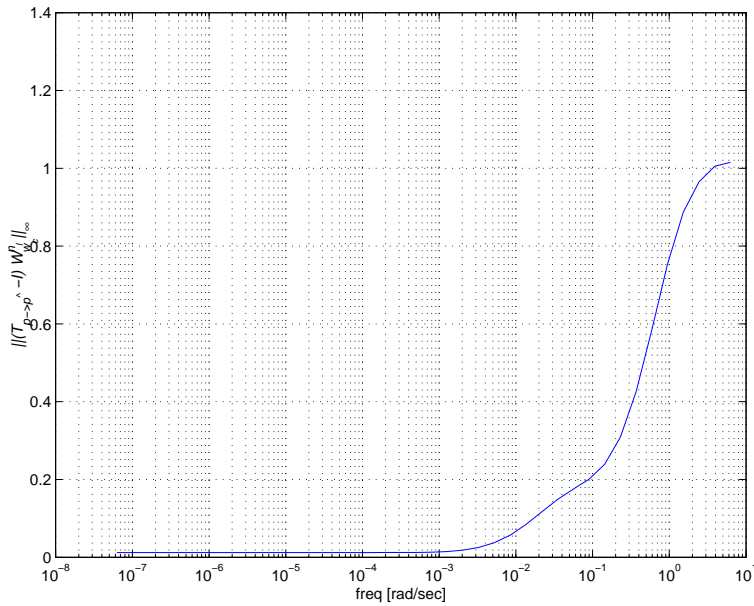


Figure 5.5.2: Analysis of the low-pass operator $T_{x_m \rightarrow \hat{x}}$. Generalized Bode plot.

used. This precludes the use of the convex optimization tools described previously. No further development on the approach required to tackle this problem will be presented in this chapter. An alternative approach will be presented in the next chapter in a time-varying setup, and that can also be adopted to solve the problem previously stated.

5.6 Conclusions and future work

A new methodology for the analysis of periodic time-varying systems was proposed and used in the direct design of a periodic estimator, resorting to LMIs. The advantages of the proposed method are evident and provide tools for a more accurate synthesis of this subclass of linear systems.

The proposed methodology can be applied to the analysis and/or to the direct synthesis of periodic controllers and multi-rate filters. Moreover, others classes of systems such that the norm computation is achievable resorting to LMIS can also be addressed. One such class consists of systems with unknown parameters bounded by polytopes, as described in the next chapter.

Chapter 6

Navigation System Design using Time-Varying Complementary Filters

6.1 Introduction

This chapter introduces a new methodology for the design of navigation systems for autonomous vehicles. Using simple kinematic relationships, the problem of estimating the velocity and position of an autonomous vehicle is solved by resorting to special bilinear time-varying filters. These are the natural generalization of linear time-invariant complementary filters that are commonly used to properly merge sensor information available at low frequency with that available in the complementary region as introduced in chapter 3.

The time-dependence is imposed by the fact that some of the sensors provide measurements in inertial coordinates, while other measurements are naturally expressed in body axis. To merge the information from both types of sensors - while being able to compensate for sensor biases - requires that the rotation matrix from inertial to body axis be explicitly included in the navigation filters.

Complementary filters lend themselves to frequency domain interpretations that provide valuable insight into the filtering design process. This chapter extends these properties to the time-varying setting by resorting to the theory of linear differential inclusions and by converting

the problem of weighted filter performance analysis into that of determining the feasibility of a related set of LMIs. The resulting filters are bilinear and time-varying, but the time-dependence is well structured. By exploiting this structure, the problem of filter design and analysis can be converted into that of determining the feasibility of a set of Linear Matrix Inequalities (LMIs) [14, 67] that arise in the theory of linear differential inclusions [8, 14]. As a consequence, the stability of the resulting filters as well as their "frequency-like" performance can be assessed using efficient numerical analysis tools that borrow from convex optimization techniques [14, 48], in a similar way as presented in the previous chapter for the class of periodic systems.

The design of a navigation system that estimates position and velocity of an autonomous vehicle by complementing position information available from GPS with the velocity information provided by a Doppler sonar system will again be used as a motivating example along this chapter. However, there are no constraints on the application of the methodology formulated along this chapter to other complementary structures as presented in chapter 3.

The chapter is organized as follows: the mathematical background that is required for complementary time-varying filter analysis and design will be reviewed in section 6.2 namely induced operator norms, and polytopic systems. Moreover, the new concepts of low and high-pass filters, introduced for periodic systems in chapter 5, are extended for linear time-varying systems. Section 6.3 describes the navigation problem addressed in this paper and formulates it mathematically in terms of an equivalent time-varying filter design problem. Section 6.4 provides the main theoretical tools for linear time-varying filter design and analysis using the theory of linear matrix inequalities. Section 6.5 describes a practical algorithm for complementary filter design and illustrates the performance of the new filtering structure in simulation. Section 6.6 discusses an extension of the results reported in previous sections to the case where accelerometers are available instead of velocity sensors. Finally, some conclusions are drawn and some goals for future work are set in section 6.7.

6.2 Mathematical background

This section summarizes the mathematical formalism that is required for the study of linear systems, both from an internal and an input-output point of view. Throughout this chapter, we will restrict ourselves to the class of linear time-varying systems \mathcal{G}_t , described as a finite-

dimensional operator where $\mathbf{x}(t) \in \mathbb{R}^n$ is the state vector, $\mathbf{u}(t) \in \mathbb{R}^m$ is the vector of inputs and disturbances, and $\mathbf{y}(t) \in \mathbb{R}^p$ is the output vector, with state-space realization

$$\Sigma_{\mathcal{G}_t} := \begin{cases} \dot{\mathbf{x}}(t) &= A(t)\mathbf{x}(t) + B(t)\mathbf{u}(t) \\ \mathbf{y}(t) &= C(t)\mathbf{x}(t) + D(t)\mathbf{u}(t) \end{cases} \quad (6.2.1)$$

of bounded, piece-wise continuous matrix functions of time. Often, we will use the same symbol \mathcal{G}_t to denote both an linear time-varying system and its particular realization $\Sigma_{\mathcal{G}_t}$, as the meaning will become clear from the context.

Throughout the text, given any $\tau \in \mathcal{R}_+$, Π_τ denotes the projection operator defined for every f by $\Pi_\tau f(t) = f(t)$ when $t \leq \tau$, and 0 otherwise. Let $L_2[0, \infty; \mathcal{R}^p]$ denote the Hilbert space of Lebesgue measurable functions endowed with the usual norm

$$\|f\|_2^2 := \int_0^\infty \|f(t)\|_2^2 dt$$

and define the extended space $L_{2e}[0, \infty; \mathcal{R}^p] := \{f \in \mathcal{X} : \Pi_\tau f \in L_2[0, \infty; \mathcal{R}^p] \text{ for all finite } \tau \text{ in } \mathcal{R}_+\}$. In the sequel we compress the notation $L_{2e}[0, \infty; \mathcal{R}^p]$ and $L_2[0, \infty; \mathcal{R}^p]$ to L_{2e}^p and L_2^p , respectively. This notation will be further simplified to L_{2e} and L_2 whenever the dimension of p is not relevant. Along this chapter, $L_\infty[0, \infty; \mathcal{R}^p]$ (abbv. L_∞) denote the space of Lebesgue measurable functions in \mathbb{R}^n , endowed with the norm

$$\|f\|_\infty := \operatorname{ess\,sup}_{t \in \mathbb{R}^+} \|f(t)\|_2.$$

If an operator \mathcal{G}_t admits a state-space representation $\Sigma_{\mathcal{G}_t}$ that is internally stable, then \mathcal{G}_t maps L_∞ to L_∞ and the corresponding induced operator norm

$$\|\mathcal{G}_t\|_{\infty, i} := \sup \left\{ \frac{\|\mathcal{G}_t f\|_\infty}{\|f\|_\infty} : f \in L_\infty, t \in \mathcal{R}_+ \right\}$$

is finite.

A realization is said to be *exponentially stable* if the null solution to the linear differential equation $d\mathbf{x}(t)/dt = A(t)\mathbf{x}(t)$ is uniformly asymptotically stable, that is, there exist positive-real constants α and β such that $\|\Phi(t, \tau)\| \leq \alpha \exp[-\beta(t - \tau)]$ for all $t \geq \tau$, where $\Phi(t, \tau)$ denotes the transition matrix associated with $A(t)$. To simplify the exposition, we will henceforth refer to an exponentially stable system as *internally stable*, while a (finite-gain) stable system will be simply called *stable*. If $\mathcal{G}_t : L_{2e} \rightarrow L_{2e}$ has an internally stable realization, then \mathcal{G}_t defines a stable operator from $L_2 \rightarrow L_2$.

The extension of these definitions to the case where the operator inputs and outputs belong to the space of essentially bounded functions of time is immediate, and can be found in [76].

6.2.1 Computation of induced operator norms. Polytopic systems.

In the following there will be considered linear time-varying systems with realizations

$$\{A(t), B(t), C(t), D(t)\} \in \Omega := \mathbf{Co}\{\{A_1, B_1, C_1, D_1\}, \dots, \{A_L, B_L, C_L, D_L\}\}$$

where

$$\mathbf{Co}S := \left\{ \sum_{i=1}^L \lambda_i \mathcal{A}_i \mid \mathcal{A}_i \in S, \lambda_1 + \dots + \lambda_L = 1 \right\}$$

is the convex hull of the set $S := \{\mathcal{A}_1, \dots, \mathcal{A}_n\}$. These systems are usually referred to in the literature as *polytopic differential inclusions* [14]. The next results gives conditions on the computation of the \mathcal{H}_∞ norm of that class of systems.

Proposition 6.2.1 [14] *Let the system $\mathcal{G}_t : \mathbf{w} \rightarrow \mathbf{z}$ described by (6.2.1) be asymptotically stable and let $\gamma > 0$ be a real number. The following statements are equivalent:*

1. $\|\mathcal{G}_t\|_\infty < \gamma$;
2. *The system is strictly dissipative, with respect to the supply function*

$$s(\mathbf{w}, \mathbf{z}) = \gamma^2 \|\mathbf{w}\|_2^2 - \|\mathbf{z}\|_2^2;$$

3. *There exists a symmetric matrix $P = P^T \in \mathbb{R}^{n \times n}$ that enables the LMIs*

$$\begin{bmatrix} A_i^T P + P A_i + C_i^T C_i & P B_i + C_i^T D_i \\ B_i^T P + D_i^T C_i & D_i^T D_i - \gamma^2 I_m \end{bmatrix} < 0. \quad (6.2.2)$$

for $i = 1, 2, \dots, L$.

Note that the LMIs used are a natural extension to the ones used in the basic result for the \mathcal{H}_∞ norm of a linear time-invariant system, presented in proposition 2.5.1. In a similar way as in the precedent chapters, checking that such a P exists can be done quite efficiently using highly efficient numerical algorithms.

The results above have their natural counterparts for the cases of operators that map L_∞ to L_∞ , as well as for the \mathcal{H}_2 norm computation of such operators. As discussed in [67], the

problem of computing the L_∞ induced norm of an operator can still be cast in the framework of LMI theory. However, the computational procedure is more complex and requires a line search over a real parameter.

6.2.2 Low and high-pass time-varying filters.

The concepts of low-pass and high-pass filters introduced previously in this work will be extended to the class of linear time-invariant systems. In a similar way as for periodic systems (see chapter 5), they will also play a key role in assessing the performance of complementary filters. The definitions of low and high-pass filters will be rewritten next for time-varying systems, based on the \mathcal{H}_∞ norm computation of an auxiliary operator.

Definition 6.2.2 Low-pass property - Let \mathcal{G}_t be a linear, internally stable time-varying system and let \mathcal{W}_ω^n be a low-pass, linear time-invariant Chebyshev filter of order n and cutoff frequency ω . The system \mathcal{G}_t is said to satisfy a low-pass property with indices (ϵ, n) over $[0, \omega_c]$ if

$$\|(\mathcal{G}_t - I)\mathcal{W}_{\omega_c}^n\|_\infty < \epsilon$$

Definition 6.2.3 Low-pass filter with bandwidth ω_c - A linear, internally stable time-varying system \mathcal{G}_t is said to be an (ϵ, n) low-pass filter with bandwidth ω_c if

- $\lim_{\omega \rightarrow 0} \|(\mathcal{G}_t - I)\mathcal{W}_\omega^n\|$ is well defined and equals 0.
- $\omega_c := \sup\{\omega : \|(\mathcal{G}_t - I)\mathcal{W}_\omega^n\| < \epsilon\}$, i.e. \mathcal{G}_t satisfies a low-pass property with indices (ϵ, n) over $[0, \omega]$ for all $\omega \in [0, \omega_c)$ but fails to satisfy that property whenever $\omega \geq \omega_c$.
- For every $\delta > 0$, there exists $\omega^* = \omega^*(\delta)$ such that $\|\mathcal{G}_t(I - \mathcal{W}_\omega^n)\| < \delta$ for $\omega > \omega^*$.

Definition 6.2.4 High-pass Filter with break frequency ω_c - A linear, internally stable time-varying system \mathcal{G}_t is said to be an (ϵ, n) high-pass filter with break frequency ω_c if $(I - \mathcal{G}_t)$ is an (ϵ, n) low-pass filter with bandwidth ω_c .

Interestingly, these definitions rely only on the computation of the \mathcal{H}_∞ norm of polytopic systems, which can be done resorting to 6.2.1. The same circle of ideas as introduced in chapter 5 can be applied to polytopic systems, therefore no further explanations will be used.

6.3 Navigation system design: problem formulation

This section describes the navigation problem that is the main focus of the chapter and formulates it mathematically in terms of an equivalent filter design problem. For the sake of clarity, we first repeat the basic notation and summarize the kinematic equations for a general vehicle.

6.3.1 Notation. Vehicle kinematics: a summary.

Let $\{\mathcal{I}\}$ be a reference frame, and let $\{\mathcal{B}\}$ denote a body-fixed frame that moves with the vehicle. Note that in this case the vehicle under consideration can be a surface craft (such as the Delfim catamaran) or an underwater vehicle (such as an autonomous underwater vehicle or a remotely operated vehicle). The following notation is therefore required:

$$\begin{aligned}
 \mathbf{p} &:= [x \ y \ z]^T && \text{- position of the origin of } \{\mathcal{B}\} \text{ measured in } \{\mathcal{I}\}; \\
 {}^{\mathcal{I}}\mathbf{v} &:= [\dot{x} \ \dot{y} \ \dot{z}]^T && \text{- linear velocity of the origin of } \{\mathcal{B}\} \text{ with respect to the} \\
 &&& \text{fixed frame } \{\mathcal{I}\}; \\
 \mathbf{v} &:= [u \ v \ w]^T && \text{- linear velocity of the origin of } \{\mathcal{B}\} \text{ with respect to the} \\
 &&& \text{inertial coordinate frame } \{\mathcal{I}\}, \text{ expressed in } \{\mathcal{B}\}, \text{ i.e.,} \\
 &&& \text{body-fixed velocity}; \\
 \boldsymbol{\lambda} &:= [\phi \ \theta \ \psi]^T && \text{- vector of roll, pitch, and yaw angles that parametrize} \\
 &&& \text{locally the orientation of } \{\mathcal{B}\} \text{ relative to } \{\mathcal{I}\}; \\
 \boldsymbol{\omega} &:= [p \ q \ r]^T && \text{- angular velocity of } \{\mathcal{B}\} \text{ with respect to } \{\mathcal{I}\}, \text{ resolved} \\
 &&& \text{in } \{\mathcal{B}\};
 \end{aligned}$$

Given two frames $\{\mathcal{A}\}$ and $\{\mathcal{B}\}$, ${}^{\mathcal{A}}\mathcal{R}$ denotes the rotation matrix from $\{\mathcal{B}\}$ to $\{\mathcal{A}\}$. In particular, ${}^{\mathcal{I}}\mathcal{R}$ (abbreviated \mathcal{R}) is the rotation matrix from $\{\mathcal{B}\}$ to $\{\mathcal{I}\}$, parametrized locally by $\boldsymbol{\lambda}$, that is, $\mathcal{R} = \mathcal{R}(\boldsymbol{\lambda})$. Since \mathcal{R} is a rotation matrix, it satisfies the orthonormality condition $\mathcal{R}^T \mathcal{R} = I$. Given the angular velocity vector $\boldsymbol{\omega}$, then

$$\dot{\boldsymbol{\lambda}} = Q(\boldsymbol{\lambda})\boldsymbol{\omega}$$

where $Q(\boldsymbol{\lambda})$ is a matrix that relates the derivative of $\boldsymbol{\lambda}$ with $\boldsymbol{\omega}$. The following kinematic relations apply [15]:

$$\frac{d}{dt}\mathbf{p} = {}^{\mathcal{I}}\mathbf{v} = \mathcal{R}\mathbf{v} \quad (6.3.1)$$

and

$$\dot{\mathcal{R}}(\boldsymbol{\lambda}) = \mathcal{R}(\boldsymbol{\lambda})\mathcal{S}(\boldsymbol{\omega}), \quad (6.3.2)$$

where

$$\mathcal{S}(\boldsymbol{\omega}) := \begin{bmatrix} 0 & -\omega_z & \omega_y \\ \omega_z & 0 & -\omega_x \\ -\omega_y & \omega_x & 0 \end{bmatrix} \quad (6.3.3)$$

is a skew symmetric matrix, that is, $\mathcal{S}^T = -\mathcal{S}$. The matrix \mathcal{S} satisfies the relationship $\mathcal{S}(a)b = a \times b$, where a, b are arbitrary vectors and \times denotes the cross product operation. Furthermore, $\|\mathcal{S}(\boldsymbol{\omega})\| = \|\boldsymbol{\omega}\|$.

6.3.2 Time-varying complementary filters. Navigation problem formulation.

We now extend the basic concepts of complementary filtering to the time-varying setting. The motivation for this work can be simply described by considering the example where one is interested in estimating the position \mathbf{p} and velocity ${}^I\mathbf{v}$ of a vehicle based on measurements \mathbf{p}_m and \mathbf{v}_m of \mathbf{p} and \mathbf{v} , respectively. In the case of an ocean surface vehicle, \mathbf{p}_m is provided by a Differential Global Positioning System (SGPS), whereas \mathbf{v}_m is provided by a Doppler sonar. In the case of a fully submerged underwater vehicle, \mathbf{p}_m can be provided by a Long Baseline System or by a GIB system [58].

It must be stressed that due to the physical characteristic of the Doppler sonar the *measurement* \mathbf{v}_m is naturally expressed in body-axis, that is, in the reference frame $\{\mathcal{B}\}$. Furthermore, Doppler bias effects are also naturally expressed in $\{\mathcal{B}\}$. This is in contrast with the measurements \mathbf{p}_m , which are directly available in the reference frame $\{\mathcal{I}\}$. These facts impose important constraints on the class of complementary filters for position and velocity estimation, as will become clear later.

The underlying process model \mathcal{M}_{pv} is depicted in figure 6.3.1, where \mathcal{E}_t is a dynamical system (filter) that operates on the measurements \mathbf{p}_m and \mathbf{v}_m to provide estimates $\hat{\mathbf{p}}$ of \mathbf{p} . In the figure, \mathbf{p}_d and \mathbf{v}_d are measurement disturbances. As detailed in the motivating example introduced in the chapter on complementary filters, we study the situation where $\mathbf{p}_d = 0$ and $\mathbf{v}_d = \mathbf{v}_{d,0}$ where $\mathbf{v}_{d,0}$ is the Doppler bias. This setup is all that is required for the design of complementary filters from a "frequency-like" domain point of view. Notice that the process model \mathcal{M}_{pv} is

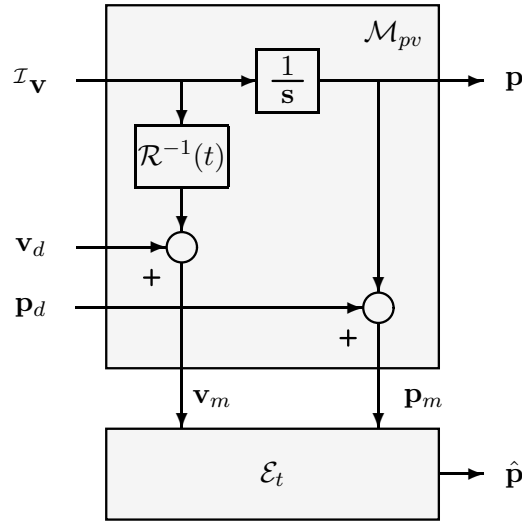


Figure 6.3.1: Process model.

time-varying due to the presence of the rotation matrix $\mathcal{R}(t)$. However, the entries of $\mathcal{R}(t)$ and their derivatives are not arbitrary functions of time but exhibit bounds that depend on each specific vehicle mission under consideration. For example, if an underwater vehicle motion is restricted to the horizontal plane and the maximum yaw rate achievable with that vehicle is r_{max} , then this information must be explicitly included in the description of the process model \mathcal{M}_{pv} as we explain below. We now introduce the following definitions.

Definition 6.3.1 Process Model \mathcal{M}_{pv} - The process model \mathcal{M}_{pv} is given by

$$\mathcal{M}_{pv} := \begin{cases} \frac{d}{dt} \mathbf{p} &= \mathcal{I} \mathbf{v} \\ \mathbf{p}_m &= \mathbf{p} \\ \mathbf{v}_m &= \mathcal{R}^{-1}(t) \mathcal{I} \mathbf{v} + \mathbf{v}_{d,0} \end{cases} \quad (6.3.4)$$

We further assume that the matrix \mathcal{R} and its derivative $\dot{\mathcal{R}}$ are constrained through the inequalities

$$|\phi(t)| \leq \phi_{max}, |\theta(t)| \leq \theta_{max} \quad (6.3.5)$$

and

$$|p(t)| \leq p_{max}, |q(t)| \leq q_{max}, |\dot{q}(t)| \leq r_{max} \quad (6.3.6)$$

for all $t \in \mathbb{R}^+$. Notice in the definition above that there are constraints on the roll and pitch angles ϕ and θ respectively, but not on the yaw angle ψ . This is due to the fact that ocean

vehicles are designed to undergo arbitrary maneuvers in yaw, but pitch and roll excursions are restricted by vehicle construction.

Definition 6.3.2 Candidate complementary filter - Consider the process model \mathcal{M}_{pv} in (6.3.4) with $\mathbf{v}_{d,0}$ an arbitrary constant, and let \mathcal{E}_t be a linear time-varying filter with realization

$$\mathcal{E}_t := \begin{cases} \dot{\mathbf{x}} &= A(t)\mathbf{x} + B_p(t)\mathbf{p}_m + B_v(t)\mathbf{v}_m \\ \hat{\mathbf{p}} &= C(t)\mathbf{x}. \end{cases} \quad (6.3.7)$$

Then, \mathcal{E}_t is said to be a *candidate complementary filter* for \mathcal{M}_{pv} if

- \mathcal{E}_t is internally stable
- For every initial conditions $\mathbf{p}(0)$ and $\mathbf{x}(0)$, $\lim_{t \rightarrow \infty} \{\mathbf{p}(t) - \hat{\mathbf{p}}(t)\} = 0$.
- \mathcal{E}_t satisfies a bias rejection property, that is, $\lim_{t \rightarrow \infty} \hat{\mathbf{p}} = 0$ when $\mathbf{v} = 0$.

Definition 6.3.3 Complementary filter with break frequency ω_c - Let \mathcal{E}_t be a candidate complementary filter for \mathcal{M}_{pv} , and let \mathcal{E}_{tp} denote the corresponding operator from \mathbf{p}_m to $\hat{\mathbf{p}}$. Then, \mathcal{E}_t is said to be an (ϵ, n) complementary filter for \mathcal{M}_{pv} with break frequency ω_c if \mathcal{E}_{tp} is an (ϵ, n) low-pass filter with bandwidth ω_c .

The discussion in the previous sections leads directly to the following filter design problem.

Problem formulation: Given the process model \mathcal{M}_{pv} in (6.3.4) and positive numbers ω_c , n , and ϵ , find an (ϵ, n) complementary filter for \mathcal{M}_{pv} with break frequency ω_c .

6.4 Complementary filter design. Main results.

This section introduces a specific candidate complementary filter structure for \mathcal{M}_{pv} and derives sufficient conditions for the existence of a complementary filter with the structure adopted that meets required bandwidth constraints.

6.4.1 Candidate complementary filter structure.

Figure 6.4.1 depicts the candidate filter structure for \mathcal{M}_{pv} that will be adopted in the chapter. The structure is motivated by the simple example described in Section 3.3, where an extra

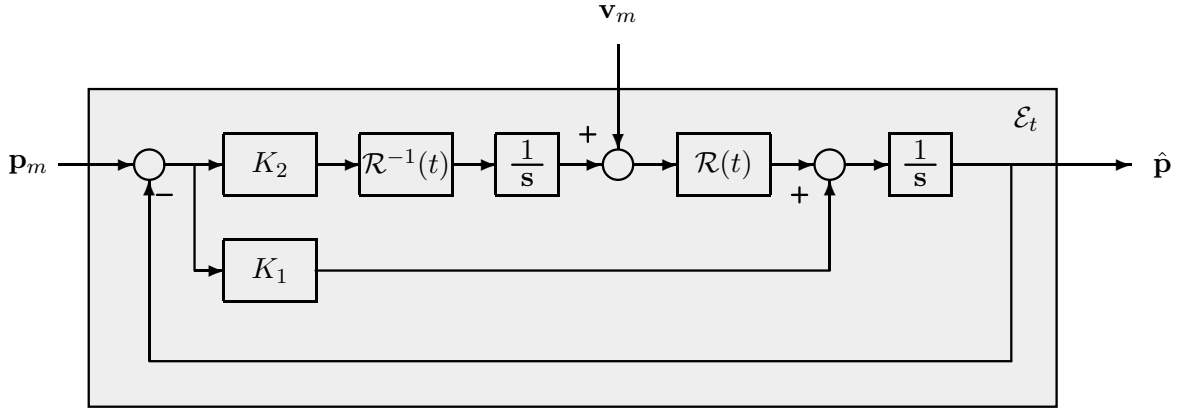


Figure 6.4.1: Non-linear time-varying complementary filter.

integrator was inserted to estimate a sensor bias. Notice however that the filter explicitly includes the rotation matrix $\mathcal{R}(t)$, which we assume is available from an attitude reference system. The issue of robust filter performance against uncertainties in the measurement of $\mathcal{R}(t)$ will be addressed later in this section. The following result is obtained.

Theorem 6.4.1 Consider the process model \mathcal{M}_{pv} and the time-varying filter

$$\mathcal{E}_t := \begin{cases} \dot{\mathbf{x}}_1 &= \mathcal{R}(t)\mathbf{v}_m + \mathcal{R}(t)\mathbf{x}_2 + K_1(\mathbf{p} - \mathbf{x}_1) \\ \dot{\mathbf{x}}_2 &= \mathcal{R}^{-1}(t)K_2(\mathbf{p} - \mathbf{x}_1) \\ \hat{\mathbf{p}} &= \mathbf{x}_1 \end{cases} \quad (6.4.1)$$

Suppose the filter \mathcal{E}_t is internally stable. Then, \mathcal{E}_t is a candidate complementary filter for \mathcal{M}_{pv} .

Proof: From the assumptions, the time-varying filter has the realization

$$\mathcal{E}_t := \begin{cases} \dot{\mathbf{x}} &= A(t)\mathbf{x} + \begin{bmatrix} B_p(t) & B_v(t) \end{bmatrix} \begin{bmatrix} \mathbf{p}_m \\ \mathbf{v}_m \end{bmatrix} \\ \hat{\mathbf{p}} &= C(t)\mathbf{x}. \end{cases}$$

where

$$A(t) = \begin{bmatrix} -K_1 & \mathcal{R}(t) \\ -\mathcal{R}^{-1}(t)K_2 & 0 \end{bmatrix}, B_p(t) = \begin{bmatrix} K_1 \\ \mathcal{R}^{-1}(t)K_2 \end{bmatrix}, B_v(t) = \begin{bmatrix} \mathcal{R}(t) \\ 0 \end{bmatrix}, C(t) = \begin{bmatrix} I \\ 0 \end{bmatrix}$$

Furthermore, $\mathbf{v}_m = \mathbf{v} + \mathbf{v}_{d,0}$, where $\mathbf{v}_{d,0}$ is an arbitrary constant vector (Doppler bias). Let $\Phi(t, \tau)$ denote the state transition matrix associated with $A(t)$. Then, using the equalities

$$B_P \mathbf{p}(\tau) = -A(\tau) \begin{bmatrix} \mathbf{p}(\tau) \\ 0 \end{bmatrix}, B_v \mathbf{v}(\tau) = \begin{bmatrix} \frac{d}{d\tau} \mathbf{p}(\tau) \\ 0 \end{bmatrix}, B_v \mathbf{v}_{d,0} = -A(\tau) \begin{bmatrix} 0 \\ \mathbf{v}_{d,0} \end{bmatrix}$$

the filter state evolution is given by

$$\begin{aligned} \begin{bmatrix} \mathbf{x}_1(t) \\ \mathbf{x}_2(t) \end{bmatrix} &= \Phi(t, t_0) \begin{bmatrix} \mathbf{x}_1(t_0) \\ \mathbf{x}_2(t_0) \end{bmatrix} + \int_{t_0}^t \Phi(t, \tau) \{B_P \mathbf{p}(\tau) + B_v(\mathbf{v}(\tau) + \mathbf{v}_{d,0})\} d\tau \\ &= \Phi(t, t_0) \begin{bmatrix} \mathbf{x}_1(t_0) \\ \mathbf{x}_2(t_0) \end{bmatrix} \\ &\quad + \int_{t_0}^t \Phi(t, \tau) \left\{ -A(\tau) \begin{bmatrix} \mathbf{p}(\tau) \\ 0 \end{bmatrix} + \begin{bmatrix} \frac{d}{d\tau} \mathbf{p}(\tau) \\ 0 \end{bmatrix} \right\} d\tau \\ &\quad + \int_{t_0}^t \Phi(t, \tau) \left\{ -A(\tau) \begin{bmatrix} 0 \\ \mathbf{v}_{d,0} \end{bmatrix} \right\} d\tau. \end{aligned} \tag{6.4.2}$$

The transition matrix $\Phi(t, \tau)$ satisfies

$$\frac{d}{d\tau} \Phi(t, \tau) = -\Phi(t, \tau) A(\tau) \tag{6.4.3}$$

and therefore 6.4.2 can also be written as

$$\begin{aligned} \begin{bmatrix} \mathbf{x}_1(t) \\ \mathbf{x}_2(t) \end{bmatrix} &= \Phi(t, t_0) \begin{bmatrix} \mathbf{x}_1(t_0) \\ \mathbf{x}_2(t_0) \end{bmatrix} + \int_{t_0}^t \left\{ \frac{d}{d\tau} \left(\Phi(t, \tau) \begin{bmatrix} p(\tau) \\ 0 \end{bmatrix} \right) \right\} d\tau \\ &\quad + \int_{t_0}^t \left\{ \frac{d}{d\tau} \left(\Phi(t, \tau) \begin{bmatrix} 0 \\ \mathbf{v}_{d,0} \end{bmatrix} \right) \right\} d\tau \\ &= \Phi(t, t_0) \begin{bmatrix} \mathbf{x}_1(t_0) \\ \mathbf{x}_2(t_0) \end{bmatrix} + \begin{bmatrix} \mathbf{p}(t) \\ 0 \end{bmatrix} - \Phi(t, t_0) \begin{bmatrix} \mathbf{p}(t_0) \\ 0 \end{bmatrix} \\ &\quad + \begin{bmatrix} 0 \\ \mathbf{v}_{d,0} \end{bmatrix} - \Phi(t, t_0) \begin{bmatrix} 0 \\ \mathbf{v}_{d,0} \end{bmatrix} \end{aligned} \tag{6.4.4}$$

Since the filter is stable, $\lim_{t \rightarrow \infty} \|\Phi(t, t_0)\| = 0$. The results follows immediately by observing that $\hat{\mathbf{p}} = \mathbf{x}_1$. ■

Notice that the state \mathbf{x}_2 of the appended integrator tends asymptotically to $-\mathbf{v}_{d,0}$. Thus, \mathbf{x}_2 provides an estimate of the Doppler bias in the body frame. This result makes perfect sense from a physical point of view since the bias is constant in the body frame (not in the reference frame \mathcal{I}).

6.4.2 The candidate complementary filter: sufficient conditions for stability and guaranteed break frequency.

The next result establishes sufficient conditions for the existence of fixed gains K_1 and K_2 such that the candidate filter is internally stable and has a guaranteed break frequency of at least ω_c , where ω_c is a design parameter. In preparation for that result we let

$$\boldsymbol{\omega}_r = [p_r \ q_r \ r_r]^T := \mathcal{R}\boldsymbol{\omega}$$

and define

$$\mathcal{S}_r := S(\boldsymbol{\omega}_r) = S(\mathcal{R}\boldsymbol{\omega})$$

Given the original design bounds (6.3.5)-(6.3.6), it is possible to compute positive upper bounds p_r^+ , q_r^+ , and r_r^+ such that

$$|p_r| \leq p_r^+, |q_r| \leq q_r^+, |r_r| \leq r_r^+. \quad (6.4.5)$$

Let $p_r^- = -p_r^+$, $q_r^- = -q_r^+$, $r_r^- = -r_r^+$ and construct the set $\{\boldsymbol{\omega}_r^i, i = \{1, \dots, 8\}\}$, where

$$\boldsymbol{\omega}_r^1 = \begin{bmatrix} p_r^- \\ q_r^- \\ r_r^- \end{bmatrix}, \boldsymbol{\omega}_r^2 = \begin{bmatrix} p_r^+ \\ q_r^- \\ r_r^- \end{bmatrix}, \boldsymbol{\omega}_r^3 = \begin{bmatrix} p_r^- \\ q_r^+ \\ r_r^- \end{bmatrix}, \boldsymbol{\omega}_r^4 = \begin{bmatrix} p_r^+ \\ q_r^+ \\ r_r^- \end{bmatrix}, \dots, \boldsymbol{\omega}_r^8 = \begin{bmatrix} p_r^+ \\ q_r^+ \\ r_r^+ \end{bmatrix}.$$

Then

$$\boldsymbol{\omega}_r \in \text{Co}\{\boldsymbol{\omega}_r^i, i = \{1, \dots, 8\}\} \text{ and}$$

$$\mathcal{S}_r \in \text{Co}\{\mathcal{S}_r^i = S(\boldsymbol{\omega}_r^i); i = \{1, \dots, 8\}\}$$

Theorem 6.4.2 Consider the linear time-varying filter (6.4.1) and assume that the bounds (6.4.5) on $\boldsymbol{\omega}_r$ apply. Given n and ω_c , let

$$\Sigma_{\mathcal{W}} := \begin{cases} \dot{\mathbf{x}}(t) &= A_W \mathbf{x}(t) + B_W \mathbf{u}(t) \\ \mathbf{y}(t) &= C_W \mathbf{x}(t) \end{cases}$$

be a minimal realization for the weighting Chebyshev filter introduced in subsection 6.2.2. Further let

$$F = \begin{bmatrix} 0 & I \\ 0 & \mathcal{S}_r \end{bmatrix}, \quad \text{and} \quad H = \begin{bmatrix} -I & 0 \end{bmatrix}.$$

Suppose that given $\epsilon > 0 \exists K \in \mathcal{R}^{6 \times 3}$, $P \in \mathcal{R}^{(6+n) \times (6+n)}$, $P > 0$, such that the linear matrix inequalities

$$L_{LP_i}(K, P, \epsilon) := \left[\begin{array}{c|c} P \begin{bmatrix} F_i + KH & KC_W \\ 0 & A_W \end{bmatrix} + \begin{bmatrix} F_i + KH & KC_W \\ 0 & A_W \end{bmatrix}^T P & P \begin{bmatrix} 0 \\ B_W \end{bmatrix} \\ \hline \begin{matrix} + \begin{bmatrix} H^T \\ -C_W^T \end{bmatrix} \\ [H \quad -C_W] \end{matrix} & -\epsilon^2 I \end{array} \right] < 0, \quad (6.4.6)$$

$$F_i = \begin{bmatrix} 0 & I \\ 0 & \mathcal{S}(\omega_r^i) \end{bmatrix}, \quad i = \{1, \dots, 8\}$$

are satisfied. Then, the constant gains

$$\begin{bmatrix} K_1 \\ K_2 \end{bmatrix} := K$$

make the filter \mathcal{E}_t internally stable. Furthermore, the operator $\mathcal{E}_{t_p} : \mathbf{p} \rightarrow \hat{\mathbf{p}}$ satisfies a low-pass property with indices (ϵ, n) over $[0, \omega_c]$, that is, $\|(\mathcal{E}_{t_p} - I)\mathcal{W}_{\omega_c}^n\| < \epsilon$.

Proof: Given the realization 6.4.1, consider the Lyapunov coordinate transformation [16]

$$\zeta(t) = \bar{P}(t)\mathbf{x}(t),$$

where

$$\bar{P}(t) = \begin{bmatrix} I & 0 \\ 0 & \mathcal{R}(t) \end{bmatrix}.$$

With this change of coordinates, the operator \mathcal{E}_{t_p} admits the realization

$$\mathcal{E}_{t_p} = \begin{cases} \dot{\zeta} &= (\bar{P}A\bar{P}^{-1} + \dot{\bar{P}}\bar{P}^{-1})\zeta + \bar{P}B_p\mathbf{p} \\ \hat{\mathbf{p}} &= C\bar{P}^{-1}\zeta \end{cases} \quad (6.4.7)$$

Using the relations

$$\bar{P}A\bar{P}^{-1} = \begin{bmatrix} -K_1 & I \\ -K_2 & 0 \end{bmatrix}$$

and

$$\dot{\bar{P}}\bar{P}^{-1} = \begin{bmatrix} 0 & 0 \\ 0 & \mathcal{R}\mathcal{S}(\omega)\mathcal{R}^{-1} \end{bmatrix} = \begin{bmatrix} 0 & 0 \\ 0 & \mathcal{S}(\mathcal{R}\omega) \end{bmatrix} = \begin{bmatrix} 0 & 0 \\ 0 & \mathcal{S}(\omega_r) \end{bmatrix}$$

(6.4.7) can be written as

$$\begin{aligned} \dot{\zeta} &= \begin{bmatrix} -K_1 & I \\ -K_2 & \mathcal{S}(\omega_r) \end{bmatrix} \zeta + \begin{bmatrix} K_1 \\ K_2 \end{bmatrix} \mathbf{p} \\ \hat{\mathbf{p}} &= [I \ 0] \zeta. \end{aligned} \quad (6.4.8)$$

Simple algebra now shows that $(\mathcal{E}_{t_p} - I)\mathcal{W}_{\omega_c}^n$ admits the state-space representation

$$(\mathcal{E}_{t_p} - I)\mathcal{W}_{\omega_c}^n := \left[\begin{array}{ccc|c} -K_1 & I & K_1 C_W & 0 \\ -K_2 & \mathcal{S}_r & K_2 C_W & 0 \\ 0 & 0 & A_W & B_W \\ \hline I & 0 & -C_W & 0 \end{array} \right] = \quad (6.4.9)$$

$$= \left[\begin{array}{cc|c} F + KH & KC_W & 0 \\ 0 & A_W & B_W \\ \hline H & -C_W & 0 \end{array} \right] \in \mathbf{Co} \left\{ \left[\begin{array}{cc|c} F_i + KH & KC_W & 0 \\ 0 & A_W & B_W \\ \hline H & -C_W & 0 \end{array} \right], i = \{1, \dots, 8\} \right\}.$$

where

$$K = \begin{bmatrix} K_1 \\ K_2 \end{bmatrix}$$

and F , H , and F_i are defined above.

Suppose $\exists P > 0$ and K such that

$$\left[\begin{array}{ccc|c} P \begin{bmatrix} F_i + KH & KC_W \\ 0 & A_W \end{bmatrix} + \begin{bmatrix} F_i + KH & KC_W \\ 0 & A_W \end{bmatrix}^T P & & & P \begin{bmatrix} 0 \\ B_W \end{bmatrix} \\ & + \begin{bmatrix} H^T \\ -C_W^T \end{bmatrix} [H \ -C_W] & & \\ \hline & [0 \ B_W^T] P & & -\epsilon^2 I \end{array} \right] < 0, \quad (6.4.10)$$

$i = \{1, \dots, 8\}$.

Then, using standard results on polytopic system analysis (see proposition 6.2.1 or equation (6.54) in [14]) it follows that $\|(\mathcal{E}_{t_p} - I)\mathcal{W}_{\omega_c}^n\| < \epsilon$. Clearly, if the inequalities (6.4.10) are satisfied

then the gains

$$\begin{bmatrix} K_1 \\ K_2 \end{bmatrix} := K \quad (6.4.11)$$

guarantee that $\|(\mathcal{E}_{t_p} - I)\mathcal{W}_{\omega_c}^n\| < \epsilon$. Notice if expression (6.4.10) is satisfied for some P and K then the matrices

$$\begin{bmatrix} F_i + KH & KC_W \\ 0 & A_W \end{bmatrix}, \quad i = 1, \dots, 8$$

are stable and therefore the polytopic system (6.4.8) with state matrix $F + KH$ is internally stable [14]. Since Lyapunov transformations preserve internal stability, the original system 6.4.1 is also internally stable. ■

The above theorem establishes sufficient conditions for the existence of fixed gains K_1 and K_2 such that the complementary filter (6.4.1) is internally stable and meets desired "frequency-like" response characteristics. However, it does not provide any results on the feasibility of the problem at hand. The theorem that follows addresses this problem partially, by showing that there always exists a set of fixed gains for which the filter (6.4.1) is internally stable.

Theorem 6.4.3 *Consider the linear time-varying filter (6.4.1). Then, for every set of finite positive numbers p_r^+ , q_r^+ , and r_r^+ such that the bounds (6.4.5) on ω_r apply there exist fixed gains K_1 and K_2 that make the filter internally stable.*

Proof: From the proof of theorem 6.4.2, the filter (6.4.1) is internally stable if and only if the unforced polytopic system

$$\dot{\zeta} = (F + KH)\zeta \quad (6.4.12)$$

is internally stable for some choice of K . Given (6.4.12), consider the related time-invariant system

$$\dot{\zeta} = (A + KH)\zeta = A_K\zeta, \quad (6.4.13)$$

where

$$A_K = A + KH; \quad A = \begin{bmatrix} 0 & I \\ 0 & 0 \end{bmatrix}.$$

The simple structures of the matrices A and H implies that (6.4.13) can be made stable by choosing $K_1 = k_1I$, $K_2 = k_2I$, where k_1 and $k_2 > 0$ are positive but otherwise arbitrary. This

stems from the fact that the closed loop eigenvalues of $A + KH$ have multiplicity three and are easily obtained from the roots of the second order polynomial $s^2 + k_1s + k_2$. Therefore, from basic Lyapunov stability theory it follows that for every $\gamma_1 > 0, \gamma_2 > 0$ there exists a positive definite matrix

$$P_1 = \begin{bmatrix} P_{11} & P_{12} \\ P_{12} & P_{22} \end{bmatrix} > 0$$

such that

$$A_K^T P_1 + P_1 A_K = -Q = \begin{bmatrix} -\gamma_1 I & 0 \\ 0 & -\gamma_2 I \end{bmatrix} \quad (6.4.14)$$

Expanding (6.4.14) we obtain

$$\left[\begin{array}{c|c} -2P_{11}K_1 - 2P_{12}K_2 & -P_{12}K_1 - P_{22}K_2 + P_{11} \\ \hline (-P_{12}K_1 - P_{22}K_2 + P_{11})^T & 2P_{12} \end{array} \right] = \begin{bmatrix} -\gamma_1 I & 0 \\ 0 & -\gamma_2 I \end{bmatrix} \quad (6.4.15)$$

and therefore $P_{12} = -(\gamma_2/2)I$. Furthermore, since K_1 and K_2 are diagonal, P_{11} and P_{22} are also diagonal. Consider now the linear time-invariant systems

$$\dot{\zeta} = (F_i + KH)\zeta = A_{K_i}\zeta \quad i = 1, \dots, 8 \quad (6.4.16)$$

with F_i defined as before. Using the relation $(S_r^i)^T = -S_r^i$ it follows that

$$A_{K_i} P_1 + P_1 A_{K_i} = \begin{bmatrix} -\gamma_1 I & P_{12} S_r^i \\ (S_r^i)^T P_{12} & -\gamma_2 I \end{bmatrix} \quad i = 1, \dots, 8 \quad (6.4.17)$$

We now show that (6.4.17) can be made negative definite for all $i = 1, 2, \dots, 8$ by suitable choice of γ_1 and γ_2 . In fact, using Schur complements [14] it easily shown that (6.4.17) is negative definite if and only if

$$\gamma_1 I - P_{12} S_r^i \gamma_2^{-1} (S_r^i)^T P_{12} = \gamma_1 I - (\gamma_2/4) S_r^i (S_r^i)^T > 0.$$

Since $\|S_r^i(\omega_r^i)\| = \|\omega_r^i\|$, the above expression is satisfied with $\gamma_2 = 4$ and $\gamma_1 > \max\{\|\omega_r^i\|^2 : i = 1, 2, \dots, 8\}$. Hence, using the theory of polytopic systems [14] the system (6.4.12) and therefore the original complementary filter are internally stable. ■

Note. From the proof of the theorem, it follows that the linear time-varying filter (6.4.1) is internally stable for any choice of constant, positive, diagonal matrices K_1 and K_2 .

We now address the issue of performance robustness of the complementary filter in the presence of measurement errors in the rotation matrix \mathcal{R} . In what follows, we let $\mathcal{R} = \mathcal{R}(\boldsymbol{\lambda})$ and

$\mathcal{R}_m = \mathcal{R}_m(\boldsymbol{\lambda}_m)$ denote the "true" and measured rotation matrices, which are functions of the "true" and measured orientation vectors $\boldsymbol{\lambda}$ and $\boldsymbol{\lambda}_m$, respectively. We further let $\mathcal{R} - \mathcal{R}_m = \Delta\mathcal{R}$ and assume that $\Delta\mathcal{R}$ is bounded, that is, there exists a positive constant δ_R such that $\|\Delta\mathcal{R}\| \leq \delta_R$.

To compute the influence of $\Delta\mathcal{R}$ on the estimation error $\mathbf{e}_p = \mathbf{p} - \hat{\mathbf{p}}$, we set $\mathbf{p}_m = \mathbf{p}$ and $\mathbf{v}_m = \mathbf{v}$. From (6.3.4) and (6.4.1) it follows that the error \mathbf{e}_p is the output of a dynamical system with input \mathbf{v} and state-space realization

$$\Sigma_{\mathcal{E}_{t_e}} := \begin{cases} \dot{\mathbf{x}}(t) &= \begin{bmatrix} -K_1 & \mathcal{R}_m \\ -\mathcal{R}_m^{-1}K_2 & 0 \end{bmatrix} \mathbf{x}(t) + \begin{bmatrix} \Delta\mathcal{R} \\ 0 \end{bmatrix} \mathbf{v}(t) \\ \mathbf{e}_p(t) &= \begin{bmatrix} I & 0 \end{bmatrix} \mathbf{x}(t) \end{cases} \quad (6.4.18)$$

The state matrix of \mathcal{E}_{t_e} equals that of \mathcal{E}_t in theorem 6.4.1. Therefore, internal stability is obtained if the conditions of theorem 6.4.2 are met with \mathcal{R} replaced by \mathcal{R}_m . In particular, if the filter gains K_1 and K_2 are constant, diagonal, and positive then internal stability is automatically ensured (see theorem 6.4.3). The issue of robust performance requires further thought, but can be addressed by viewing \mathcal{E}_{t_e} as an input-output operator with realization

$$\Sigma_{\bar{\mathcal{E}}_{t_e}} := \begin{cases} \dot{\mathbf{x}}(t) &= \begin{bmatrix} -K_1 & \mathcal{R}_m \\ -\mathcal{R}_m^{-1}K_2 & 0 \end{bmatrix} \mathbf{x}(t) + \begin{bmatrix} I \\ 0 \end{bmatrix} \mathbf{u}(t) \\ \mathbf{e}_p(t) &= \begin{bmatrix} I & 0 \end{bmatrix} \mathbf{x}(t) \end{cases} \quad (6.4.19)$$

and input $\mathbf{u} = \Delta\mathcal{R}\mathbf{v}$. If \mathbf{v} is bounded uniformly in time, that is, $\|\mathbf{v}\|_\infty = \mathbf{v}_\infty < \infty$ then

$$\|\mathbf{u}\|_\infty \leq \|\Delta\mathcal{R}\| \|\mathbf{v}\|_\infty = \delta_R \mathbf{v}_\infty$$

Since $\bar{\mathcal{E}}_{t_e}$ is internally stable, the induced norm $\|\bar{\mathcal{E}}_{t_e}\|_{\infty,i}$ of the corresponding operator is finite. Therefore,

$$\|\mathbf{e}(t)\|_2 \leq \|\mathbf{e}\|_\infty \leq \|\bar{\mathcal{E}}_{t_e}\|_{\infty,i} \delta_R \mathbf{v}_\infty$$

for all t in \mathcal{R}_+ . Thus, *the estimation error $\mathbf{e}(t)$ remains bounded for all t in the presence of measurement errors in \mathcal{R} and decreases uniformly to zero as δ_R approaches zero.*

From the discussion above, it follows that the induced operator norm $\|\bar{\mathcal{E}}_{t_e}\|_{\infty,i}$ is the correct measure of performance robustness of the filter against measurement perturbations in the rotation matrix \mathcal{R} . A constraint on $\|\bar{\mathcal{E}}_{t_e}\|_{\infty,i}$ can be included in the filter design process by using the circle of ideas discussed in [67].

6.5 Filter Design: a practical algorithm. Simulation results.

The previous section introduced the mathematical tools that are required to design a candidate complementary filter with a guaranteed break frequency. Notice, however, that the outcome of the design process may very well be a filter with an effective bandwidth that is greater than the one required. Clearly, the set of possible solutions must be further constrained so that the designer have an extra design parameter at his disposal to select one solution (if it exists) that meets the required break frequency criterion. This situation is identical to what happens in the case of filter design using Kalman-Bucy theory, where the noise covariances play the role of "tuning knobs" to shape the filter characteristics.

In the linear time-invariant case, a simple analysis of a Bode diagram indicates that an expedite way of setting an upper bound on the break frequency is to make the filter "roll-off" sufficiently fast. In the time-varying setting, this corresponds to making $\|\mathcal{E}_{tp}\mathcal{W}_{\omega_h}^{n_h}\| < \gamma$, where $\mathcal{W}_{\omega_h}^{n_h}$ is a high-pass Chebyshev filter and ω_h and γ play the role of "tuning parameters". In practice, it is sufficient to vary the value of the parameter γ .

These considerations lead directly to a *practical algorithm* for the *design* of a time-varying complementary filter with a desired break frequency ω_c . This is done by using theorem 6.4.2 with the additional "high-frequency" constraint described above, which can be also cast as a LMI. The underlying optimization problem can be formulated as follows:

$$\begin{aligned}
 & \min \gamma \\
 & K \\
 & \text{subject to:} \\
 & \|(I - \mathcal{E}_{tp})\mathcal{W}_{\omega_c}^n\|_\infty < \epsilon_0, \\
 & \|\mathcal{E}_{tp}\mathcal{W}_{\omega_h}^{n_h}\|_\infty < \gamma,
 \end{aligned} \tag{6.5.1}$$

where the minimization is performed over the the set of gain matrices $K \in \mathcal{R}^{6 \times 3}$ and ϵ_0 captures the low-pass requirement constraint. It is simple to see that the high-pass constraint $\|\mathcal{E}_{tp}\mathcal{W}_{\omega_h}^{n_h}\| < \gamma$ is satisfied if $\exists Y > 0$ and K such that

$$L_{HP_i}(Y, K, \gamma) := \left[\begin{array}{c|c} Y \left[\begin{array}{cc} F_i + KH & KC_{W_h} \\ 0 & A_{W_h} \end{array} \right] + \left[\begin{array}{cc} F_i + KH & KC_{W_h} \\ 0 & A_{W_h} \end{array} \right]^T Y & \\ \hline \left[\begin{array}{c} H^T \\ 0 \end{array} \right] & \left[\begin{array}{cc} H & 0 \end{array} \right] \\ \hline [KD_{W_h} \quad B_{W_h}^T] Y & -\gamma^2 I \end{array} \right] < 0, \quad (6.5.2)$$

$i = \{1, \dots, 8\},$

where

$$\Sigma_{W_h} := \begin{cases} \dot{\mathbf{x}}(t) = A_{W_h} \mathbf{x}(t) + B_{W_h} \mathbf{u}(t) \\ \mathbf{y}(t) = C_{W_h} \mathbf{x}(t) + D_{W_h} \mathbf{u}(t). \end{cases}$$

The optimization problem (6.5.1) can now be cast in the LMI framework as follows. For given numbers $\epsilon > 0$ and $\gamma > 0$ define the sets

$$\Phi_{LP}(\epsilon) = \{K, P : P > 0, L_{LP_i}(K, P, \epsilon) < 0, \forall i = 1, \dots, 8\}, \quad (6.5.3)$$

$$\Phi_{HP}(\gamma) = \{K, Y : Y > 0, L_{HP_j}(K, Y, \gamma) < 0, \forall j = 1, \dots, 8\}, \quad (6.5.4)$$

where the expressions $L_{LP_i}(K, P, \epsilon)$ and $L_{HP_j}(K, Y, \gamma)$ were defined in (6.4.6) and (6.5.2), respectively. Then the solution K to the optimization problem (6.5.1) can be obtained by solving the following constrained optimization problem:

$$\min_{(K, P) \in \Phi_{LP}(\epsilon_0); (K, Y) \in \Phi_{HP}(\gamma)} \gamma. \quad (6.5.5)$$

The optimization problem (6.5.5) is non-convex. However, the matrix inequalities $L_{LP_i}(K, P, \epsilon) < 0$ and $L_{HP_j}(K, Y, \gamma) < 0$ are jointly linear in the parameters P , K and Y . Therefore, for fixed K the expressions $L_{LP_i}(K, P, \epsilon)$ and $L_{HP_j}(K, Y, \gamma)$ are linear in P and Y respectively, and for fixed P and Y they are linear in K . This observation suggests the following numerical solution/design procedure to solve the above constrained optimization problem (see [29] and references therein for similar approaches reported in the literature):

I Initialization

- 1 Fix $\epsilon > \epsilon_0 > 0$. From operational conditions, determine the operating range of angular velocities p_r, q_r, r_r :

$$|p_r| \leq p_r^+, |q_r| \leq q_r^+, |r_r| \leq r_r^+.$$

- 2 Specify the frequency ω_c and use it to construct the low-pass weight $\mathcal{W}_{\omega_c}^n$.
- 3 Specify the bandwidth ω_t of the high-pass weight $\mathcal{W}_{\omega_h}^n$. (As a rule-of-thumb choose $\omega_t \gg \omega_c$).
- 4 Select initial values for the gains K_1, K_2 . (As suggested by the theorem 6.4.3 any gains of the form $\gamma_1 I, \gamma_2 I, \gamma_1 > 0, \gamma_2 > 0$ will do.)

II Numerical optimization

- 1 Low-pass constraint. Solve

$$\min_{(P,K) \in \Phi_{LP}(\epsilon), \epsilon \geq \epsilon_0} \epsilon. \quad (6.5.6)$$

Use $K = [\gamma_1^T \ \gamma_2^T]$ obtained in step I.4 to initialize K , then iterate over P and K to solve the optimization problem (6.5.6). If no solution is found, increase ϵ_0 .

- 2 High-pass constraint. Let (P^*, K^*) denote the solution to the optimization problem (6.5.6). Solve

$$\min_{(Y,K) \in \Phi_{HP}(\gamma), (P^*, K) \in \Phi_{LP}(\epsilon_0)} \gamma. \quad (6.5.7)$$

Use K^* as an initial value for K , then iterate over Y and K to solve the optimization problem (6.5.7).

Due to non-convexity the numerical solutions proposed in Steps II.1 and II.2 are not guaranteed to converge to a local minimum [29]. Therefore, the algorithm should be run for multiple initial conditions. It is then up to the system designer to select appropriate values of the tuning parameters to try and meet all the criteria that must be satisfied by a complementary filter with a desired break frequency. See the definitions of *complementary filter with break frequency ω_c* and *low-pass filter with bandwidth ω_c* introduced early in this chapter.

To illustrate the performance of the complementary filtering structure, a simple filter design exercise was carried out for an autonomous surface vehicle undergoing rotational maneuvers in the horizontal plane. In this case, the navigation system is required to provide accurate estimates of the vehicle's position based on position and velocity measurements provided by a DGPS and a Doppler sonar, respectively. In the scenario adopted the vehicle progresses at a constant speed of $2m/s$ while it executes repeated turns at a maximum yaw rate of $3rad/s$. The Doppler sonar is assumed to introduce a constant bias term $\mathbf{v}_{d,0} = [0.1m/s, 0.2m/s]^T$. The selected break frequency for the complementary filter was $\omega_c = 4rad/s$.

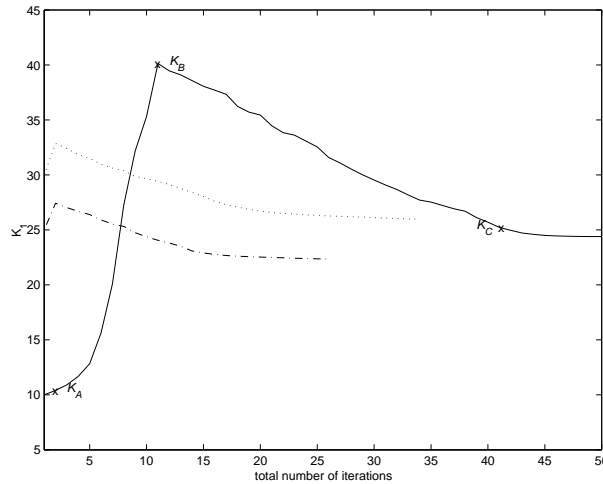


Figure 6.5.1: Filter gain K_1 versus iteration number.

The design procedure is illustrated in figures 6.5.1 - 6.5.3. In the design, the orders n and n_h of the Chebyshev weights $\mathcal{W}_{\omega_c}^n$ and $\mathcal{W}_{\omega_h}^{n_h}$ were selected as 2. Furthermore, ω_h was set arbitrarily to 60rad/s . The performance parameter ϵ_0 for the low-pass filter was chosen as 0.2.

Figure 6.5.1 shows the evolution of the complementary filter gain K_1 for three different initial values. The bold curve shows clearly the general tendency for the case where the initial values are small: the filter does not exhibit a high enough break frequency, and therefore the gains are increased until the low-pass requirement is met, possibly with a certain margin (the margin depends on the particular sequence of iterations obtained by running the first minimization problem in (6.5.6)). At this point, the high-pass constraint comes into play, forcing the gains to change until the low-pass constraint is met, without incurring too much spillover at high frequencies.

The three lower curves in figure 6.5.2 are plots of $\|(\mathcal{E}_{tp} - I)\mathcal{W}_{\omega_c}^n\|$ as a function of ω_c , the operator \mathcal{E}_{tp} being computed with the gains obtained at steps A , B , and C of figure 6.5.1. The top curve I shows the case where the filter gains were set to values much smaller than those obtained in step A . Henceforth, we will refer to such plots as *generalized Bode plots*. The figure shows clearly that the filter starts with a break frequency that is smaller than that required, that frequency being increased until the break frequency requirement is met. It is the role of the "high-pass" constraint to guarantee that the low-pass requirement be met while reducing the spillover at high frequencies. Figure 6.5.3 shows the evolution of $\|\mathcal{E}_{tp}\mathcal{W}_{\omega_h}^{n_h}\|$ as a function of

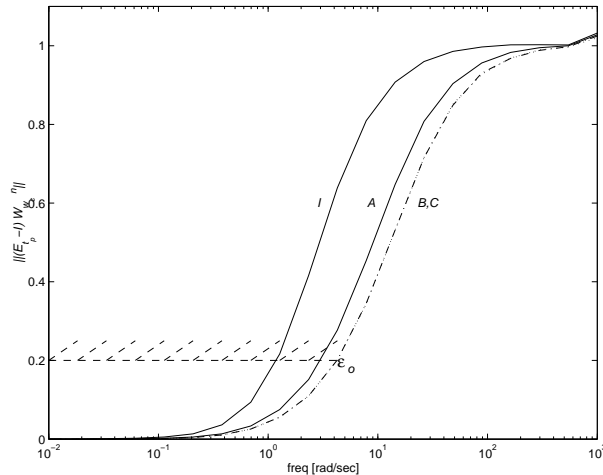


Figure 6.5.2: Generalized bode plots - low-pass property

ω_h . The iterative procedure described above aims at minimizing the value γ of these generalized Bode plots at $\omega = 60\text{rad/s}$ subject to the low-pass constraint described before. The cases *I* and *A* violate the low-pass constraint and are therefore not important to examine. Notice, however, how the value of γ decreases from iteration *B* to *C*, thus showing that in case *C* less spillover is introduced at high frequency.

The performance of the resulting filter was assessed in simulation. Figure 6.5.4 shows the actual and estimated vehicle position when the initial state of the filter was set to $\mathbf{x}_1 = [10\text{m}, 20\text{m}]^T$ and $\mathbf{x}_2 = [0\text{m/s}, 0\text{m/s}]^T$. Figure 6.5.5 captures the evolution of the first component of the Doppler bias estimate. It can be concluded from the figures that the filter provides good tracking of the actual inertial trajectory and rejects the bias introduced by the Doppler unit in the body-axis.

6.6 Extension to Accelerometers

In this section we extend the results discussed above to include the case of complementing position information with that available from on-board accelerometers. This is a scenario commonly encountered in the case of air vehicles. First, we introduce additional notation:

- ${}^I\mathbf{a}$ - linear acceleration of the origin of $\{\mathcal{B}\}$ measured in $\{\mathcal{I}\}$.
- \mathbf{a} - linear acceleration of the origin of $\{\mathcal{B}\}$ with respect to $\{\mathcal{I}\}$, resolved in $\{\mathcal{B}\}$

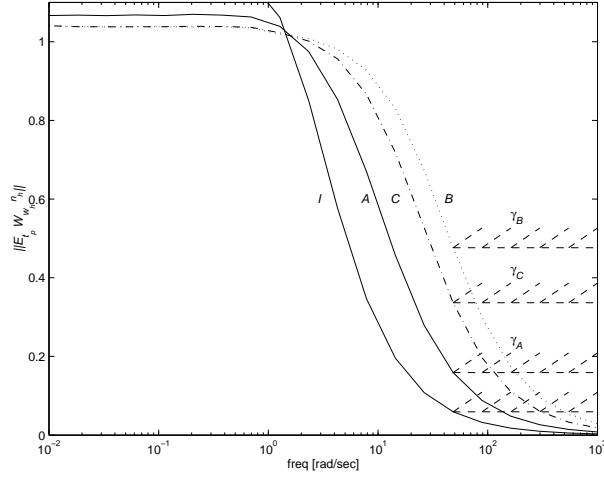


Figure 6.5.3: Generalized bode plots - high-pass property

Using this notation we establish the following kinematic relationships for the case of accelerometers:

$$\begin{aligned}
 \frac{d}{dt} \mathbf{p} &= I \mathbf{v} \\
 \frac{d}{dt} I \mathbf{v} &= I \mathbf{a} = \mathcal{R}(\boldsymbol{\lambda}) \mathbf{a} \\
 \frac{d}{dt} \mathcal{R}(\boldsymbol{\lambda}) &= \mathcal{R}(\boldsymbol{\lambda}) S(\boldsymbol{\omega}),
 \end{aligned} \tag{6.6.1}$$

The underlying process model \mathcal{M}_{pa} is depicted in figure 6.6.1, where \mathcal{E}_t is a dynamical system (filter) that operates on the measurements \mathbf{p}_m and \mathbf{a}_m to provide estimates $\hat{\mathbf{p}}$ of \mathbf{p} . In the figure, \mathbf{p}_d and \mathbf{a}_d are measurement disturbances. As in section 6.4, we study the situation where $\mathbf{p}_d = 0$ and $\mathbf{a}_d = \mathbf{a}_{d,0}$ where $\mathbf{a}_{d,0}$ is the accelerometer bias.

Definition 6.6.1 Process Model \mathcal{M}_{pa} . *The process model \mathcal{M}_{pa} is given by*

$$\mathcal{M}_{pa} := \begin{cases} \frac{d}{dt} \mathbf{p} &= I \mathbf{v} \\ \frac{d}{dt} I \mathbf{v} &= I \mathbf{a} \\ \mathbf{p}_m &= \mathbf{p} \\ \mathbf{a}_m &= \mathcal{R}^{-1}(t) I \mathbf{a} + \mathbf{a}_{d,0} \end{cases} \tag{6.6.2}$$

The discussion in the previous sections leads directly to the following filter design problem.

Problem formulation. *Given the process model \mathcal{M}_{pa} in (6.6.2) and positive numbers ω_c , n , and ϵ , find an (ϵ, n) complementary filter for \mathcal{M}_{pa} with break frequency ω_c .*

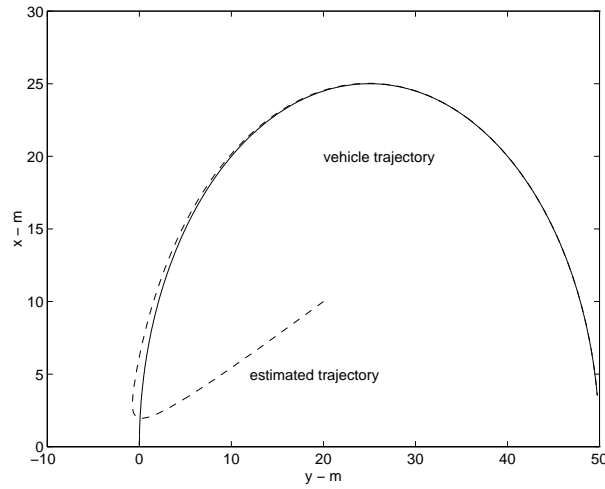


Figure 6.5.4: Actual and estimated vehicle trajectory.

The theorem that follows introduces a candidate complementary filter for \mathcal{M}_{pa} (see figure 6.6.2). The filter structure is motivated by the results presented in previous sections, where an extra integrator was inserted to estimate the Doppler bias.

Theorem 6.6.2 Consider the process model \mathcal{M}_{pa} and the time-varying filter

$$\mathcal{E}_{ta} := \begin{cases} \dot{\mathbf{x}}_1 &= \mathbf{x}_2 + K_1(\mathbf{p} - \mathbf{x}_1) \\ \dot{\mathbf{x}}_2 &= \mathcal{R}(t)\mathbf{a}_m + \mathcal{R}(t)\mathbf{x}_3 + K_2(\mathbf{p} - \mathbf{x}_1) \\ \dot{\mathbf{x}}_3 &= \mathcal{R}^{-1}(t)K_3(\mathbf{p} - \mathbf{x}_1) \\ \hat{\mathbf{p}} &= \mathbf{x}_1 \end{cases} \quad (6.6.3)$$

Suppose the filter \mathcal{E}_{ta} is internally stable. Then, \mathcal{E}_t is a candidate complementary filter for \mathcal{M}_{pa} .

The next result establishes sufficient conditions for the existence of fixed gains K_1 , K_2 and K_3 such that the candidate filter is internally stable and has a guaranteed break frequency of at least ω_c , where ω_c is a design parameter.

Theorem 6.6.3 Consider the linear time-varying filter (6.6.3) and assume that the bounds (6.4.5) on ω_r apply. Given n and ω_c , let $\mathcal{W}_{\omega_c}^n$ be given by theorem 6.4.2. Further let

$$F = \begin{bmatrix} 0 & I & 0 \\ 0 & 0 & I \\ 0 & 0 & \mathcal{S}_r \end{bmatrix}, \quad H = [I \ 0 \ 0].$$

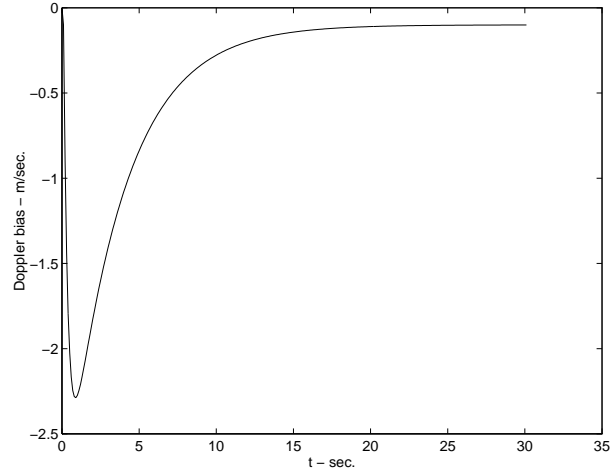


Figure 6.5.5: Doppler bias estimate.

Suppose that given $\epsilon > 0 \exists K \in \mathcal{R}^{9 \times 3}$, $P \in \mathcal{R}^{(9+n) \times (9+n)}$, $P > 0$ such that the linear matrix inequalities

$$\left[\begin{array}{c|c} P \begin{bmatrix} F_i + KH & KC_W \\ 0 & A_W \end{bmatrix} + \begin{bmatrix} F_i + KH & KC_W \\ 0 & A_W \end{bmatrix}^T P & P \begin{bmatrix} 0 \\ B_W \end{bmatrix} \\ \hline \begin{bmatrix} H^T \\ -C_W^T \end{bmatrix} [H \quad -C_W] & -\epsilon^2 I \end{array} \right] < 0, \quad (6.6.4)$$

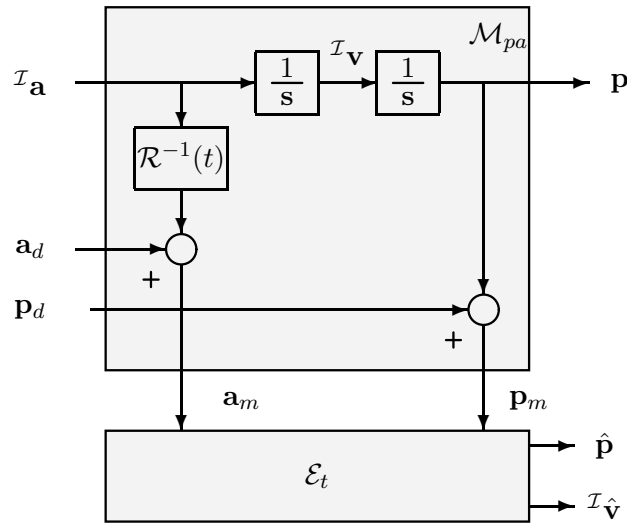
$$F_i = \begin{bmatrix} 0 & I & 0 \\ 0 & 0 & I \\ 0 & 0 & \mathcal{S}(\omega_r^i) \end{bmatrix}, \quad i = \{1, \dots, 8\}$$

are satisfied. Then, the constant gains

$$\begin{bmatrix} K_1 \\ K_2 \\ K_3 \end{bmatrix} := K$$

make the filter \mathcal{E}_{t_a} internally stable. Furthermore, the operator $\mathcal{E}_{t_p} : \mathbf{p} \rightarrow \hat{\mathbf{p}}$ satisfies a low-pass property with indices (ϵ, n) over $[0, \omega_c]$, that is, $\|(\mathcal{E}_{t_p} - I)\mathcal{W}_{\omega_c}^n\| < \epsilon$.

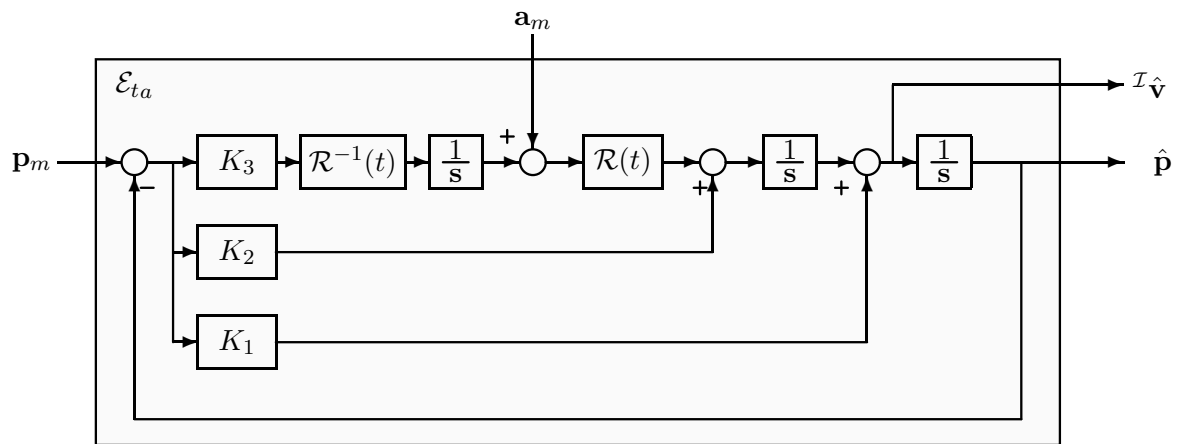
The proofs of theorems 6.6.2 and 6.6.3 follow directly from the proofs of theorems 6.4.1 and 6.4.2 and will be omitted. The robustness of the filter \mathcal{E}_t with respect to uncertainties in the rotation matrix $R(t)$ can be analyzed using the steps outlined in Section 6.4. Similarly, the filter design procedure given in Section 6.5 applies to the design of filter 6.6.3.

Figure 6.6.1: Process model \mathcal{M}_{pa}

6.7 Conclusions and future work

This chapter extended the theory of complementary filtering to the time-varying setting. In particular, the frequency domain interpretations of complementary filters were extended by resorting to the theory of linear differential inclusions and by converting the problem of weighted filter performance analysis into that of determining the feasibility of a related set of Linear Matrix Inequalities (LMIs). Using this setup, it has been shown how the stability of the resulting filters as well as their "frequency-like" performance can be assessed using efficient numerical analysis tools that borrow from convex optimization techniques. The cases of complementing position information with that available from on-board Doppler sonar and accelerometers have been considered, however nothing precludes the use of the methodology proposed to other complementary filters. The resulting design methodology was successfully applied to a design example. Future work will aim at extending these results to the discrete-time, multi-rate case.

Numerical methods to solve Bilinear Matrix Inequalities (BMIs) constitute an active field of research, with interesting results recently brought to light (see [68] and references therein). The use of these new algorithms can help to solve the problem at hand, addressing the optimization procedure directly and can pave the way to the solution of difficult problems to solve with the tools available until recently.

Figure 6.6.2: Complementary filter \mathcal{E}_{ta} .

Chapter 7

Non-linear Tracker for Joint ASC/AUV Oceanic Missions

7.1 Introduction

In recent years there has been increasing interest in the use of fleets of autonomous vehicles to perform complex missions. Air, land, and sea examples of such cooperative missions can be found in [70, 4] and in the references therein. See also [59, 3] for an example of cooperative motion control of the DELFIM Autonomous Surface Craft (ASC) and the INFANTE Autonomous Underwater Vehicle (AUV) for marine applications. The Delfim ASC / Infante AUV ensemble is being used to study the extent of shallow water hydro-thermalism and to determine the patterns of community diversity at the vents in the D. João de Castro bank in the Azores. To that purpose on-board sensors such as a video camera and a sonar are carried by the AUV to collect scientific data on a pre-specified survey area.

In the latter case, data exchange between the two vehicles must rely on acoustic communications due to the strong attenuation experienced by electromagnetic waves in the water. In order to have access to higher bandwidth acoustic communications, the vertical channel must be used [3]. This constraint motivated the design of joint cooperative missions where the ASC Delfim will be positioned in a vicinity of the vertical position of the AUV Infante with minimal or no exchange of navigation data among both platforms (see figure 7.1.1).

These requirements lead naturally to the need of implementing a tracker on-board the ASC



Figure 7.1.1: Joint mission of the Delfim ASC and the Infante AUV.

to provide estimates of the relative position and velocity of both platforms. Traditional solutions rely on the use of Ultra-Short Baseline positioning systems (USBL) or, more recently, on a GPS Intelligent Buoy tracker system (GIB) [58]. However, their high price, complex installation, and precise calibrating requirements lead one to pursue alternative solutions. This work proposes a structure for the tracker that complements data from a camera with that available from other motions sensors. This solution is plausible in shallow water and under high visibility conditions, when an artificial feature associated with the AUV can be extracted from the image obtained on-board the ASC.

Classically, trackers are based on the so-called proportional navigation law (PNG) [32]. However, the issues of stability and capturability are still active domains of research (see [55]). Interacting Multi Model (IMM) strategies have been proposed during the last decade [6] to take into consideration the manoeuvres by the tracking targets, but the complexity and computational power required to solve the complete problem preclude the implementation of the general solution, as convincingly argued in [49]. Sub-optimal strategies are usually implemented with some degradation of the resulting performance, but no reliable analysis are available.

Position, velocity, and attitude estimates (see chapter 4) are available for the ASC, provided by a navigation system installed on-board [57], based on measurements from a DGPS, a Doppler

Sonar log, and an Attitude and Heading Reference System (AHRS). The installation of a calibrated video camera on the ASC is required to provide access to the coordinates of an artificial feature of the AUV in the image, such as a strobe light. To solve the ambiguity associated with the image sensor, that maps the 3D world into 2D image coordinates, an additional measurement of the AUV position is required. Alternative measurements such as AUV depth or the distance between the two vehicles can be provided by a depth cell or by an acoustic ranging sensor, respectively, and will be discussed along this chapter. Moreover, in the case where the previously specified depth for the AUV is used by the tracker, only data relative to deviations from the mission plan are required to be transmitted through the acoustic communication link.

The key contribution of this work is the development of a vision based non-linear tracker that departs considerably from classical solutions. The methodology developed for system design builds on the theory of Linear Parametrically Varying (LPV) Systems [68], which are shown to provide a new powerful framework for the design of navigation filters for autonomous vehicles that rely on inertial and vision sensors. The new methodology leads to filter structures that are intuitively appealing. Furthermore, it provides tools to assess regional (non-local) stability and performance.

The work presented along this chapter builds on a key result presented in [64] relating the errors on the image plane with the errors observed in the inertial frame, assuming a perspective projection map. This algebraic relation allows for the design of an estimator that solves implicitly the triangulation problem for the data from the video camera.

The organization of the chapter is as follows: section 7.2 reviews some background material on linear time-varying systems, induced operator norms, and on linear parametrically time-varying (LPV) systems. In section 7.3, some notation and the basic kinematic relations for the autonomous vehicles present in the mission scenarios envisioned are described. The sensor suite to be installed on board is discussed and the resulting non-linear synthesis model to be used in the tracker design problem is introduced. Section 7.4 presents the main results of the paper by providing a solution to the tracking problem considered. Section 7.5 discusses simulation results. The non-linear tracker problem is revisited in section 7.6, where instead of using the AUV depth, a ranging sonar providing measurements on the distance between the two platforms is used. Results for this sensor suite are presented along with a simulation experiment to assess the performance. Finally, conclusions and some areas for further work are outlined in section

7.7.

7.2 Mathematical background

This section introduces some technical results for the study of linear parametrically varying (LPV) systems as a special case of linear time-varying systems. The notation and the basic theory are by now standard, see [8], [14], [68] and [76].

Let \mathcal{Q} (a compact subset of \mathcal{R}^p) denote a parameter variation set and let \mathcal{F}_ρ be the set of all continuous functions mapping \mathcal{R}^+ to \mathcal{Q} . We will restrict ourselves to the class of LPV systems $\mathcal{G}_{\mathcal{F}_\rho}$ with finite-dimensional state-space realizations

$$\Sigma_{\mathcal{G}_{\mathcal{F}_\rho}} = \begin{cases} \dot{\mathbf{x}} &= A(\rho(t))\mathbf{x} + B(\rho(t))\mathbf{w}, \\ \mathbf{z} &= C(\rho(t))\mathbf{x} \end{cases} \quad (7.2.1)$$

where $\rho \in \mathcal{F}_\rho$, $\mathbf{x} \in \mathbb{R}^n$ is the state, $\mathbf{w} \in \mathcal{W} = \mathbb{R}^m$ is the input, and $\mathbf{z} \in \mathcal{Z} = \mathbb{R}^p$ is the system output. The symbols $A(\rho(t))$, $B(\rho(t))$, and $C(\rho(t))$ denote matrices of bounded, piece-wise continuous functions of time, depending on a continuous time-varying parameter $\rho(t)$ of proper dimensions. See [8, 14, 68] and references therein for an introduction to the subject. In an LPV system the parameter $\rho \in \mathcal{F}_\rho$ is assumed to be unknown but measurable online. Note that the symbol $\mathcal{G}_{\mathcal{F}_\rho}$ denotes both an LPV system and its particular realization $\Sigma_{\mathcal{G}_{\mathcal{F}_\rho}}$, as the meaning will become clear from the context.

An LPV system $\mathcal{G}_{\mathcal{F}_\rho} : L_2 \rightarrow L_2$ is said to be stable if its \mathcal{L}_2 induced operator norm

$$\|\mathcal{G}_{\mathcal{F}_\rho}\|_{2,i} = \sup_{\rho \in \mathcal{Q}} \|\mathcal{G}_\rho\|_{2,i} = \sup_{\rho \in \mathcal{Q}} \sup \left\{ \frac{\|\mathcal{G}_\rho \mathbf{w}\|_2}{\|\mathbf{w}\|_2} : \mathbf{w} \in L_2, \|\mathbf{w}\|_2 \neq 0 \right\} \quad (7.2.2)$$

is well defined and finite. The following result is instrumental in computing the \mathcal{L}_2 induced operator norm of a system.

Theorem 7.2.1 [8] *Consider the LPV system $\mathcal{G}_{\mathcal{F}_\rho} : \mathcal{W} \rightarrow \mathcal{Z}$ with realization (7.2.1). Suppose there exists a positive definite, symmetric matrix $X \in \mathbb{R}^{n \times n}$ such that for all $\rho \in \mathcal{Q}$*

$$A^T(\rho(t))X + XA(\rho(t)) + XB(\rho(t))B^T(\rho(t))X + \frac{C(\rho(t))C^T(\rho(t))}{\gamma^2} < 0. \quad (7.2.3)$$

Then, for $x(0) = 0$, $w \in L_2$, $\|w\|_2 < 1$ and $\forall \rho \in \mathcal{Q}$

$$\lim_{t \rightarrow \infty} x(t) = 0.$$

and $\|\mathcal{G}_{\mathcal{F}_\rho}\|_{2,i} < \gamma$.

The extension of these definitions to the case where the operator inputs and outputs belong to the space of essentially bounded functions of time is immediate, and can be found in [76].

A system $\mathcal{G}_{\mathcal{F}_p} : \mathcal{L}_2 \rightarrow \mathcal{L}_\infty$ described by equation (7.2.2) is said to be finite-gain stable if its $\|\mathcal{G}_{\mathcal{F}_p}\|_{2,\infty}$ induced norm defined as

$$\|\mathcal{G}_{\mathcal{F}_p}\|_{2,\infty} = \sup_{\rho \in \mathcal{Q}} \|\mathcal{G}_\rho\|_{2,\infty} = \sup_{\rho \in \mathcal{Q}} \sup \left\{ \frac{\|\mathcal{G}_\rho \mathbf{w}\|_\infty}{\|\mathbf{w}\|_2} : \mathbf{w} \in L_2, \|\mathbf{w}\|_2 \neq 0 \right\}$$

is well defined and finite.

The $\mathcal{G}_{\mathcal{F}_p}$ induced norm is also referred to as generalized \mathcal{H}_2 norm (in an analogous way as in chapter 2). See [68] for the computation of $\|\mathcal{G}_{\mathcal{F}_p}\|_{2,\infty}$ by resorting to linear matrix inequalities, as presented in the next result:

Theorem 7.2.2 [68] *Consider the LPV system $\mathcal{G}_{\mathcal{F}_p} : \mathcal{W} \rightarrow \mathcal{Z}$ with realization (7.2.1) and let $\alpha > 0$. Suppose that $\rho(t) \in \mathcal{Q}$ for all $t \geq 0$ and that there exists a positive definite, symmetric matrix $Y \in \mathbb{R}^{n \times n}$ such that for all $\rho \in \mathcal{Q}$*

$$A^T(\rho(t))Y + YA(\rho(t)) + YB(\rho(t))B^T(\rho(t))Y < 0, \quad \text{and} \quad (7.2.4)$$

$$Y - \frac{C^T(\rho(t))C(\rho(t))}{\alpha^2} > 0, \quad (7.2.5)$$

then $\|\mathcal{G}_{\mathcal{F}_p}\|_{2,\infty} < \alpha$.

The following result, giving an upper bound on the L_∞ norm of the output signal of an LPV given a nonzero initial condition, completes the set of results that will be needed.

Theorem 7.2.3 [68] *Consider the LPV system $\mathcal{G}_{\mathcal{F}_p} : \mathcal{W} \rightarrow \mathcal{Z}$ with realization (7.2.1), with $w = 0$ and $\beta > 0$. Suppose that $\rho(t) \in \mathcal{Q}$ for all $t \geq 0$, and that there exists a positive definite, symmetric matrix $Z \in \mathbb{R}^{n \times n}$ such that for all $\rho \in \mathcal{Q}$ such that for all $\rho \in \mathcal{Q}$*

$$A^T(\rho(t))Z + ZA(\rho(t)) < 0, \quad (7.2.6)$$

$$Z - \frac{C^T(\rho(t))C(\rho(t))}{\beta^2} > 0 \quad \text{and} \quad (7.2.7)$$

$$x^T(0)Zx(0) < 1, \quad (7.2.8)$$

then $\|z\|_\infty < \beta$. Furthermore, $x(t) \rightarrow 0$ as $t \rightarrow \infty$.

Equipped with this set of results the tracking problem will be set and a solution will be proposed and studied.

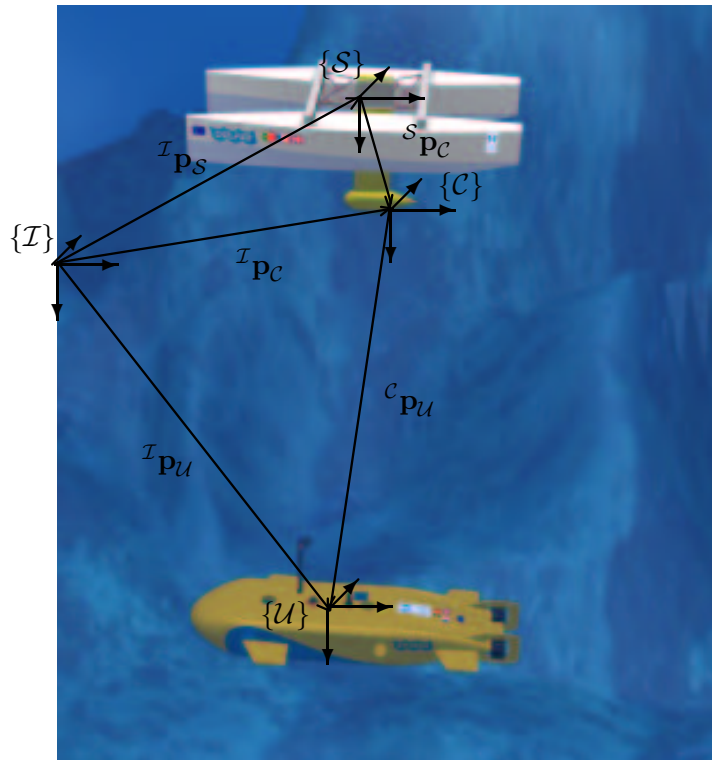


Figure 7.3.1: Mission coordinate frames and notation.

7.3 Tracker design: problem formulation

This section describes the tracker problem that is the main focus of this chapter. For the sake of clarity, we first introduce some basic notation and summarize the kinematic relations. Next, the sensor suite is discussed for the envisioned mission scenario, as depicted in figure 7.3.1, and the corresponding measurements are related according to the kinematics of the problem at hand. Finally, the underlying non-linear tracker synthesis model is presented.

7.3.1 Notation

Let $\{Z\}$ be an inertial reference frame located in the pre-specified mission scenario origin, at mean sea level, and let $\{S\}$ and $\{U\}$ denote body-fixed frames that move with the ASC and AUV, respectively, as depicted in figure 7.3.1. The following notation is required:

$$\begin{aligned}
{}^{\mathcal{I}}\mathbf{p}_{\mathcal{S}} &:= \begin{bmatrix} {}^{\mathcal{I}}x_s & {}^{\mathcal{I}}y_s & {}^{\mathcal{I}}z_s \end{bmatrix}^T & - \text{position of the origin of } \{\mathcal{S}\} \text{ in } \{\mathcal{I}\}; \\
{}^{\mathcal{I}}\mathbf{p}_{\mathcal{U}} &:= \begin{bmatrix} {}^{\mathcal{I}}x_u & {}^{\mathcal{I}}y_u & {}^{\mathcal{I}}z_u \end{bmatrix}^T & - \text{position of the origin of } \{\mathcal{U}\} \text{ in } \{\mathcal{I}\}; \\
\mathbf{p} &:= \begin{bmatrix} x & y & z \end{bmatrix}^T & - \text{position of the origin of } \{\mathcal{U}\} \text{ relative to } \{\mathcal{S}\}, \text{ ex-} \\
&&&& \text{pressed in } \{\mathcal{I}\}, \text{ i.e., } \mathbf{p} = {}^{\mathcal{I}}\mathbf{p}_{\mathcal{U}} - {}^{\mathcal{I}}\mathbf{p}_{\mathcal{S}}; \\
{}^{\mathcal{I}}\mathbf{v}_{\mathcal{S}} &:= \begin{bmatrix} {}^{\mathcal{I}}\dot{x}_s & {}^{\mathcal{I}}\dot{y}_s & {}^{\mathcal{I}}\dot{z}_s \end{bmatrix}^T & - \text{linear velocity of the origin of } \{\mathcal{S}\} \text{ in } \{\mathcal{I}\}; \\
{}^{\mathcal{I}}\mathbf{v}_{\mathcal{U}} &:= \begin{bmatrix} {}^{\mathcal{I}}\dot{x}_u & {}^{\mathcal{I}}\dot{y}_u & {}^{\mathcal{I}}\dot{z}_u \end{bmatrix}^T & - \text{linear velocity of the origin of } \{\mathcal{U}\} \text{ in } \{\mathcal{I}\}; \\
\boldsymbol{\lambda} &:= \begin{bmatrix} \phi & \theta & \psi \end{bmatrix}^T & - \text{vector of roll, pitch, and yaw angles that param-} \\
&&&& \text{eterize locally the orientation of frame } \{\mathcal{S}\} \text{ with} \\
&&&& \text{respect to } \{\mathcal{I}\}; \\
\boldsymbol{\omega} &:= \begin{bmatrix} p & q & r \end{bmatrix}^T & - \text{angular velocity of } \{\mathcal{S}\} \text{ with respect to } \{\mathcal{I}\}, \text{ re-} \\
&&&& \text{solved in } \{\mathcal{S}\};
\end{aligned}$$

7.3.2 Vehicles kinematics and the sensor suite measurements

Given two frames $\{\mathcal{A}\}$ and $\{\mathcal{B}\}$, ${}^{\mathcal{A}}\mathcal{R}$ denotes the rotation matrix from $\{\mathcal{B}\}$ to $\{\mathcal{A}\}$. In particular, ${}^{\mathcal{I}}\mathcal{R}(\boldsymbol{\lambda})$ is the rotation matrix from $\{\mathcal{S}\}$ to $\{\mathcal{I}\}$, parameterized locally by $\boldsymbol{\lambda}$. Since \mathcal{R} is a rotation matrix, it satisfies the orthogonality condition $\mathcal{R}^T = \mathcal{R}^{-1}$ or $\mathcal{R}^T\mathcal{R} = I$.

Given the angular velocity vector $\boldsymbol{\omega}$, then

$$\dot{\boldsymbol{\lambda}} = Q(\boldsymbol{\lambda})\boldsymbol{\omega},$$

where $Q(\boldsymbol{\lambda})$ is a matrix that relates the derivative of $\boldsymbol{\lambda}$ with $\boldsymbol{\omega}$. The following kinematic relations for the ASC apply [15]:

$$\frac{d}{dt}{}^{\mathcal{I}}\mathbf{p}_{\mathcal{S}} = {}^{\mathcal{I}}\mathbf{v}_{\mathcal{S}} = {}^{\mathcal{I}}\mathcal{R}(\boldsymbol{\lambda}) {}^{\mathcal{S}}({}^{\mathcal{I}}\mathbf{v}_{\mathcal{S}}) \quad \text{and} \quad (7.3.1)$$

$$\frac{d}{dt}{}^{\mathcal{I}}\mathcal{R}(\boldsymbol{\lambda}) = {}^{\mathcal{I}}\mathcal{R}(\boldsymbol{\lambda}) \mathcal{S}(\boldsymbol{\omega}), \quad (7.3.2)$$

where ${}^{\mathcal{S}}({}^{\mathcal{I}}\mathbf{v}_{\mathcal{S}})$ is the ASC velocity relative to the inertial frame, expressed in \mathcal{S} (i.e., the body-fixed velocity) and where

$$\mathcal{S}(\boldsymbol{\omega}) := \begin{bmatrix} 0 & -\omega_z & \omega_y \\ \omega_z & 0 & -\omega_x \\ -\omega_y & \omega_x & 0 \end{bmatrix} \quad (7.3.3)$$

is a skew symmetric matrix, that is, $\mathcal{S}^T = -\mathcal{S}$. The matrix \mathcal{S} satisfies the relationship $\mathcal{S}(a)b = a \times b$, where a and b are arbitrary vectors and \times denotes the cross product operation. Furthermore, $\|\mathcal{S}(\boldsymbol{\omega})\| = \|\boldsymbol{\omega}\|$.

It is assumed that the ASC is equipped with a set of sensors and its own navigation system, as shown in detail in the design example described in chapter 4, that provides estimates on the position and velocity of the body-fixed frame $\{\mathcal{S}\}$, relative to the inertial frame $\{\mathcal{I}\}$, ${}^{\mathcal{I}}\mathbf{p}_{\mathcal{S}}$ and ${}^{\mathcal{I}}\mathbf{v}_{\mathcal{S}}$, respectively. Estimates for the attitude $\boldsymbol{\lambda}$ are also available and, as a consequence, ${}^{\mathcal{I}}\mathcal{R}(\boldsymbol{\lambda})$ is assumed to be known.

The tracker design problem at hand will be cast in a structure similar to a complementary filter (see chapter 3), based on measurements from a set of sensors installed on-board. The sensor suite to be used and the available measurements will be discussed in the following. A video camera pointing down, able to discriminate some artificial feature of the AUV such as a strobe light, will be installed on-board the ASC. The camera position and orientation, ${}^{\mathcal{I}}\mathbf{p}_{\mathcal{C}}$ and ${}^{\mathcal{I}}\mathcal{R}$ are given by (see figure 7.3.1)

$${}^{\mathcal{I}}\mathbf{p}_{\mathcal{C}} = {}^{\mathcal{I}}\mathbf{p}_{\mathcal{S}} + {}^{\mathcal{I}}\mathcal{R}(\boldsymbol{\lambda}) {}^{\mathcal{S}}\mathbf{p}_{\mathcal{C}} \quad (7.3.4)$$

and

$${}^{\mathcal{I}}\mathcal{R}(\boldsymbol{\lambda}) = {}^{\mathcal{I}}\mathcal{R}(\boldsymbol{\lambda}) {}^{\mathcal{S}}\mathcal{R},$$

respectively, where the dependence on the position ${}^{\mathcal{S}}\mathbf{p}_{\mathcal{C}}$ and the orientation ${}^{\mathcal{S}}\mathcal{R}$ due to the installation procedure is obvious. The coordinates of the AUV in the $\{\mathcal{I}\}$ and $\{\mathcal{C}\}$ coordinate frames can be related by

$${}^{\mathcal{I}}\mathbf{p}_{\mathcal{U}} = {}^{\mathcal{I}}\mathbf{p}_{\mathcal{C}} + {}^{\mathcal{I}}\mathcal{R}(\boldsymbol{\lambda}) {}^{\mathcal{C}}\mathbf{p}_{\mathcal{U}}. \quad (7.3.5)$$

Using the relations (7.3.4) and (7.3.5), the coordinates of $\{\mathcal{U}\}$ in the camera frame $\{\mathcal{C}\}$ are

$${}^{\mathcal{C}}\mathbf{p}_{\mathcal{U}} = {}^{\mathcal{C}}\mathcal{R} {}^{\mathcal{S}}\mathcal{R}(\boldsymbol{\lambda}) ({}^{\mathcal{I}}\mathbf{p}_{\mathcal{U}} - {}^{\mathcal{I}}\mathbf{p}_{\mathcal{S}} - {}^{\mathcal{I}}\mathcal{R}(\boldsymbol{\lambda}) {}^{\mathcal{S}}\mathbf{p}_{\mathcal{C}}).$$

Assuming without loss of generality that ${}^{\mathcal{C}}\mathcal{R} = I$ and ${}^{\mathcal{S}}\mathbf{p}_{\mathcal{C}} = 0$, this relation degenerates into

$${}^{\mathcal{C}}\mathbf{p}_{\mathcal{U}} = [x_c \ y_c \ z_c]^T = {}^{\mathcal{C}}\mathcal{R}(\boldsymbol{\lambda}) ({}^{\mathcal{I}}\mathbf{p}_{\mathcal{U}} - {}^{\mathcal{I}}\mathbf{p}_{\mathcal{S}}), \quad (7.3.6)$$

which can be written in compact form as ${}^{\mathcal{C}}\mathbf{p} = {}^{\mathcal{C}}\mathcal{R}(\boldsymbol{\lambda})\mathbf{p}$. Setting an artificial feature coincident with the origin of $\{\mathcal{U}\}$ (such as a strobe light), processing the video images (i.e., threshold detection) can be used to extract its 2D coordinates

$$\begin{bmatrix} u_c \\ v_c \end{bmatrix} = \begin{bmatrix} f x_c / z_c \\ f y_c / z_c \end{bmatrix}, \quad (7.3.7)$$

on the image plane, where f is the focal distance for the pinhole model of the imaging system. This key relation in the computer vision area [36] corresponds to a non-linear mapping from \mathcal{R}^3 to \mathcal{R}^2 , leading to an ambiguity in the coordinate measurements in the image plane. To solve this ambiguity, an additional measurement on the AUV position is required, such as the depth or the distance between the two vehicles. In what follows we assume that a depth cell is used¹.

Assuming the ASC is at depth zero, the relative z coordinate (which equals the AUV depth) is obtained from the third row of equation (7.3.6) as

$$z = -\sin(\theta)x_c + \cos(\theta)\sin(\phi)y_c + \cos(\theta)\cos(\phi)z_c, \quad (7.3.8)$$

where ϕ and θ are the Euler angles of roll and pitch, respectively. This relation assumes that wave effects can be removed due to the existence of a navigation system on-board the ASC. The measurement of this variable, performed in the AUV using a depth cell, should be sent to the ASC via the communications channel or using the delay between two signals emitted from the AUV (see [58], where this simplified communication method was used). As a cooperative mission is envisioned for the two vehicles, the actual values should be sent to the ASC only when some deviation from the original plan occurs. In this manner dependence on the acoustic signals diminishes and the required bandwidth is reduced to a minimum.

In order to implement the desired estimator structure, the complementary measurement of the AUV velocity relative to the ASC is required. A sensor that would measure this relative velocity, based on the Doppler effect experienced by acoustic waves travelling between the two vehicles, would be a possibility. However, this option requires sensors that are expensive or difficult to implement and will therefore not be used in the proposed framework. Instead, an approximate relation that is introduced next will be exploited along this work. The relationship builds on the assumption that the AUV travels at constant velocity.

Consider the position of the AUV relative to the ASC (as depicted in figure 7.3.1), written as

$${}^{\mathcal{I}}\mathbf{p}_{\mathcal{U}} = {}^{\mathcal{I}}\mathbf{p}_{\mathcal{S}} + {}^{\mathcal{I}}_{\mathcal{C}}\mathcal{R}(\boldsymbol{\lambda}) {}^{\mathcal{C}}\mathbf{p},$$

where ${}^{\mathcal{C}}\mathbf{p}$ is the relative position, expressed in the camera frame $\{\mathcal{C}\}$. The velocities of both

¹In section 7.6, the problem at hand will be revisited supported by sonar ranging measurements of the relative distance between platforms.

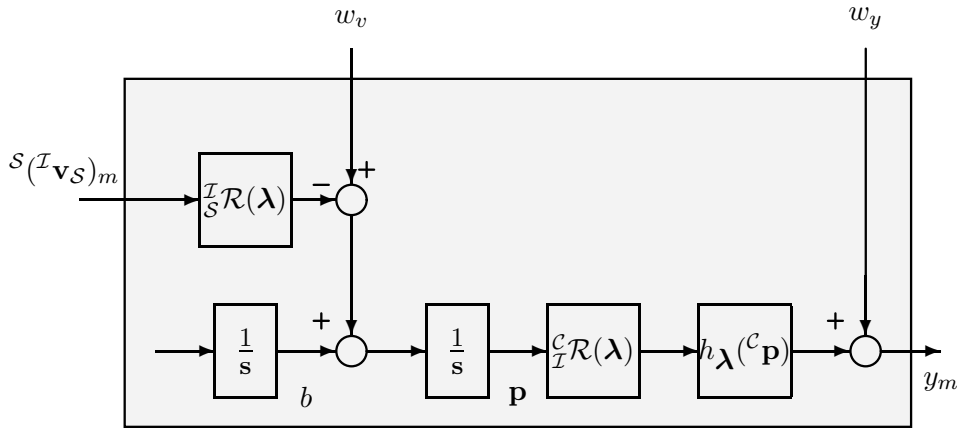


Figure 7.3.2: Estimator model.

platforms can be related as

$$\mathcal{I}\mathbf{v}_U = \mathcal{I}\mathbf{v}_S + \frac{d}{dt}(\frac{\mathcal{I}}{\mathcal{C}}\mathcal{R}^c\mathbf{p}). \quad (7.3.9)$$

Consider for the time being that the the velocity of the AUV is zero (this restriction will be lifted shortly). Then,

$$\frac{d}{dt}(\frac{\mathcal{I}}{\mathcal{C}}\mathcal{R}^c\mathbf{p}) = -\mathcal{I}\mathbf{v}_S,$$

i.e., the velocity of the AUV seen by the catamaran and expressed in the inertial frame $\{\mathcal{I}\}$ is the same as the velocity of the catamaran in $\{\mathcal{I}\}$, apart from a change in signal. Moreover, using the fact that a Doppler Sonar log is installed on-board the ASC, this relation can be rewritten using (7.3.1) as

$$\frac{d}{dt}(\frac{\mathcal{I}}{\mathcal{C}}\mathcal{R}^c\mathbf{p}) = -\frac{\mathcal{I}}{\mathcal{S}}\mathcal{R}(\lambda)s^{(\mathcal{I}\mathbf{v}_S)}.$$

The assumption above motivates the use of an estimator with a bank of integrators aimed at estimating biases in the velocity measurements. The estimated biases corresponds to the deviation in the estimated ASC velocity due to the actual AUV velocity, which is different from zero.

7.3.3 Design Model

In the following, the underlying design model that plays a central role in the design of the envisioned tracker is presented. The model is based on the kinematic relations presented above

and the resulting system \mathcal{G} has the realization

$$\Sigma_{\mathcal{G}} = \begin{cases} \dot{\mathbf{p}} &= -\frac{\mathcal{I}}{\mathcal{S}}\mathcal{R}(\boldsymbol{\lambda})^S (\mathcal{I}\mathbf{v}_S)_m + b + w_v \\ \dot{b} &= 0 \\ y_m &= h_{\boldsymbol{\lambda}}(\mathcal{C}\mathbf{p}) + w_y, \end{cases} \quad (7.3.10)$$

where y_m is the measurement of $y = [u_c \ v_c \ z]^T$, i.e., the column vector of the variables from the sensors' measurements and $h_{\boldsymbol{\lambda}}(\mathcal{C}\mathbf{p}) : \mathcal{R}^3 \rightarrow \mathcal{R}^3$ is obtained by putting together relations (7.3.7) and (7.3.8) for the camera model and depth measurement, respectively. Vector b denotes velocity bias that must be estimated. The velocity of the ASC is considered as an input to the model. The overall model structure is depicted in the block diagram of figure 7.3.2.

7.4 Tracker design and analysis

The problem at hand can be described as that of determining estimates of the relative position and velocity of the AUV with respect to the ASC, based on the sensor package described above. The filter design model is the one in figure 7.3.2. In this section, a structure for a non-linear estimator is proposed and analyzed.

Consider that the orientation of the camera frame installed on-board the ASC is constrained to be in the compact set given by

$$\Lambda_c = \{\boldsymbol{\lambda} = [\phi \ \theta \ \psi]^T : |\phi| \leq \phi_{max}, |\theta| \leq \theta_{max}\}, \quad (7.4.1)$$

and that the relative position of the AUV relative to the ASC, expressed in $\{\mathcal{C}\}$, is constrained to be in

$$\mathcal{P}_c = \{\mathcal{C}\mathbf{p} = [x_c \ y_c \ z_c]^T : \underline{x} \leq x_c \leq \bar{x}, \underline{y} \leq y_c \leq \bar{y}, 0 < \underline{z} \leq z_c \leq \bar{z}\}. \quad (7.4.2)$$

Notice that the yaw angle ψ is not constrained, $\underline{x} \dots \bar{z}$ can be chosen according to the mission scenario and the expected vehicles dynamics, and z_c is positive given the fact that we are dealing with an underwater vehicle and the inertial frame origin $\{\mathcal{I}\}$ is located at mean sea level. Let the estimates of the relative position $\mathcal{C}\mathbf{p}$ and velocity $\mathcal{C}\mathbf{v}$ be written as $\hat{\mathbf{p}}_c$ and $\hat{\mathbf{v}}_c$, respectively. It will be required that the relative position estimate $\mathcal{C}\hat{\mathbf{p}}$ lie in the compact set

$$\hat{\mathcal{P}}_c = \{\mathcal{C}\hat{\mathbf{p}} = [\hat{x}_c \ \hat{y}_c \ \hat{z}_c]^T : |\hat{x}_c - x_c| \leq \bar{x} - \underline{x} + dx, |\hat{y}_c - y_c| \leq \bar{y} - \underline{y} + dy, |\hat{z}_c - z_c| \leq \bar{z} - \underline{z} + dz, \},$$

where dx , dy , and dz are positive numbers and $dz < \underline{z}$.

The estimator structure proposed along this chapter builds on a key result that was introduced in [64]. See also [37], where the same structure is used on a navigation system used to assist on the automatic landing of an autonomous aircraft. This algebraic result, which relates errors in the image plane with errors observed in the inertial frame, is stated in the following lemma:

Lemma 7.4.1 [64] *Let $h_{\lambda}(\dots)$ be the mapping function introduced in section 7.3. Then*

$$h_{\lambda}({}^c\hat{\mathbf{p}}) - h_{\lambda}({}^c\mathbf{p}) = L({}^c\hat{\mathbf{p}}, {}^c\mathbf{p})H({}^c\hat{\mathbf{p}})({}^c\hat{\mathbf{p}} - {}^c\mathbf{p}), \quad (7.4.3)$$

where

$$L({}^c\hat{\mathbf{p}}, {}^c\mathbf{p}) = \begin{bmatrix} \hat{z}_c/z_c & 0 & 0 \\ 0 & \hat{z}_c/z_c & 0 \\ 0 & 0 & 1 \end{bmatrix},$$

and $H({}^c\hat{\mathbf{p}})$ denotes the Jacobian of $h_{\lambda}({}^c\hat{\mathbf{p}})$, with respect to ${}^c\hat{\mathbf{p}}$.

According to the definition of $h_{\lambda}({}^c\hat{\mathbf{p}})$, the Jacobian is given by

$$H({}^c\hat{\mathbf{p}}) = \begin{bmatrix} f/\hat{z}_c & 0 & -f\hat{x}_c/\hat{z}_c^2 \\ 0 & f/\hat{z}_c & -f\hat{y}_c/\hat{z}_c^2 \\ -\sin(\theta) & \cos(\theta)\sin(\phi) & \cos(\theta)\cos(\phi) \end{bmatrix} \text{ and}$$

and verifies

$$|H({}^c\hat{\mathbf{p}})| = \frac{f}{\hat{z}_c^3}z,$$

therefore is invertible in the compact set of positions where the missions will take place. As a motivation to the structure of the estimator to be proposed, invert expression (7.4.3) to obtain

$${}^c\hat{\mathbf{p}} - {}^c\mathbf{p} = H^{-1}({}^c\hat{\mathbf{p}})L^{-1}({}^c\hat{\mathbf{p}}, {}^c\mathbf{p})(h_{\lambda}({}^c\hat{\mathbf{p}}) - h_{\lambda}({}^c\mathbf{p})).$$

Assuming that $\hat{z}_c/z_c \approx 1$ yields $L({}^c\hat{\mathbf{p}}, {}^c\mathbf{p}) \approx I$, i.e.,

$$({}^c\hat{\mathbf{p}} - {}^c\mathbf{p}) = H({}^c\hat{\mathbf{p}})^{-1}(h_{\lambda}({}^c\hat{\mathbf{p}}) - h_{\lambda}({}^c\mathbf{p})). \quad (7.4.4)$$

The importance of this non-linear relation is twofold: i) it can be used in the estimator as a way to relate errors in the sensor measurements with state variable errors, and ii) it holds the key to bring the estimator dynamics into the form of a LPV system.

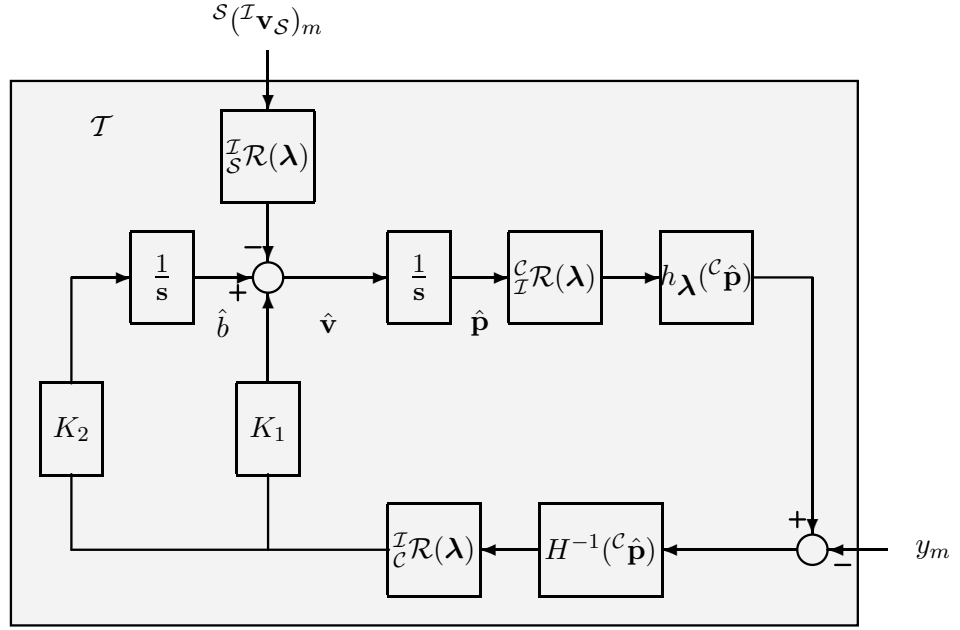


Figure 7.4.1: Non-linear tracker structure.

An alternative way to arrive at this relation is by expanding $h_{\lambda}(^C \mathbf{p})$ in its first order Taylor series, in the vicinity of $^C \hat{\mathbf{p}}$

$$h_{\lambda}(^C \mathbf{p}) = h_{\lambda}(^C \hat{\mathbf{p}}) + H(^C \hat{\mathbf{p}})(^C \mathbf{p} - ^C \hat{\mathbf{p}}) + \mathcal{O}(^C \mathbf{p} - ^C \hat{\mathbf{p}}),$$

which for negligible residuals ($\mathcal{O}(^C \mathbf{p} - ^C \hat{\mathbf{p}}) \approx 0$) becomes identical to relation (7.4.4). Note that in the work of [37] a similar relation was used, based however on the transposed Jacobian. These circle of ideas leading to alternative solutions are also discussed in the framework of robotics in [66] and in the references therein.

7.4.1 Proposed solution

Motivated by the relation in (7.4.4), the solution proposed for the problem addressed in this paper is the tracker with realization

$$\Sigma_{\mathcal{T}} = \begin{cases} \dot{\hat{\mathbf{p}}} &= -\frac{I}{S} \mathcal{R}(\lambda) s^{(I \mathbf{v}_S)_m} + \hat{b} + K_1 \frac{I}{C} \mathcal{R}(\lambda) H^{-1}(^C \hat{\mathbf{p}}) (h_{\lambda}(^C \hat{\mathbf{p}}) - y_m) \\ \dot{\hat{b}} &= K_2 \frac{I}{C} \mathcal{R}(\lambda) H^{-1}(^C \hat{\mathbf{p}}) (h_{\lambda}(^C \hat{\mathbf{p}}) - y_m), \end{cases} \quad (7.4.5)$$

where $\hat{\mathbf{p}}$ is the relative position estimate, \hat{b} is the bias estimate, and K_1 and K_2 are gains to be computed so as to meet adequate stability and performance criteria. The estimator structure

is depicted in figure 7.4.1. The input, state and output vectors are three dimensional. Clearly, this is an LPV system.

We now address the problems of regional stability and performance of the filter proposed, referred to as \mathbf{P}_1 and \mathbf{P}_2 respectively, below.

P₁ Regional Stability - Consider the design model and the estimator structure introduced before. Further assume that $w_v = w_y = 0$. Given an envisioned mission scenario defined by \mathcal{P}_c , find a number $\alpha > 0$ and observer parameters such that the estimates $\hat{\mathbf{p}}$ of \mathbf{p} and $\hat{\mathbf{v}}$ of \mathbf{v} verify the relationships

$$\text{a) } {}^c\hat{\mathbf{p}} \in \hat{\mathcal{P}}_c \text{ for } t > 0,$$

$$\text{b) } \|\hat{\mathbf{p}} - \mathbf{p}\| + \|\hat{\mathbf{v}} - \mathbf{v}\| \rightarrow 0 \text{ as } t \rightarrow \infty$$

$$\text{whenever } \|[(\hat{\mathbf{p}}(0) - \mathbf{p}(0))^T, (\hat{\mathbf{b}}(0) - \mathbf{b}(0))^T]^T\|_\infty < \alpha.$$

In order to be able to state a result on the stability of the proposed solution, some auxiliary results are needed. First, some auxiliary mappings and some properties to be used later will be introduced.

Lemma 7.4.2 [37] *Let $\phi : \mathcal{R}^6 \rightarrow \mathcal{R}^{3 \times 3}$ and $\phi_1 : \mathcal{R}^3 \rightarrow \mathcal{R}^{3 \times 3}$ be the operators defined by*

$$\phi({}^c\hat{\mathbf{p}}, {}^c\mathbf{p}) = H^T({}^c\hat{\mathbf{p}})L({}^c\hat{\mathbf{p}}, {}^c\mathbf{p})H({}^c\hat{\mathbf{p}}), \quad (7.4.6)$$

and $\phi_1({}^c\hat{\mathbf{p}}) = H^T({}^c\hat{\mathbf{p}})H({}^c\hat{\mathbf{p}})$. Then,

$$\phi({}^c\hat{\mathbf{p}}, {}^c\mathbf{p}) > 0, \phi_1({}^c\hat{\mathbf{p}}) > 0, \forall {}^c\mathbf{p} \in \mathcal{P}_c \text{ and } {}^c\hat{\mathbf{p}} \in \hat{\mathcal{P}}_c.$$

Lemma 7.4.3 *Let $\phi_2 : \mathcal{R}^6 \rightarrow \mathcal{R}^{3 \times 3}$ be the operator defined by*

$$\phi_2({}^c\hat{\mathbf{p}}, {}^c\mathbf{p}) = H^{-1}({}^c\hat{\mathbf{p}})L({}^c\hat{\mathbf{p}}, {}^c\mathbf{p})H({}^c\hat{\mathbf{p}}), \quad (7.4.7)$$

Then,

$$\phi_2({}^c\hat{\mathbf{p}}, {}^c\mathbf{p}) > 0, \forall {}^c\mathbf{p} \in \mathcal{P}_c \text{ and } {}^c\hat{\mathbf{p}} \in \hat{\mathcal{P}}_c.$$

Proof: If ϕ_2 were not positive definite there would exist at least one eigenvalue $\lambda^* < 0$ verifying

$$H^{-1}({}^c\hat{\mathbf{p}})L({}^c\hat{\mathbf{p}}, {}^c\mathbf{p})H({}^c\hat{\mathbf{p}})v = \lambda^*v.$$

Pre-multiplying by $H({}^c\hat{\mathbf{p}})$ and $H^T({}^c\hat{\mathbf{p}})$, consecutively, this expression becomes

$$H^T({}^c\hat{\mathbf{p}})L({}^c\hat{\mathbf{p}}, {}^c\mathbf{p})H({}^c\hat{\mathbf{p}})v = \lambda^*H^T({}^c\hat{\mathbf{p}})H({}^c\hat{\mathbf{p}})v,$$

but according with the results in lemma 7.4.2 both sides of this expression are positive. Therefore λ^* can not be negative. \blacksquare

In the following the error dynamics for the proposed estimator will be presented, with a similar form to the dynamics introduced for a generic LPV system (7.2.1). Using the design model (7.3.10) and the proposed estimator with realization (7.4.5), define the auxiliary estimator error variables $e_1 = \hat{\mathbf{p}} - \mathbf{p}$ and $e_2 = \hat{b} - b$. The error dynamics can be written as

$$\begin{cases} \dot{e}_1 &= e_2 + K_1^T \mathcal{R} H^{-1}(h_{\lambda}({}^c\hat{\mathbf{p}}) - h_{\lambda}({}^c\mathbf{p}) - w_y) - w_v, \\ \dot{e}_2 &= K_2^T \mathcal{R} H^{-1}(h_{\lambda}({}^c\hat{\mathbf{p}}) - h_{\lambda}({}^c\mathbf{p}) - w_y), \end{cases}$$

where H^{-1} stands as an abbreviation for $H^{-1}({}^c\hat{\mathbf{p}})$. Using lemma 7.4.1 and writing the error dynamics in vector form such that $e = [e_1^T \ e_2^T]^T$ and $w = [w_y^T \ w_v^T]^T$, the previous expressions becomes

$$\dot{e} = \begin{bmatrix} K_1^T \mathcal{R} H^{-1} L H^c \mathcal{R} & I \\ K_2^T \mathcal{R} H^{-1} L H^c \mathcal{R} & 0 \end{bmatrix} e - \begin{bmatrix} K_1^T \mathcal{R} H^{-1} & I \\ K_2^T \mathcal{R} H^{-1} & 0 \end{bmatrix} w,$$

where L stands as an abbreviation for $L({}^c\hat{\mathbf{p}}, {}^c\mathbf{p})$. Let $K = [K_1^T \ K_2^T]^T$, $F = \begin{bmatrix} 0 & I \\ 0 & 0 \end{bmatrix}$, and $C = [I \ 0]$. Using lemma 7.4.3, this relation can be written in a more compact form as

$$\dot{e} = (F + K^T \mathcal{R} \phi_2({}^c\hat{\mathbf{p}}, {}^c\mathbf{p})^c \mathcal{R} C) e - (F + K^T \mathcal{R} H^{-1} C) w, \quad (7.4.8)$$

and $z = Ce$. Notice that the system describing the error dynamics is an LPV that depends on ${}^c\mathbf{p}$ and on ${}^c\hat{\mathbf{p}}$.

The next theorem gives conditions under which \mathbf{P}_1 has a solution. See theorem 4.3 in [37] for a similar result.

Theorem 7.4.4 *Consider a mission scenario where the orientation and position variables are constrained by (7.4.1) and (7.4.2) respectively, and let $\hat{\mathcal{P}}_c$ be given. Let $\alpha < \min(\bar{x} - \underline{x} + dx, \bar{y} -$*

$\underline{y} + dy, \bar{z} - \underline{z} + dz$) be a positive number and define $r_z = \frac{\bar{z} - \underline{z} + dz}{\underline{z}} < 1$. Further let

$$F := \begin{bmatrix} 0 & I \\ 0 & 0 \end{bmatrix} \quad (7.4.9)$$

and $C = [I \ 0]$. Suppose there exists a matrix $P = P^T \in \mathcal{R}^{6 \times 6}$ such that

$$P > 0, \quad (7.4.10)$$

$$F^T P + PF + \begin{bmatrix} -2(1 - r_z)^2 I & 0 \\ 0 & 0 \end{bmatrix} < 0, \quad (7.4.11)$$

$$P - \max \left(\begin{array}{c} \frac{1}{(\bar{x} - \underline{x} + dx)^2}, \\ \frac{1}{(\bar{y} - \underline{y} + dy)^2}, \\ \frac{1}{(\bar{z} - \underline{z} + dz)^2} \end{array} \right) C^T C > 0, \quad (7.4.12)$$

$$\frac{I}{\alpha^2} - P > 0, \quad (7.4.13)$$

Then the filter with realization (7.4.5) and parameters $K = [K_1^T \ K_2^T]^T = -P^{-1}(1 - r_z)C^T$ solves the filtering problem \mathbf{P}_1 .

Proof:

The results expressed in theorem 7.2.3 will be used in the proof that follows. Condition (7.2.6) of theorem 7.2.3 is verified for the deterministic version of the error dynamics in (7.4.8) if

$$F^T P + C^T \mathcal{I}_C^T \mathcal{R} \phi_2^T(\mathcal{C} \hat{\mathbf{p}}, \mathcal{C} \mathbf{p}) \mathcal{I}_C^C \mathcal{R} K^T P + PF + PK \mathcal{I}_C^T \mathcal{R} \phi_2(\mathcal{C} \hat{\mathbf{p}}, \mathcal{C} \mathbf{p}) \mathcal{I}_C^C \mathcal{R} C < 0.$$

Setting $K = -P^{-1}(1 - r_z)C^T$ as suggested in [37], and using lemma 7.4.3 this relation can be simplified as

$$F^T P + \begin{bmatrix} -(1 - r_z) \mathcal{I}_C^T \mathcal{R} H^T L H^{-T} \mathcal{I}_C^C \mathcal{R} & 0 \\ 0 & 0 \end{bmatrix} + PF + \begin{bmatrix} -(1 - r_z) \mathcal{I}_C^T \mathcal{R} H^{-1} L H \mathcal{I}_C^C \mathcal{R} & 0 \\ 0 & 0 \end{bmatrix} < 0.$$

Using the fact that in the set $\mathcal{S} = \{\forall e : e^T P e < 1\}$

$$L = I + \begin{bmatrix} \frac{\hat{z}_c - z_c}{z_c} & 0 & 0 \\ 0 & \frac{\hat{z}_c - z_c}{z_c} & 0 \\ 0 & 0 & 0 \end{bmatrix} > (1 - r_z)I,$$

the second and fourth terms can be rewritten, resulting in

$$F^T P + PF + \begin{bmatrix} -2(1-r_z)^2 I & 0 \\ 0 & 0 \end{bmatrix} < 0$$

which implies condition (7.2.6). The second condition is guaranteed by the condition (7.4.12), and the third condition of theorem 7.2.3 holds due to (7.4.13), with the assumption that $\alpha < \min(\bar{x} - \underline{x} + dx, \bar{y} - \underline{y} + dy, \bar{z} - \underline{z} + dz)$.

Now, after deducing that the given LMIs imply theorem 7.2.3, we can conclude that $\|e_1\|_\infty < \min(\bar{x} - \underline{x} + dx, \bar{y} - \underline{y} + dy, \bar{z} - \underline{z} + dz)$ and that $e(t) \rightarrow 0$ as $t \rightarrow \infty$. Furthermore, in this case $e_2 = \hat{b} - b \rightarrow 0$ implies $\hat{\mathbf{v}} \rightarrow \mathbf{v}$, which completes the proof proposition **P**₁. ■

The stability of the deterministic version of the estimator error dynamics proposed to solve the tracking problem at hand has been proven, however we now address the more complex problem of filter performance in the presence of sensor noise. Notice how filter performance is captured in terms of a bound on the induced norm of a suitably defined operator.

P₂ **Regional Stability and Performance** - Consider a mission scenario defined by \mathcal{P}_c and $\hat{\mathcal{P}}_c$ in (7.4.2). Consider also the design model (7.3.10), with $w = [w_y^T w_v^T]^T \in L_2$ and $\|w\|_2 < 1$. Given positive numbers $\gamma > 0$ and $\alpha > 0$ find (if possible) the observer parameters such that

- a) $\|T_{ew}\|_{2,\infty} < \gamma$, where $\mathbf{e} = [(\hat{\mathbf{p}} - \mathbf{p})^T (\hat{b} - b)^T]^T$ and $T_{ew} : w \rightarrow \mathbf{e}$;
- b) $\mathcal{C}\hat{\mathbf{p}} \in \hat{\mathcal{P}}_c$ for $t > 0$;
- c) $e(t) \rightarrow 0$ as $t \rightarrow \infty$ when $w = 0$ and $\|[(\hat{\mathbf{p}}(0) - \mathbf{p}(0))^T, (\hat{b}(0) - b(0))^T]^T\|_\infty < \alpha$

The next theorem gives conditions under which **P**₂ has a solution.

Theorem 7.4.5 *Consider a mission scenario where the orientation and position variables are constrained by (7.4.1) and (7.4.2) respectively, and let $\hat{\mathcal{P}}_c$ be given. Let $\alpha < \min(\bar{x} - \underline{x} + dx, \bar{y} - \underline{y} + dy, \bar{z} - \underline{z} + dz)$ be a positive number and define $r_z = \frac{\bar{z} - \underline{z} + dz}{\underline{z}} < 1$. Let*

$$\begin{aligned} \epsilon &= \min_{\hat{\mathbf{p}}_c \in \hat{\mathcal{P}}_c} \lambda_{\min}(H^{-1}(\mathcal{C}\hat{\mathbf{p}})H^{-T}(\mathcal{C}\hat{\mathbf{p}})) \\ &= \min_{\hat{\mathbf{p}}_c \in \hat{\mathcal{P}}_c} \lambda_{\max}(H(\mathcal{C}\hat{\mathbf{p}})H^T(\mathcal{C}\hat{\mathbf{p}})) \end{aligned} \tag{7.4.14}$$

Given γ , suppose there exists a matrix $P = P^T \in \mathcal{R}^{6 \times 6}$ such that

$$P > 0, \quad (7.4.15)$$

$$\left[\begin{array}{c|c} F^T P + PF + \left[\begin{array}{c|c} \frac{I}{\gamma^2} & 0 \\ \hline -(1-r_z)^2(2-\epsilon)I & 0 \\ \hline 0 & 0 \end{array} & PF \\ \hline F^T P & -I \end{array} \right] < 0, \quad (7.4.16)$$

$$P - 4 \max \left(\begin{array}{c} \frac{1}{(\bar{x}-x+dx)^2}, \\ \frac{1}{(\bar{y}-y+dy)^2}, \\ \frac{1}{(\bar{z}-z+dz)^2} \end{array} \right) C^T C > 0, \quad (7.4.17)$$

$$\frac{I}{\alpha^2} - P > 0. \quad (7.4.18)$$

Then the filter with realization (7.4.5) and parameters $K = [K_1^T \ K_2^T]^T = -P^{-1}(1-r_z)C^T$ solves problem \mathbf{P}_2 if $\|[(\hat{\mathbf{p}}(0) - \mathbf{p}(0))^T, (\hat{\mathbf{b}}(0) - \mathbf{b}(0))^T]^T\|_\infty < \alpha$.

Proof: The proof for this theorem will be shown in the following steps:

1. Requirement a) of proposition \mathbf{P}_2 will be proven by resorting to the results presented in theorems 7.2.2 and 7.2.3, for the generalized H_2 induced norm and for the initial conditions on the filter, respectively;
2. Requirement b) of proposition \mathbf{P}_2 will be proven by resorting to the result presented in theorem 7.2.1;
3. The third and last requirement of proposition \mathbf{P}_2 follows as a consequence of the use of theorem 7.2.3 in the proof of requirement a).

Step 1 Given the error dynamics (7.4.8) for the proposed estimator, and again using $K = -P^{-1}(1-r_z)C^T$ and lemma 7.4.3, condition (7.2.3) in theorem 7.2.1 is verified if

$$\left[\begin{array}{c|c} F^T P + PF + PFF^T P + \frac{C^T C}{\gamma^2} + \\ \left[\begin{array}{c|c} -2(1-r_z) \frac{\mathcal{I}}{C} \mathcal{R} H^{-1} L H \frac{C}{\mathcal{I}} \mathcal{R} + (1-r_z) \frac{2\mathcal{I}}{C} \mathcal{R} H^{-1} H^{-T} \frac{C}{\mathcal{I}} \mathcal{R} & 0 \\ \hline 0 & 0 \end{array} \right] & 0 \end{array} \right] < 0,$$

where the explicit dependence of the Jacobian in ${}^c\hat{\mathbf{p}}$ and of the auxiliary matrix L in ${}^c\hat{\mathbf{p}}$ and ${}^c\mathbf{p}$ was suppressed. Using the fact that $L > (1 - r_z)I$ in the set $\mathcal{S} = \{\forall e : e^T P e < 1\}$, the previous relation can be further simplified, resulting in

$$F^T P + P F + P F F^T P + \begin{bmatrix} \frac{I}{\gamma^2} - 2(1 - r_z)^2 I + (1 - r_z)^2 \epsilon I & 0 \\ 0 & 0 \end{bmatrix} < 0.$$

Using Schur complements [14], this relation becomes

$$\left[\begin{array}{c|c} F^T P + P F + \begin{bmatrix} \frac{I}{\gamma^2} - 2(1 - r_z)^2 I + (1 - r_z)^2 \epsilon I & 0 \\ 0 & 0 \end{bmatrix} & P F \\ \hline F^T P & -I \end{array} \right] < 0,$$

which implies condition (7.2.3) of theorem 7.2.1. In this way, for all $w \in L_2$, $\|T_{ew}\|_{(2,i)} < \gamma$, where $\mathbf{e} = [(\hat{\mathbf{p}} - \mathbf{p})^T (\hat{\mathbf{b}} - \mathbf{b})^T]^T$ and $T_{ew} : w \rightarrow \mathbf{e}$.

Step 2 Requirement b) in proposition \mathbf{P}_2 will be proven taking into consideration that (7.4.8) is an LPV system. Therefore its solution will be composed of two terms as given by the variation of constants formula, one due to the initial conditions and another driven by the stochastic input. According to the definition, the output $z = C e$ is $z = \hat{\mathbf{p}} - \mathbf{p}$. Moreover, the norm of the output can be written as

$$\|z\|_\infty \leq \|\hat{\mathbf{p}} - \mathbf{p}\|_{\infty|e(0)=0, \|w\|_2 < 1} + \|\hat{\mathbf{p}} - \mathbf{p}\|_{\infty|w=0, \|e(0)\|_\infty < \alpha}$$

and each of the two terms in this inequality can be bounded by the same quantity, without loss of generality, with the result

$$\|\hat{\mathbf{p}} - \mathbf{p}\|_{\infty|e(0)=0, \|w\|_2 < 1} < \frac{1}{2} \min(\bar{x} - \underline{x} + dx, \bar{y} - \underline{y} + dy, \bar{z} - \underline{z} + dz) \quad (7.4.19)$$

and

$$\|\hat{\mathbf{p}} - \mathbf{p}\|_{\infty|w=0, \|e(0)\|_\infty < \alpha} < \frac{1}{2} \min(\bar{x} - \underline{x} + dx, \bar{y} - \underline{y} + dy, \bar{z} - \underline{z} + dz). \quad (7.4.20)$$

To prove the relation in (7.4.19) we will use the result presented in theorem 7.2.2. Given the estimator error dynamics (7.4.8) and the gain $K = -P^{-1}(1 - r_z)C^T$ as above and

using lemma 7.4.3, condition (7.2.4) is verified if

$$F^T P + PF + PFF^T P + \begin{bmatrix} -2(1-r_z)\frac{\mathcal{I}}{c}\mathcal{R}H^{-1}LH\frac{c}{\mathcal{I}}\mathcal{R} & 0 \\ 0 & 0 \end{bmatrix} + \begin{bmatrix} (1-r_z)^2\frac{\mathcal{I}}{c}\mathcal{R}H^{-1}H^{-T}\frac{c}{\mathcal{I}}\mathcal{R} & 0 \\ 0 & 0 \end{bmatrix} < 0.$$

Using Schur complements [14], this relation becomes

$$\left[\begin{array}{c|c} F^T P + PF + \begin{bmatrix} -2(1-r_z)^2 I + (1-r_z)^2 \epsilon I & 0 \\ 0 & 0 \end{bmatrix} & PF \\ \hline F^T P & -I \end{array} \right] < 0,$$

which clearly is guaranteed if the LMI in (7.4.16) is feasible, as required in Step 1.

To obtain the bound on (7.4.20), the result presented in theorem 7.2.3 must be used in a similar way to that presented in theorem 7.4.4.

In conclusion, if the LMIs (7.4.15), (7.4.16), (7.4.17), and (7.4.18) are observed, proposition **P₂** is true for the proposed estimator. ■

Theorems 7.4.4 and 7.4.5 are the tools that allow for the design and analysis of the proposed estimator, with complementary filter properties, for the envisioned tracker problem. Moreover, according to theorem 4.5 of [37], the LMI in (7.4.16) is equivalent to computing

$$\gamma^2 > \frac{1}{(1-r_z)^2(2-\epsilon)},$$

which is a lower bound on the $\|T_{ew}\|_{2,\infty}$.

7.5 Experimental results

This section summarizes the design and analyzes briefly the performance of a non linear tracker with the structure proposed in (7.4.5) for a simulated mission scenario that requires the concerted operation of the AUV and the ASC.

The nominal trajectories performed by the ASC and the AUV are square shaped in the horizontal plane, with constant nominal velocities $^S(\mathcal{I}\mathbf{v}_S) = [1.500]^T m/s$ and $^U(\mathcal{I}\mathbf{v}_U) = [1.000]^T m/s$,

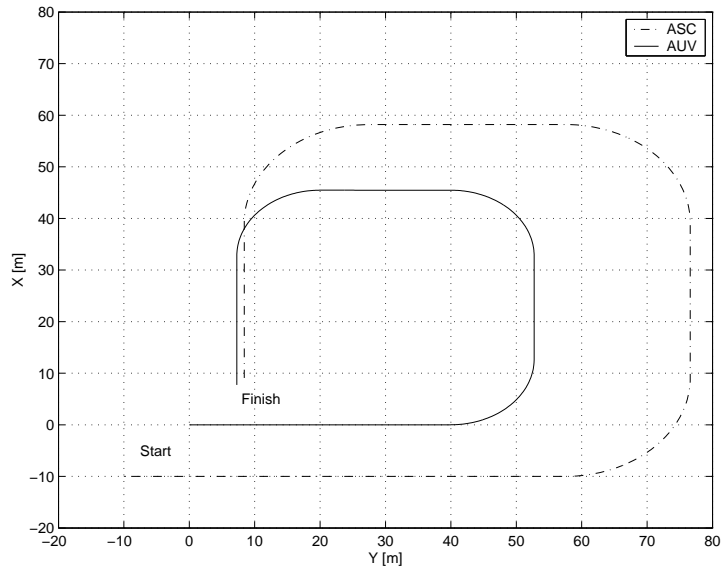


Figure 7.5.1: ASC and AUV inertial coordinates on the horizontal plane.

respectively. The ASC remains at the sea surface (${}^I z_s = 0\text{ m}$) and the AUV starts the mission at a depth of ${}^I z_u = 30\text{ m}$. From time $t = 60\text{ s}$ until $t = 80\text{ s}$ the AUV changes its depth with a constant vertical velocity of ${}^I \dot{z}_u = 0.25\text{ m/s}$.

The envisioned missions are naturally constrained by the ability of the video camera installed on-board the ASC to detect artificial features on the AUV. This impacted on the choice of the parameters for the compact sets \mathcal{P}_c and $\hat{\mathcal{P}}_c$, as shown in table 1. The value of γ in theorem 7.4.5 has a lower bound of $\gamma^2 > 55.8$, which is a lower bound on the induced norm $\|T_{ew}\|_{(2,i)}$.

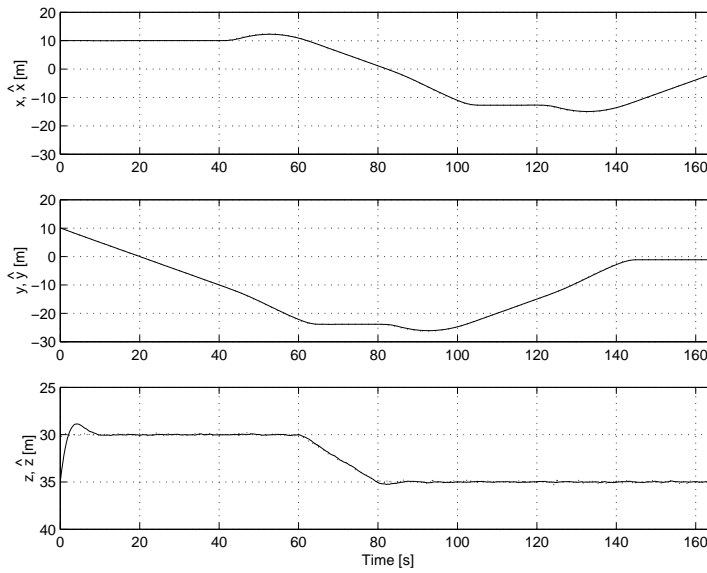
From the LMIs introduced in theorems 7.4.4 and 7.4.5 and from the aforementioned parameters, the value for the estimator gains are $K_1 = 0.74 I_{3 \times 3}$ and $K_2 = 0.30 I_{3 \times 3}$, respectively.

In the first experiment, additive gaussian noise with zero mean and a standard deviation of 0.1 m for the depth sensor was considered. The relative z coordinate was initialized at 35 m when the nominal value was 30 m . The results for the relative position \mathbf{p} are depicted in figure 7.5.2, which shows very small estimation errors. A stronger impact of depth sensor noise on the AUV vertical velocity estimate can be observed in figure 7.5.3, due to the structure of the estimator chosen. However, the vertical velocity changes are accurately estimated. Finally, the coordinates on the camera plane, after compensation for the focal length frame and without taking into consideration the resolution of the sensing system, are depicted in figure 7.5.4 (continuous line).

A second experiment was conducted to evaluate the overall performance of the tracker in the

	Parameter	Value
Λ_c	ϕ_{max}	5°
	θ_{max}	5°
\mathcal{P}_c	$\underline{x} = \underline{y}$	$-20\ m$
	$\bar{x} = \bar{y}$	$20\ m$
	\underline{z}	$20\ m$
	\bar{z}	$38\ m$
$\hat{\mathcal{P}}_c$	dx	$0.1\ m$
	dy	$0.1\ m$
	dz	$0.1\ m$
Theorems 7.4.4 and 7.4.5	α	$18.1\ m$
	r_z	$0.905\ m$
Theorem 7.4.5	ϵ	0.0132

Table 7.5.1: Non-linear tracker design parameters.

Figure 7.5.2: Relative position coordinates \mathbf{p} (dashed) and estimates $\hat{\mathbf{p}} = [\hat{x}\ \hat{y}\ \hat{z}]^T$.

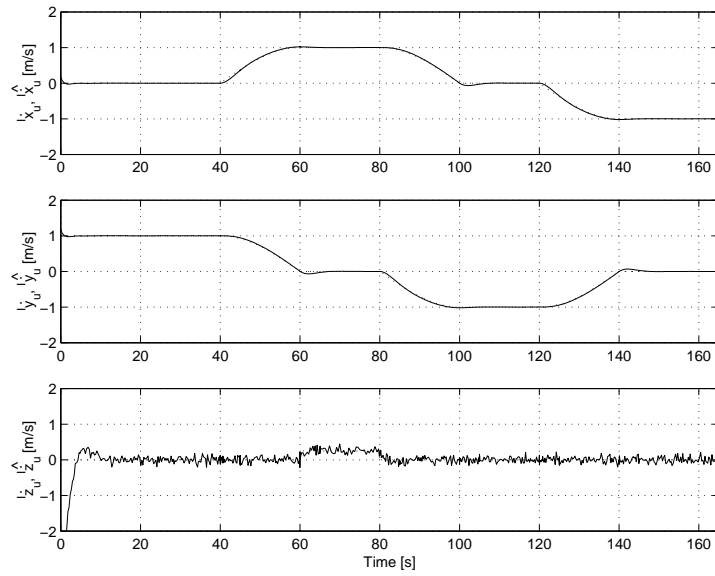


Figure 7.5.3: AUV velocity in the inertial frame $\{I\}$ ${}^I\mathbf{v}_U = [{}^I\dot{x}_u \ {}^I\dot{y}_u \ {}^I\dot{z}_u]^T$ (dashed) and respective estimates ${}^I\hat{\dot{x}}_u$, ${}^I\hat{\dot{y}}_u$ and ${}^I\hat{\dot{z}}_u$.

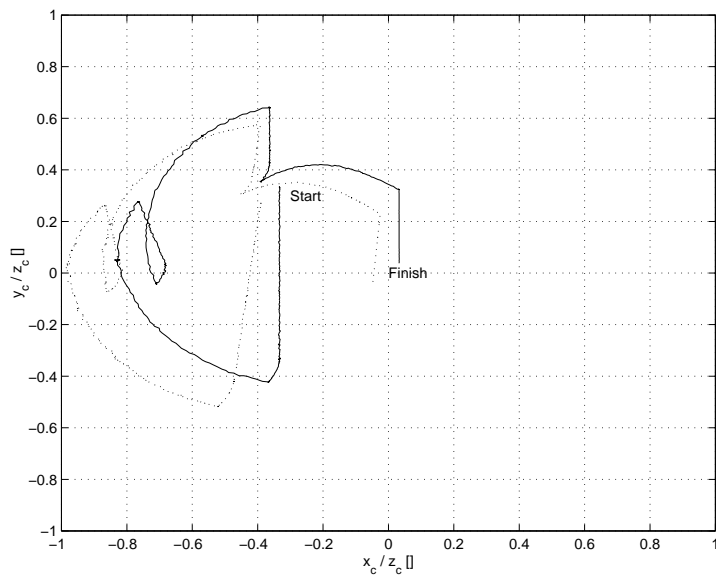


Figure 7.5.4: Camera plane coordinates after compensation for the simulated camera parameters. Exact knowledge of the camera position and orientation in the first experiment (continuous line) and misplaced and misdirected (dashed line).

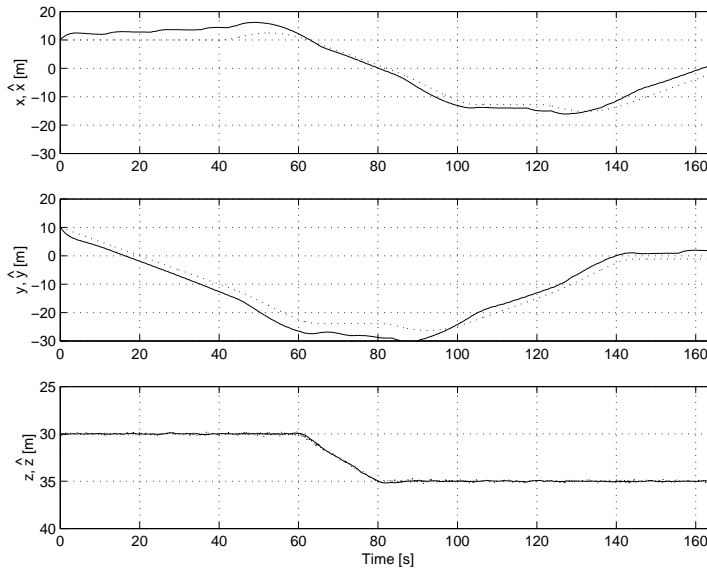


Figure 7.5.5: Relative position coordinates \mathbf{p} (dashed) and estimates \hat{x} , \hat{y} and \hat{z} .

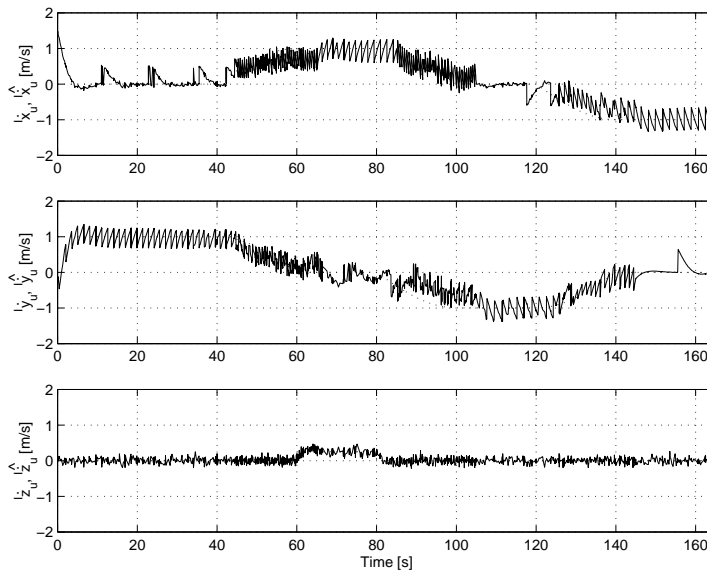


Figure 7.5.6: AUV velocity in the inertial frame $\{I\}^I \mathbf{v}_U = [{}^I \dot{x}_u \ {}^I \dot{y}_u \ {}^I \dot{z}_u]^T$ (dashed) and respective estimates ${}^I \hat{\dot{x}}_u$, ${}^I \hat{\dot{y}}_u$ and ${}^I \hat{\dot{z}}_u$.

presence of a more realistic vision sensor. To that purpose, a resolution grid was set so that a 1 m displacement at a distance of 40 m, in the plane parallel to the camera, corresponded to one pixel. Moreover, an installation error on the camera, corresponding to a rotation on roll, pitch, and yaw angles of 0.1 rad and a misplacement of 0.1 m in all axes was set. The camera plane coordinates are also depicted in figure 7.5.4 (dashed line). The impact of such disturbances on the tracking system can be observed in figure 7.5.5. Notice that though the estimates on the relative position becomes biased the tracker exhibits stable characteristics. The performance on velocity estimates is very poor due to the structure of the tracker, where the bank of integrators used to estimate the velocity bias is now also being used to absorb errors due to finite resolution of the video sensor.

7.6 Non-linear tracker revisited

This section introduces a tracker based on an alternative sensor suite, composed of a video camera, a Doppler log, and a sonar ranging system. The last sensor can be implemented using a pinger, located on the ASC, emitting an interrogation acoustic wave that a transponder, located on the AUV, detects and *answers* to with a signal recognizable by the pinger unit. In this way the round trip travel time corresponds to twice the distance between the two vehicles in the joint oceanic mission, assuming negligible velocities for both vehicles when compared with the speed of sound in the water. This type of acoustic ranging sonar systems is common in Long Baseline positioning systems and is commercially available. The algebraic relations as well as their properties and the results introduced in section 7.4 will be revisited and written for this alternative sensor suite.

Let us assume, without loss of generality, that the acoustic transducers of the pinger and the transponder are installed in the origin of the frames \mathcal{S} and \mathcal{U} , respectively. From the round trip acoustic travel time and assuming a constant (known) velocity for the acoustic waves in the water v_{sound} , the distance between both vehicles can be computed as

$$d = \frac{\tau v_{sound}}{2} = \sqrt{(I x_u - I x_s)^2 + (I y_u - I y_s)^2 + (I z_u - I z_s)^2},$$

where τ is the total round trip travel time of the acoustic waves. Using the notation previously introduced for the position of the ASC and the AUV and using the identity $\frac{\mathcal{I}}{c}\mathcal{R}(\boldsymbol{\lambda})\frac{c}{\mathcal{I}}\mathcal{R}(\boldsymbol{\lambda}) = I$,

this expression can be written as

$$d = \sqrt{(\mathcal{I}\mathbf{p}_u - \mathcal{I}\mathbf{p}_s)^T \frac{\mathcal{I}}{c} \mathcal{R}(\boldsymbol{\lambda}) \frac{c}{\mathcal{I}} \mathcal{R}(\boldsymbol{\lambda}) (\mathcal{I}\mathbf{p}_u - \mathcal{I}\mathbf{p}_s)} = \sqrt{{}^c\mathbf{p}_u^T {}^c\mathbf{p}_u}. \quad (7.6.1)$$

We will work with the square of the distance, the advantages being evident in what follows. The measurements from the video camera and from the sonar ranging sensor to be used by the tracker are stacked together resulting in $h_{\boldsymbol{\lambda}}({}^c\mathbf{p}) : \mathcal{R}^3 \rightarrow \mathcal{R}^3$:

$$h_{\boldsymbol{\lambda}}({}^c\mathbf{p}) = \begin{bmatrix} u_c \\ v_c \\ d^2 \end{bmatrix} = \begin{bmatrix} fx_c/z_c \\ fy_c/z_c \\ x_c^2 + y_c^2 + z_c^2 \end{bmatrix}. \quad (7.6.2)$$

Motivated by the alternative way to obtain the key algebraic relation presented in section 7.3, based in the Taylor series expansion, the expression for the square of the distance in (7.6.1) can be expanded in the exact second order Taylor series around the point ${}^c\hat{\mathbf{p}}$, i.e.

$$d^2 = \hat{d}^2 + \nabla f^T({}^c\hat{\mathbf{p}})({}^c\mathbf{p} - {}^c\hat{\mathbf{p}}) + \frac{1}{2}({}^c\mathbf{p} - {}^c\hat{\mathbf{p}})^T \mathcal{H}({}^c\hat{\mathbf{p}})({}^c\mathbf{p} - {}^c\hat{\mathbf{p}}),$$

where $\nabla f({}^c\hat{\mathbf{p}}) = \begin{bmatrix} 2\hat{x}_c & 2\hat{y}_c & 2\hat{z}_c \end{bmatrix}^T$ is the gradient and $\mathcal{H}({}^c\hat{\mathbf{p}}) = 2I_{3 \times 3}$ is the constant Hessian matrix. Note that this equality precludes the amplification of the noise that could be added due to the use of the square of distance.

The modified key algebraic relation is now presented along with the matrices relating the relevant qualities.

Lemma 7.6.1 *Let $h_{\boldsymbol{\lambda}}(\dots)$ be the mapping function introduced in (7.6.2), then the following relation holds:*

$$h_{\boldsymbol{\lambda}}({}^c\hat{\mathbf{p}}) - h_{\boldsymbol{\lambda}}({}^c\mathbf{p}) = (L({}^c\hat{\mathbf{p}}, {}^c\mathbf{p})H({}^c\hat{\mathbf{p}}) + M({}^c\hat{\mathbf{p}}, {}^c\mathbf{p}))({}^c\hat{\mathbf{p}} - {}^c\mathbf{p}), \quad (7.6.3)$$

where

$$L({}^c\hat{\mathbf{p}}, {}^c\mathbf{p}) = \begin{bmatrix} \hat{z}_c/z_c & 0 & 0 \\ 0 & \hat{z}_c/z_c & 0 \\ 0 & 0 & 1 \end{bmatrix},$$

$H({}^c\hat{\mathbf{p}})$ denotes the Jacobian of $h_{\boldsymbol{\lambda}}({}^c\hat{\mathbf{p}})$, with respect to ${}^c\hat{\mathbf{p}}$ and

$$M({}^c\hat{\mathbf{p}}, {}^c\mathbf{p}) = \begin{bmatrix} 0 \\ 0 \\ ({}^c\hat{\mathbf{p}} - {}^c\mathbf{p})^T \end{bmatrix}$$

accounts for the Hessian term of the last row, corresponding to the sonar ranging sensor.

According to the definition of $h_{\lambda}(\mathcal{C}\hat{\mathbf{p}})$, the Jacobian is given by

$$H(\mathcal{C}\hat{\mathbf{p}}) = \begin{bmatrix} f/\hat{z}_c & 0 & -f\hat{x}_c/\hat{z}_c^2 \\ 0 & f/\hat{z}_c & -f\hat{y}_c/\hat{z}_c^2 \\ 2\hat{x}_c & 2\hat{y}_c & 2\hat{z}_c \end{bmatrix},$$

with a determinant $|H(\mathcal{C}\hat{\mathbf{p}})| = 2f^2d^2/\hat{z}_c^3$ that allows one to conclude that it is invertible in the compact set of positions where the missions will take place.

As discussed earlier, this relation can be used in the estimator as a way to relate errors in the sensor measurements with state variable errors and it is a non-linear relation that makes the estimator dynamics an LPV system. Therefore, in this case the underlying design model is also given by the relations in (7.4.5) which corresponds to a structure as depicted in figure 7.4.1. Lemmas 7.4.2 and 7.4.3 are also true for the relation obtained (please refer to section 7.4 and to [37]).

In the following the error dynamics for the proposed estimator using the present sensor suite will be presented in a similar form to the dynamics introduced for the LPV estimator in (7.4.8). Using the design model (7.3.10), the proposed estimator with realization (7.4.5), and lemma 7.6.1, the error dynamics can be written as

$$\dot{e} = \begin{bmatrix} K_1^T \mathcal{C} \mathcal{R} H^{-1} (LH + M) \mathcal{C}^T \mathcal{R} & I \\ K_2^T \mathcal{C} \mathcal{R} H^{-1} (LH + M) \mathcal{C}^T \mathcal{R} & 0 \end{bmatrix} e - \begin{bmatrix} K_1^T \mathcal{C} \mathcal{R} H^{-1} & I \\ K_2^T \mathcal{C} \mathcal{R} H^{-1} & 0 \end{bmatrix} w,$$

where H , L and H^{-1} are the same abbreviations as before and M is an abbreviation for $M(\mathcal{C}\hat{\mathbf{p}}, \mathcal{C}\mathbf{p})$ introduced in lemma 7.6.1. Let $K = [K_1^T K_2^T]^T$, $F = \begin{bmatrix} 0 & I \\ 0 & 0 \end{bmatrix}$, $C = [I \ 0]$, and using lemma 7.4.3, this relation can be written in a more compact form as

$$\dot{e} = (F + K^T \mathcal{C} \mathcal{R} \phi_2(\mathcal{C}\hat{\mathbf{p}}, \mathcal{C}\mathbf{p}) \mathcal{C}^T \mathcal{R} C + K^T \mathcal{C} \mathcal{R} H^{-1} M \mathcal{C}^T \mathcal{R} C) e - (F + K^T \mathcal{C} \mathcal{R} H^{-1} C) w, \quad (7.6.4)$$

with $z = Ce$. Notice that the system describing the error dynamics is again an LPV that depends on $\mathcal{C}\mathbf{p}$ and on $\mathcal{C}\hat{\mathbf{p}}$ and that a new term appears in the system dynamics matrix.

For the system at hand it is also important to proof that propositions \mathbf{P}_1 and \mathbf{P}_2 are verified. To achieve that purpose two theorems similar to theorems 7.4.4 and 7.4.5 will be presented, with only a partial demonstration due to the similarity of the two cases.

Theorem 7.6.2 Consider a mission scenario where the orientation and position variables are constrained by (7.4.1) and (7.4.2), respectively and let \hat{P}_c be given. Let $\alpha < \min(\bar{x} - \underline{x} + dx, \bar{y} - \underline{y} + dy, \bar{z} - \underline{z} + dz)$ be a positive number, let $r_z = \frac{\bar{z} - \underline{z} + dz}{z} < 1$, and let $\delta < -(\bar{x} - \underline{x} + dx + \bar{y} - \underline{y} + dy + \bar{z} - \underline{z} + dz)/2$.

Suppose there exists a matrix $P = P^T \in \mathcal{R}^{6 \times 6}$ such that

$$P > 0, \quad (7.6.5)$$

$$F^T P + P F + \begin{bmatrix} -2(1 - r_z)^2 I - 2(1 - r_z)\delta I & 0 \\ 0 & 0 \end{bmatrix} < 0, \quad (7.6.6)$$

$$P - \max \left(\frac{1}{(\bar{x} - \underline{x} + dx)^2}, \frac{1}{(\bar{y} - \underline{y} + dy)^2}, \frac{1}{(\bar{z} - \underline{z} + dz)^2} \right) C^T C > 0, \quad (7.6.7)$$

$$\frac{I}{\alpha^2} - P > 0, \quad (7.6.8)$$

with F and C as defined above. The filter with the realization given by (7.4.5) solves the filtering problem expressed in proposition **P₁**.

Proof:

The proof of this theorem follows along the lines of theorem 7.4.4. The only difference is the fact that the system dynamics equation has a new term. Condition (7.2.6) of theorem 7.2.3 is verified for the deterministic version of the error dynamics in (7.6.4) if

$$F^T P + P F + \begin{bmatrix} -2(1 - r_z)^2 I & 0 \\ 0 & 0 \end{bmatrix} + \begin{bmatrix} -2(1 - r_z) \frac{I}{c} \mathcal{R} H^{-1} M_{\mathcal{I}}^c \mathcal{R} & 0 \\ 0 & 0 \end{bmatrix} < 0.$$

Using the fact that in the set $\mathcal{S} = \{\forall e : e^T P e < 1\}$

$$H^{-1} M = \begin{bmatrix} \cdot & \cdot & \frac{\hat{x}_c}{2(\hat{x}_c^2 + \hat{y}_c^2 + \hat{z}_c^2)} \\ \cdot & \cdot & \frac{\hat{y}_c}{2(\hat{x}_c^2 + \hat{y}_c^2 + \hat{z}_c^2)} \\ \cdot & \cdot & \frac{\hat{z}_c}{2(\hat{x}_c^2 + \hat{y}_c^2 + \hat{z}_c^2)} \end{bmatrix} \begin{bmatrix} 0 & 0 & 0 \\ 0 & 0 & 0 \\ x_c - \hat{x}_c & y_c - \hat{y}_c & z_c - \hat{z}_c \end{bmatrix}$$

verifies

$$H^{-1} M > -\frac{1}{2}(\bar{x} - \underline{x} + dx + \bar{y} - \underline{y} + dy + \bar{z} - \underline{z} + dz) I,$$

the new terms can be rewritten, with the result that (7.6.6) implies condition (7.2.6). The remaining conditions are guaranteed using the same arguments as in theorem 7.4.4, concluding the proof of proposition **P₁**, for this case. ■

Note that the extra term on this theorem can be understood as a bound on the added noise due to the use of the square of distance, in the sensor package proposed. The next theorem states the conditions when proposition **P₂** is satisfied. The proof follows along the lines of theorem 7.4.5 and the new term in the system dynamics has a similar impact as in the previous theorem.

Theorem 7.6.3 *Consider a mission scenario where the orientation and position variables are constrained by (7.4.1) and (7.4.2), respectively, and let $\hat{\mathcal{P}}_c$ be given. Let F , α , r_z , and δ be defined as above. Define*

$$\epsilon = \min_{\hat{\mathbf{p}}_c \in \hat{\mathcal{P}}_c} \lambda_{\min}(H^{-1}(\mathcal{C}\hat{\mathbf{p}})H^{-T}(\mathcal{C}\hat{\mathbf{p}})) = \min_{\hat{\mathbf{p}}_c \in \hat{\mathcal{P}}_c} \lambda_{\max}(H(\mathcal{C}\hat{\mathbf{p}})H^T(\mathcal{C}\hat{\mathbf{p}}))$$

and for a given γ , suppose there exists a matrix $P = P^T \in \mathcal{R}^{6 \times 6}$ such that

$$P > 0, \quad (7.6.9)$$

$$\left[\begin{array}{c|c} F^T P + P F + \left[\begin{array}{cc} \frac{I}{\gamma^2} - (1 - r_z)^2(2 - \epsilon)I - 2(1 - r_z)\delta I & 0 \\ 0 & 0 \end{array} \right] & P F \\ \hline F^T P & -I \end{array} \right] < 0, \quad (7.6.10)$$

$$P - 4 \max \left(\frac{1}{(\bar{x} - \underline{x} + dx)^2}, \frac{1}{(\bar{y} - \underline{y} + dy)^2}, \frac{1}{(\bar{z} - \underline{z} + dz)^2} \right) C^T C > 0, \quad (7.6.11)$$

$$\frac{I}{\alpha^2} - P > 0. \quad (7.6.12)$$

Then the filter with realization (7.4.5) and parameters $K = [K_1^T \ K_2^T]^T = -P^{-1}(1 - r_z)C^T$ solves problem **P₂** if $\|[(\hat{\mathbf{p}}(0) - \mathbf{p}(0))^T, (\hat{\mathbf{b}}(0) - \mathbf{b}(0))^T]^T\|_\infty < \alpha$.

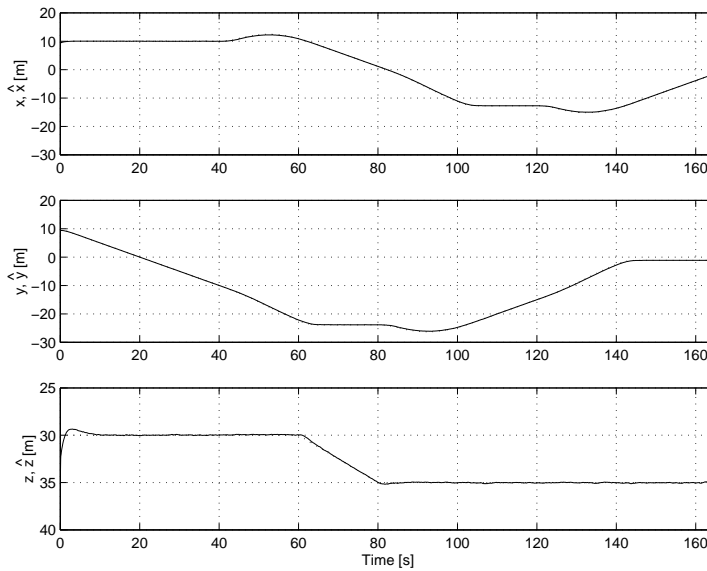
Theorems 7.6.2 and 7.6.3 are again the tools that allow for the design and analysis of the proposed estimator, with complementary filter properties, for the envisioned tracker problem at hand and the sensor suite presented at the beginning of this section.

To assess the performance of the proposed structure the results of a simulation experiment is reported, where the nominal trajectories are identical to those described in section 7.5.

The envisioned missions are naturally constrained by the visibility of the artificial feature of the AUV by the video camera installed on-board the ASC. Therefore, the parameters for the position compact sets \mathcal{P}_c and $\hat{\mathcal{P}}_c$ were chosen accordingly, as described in table 2. From

	Parameter	Value
Λ_c	ϕ_{max}	5°
	θ_{max}	5°
\mathcal{P}_c	$\underline{x} = \underline{y}$	$-15\ m$
	$\bar{x} = \bar{y}$	$15\ m$
	\underline{z}	$20\ m$
	\bar{z}	$38\ m$
$\hat{\mathcal{P}}_c$	dx	$0.1\ m$
	dy	$0.1\ m$
	dz	$0.1\ m$
Theorems 7.6.2 and 7.6.3	α	$18.1\ m$
	r_z	0.905
	δ	$-39.15\ m$
Theorem 7.6.3	ϵ	1.32×10^{-4}

Table 7.6.1: Non-linear tracker design parameters for the new sensor suite.

Figure 7.6.1: Relative position coordinates \mathbf{p} (dashed) and estimates \hat{x} , \hat{y} and \hat{z} .

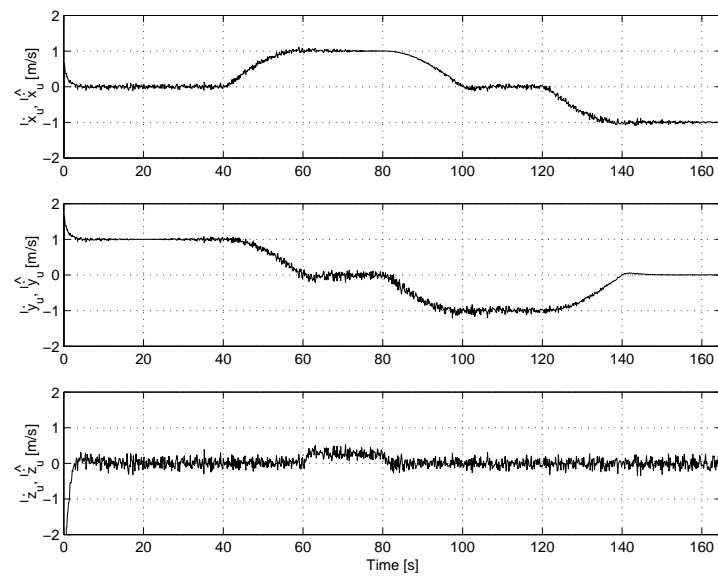


Figure 7.6.2: AUV velocity in the inertial frame $\{I\}$ ${}^I\mathbf{v}_U = [{}^I\dot{x}_u \ {}^I\dot{y}_u \ {}^I\dot{z}_u]^T$ (dashed) and respective estimates ${}^I\hat{\dot{x}}_u$, ${}^I\hat{\dot{y}}_u$ and ${}^I\hat{\dot{z}}_u$.

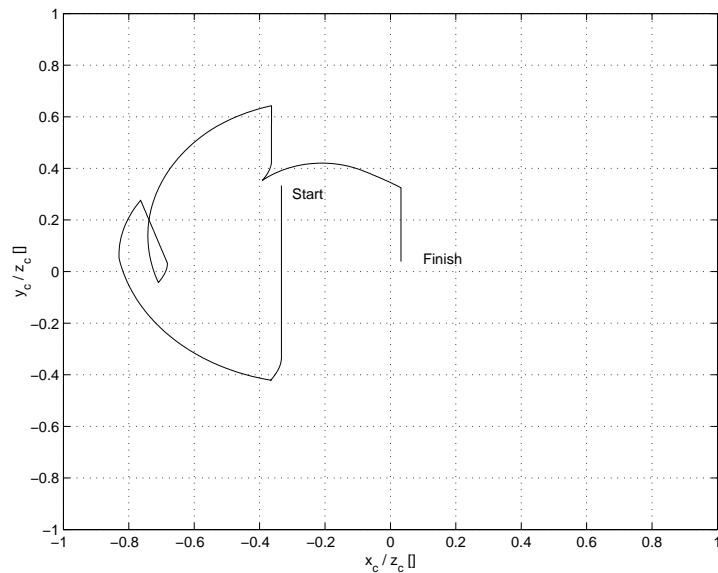


Figure 7.6.3: Camera plane coordinates after compensation for the simulated camera parameters.

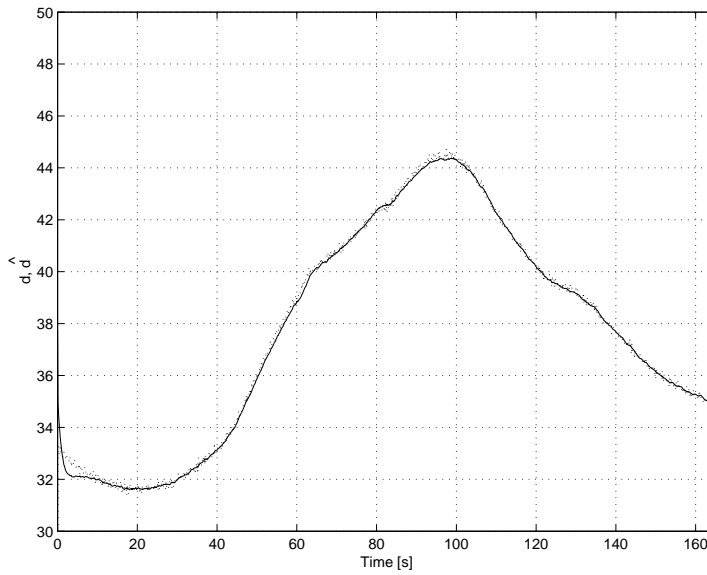


Figure 7.6.4: Distance measured d (dashed) and estimated between both vehicles.

the LMIs introduced in theorems 7.4.4 and 7.4.5 and from the aforementioned parameters, the values for the estimator gains are $K_1 = 0.92 I_{3 \times 3}$ and $K_2 = 0.22 I_{3 \times 3}$, respectively.

During the simulation, an additive gaussian noise with zero mean and a standard deviation of 0.1 m for the sonar ranging sensor was set. A delay of $2\delta v_{sound}$ was also introduced in the measurements of the aforementioned sensor. The results for the relative position \mathbf{p} are depicted in figure 7.6.1, where minor impact on the performance of the tracker was observed in the described conditions.

A stronger impact of the additive noise on the velocity estimate can be observed in figure 7.6.2, due to the structure of the estimator chosen, as was seen in the earlier experiment reported. The coordinates on the camera plane, after compensation for the focal length frame and without taking into consideration the resolution of the sensing system, are depicted in figure 7.6.3. In figure 7.6.4 the distance measured by the sonar ranging sensor and the corresponding estimated value is depicted. In conclusion, the overall performance of the proposed non-linear tracker seems to be promising for the problem at hand, though a set of field tests will need to be performed to assess the viability of such non-linear tracker in realistic oceanic conditions.

7.7 Conclusions

A non-linear tracker structure was proposed to solve a specific tracking problem resulting from the use of autonomous vehicles in oceanography. However, nothing precludes the application of the methodology followed along this chapter to other generic tracking problems such as hovering and feature-based navigation. Moreover, the approach consisting of designing feedback systems in the sensors' coordinates constitute a natural solution to a large class of estimation and control problems in robotics.

The properties of the proposed non-linear trackers revealed as an interesting solution to the problem at hand. A systematic methodology for the analysis and design of the resulting LPV systems was presented. The simulation results provide confidence on the practical implementation of such non-linear estimators in a realistic setup, on-board a small autonomous surface craft.

Due to the discrete-time nature of the measurements available from the sensor package to be used, the development of a discrete-time version of such tracker is of utmost importance. Moreover, since data from the sensors to be used is made available at different rates, the study of a multi-rate version of such non-linear tracker should be further investigated. The time independence of the key algebraic relation used to solve the tracker design problem at hand along this chapter is a major feature toward achieving these goals.

Chapter 8

Conclusion

This thesis started by reviewing a recently introduced framework for the characterization of classical concepts in systems and control theory - Linear Matrix Inequalities (LMIs). Concepts such as dissipativity of linear systems, stability of non-linear and linear systems, the \mathcal{H}_∞ , \mathcal{H}_2 , and the generalized \mathcal{H}_2 norms computation of finite-dimensional, linear, time-invariant systems were reviewed and formulated using LMIs, both in continuous and in discrete-time setups. Convex constraints on regional placement of the eigenvalues of the systems at hand in terms of LMIs were also presented. Moreover, two setups for closed loop estimation were introduced and a discussion of the solutions obtained was outlined. The results obtained are easily implementable in commercially available packages such as the MATLAB LMI Optimization Toolbox and they pave the way for the design of estimators with multiple constraints.

Chapter 3 reviewed a methodology for the design of estimators, rooted on classic work done by Wiener - Complementary Filters (CFs). The framework proposed, based on a stationary stochastic characterization of the signals under consideration and on linear time-invariant systems, leads to a linear time-invariant solution resorting to spectral factorization techniques. This approach is simpler than the stochastic setting proposed by Kalman, which requires a complete characterization of process and observation noises. In real applications this a task that may be difficult, costly, or not suited to the problem at hand. In a great number of practical applications the filter design process is entirely dominated by constraints that are naturally imposed by the sensor bandwidths as shown in a motivating example presented in the chapter. Moreover, the relation between complementary filters and Wiener and Kalman filters was discussed.

The study of periodic and multi-rate systems was one of the main thrusts of this thesis. To that purpose, in chapter 4 the synthesis of periodic estimators for periodic and multi-rate systems was described in detail. The definition of multi-rate systems as periodic systems was presented and the description of linear systems as operators was introduced, with an emphasis on the properties of linear, periodically time-varying systems. New theoretical results on the \mathcal{H}_2 norm computation of periodic systems were deduced. The estimators structure introduced previously was revisited and the solutions obtained were discussed in detail, based on the new results for this subclass of systems. The methodology proposed, resorting to convex optimization procedures, is based on minimization of the \mathcal{H}_2 and/or \mathcal{H}_∞ norms from auxiliary inputs to auxiliary outputs, constrained by the norms of other input/output signals. This new synthesis methodology was successfully applied to the design of a periodic navigation system, validated with simulation results and during sea trials with an autonomous surface craft. The results obtained with this powerful new methodology pave the way for the use of such a framework in periodic feedback control and multi-rate filter design, which will be subject of future work.

Chapter 5 addressed the analysis problem for periodically time-varying linear systems, complementing the previous chapter. Classically, the isomorphic properties of the \mathbf{z} transform in the case of linear, time-invariant systems have been commonly used to understand the frequency-response for a given system. However, in the case of linear, periodically time-varying systems the notion of frequency-response is not so clear. Some classical methods were reviewed with emphasis on the difficulties in interpretation. Based on the results presented in the previous chapter, a new methodology was presented, using the computation of the \mathcal{H}_∞ norm of a difference between two signals. The close relation to the classical frequency-response computation (the Bode plot) and the broad class of systems that can be analyzed are the the main advantages of the proposed approach. In order to get insight to the proposed method, the periodic estimation problem solved in the previous chapter was analyzed. Finally, direct incorporation of the frequency domain properties led to formulating a non-convex optimization problem.

Chapter 6 extended the theory of complementary filtering to the time-varying setting. In particular, the frequency domain interpretations of complementary filters were extended by resorting to the theory of linear differential inclusions and by converting the problem of weighted filter performance analysis into that of determining the feasibility of a related set of Linear Matrix Inequalities (LMIs). Using this setup, it was shown how the stability of the resulting

filters as well as their “frequency-like” performance can be assessed using efficient numerical analysis tools that borrow from convex optimization techniques. The cases of complementing position information with that available from on-board Doppler sonar and accelerometers were also considered. The resulting design methodology was successfully applied to a design example. Future work will aim at extending these results to the discrete-time, multi-rate case.

A non-linear tracker structure was proposed in chapter 7 to solve a specific target tracking problem resulting from the use of autonomous vehicles in oceanography. The approach, consisting of designing estimators on the sensors’ coordinates, constitutes a natural solution to a large class of estimation and control problems in robotics. Sufficient conditions for stability and performance of the proposed non-linear target trackers were found, resulting in an interesting solution to the problem at hand. A systematic methodology for analysis and design of the resulting LPV systems was presented. The simulation results provide confidence on the practical implementation of such non-linear estimator in a realistic setup, on-board a small autonomous surface craft. Due to the discrete-time nature of the measurements available from the sensor package to be used, the development of a discrete-time version of such tracker is of major importance and will be the subject of further development in the near future. Moreover, since data from the sensors to be used is made available at different rates, the study of a multi-rate version of such non-linear tracker should also be further investigated. The time independence of the key algebraic relation used to solve the tracker design problem at hand in this chapter will be a major feature in achieving these goals. Further, nothing precludes the application of the methodology outlined here to other generic tracking problems such as hovering and feature-based navigation problems.

Bibliography

- [1] J. Alves, P. Oliveira, A. Pascoal, M. Rufino, L. Sebastião and C. Silvestre, “DELFIN - An Autonomous Surface Craft for Ocean Operations,” to appear in *Proceedings OCEANS 2001 MTS/IEEE*, USA, 2001.
- [2] B. Anderson and J. Moore, *Optimal Filtering*, Information and System Sciences Series, Prentice-Hall, Inc. Englewood Cliffs, 1979.
- [3] *Advanced System Integration for Managing the Coordinated Operation of Robotic Ocean Vehicles - ASIMOV*, Technical Reports No. 1 (1998) and No. 2 (1999), ISR-IST, Lisbon, Portugal.
- [4] T. Balch and R. Arkin, “Communication in Reactive Multiagent Robotic Systems,” *Autonomous Robots*, No. 1, pp. 1-25, 1994.
- [5] B. Bamieh and J. Pearson, “The \mathcal{H}_2 problem for sampled data systems,” *Systems and Control Letters*, Vol. 19, pp. 1-12, 1992.
- [6] Y. Bar-Shalom, and X.R. Li, *Estimation and Tracking: Principles, Techniques and Software*, Dedham, MA: Artech House, 1993.
- [7] I. Bar-Itzhack and I. Ziv, “Frequency and time domain designs of strapdown vertical determination systems,” *Proc. AIAA Guidance, Navigation and Control*, Williamsburgh, pp. 505-515, 1986.
- [8] G. Becker and A. Packard, “Robust performance of linear, parametrically varying systems using parametrically dependent linear, dynamic feedback,” *Systems and Control Letters*, 1993.

- [9] J. Bernussou, J. Geromel and P. Peres, "A linear programming oriented procedure for quadratic stabilization of uncertain systems," *System and Control Letters*, Vol. 13, pp. 65-72, 1989.
- [10] S. Bittanti, P. Colaneri and G. Nicolau, "The Difference Riccati Equation for the Periodic Prediction Problem," *IEEE Transactions on Circuits and Systems*, No. 8, pp. 706-712, 1988.
- [11] S. Bittanti, Ed., *The Riccati Equation*, Springer Verlag, 1991.
- [12] S. Bittanti and F. Cuzzola, "An LMI approach to periodic discrete-time unbiased filtering," *System and Control Letters*, Vol. 41, No. 1, pp. 21-35, 2001.
- [13] S. Boyd and C. Barrat, *Linear Control Design: Limits of Performance*, Prentice-Hall, 1991.
- [14] S. Boyd, L. El Ghaoui, E. Feron and B. Balakrishnan, *Linear Matrix Inequalities in Systems and Control Theory*, SIAM Studies in Applied Mathematics, Philadelphia, 1994.
- [15] K. Britting. *Inertial Navigation System Analysis*, Wiley-Interscience, 1971.
- [16] R. Brockett, *Finite Dimension Linear Systems*, John Wiley and Sons, New York, 1970.
- [17] R. Brown and P. Hwang. *Introduction to Random Signals and Applied Kalman Filtering*, Second Edition, John Wiley and Sons, Inc., 1992.
- [18] R. Brown, "Integrated navigation systems and Kalman filtering: a perspective," *Journal of the Institute of Navigation*, Vol. 19, No. 4, pp. 355-362, 1972.
- [19] T. Chen and B. Francis, *Optimal Sampled-Data Control Systems*, Communications and Control Engineering Series, Springer, 1994.
- [20] T. Chen and L. Qiu, " \mathcal{H}_∞ Design of General Multirate Sampled-data Control Systems," *Automatica*, Vol. 30, No. 7, pp. 1139-1152, 1994.
- [21] M. Chilali and P. Gahinet, " \mathcal{H}_∞ design with pole placement constraints: an LMI approach," *IEEE Transactions on Automatic Control*, Vol. 41, No. 4, pp. 358-367, 1996.

- [22] P. Colaneri, S. Bittanti and G. Nicolau, "An algebraic Riccati equation for the discrete-time periodic prediction problem," *Systems & Control Letters*, pp. 71-78, 1990.
- [23] R. Crochiere and L. Rabiner, *Multirate Digital Signal Processing*, Prentice-Hall Inc, 1980.
- [24] J. H. Davis, "Stability conditions derived from spectral theory: discrete system with periodic feedback," *SIAM Journal of Control*, Vol. 10, pp. 1-13, 1972.
- [25] C. Desoer and M. Vidyasagar, *Feedback Systems: Input-Output Properties*, Academic Press, 1975.
- [26] Friedland, B., "Sampled-data control systems containing periodically varying members," *Proc. First IFAC Congress*, 1960.
- [27] Fryxell, D., P. Oliveira, A. Pascoal and C. Silvestre. "An integrated approach to the design and analysis of navigation, guidance and control systems for AUVs. *Proc. Symposium on Autonomous Underwater Vehicle Technology*, Cambridge, Massachusetts, USA, 1994.
- [28] J. Geromel, "Optimal linear filtering under parameter uncertainty," *IEEE Transactions on Signal Processing*, Vol. 47, No. 2, pp. 168-175, 1999.
- [29] K. C. Goh, L. Turan, M. G. Safonov, G. P. Papavassilopoulos, and J. H. Ly, "Biaffine Matrix Inequality Properties and Computational Methods," *Proc 1994 American Control Conference*, Baltimore, MD, pp. 850-855, 1994.
- [30] G. Goodwin and M. Seron, "Fundamental design tradeoffs in filtering, prediction, and smoothing," *IEEE Trans. Automatic Control*, Vol. 42, No. 9, pp. 1240-1251, 1997.
- [31] M. Green and D. Limebeer. *Linear Robust Control*. Prentice-Hall, 1995.
- [32] M. Guelman, "Proportional navigation with a maneuvering target," *IEEE Transactions on Aerospace and Electronic Systems*, Vol. 8, No. 5, pp. 364-371, 1972.
- [33] M. Green and D. Limebeer, *Linear Robust Control*, Prentice-Hall, 1995.
- [34] K. Grigoriadis and J. Watson, "Reduced-order \mathcal{H}_∞ and $\mathcal{L}_2 - \mathcal{L}_\infty$ filtering via linear matrix inequalities," *IEEE Trans. Aerospace and Electronic Systems*, Vol. 33, No. 4, pp. 1326-1338, 1997.

- [35] J. Hespanha, *Controladores Periódicos e Multi Ritmo para Sistemas Invariantes no Tempo*, Master thesis, Universidade Técnica de Lisboa, 1993.
- [36] B. Horn, *Robot Vision*, MIT Press, Cambridge, MA, 1985.
- [37] I. Kaminer, A. Pascoal, W. Kang and O. Yakimenko, "Integrated Vision/Inertial Navigation System Design Using Nonlinear Filtering," *Proceedings of the 1999 American Control Conference*, San Diego, June 1999.
- [38] D. Jourdan, "Doppler sonar navigation error propagation and correction" *Journal of the Institute of Navigation*, Vol. 32, No. 1, pp. 29-56, Spring 1985.
- [39] T. Kailath, *Lectures on Wiener and Kalman Filtering*, Springer-Verlag, 1981.
- [40] R. Kalman, "Lyapunov functions for the problem of Lur'e in automatic control," *Proceedings National Academy of Sciences*, Vol. 49, pp. 201-205, 1963.
- [41] M. Kayton and W. Fried (ed.). *Avionics Navigation Systems*. John Wiley and Sons, Inc., New York, 1969.
- [42] P. Khargonekar, P. Poola and A. Tannenbaum, "Robust control of linear time-invariant plants using periodic compensation," *IEEE Transactions on Automatic Control*, Vol. 21, No. 11, pp. 1088-1096, 1985.
- [43] G. Kranc, "Input-Output Analysis of Multirate Feedback Systems," *IRE Transactions on Automatic Control*, pp. 21-28, Nov 1957.
- [44] C. Lin. *Modern Navigation, Guidance, and Control Processing*, Prentice-Hall, 1991.
- [45] D. Luenberger, "Observing the state of a linear system," *IEEE Transactions on Military Electronics*, Vol. 8, pp. 74-80, 1964.
- [46] A. Lur'e, *Some Nonlinear Problems in the Theory of Automatic Control*, H. Stationery Off., London, 1957. Original in Russian, 1957.
- [47] A. Lyapunov, *Problème General de la Stabilité du Mouvement*, *Annals of Mathematical Studies*, Princeton University Press, Princeton, 1947.

- [48] MATLAB, LMI Control Toolbox, *The Math Works Inc.*, 1997.
- [49] E. Mazor, A. Averbuch, Y. Bar-Shalom, and J. Dayan, "Interacting Multiple Model Methods in Target Tracking: A Survey," *IEEE Transactions on Aerospace and Electronic Systems*, Vol. 34, No. 1, pp. 103-122, 1998.
- [50] S. Merhav. *Aerospace Sensor Systems and Applications*, Springer-Verlag, 1996.
- [51] D. Meyer, "A New Class of Shift-Varying Operators, Their Shift-Invariant Equivalent and Multirate Digital Systems, " *IEEE Transactions on Automatic Control*, Vol. 25, No. 4, pp. 429-433, 1990.
- [52] R. Meyer and C. Burrus, "A unified analysis of multirate and periodically time-varying digital filters," *IEEE Transactions on Circuits and Systems*, No. 3, pp. 162-168, 1975.
- [53] K. Nagpal and P. Khargonekar, "Filtering and smoothing in an H_∞ setting," *IEEE Trans. Automatic Control*, Vol. 36, No. 1, pp. 152-166, 1991.
- [54] Y. Nestorov and A. Nemirovski, *Interior Point Polynomial Methods in Convex Programming: Theory and Applications*, SIAM Studies in Applied Mathematics, Philadelphia, 1994.
- [55] J. Oh, and I. Ha, "Capturability of the 3-Dimensional Pure PNG Law," *IEEE Transactions on Aerospace and Electronic Systems*, Vol. 35, No. 4, pp. 491-502, 1999.
- [56] M. Oliveira, *Controle de sistemas lineares baseado nas desigualdades matriciais lineares*, Ph.D. Thesis, Universidade Estadual de Campinas, 1999.
- [57] P. Oliveira, A. Pascoal, C. Silvestre, "Guidelines to the Design of a Navigation System for an Autonomous Underwater System," *ISR Internal report*, 1994.
- [58] The GIB System, *User Manual*, 1999.
- [59] Pascoal, A., P. Oliveira, C. Silvestre and et al, "Robotic ocean vehicles for marine science applications: the european asimov project," *MTS/IEEE Oceans 2000 Conference*, 2000.
- [60] A. Papoulis, *Probability, Random Variables, and Stochastic Processes*, McGraw Hill, 1984.

- [61] C. Pirie, *Controller Synthesis for Uncertain Time-Varying Discrete-Time Systems*, Master thesis, Waterloo, Ontario, Canada, 1999.
- [62] E. Pyatnitskii and V. Skorodinskii, "Numerical methods of Lyapunov function construction and their application to the absolute stability problem," *System and Control Letters*, Vol. 2, pp. 130-135, 1982.
- [63] R. Ravi, P. Khargonekar, K. Minto and C. Nett, "Controller Parametrization for Time-Varying Multirate Plants," *IEEE Transactions on Automatic Control*, Vol. 35, No. 11, pp. 1259-1262, 1990.
- [64] A. Rizzi and D. Koditscheck, "An Active Visual Estimator for Dextrous Manipulation," *IEEE Transactions on Robotics and Automation*, Vol. 12, No. 5, pp. 697-713, 1996.
- [65] H. L. Royden, *Real Analysis*, Macmillan Publishing Company, 1988.
- [66] C. Samson, M. Le Borgne and B. Espiau, *Robot Control, The Task Function Approach*, Clarendon Press, Oxford, 1991.
- [67] C. Scherer, P. Gahinet and M. Chilali, "Multiobjective output-feedback control via LMI optimization," *IEEE Trans. Automatic Control*, Vol. . 42, No. 7, pp. 896-911, 1997.
- [68] C. Scherer, and S. Weiland, *Linear Matrix Inequalities in Control*, Class notes, October 2000.
- [69] C. Scherer (1997), "Mixed H_2/H_∞ control for time-varying and linear parametrically-varying systems," *Int. J. of Robust and Nonlinear Control*, pp. 929-952, 1996.
- [70] Special Electronic Mission Aircraft (SEMA) Conference, Ft. Huachuca, USA.
- [71] C. Silvestre, *Multi-Objective Optimization Theory with Applications to the Integrated Design of Controllers/Plants for Autonomous Vehicles*, Ph. D. thesis, Universidade Técnica de Lisboa, 2000.
- [72] G. Siouris. *Aerospace Avionics Systems: a Modern Synthesis*, Academic Press Inc., 1993.
- [73] C. Souza, "Periodic Strong Solutions for the Optimal Filtering Problem of Linear Discrete-Time Periodic Systems," *IEEE Transactions on Automatic Control*, Vol. . 36, No. 3, pp. 333-337, 1991.

- [74] H. Sorenson, *Kalman Filtering: Theory and Application*, IEEE Press, 1985.
- [75] J. Stambaugh and R. Thibault, "Navigation requirements for autonomous underwater vehicles," *Journal of the Institute of Navigation*, Vol. 39, n. 1, pp. 79-92, Spring 1992.
- [76] M. Vidyasagar, *Control System Synthesis: a Factorization Approach*, MIT Press, 1985.
- [77] J. Willems, "Dissipative dynamic systems," *Arch. Rational Mech. Anal*, Vol. 45, pp. 321-393, 1971.
- [78] R. Wiśniewski and J. Stoustrup, "Generalized \mathcal{H}_2 Control Synthesis for Periodic Systems," *ACC 2001*, Arlington, Virginia, June, 2001.
- [79] V. Yakubovich, "The solution of certain matrix inequalities in automatic control theory," *Soviet Math Dokl.*, Vol. . 5, pp. 620-623, 1964.
- [80] J. Youngberg, "A novel method for extending GPS to underwater vehicles," *Journal of the Institute of Navigation*, Vol. 38, No. 3, pp. 263-271, Fall 1991.

